Context-dependent effects of Ascl1 on glial cell lineage decisions in the injured adult mouse cortex

Dissertation

Zur Erlangung des Grades
Doktor der Naturwissenschaften
Am Fachbereich Biologie
Der Johannes-Gutenberg-Universität Mainz

Catarina de Sá Fernandes
geb. am 19.10.1996 in Lissabon, Portugal

Mainz, 2026

Dekan:

1. Berichterstatter:

2. Berichterstatter:

Tag der mündlichen Prüfung:

Versicherung

Hiermit versichere ich gemäß §12, Abs. 2 der Promotionsordnung vom 01.04.2018, dass ich die heute als Dissertation vorgelegte Arbeit selbst angefertigt und alle benutzten Hilfsmittel in der Arbeit angegeben habe. Ich habe oder hatte die jetzt als Dissertation vorgelegte Arbeit nicht als Prüfungsarbeit für eine staatliche oder andere wissenschaftliche Prüfung eingereicht. Ich habe weder die jetzt als Dissertation vorgelegte Arbeit noch Teile einer Abhandlung bei einer anderen Fakultät bzw. einem anderen Fachbereich als Dissertation eingereicht. Ich habe noch kein Promotions-, PhD- oder vergleichbares Graduierungsverfahren im Promotionsfach erfolglos oder erfolgreich beendet. Für die Anfertigung der vorgelegten Arbeit wurde keine entgeltliche Hilfe Dritter, insbesondere eine Promotionsberatung oder -vermittlung, in Anspruch genommen.

Mainz, den

Unterschrift

"Só se nos detivermos a pensar nas pequenas coisas chegaremos a compreender as grandes"

———— José Saramago————

Acknowledgments

Table of Contents

Zusammenfassung

Hirnverletzungen führen typischerweise zu neuronalem oder oligodendroglialem Zellverlust, begleitet von anhaltenden funktionellen Beeinträchtigungen aufgrund der begrenzten Regenerationsfähigkeit des adulten Säugetiergehirns. Die *in vivo* Konversion nicht-neuronaler Zellen in Neurone oder Oligodendrozyten hat sich als vielversprechende Strategie für den Zellersatz und die Hirnreparatur etabliert. Der proneuronale Transkriptionsfaktor Ascl1 wurde umfassend als Reprogrammierungsfaktor untersucht, wobei seine neurogene Kapazität maßgeblich durch posttranslationale Phosphorylierung beeinflusst wird. Während der frühen postnatalen Entwicklung wurde festgestellt, dass die Überexpression einer phosphorylierungsdefizienten Mutante von Ascl1, Ascl1SA6, Astrozyten effizient in induzierte Neurone (iNs) konvertiert, während Wildtyp-Ascl1 die Proliferation von Oligodendrozyten-Vorläuferzellen (OPCs) fördert. Diese Befunde weisen auf potenzielle Strategien zur Regeneration von Neuronen bzw. zur Expansion von OPCs hin, jedoch ist unklar, ob diese Reaktionen auch im Kontext einer adulten Hirnverletzung noch ausgelöst werden können.

In dieser Studie habe ich die Auswirkungen einer entzündlichen Umgebung auf die Effekte von Ascl1 auf die gliale Zelllinie unter Verwendung des kortikalen Stichwunden-Läsionsmodells bei adulten Mäusen untersucht. Hierfür wurden die Reprogrammierungsergebnisse nach retroviral-vermittelter Expression von Ascl1 oder Ascl1SA6, allein oder in Kombination mit Bcl2 in reaktiven Gliazellen, im verletzten adulten Kortex bewertet. Dies ist ein Milieu, das durch entzündliche Merkmale einschließlich der Anwesenheit C3-exprimierender neurotoxischer reaktiver Astrozyten gekennzeichnet ist. In diesem Kontext zeigte Ascl1SA6 allein nur eine marginale neurogene Kapazität, während die Ko-Expression von Bcl2 die neuronale Konversionseffizienz signifikant steigerte, wobei iNs über die Zeit überlebten, jedoch teilweise unreif blieben. Genetisches Fate-Mapping ergab, dass iNs überwiegend von OPCs abstammten und nicht von reaktiven Astrozyten, die in diesem Modell refraktär erschienen. Im Gegensatz dazu förderte die ektopische Expression von Ascl1 allein oder in Kombination mit Bcl2 eine robuste und zellautonome proliferative Antwort in OPCs nach kortikaler Verletzung. Dieser proliferative Effekt erweiterte die oligodendrogliale Population, die überwiegend von präexistierenden OPCs abstammte. Bemerkenswerterweise war der Ascl1-vermittelte Effekt auf OPCs langfristig anhaltend, ohne deren Kompetenz zur Differenzierung zu beeinträchtigen, da Ascl1-überexprimierende OPCs prämyelinisierende und reife Oligodendrozyten im adulten verletzten Kortex hervorbrachten.

Zusammenfassend zeigt diese Studie, dass die entzündliche Umgebung des verletzten adulten Kortex die Wirksamkeit von phosphorylierungsdefizientem Ascl1 zur Konversion von Gliazellen in Neurone erheblich einschränkt, während Wildtyp-Ascl1 dennoch in der Lage ist, die OPC-Expansion signifikant zu fördern. Somit liefert diese Studie eine Grundlage für zukünftige Arbeiten zur neuronalen Ersatztherapie und Remyelinisierung.

Abstract

Brain injury typically results in neuronal or oligodendroglial loss accompanied by persistent functional impairment due to the limited regenerative capacity of the adult mammalian brain. *In vivo* conversion of non-neuronal cells into neurons or oligodendrocytes has emerged as a promising strategy for cell replacement and brain repair. The proneural transcription factor Ascl1 has been extensively investigated as a reprogramming factor, and its neurogenic capacity is strongly influenced by post-translational phosphorylation. During early postnatal development overexpression of a phospho-deficient mutant of Ascl1, Ascl1SA6, has been found to efficiently convert astrocytes into induced neurons (iNs), while wild-type Ascl1 enhances oligodendrocyte precursor cell (OPC) proliferation. These findings highlight potential strategies for regenerating neurons or expanding OPCs, respectively, but it is unclear whether these responses can be still elicited in the context of an adult brain injury.

In this study, I set out to examine the consequences of an inflammatory environment on the effects of Ascl1 on glial cell lineage using the adult cortical stab wound lesion model. Towards this, the reprogramming outcomes following retroviral-mediated expression of Ascl1 or Ascl1SA6 alone, or in combination with Bcl2, in reactive glia were assessed in the injured adult cortex. This milieu is characterized by inflammatory hallmarks including the presence of C3-expressing neurotoxic reactive astrocytes. In this context, Ascl1SA6 alone displayed only marginal neurogenic capacity, while co-expression of Bcl2 significantly enhanced neuronal conversion efficiency, with iNs surviving over time, despite remaining partially immature. Genetic fate-mapping revealed that iNs predominantly derived from OPCs rather than reactive astrocytes, which appeared refractory in this model. In contrast, ectopic expression of Ascl1 alone, or combined with Bcl2, promoted a robust and cell-autonomous proliferative response in OPCs following cortical injury. This proliferative effect expanded the oligodendroglial population which derived predominantly from pre-existing OPCs. Notably, Ascl1-mediated effect on OPCs was sustained in the long-term without altering their competence to undergo differentiation, as Ascl1 overexpressing OPCs gave rise to pre-myelinating and mature oligodendrocytes in the adult injured cortex.

Altogether, this study demonstrates that while the inflammatory environment of the injured adult cortex significantly constrains the efficacy of phospho-deficient Ascl1 to convert glia into neurons, wild-type Ascl1 is still capable of significantly enhancing OPC expansion. Thus, this study provides a basis for future work aimed at neuronal replacement and remyelination.

List of Abbreviations

°C	Celsius degree
AAV	Adeno-associated virus
AEP	Anterior entopeduncular area
Aldh1l1	Aldehyde dehydrogenase 1 family member L1
ANOVA	Analysis of Variance
Ascl1	Achaete-Scute complex homolog 1
ATP	Adenosine triphosphate
BAM	Brn2, Ascl1 and Myt1l
BBB	Blood Brain Barrier
BCAS1	Breast carcinoma amplified sequence 1
Bcl2	B-cell leukemia/lymphoma 2
bHLH	Basic Helix Loop Helix
BMP	Bone Morphogenetic Protein
bp	Base pairs
C1q	Complement component 1q
C3	Complement 3
CAG	Chicken β-Actin Promoter
CC1	Anti-adenomatous polyposis coli clone
CCI	Controlled cortical impact
CD45	Leucocyte common antigen

CDK	Cyclin-dependent kinase
CGE	Caudal ganglionic eminence
CNPase	2′,3′-cyclic nucleotide 3′-phosphodiesterase
CNS	Central Nervous System
DAMPS	Damage-associated molecular patterns
DAPI	4',6-diamidino-2-phenylindole
DCX	Doublecortin
DG	Dentate gyrus
Dlx2	Distal-Less Homeobox 2 gene
DMEM	Dulbecco's Modified Eagle's Medium
DMSO	Dimethyl Sulfoxide
DNA	Deoxyribonucleic acid
dpi	Days post-injection
DsRed	Discosoma red fluorescent protein
ECM	Extracellular matrix
EDTA	Ethylenediaminetetraacetic acid
EdU	5-ethynyl-2′-deoxyuridine
EGF	Epidermal growth factor
eGFP	Enhanced green fluorescent protein
ERK	Extracellular signal-regulated kinase
FBS	Fetal Bovine Serum
FGF	Fibroblast growth factor

GFAP	Glial Fibrillary Acidic Protein
GFP	Green Fluorescent Protein
h	Hours
Hes	Hairy and enhancer of split
i.p	Intra-peritoneal
Iba1	Ionized calcium-binding adapter molecule 1
IFN-γ	Interferon gamma
IL	Interleukin
iNs	Induced neurons
iPSC	Induced pluripotent stem cells
IRES	Internal ribosome entry site
kg	Kilogram
LGE	Lateral ganglionic eminence
LTR	Long Terminal Repeat
MBP	Myelin basic protein
MGE	Medial ganglionic eminence
min	Minutes
ml	Milliliter
mM	Millimolar
MMLV	Moloney Murine Leukemia Virus
MMPs	Matrix metalloproteinases
MOG	Myelin oligodendrocyte glycoprotein

MyoD	Myoblast Determination protein 1
Myrf	Myelin regulatory factor
n	Number of biological replicates
NaCl	Sodium Chloride
NeuN	Neuronal nuclei antigen
NeuroD1	Neuronal Differentiation 1
Neurog2	Neurogenin 2
NG2	Chondroitin sulfate proteoglycan
OB	Olfactory bulb
Olig2	Oligodendrocyte Transcription Factor 2
OPC	Oligodendrocyte progenitor cell
P	Postnatal day
PB	Phosphate Buffer
PBS	Phosphate Buffered Saline
PCR	Polymerase chain reaction
PDGF	Platelet-derived growth factor
PDGFRα	Platelet-Derived Growth Factor Receptor Alpha
PEI	Polyethyleneimine
PFA	Paraformaldehyde
PV	Parvalbumin
REST	RE1-silencing transcription factor
RFP	Red Fluorescent Protein

RNA	Ribonucleic acid
ROI	Region of Interest
ROS	Reactive Oxygen Species
RT	Room temperature
RV	Retrovirus
s.c	Subcutaneous
SA	Serine-Alanine
SD	Standard deviation
SGZ	Subgranular zone
Shh	Sonic hedgehog
smFISH	Single-molecule fluorescent in situ hybridization
Sox	Sex-determining region Y-box
SP	Serine-proline
SVZ	Subventricular zone
SWI	Stab-wound injury
TBI	Traumatic Brain Injury
TBS	Tris-Buffered Saline
TF	Transcription factor
TGF-β2	Transforming growth factor-beta 2
TNF-α	Tumor necrosis factor alpha
VSV-G	Vesicular stomatitis virus glycoprotein
WPRE	Woodchuck hepatitis virus posttranscriptional regulatory element

WT	Wild-type
µg	Microgram
µl	Microliter

List of figures and tables

1 Introduction

1.1 Brain injury and limited endogenous regenerative capacity

The notion that the adult central nervous system (CNS) is fundamentally restricted in its regenerative capacity was introduced over a century ago by Santiago Ramón y Cajal, who proposed that the adult brain is incapable of regenerating lost neurons (Ramón y Cajal, 1909). Although this view has since been revised following the discovery of adult neurogenesis in specific brain regions, regeneration remains limited or absent in the cerebral cortex (Alshebib et al., 2023; Jurkowski et al., 2020). Consequently, injury caused either by acute trauma or chronic neurodegeneration generally leads to irreversible neuronal loss. Unlike peripheral tissues, the adult CNS lacks efficient endogenous cell replacement mechanisms, resulting in long-lasting functional deficits (reviewed in Varadarajan et al., 2022). In contrast, lower vertebrates, such as zebrafish and axolotls, exhibit robust regenerative responses, efficiently replacing lost neurons after injury and display enhanced regenerative competence (Amamoto et al., 2016; Labusch et al., 2020).

Traumatic brain injury (TBI) is a leading cause of disability and death worldwide (Menon et al., 2010; Yan et al., 2025). TBI is characterized by focal or diffuse damage that results in extensive neuronal loss and long-term functional impairment (Ghajar, 2000). While TBI can stimulate proliferation of neural progenitors within canonical neurogenic niches, it fails to promote restoration of neuronal populations in the cerebral cortex (Chang et al., 2016; Gao & Chen, 2013). Therefore, TBI provides a clinically relevant context for examining the fundamental limitations of endogenous brain repair.

1.1.1. Traumatic brain injury: experimental models

TBI is defined as an insult or damage caused by an external mechanical force, such as impact, acceleration-deceleration or penetration by an object. TBI exhibits substantial heterogeneity based on severity, anatomical location, and temporal progression following the initial insult (Menon et al., 2010). The pathophysiology of TBI is commonly described in two phases, the primary injury, which occurs at the moment of impact and involves immediate mechanical disruption of brain tissue, blood vessels and axons. This is followed by secondary injury, a delayed cascade of molecular and cellular events that evolves over hours to days following the initial insult. Secondary injury mechanisms include excitotoxicity, inflammation, oxidative stress,

edema and progressive cell death, which increases the initial damage and represents a critical window for therapeutic intervention (Katayama et al., 1990; Povlishock & Jenkins, 1995; Shohami et al., 1994). The heterogeneity and complexity of TBI poses challenges for investigating its underlying mechanisms and cellular responses, motivating the development of experimental TBI animal models to recapitulate distinct aspects of TBI pathology and enable systematic examination of potential therapeutic strategies. Experimental models of TBI have been widely employed, as they allow the controlled manipulation of injury severity, anatomical location, and timing under defined experimental conditions, and are generally classified into diffuse or focal injury paradigms (Xiong et al., 2013).

Diffuse injury models typically result from rapid acceleration-deceleration or rotational forces, and are characterized by extensive tissue deformation without a defined lesion core, often accompanied by diffuse axonal injury. One of the earliest and more extensively used models of diffuse TBI is fluid percussion injury, which involves a brief fluid-pressure pulse to the dura, inducing transient deformation of the brain (McIntosh et al., 1989). While this model mimics injury patterns that closely resemble aspects of human TBI, and has been used to study axonal injury and secondary injury mechanisms, it has limited standardized parameters and can produce variable injury outcomes (Fesharaki-Zadeh & Datta, 2024; Povlishock & Katz, 2005).

In contrast, focal injuries result from direct impact or penetration of the skull, producing localized lesions characterized by neuronal loss and vascular disruption, enabling the investigation of cellular responses and repair mechanisms within specific cortical regions (Osier & Dixon, 2016). Common focal TBI paradigms include weight drop models, which rely on gravitational force from a falling weight to the intact dura (Feeney et al., 1981), and controlled cortical impact (CCI), in which a mechanical pistol delivers a controlled mechanical impact to the exposed cortex (Edward Dixon et al., 1991; Lighthall, 1988). The CCI model closely replicates pathological hallmarks of human cortical contusion injuries, including focal tissue loss, hemorrhage, and inflammation, and has been widely used to study underlying mechanisms of TBI for its precision and reproducibility (Fesharaki-Zadeh & Datta, 2024; Osier & Dixon, 2016).

Beyond impact-based paradigms, penetrating injury models were developed to examine the consequences of direct cortical disruption. Penetrating ballistic-like injury models recapitulate features such as intracranial hemorrhage, edema, and ischemia, but are often associated with higher mortality and experimental variability (Williams et al., 2005). To overcome these limitations, simplified penetrating injury paradigms have been developed to generate spatially confined lesions that enable high-resolution

analysis of cortical damage and glial responses. Among these, the cortical stab-wound injury (SWI) involves mechanical penetration of the cortex with a blade or needle to create a defined lesion tract (Buffo et al., 2005). SWI is commonly used to assess pathological features of human TBI, such as disruption of the dura and cortical grey matter, vascular damage, cell death, robust inflammatory responses, and reactive gliosis (Bardehle et al., 2013; Buffo et al., 2008; Cieri et al., 2023; Koupourtidou et al., 2024). Despite not accurately replicating common causes of penetrative TBI, SWI provides a simplified, reproducible model to interrogate localized cortical injury responses, explore the limitations of endogenous regeneration, and test brain repair strategies (Buffo et al., 2005; Mattugini et al., 2018).

1.1.2. Inflammatory and glial responses in the injured cortex

Cortical TBI initiates a complex and highly coordinated inflammatory response that unfolds in temporally distinct phases and involves activation of resident glial populations, together with infiltration of peripheral immune cells. While these responses are essential for wound containment and debris clearance, they also generate a hostile inflammatory environment that limits neuronal survival, regeneration and functional recovery (Russo & McGavern, 2016; Simon et al., 2017).

The primary mechanical insult causes immediate disruption of brain parenchyma, blood vessels, and axons, leading to necrotic and apoptotic cell death. Within minutes of the mechanical insult, injured cells release damage-associated molecular patterns (DAMPs), such as adenosine triphosphate (ATP) and heat shock proteins, which activate pattern recognition receptors on resident glial cells. This triggers secondary injury mechanisms characterized by neuroinflammation, glutamate excitotoxicity, cerebral edema, oxidative stress and mitochondrial dysfunction, all of which exacerbate tissue damage over hours to days following the initial insult and contribute to ongoing neuronal death (Bodnar et al., 2021; Cook et al., 2024; Gyoneva & Ransohoff, 2015).

Hallmarks of cortical TBI include disruption of the blood-brain barrier (BBB), which occur as a result of direct mechanical rupture or subsequent inflammatory signaling. This process is further exacerbated by the release of matrix metalloproteinases (MMPs) and pro-inflammatory cytokines, including interleukin 1 beta (IL-1 β), IL-6, and tumor necrosis factor alpha (TNF-α), which compromise vascular stability and tight junction integrity (Alves, 2014; Guilfoyle et al., 2015). Increased BBB permeability enables the rapid infiltration of peripheral immune cells, including monocytes, lymphocytes and neutrophils. These infiltrating immune cells

interact with resident glial cells and together secrete additional pro-inflammatory cytokines that amplify the inflammatory response and further hinder regeneration (Bodnar et al., 2021; Frik et al., 2018; Lange Canhos et al., 2021). In addition, injury induces the formation of a dense glial scar surrounding the lesion core, which comprises reactive astrocytes, oligodendrocyte precursor cells, extracellular matrix proteins, and pericyte-derived fibrotic cells that form the lesion core (Dias & Göritz, 2018). While this structure contributes to damage and inflammation containment, by isolating damaged from healthy tissue, it also represents a physical obstacle to axonal regrowth and remyelination, due in part to chondroitin sulfate proteoglycans that inhibit axonal regrowth (Cieri & Ramos, 2025).

The injury response evolves through three temporally distinct phases, each characterized by specific cellular and molecular signatures (Figure 1.1). The acute phase, occurring between the first 24 to 48 hours post-injury, is dominated by cell death, rapid activation of resident microglia, recruitment of peripheral immune cells, with peak neutrophil infiltration, and initiation of debris removal. The subacute phase, occurring between two days and three weeks after injury, is marked by robust glial proliferation and migration, peak monocyte accumulation and tissue remodeling including the progressive formation of an astrocytic scar. Finally, the chronic phase, extending beyond three weeks, is marked by stabilization of a permanent astrocytic and fibrotic scar and persistent but attenuated glial activation that may contribute to impaired functional recovery (Amlerova et al., 2024; Burda & Sofroniew, 2014).

Within the inflammatory milieu, resident glial cells adopt reactive states that are shaped by injury severity, spatial proximity to the lesion, and local signaling cues. While these responses exert protective functions, including damage containment, they also impose molecular and physical barriers that restrict regenerative outcomes in the adult cortex (Amlerova et al., 2024; Koupourtidou et al., 2024), as detailed below.

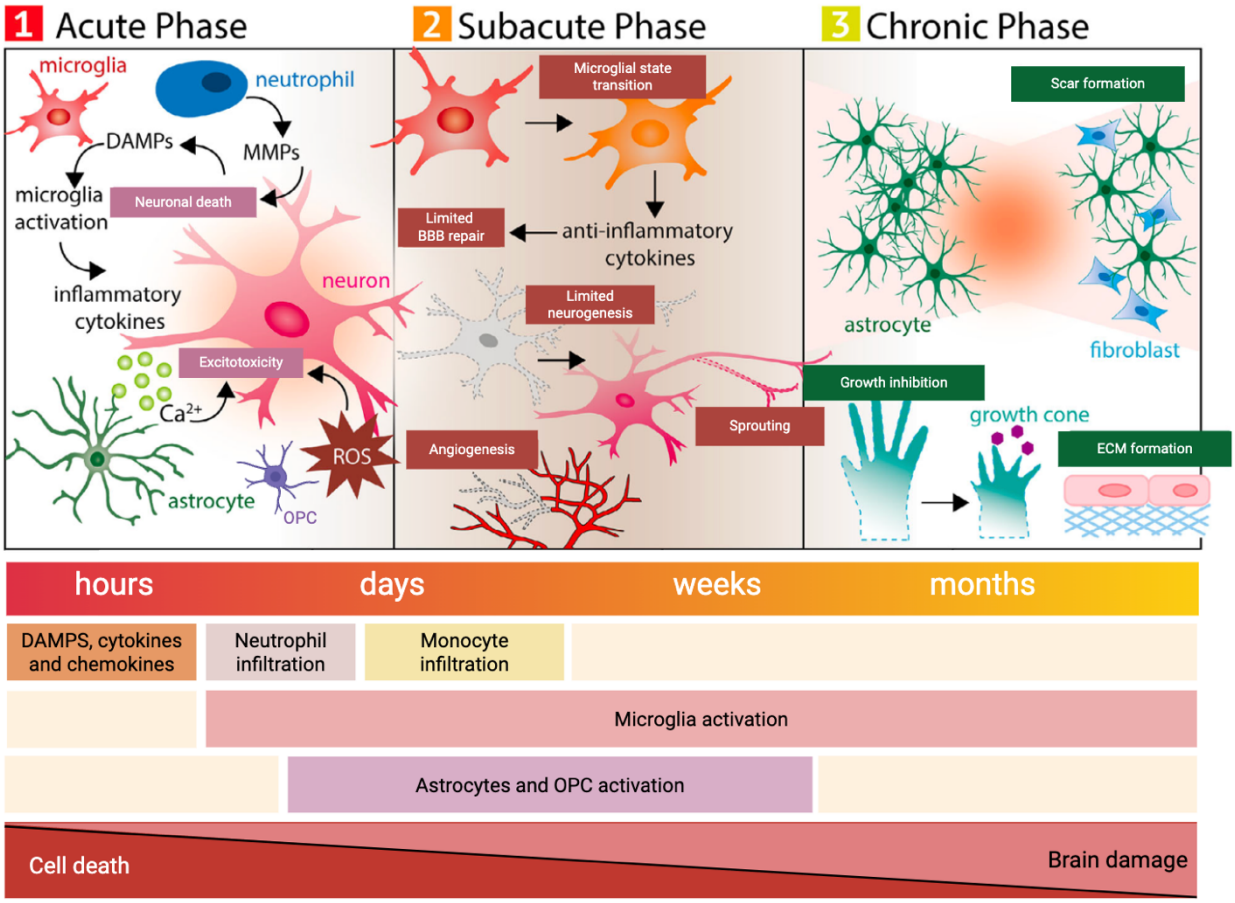

Figure 1.1: Temporal progression of inflammatory and cellular responses in TBI. TBI induces a series of cellular and molecular events that evolve across acute, subacute and chronic phases. Acute phase (hours to days) is characterized by cell death, which leads to the release of DAMPS, microglial activation and infiltration of peripheral immune cells, namely neutrophils. These events are accompanied by excitotoxicity, oxidative stress and pro-inflammatory cytokine production. During the subacute phase (days to weeks), microglia undergo reactive state transitions while reactive astrocytes and OPCs become activated and proliferate. This phase is associated with tissue remodeling processes, such as angiogenesis and limited neurogenic responses. In the chronic phase (weeks to months), glial scar formation stabilizes in the lesion environment, extracellular matrix (ECM) deposition and growth-inhibitory cues restrict axonal regeneration, while prolonged glial activation contributes to long-term functional deficits (adapted from Alam et al., 2020; Yin et al., 2025, created with Biorender).

1.1.2.1. Microglial response:

Microglia are the primary immune responders in the injured cortex and undergo morphological and transcriptional activation within hours to days of injury (Figure 1.2). Microglia transition from a ramified, surveying state to hypertrophic and

amoeboid states upon activation. This activation is initiated through recognition of DAMPs released from damaged cells, signaling via pattern recognition receptors such as Toll-like receptor 4 to activate the Nuclear Factor Kappa B (NF-κB) pathway. This induces microglia to rapidly proliferate and migrate towards the lesion site, where they participate in debris clearance through phagocytosis, modulation of the local inflammatory environment and tissue remodeling (Amlerova et al., 2024; Gyoneva & Ransohoff, 2015; Povlishock & Jenkins, 1995). In addition, activated microglia produce inflammatory mediators, such as cytokines and reactive oxygen species (ROS) that can increase BBB permeability and facilitate the recruitment of peripheral immune cells (Shigemoto-Mogami et al., 2018).

Historically, microglia activation states were simplified into M1-like (pro-inflammatory), a detrimental phenotype associated with the release of neurotoxic mediators, including pro-inflammatory cytokines, and M2-like (anti-inflammatory) phenotype, a beneficial state that promotes the release of neurotrophic factors and anti-inflammatory cytokines (Loane & Kumar, 2016). Following TBI, microglial responses unfold in temporally distinct phases, namely an early response characterized by mixed M1/M2 states with M2 state peaking around day 5 to 7 post-injury, followed by a chronic phase dominated by the M1 phenotype that can persist for months and correlates with progressive neurodegeneration (Donat et al., 2017; Loane & Kumar, 2016). However, recent transcriptomic studies reveal a far more complex spectrum of intermediate reactive states. For example, distinct microglial subclusters exhibited divergent functional signatures, including populations enriched for phagocytic or cell cycle- related genes, while others expressed inflammatory markers and show loss of homeostatic markers (Koupourtidou et al., 2024).

While acute microglial activation is essential for wound containment and clearance of damaged tissue, chronic and persistent activation is associated with secondary neuronal loss and impaired functional recovery, through excessive pruning and transcriptional suppression of neuronal pathways (Loane & Kumar, 2016). Importantly, microglia actively influence the reactivity of other glial cells, such as reactive astrocytes through cytokine and complement-mediated signaling, highlighting their central role in modulating the glial response to injury (Greenhalgh et al., 2020; Liddelow et al., 2017, 2020). In addition, activated microglia can also compromise oligodendrocyte survival and actively block oligodendrogenesis, hindering remyelination and axonal regeneration following TBI. Conversely, microglia that adopt reparative phenotypes can promote OPC differentiation and remyelination, as M2-microglia secrete activin-A, which drives oligodendrocyte differentiation during CNS repair (Miron et al., 2013). This indicates that microglia can exert both detrimental

and beneficial functions in the injured brain (Amlerova et al., 2024; Greenhalgh et al., 2020; Loane & Kumar, 2016; Miron et al., 2013; Waisman et al., 2015).

1.1.2.2. Reactive astrocyte response:

Astrocytes, the most abundant cells in the CNS, undergo extensive morphological, molecular and functional changes in response to injury, a process collectively referred to as reactive astrogliosis. This response involves morphological hypertrophy, upregulation of intermediate filament proteins such as glial fibrillary acidic protein (GFAP) and vimentin, and extensive transcriptional remodeling (Clayton & Liddelow, 2025; Escartin et al., 2021; Sofroniew, 2009).

Following cortical SWI, astrocytes near the lesion site re-enter cell cycle, with proliferation peaking within the first week post-injury (Figure 1.2). Reactive astrocytes do not migrate over long distances and instead rely on local proliferation and spatial organization to increase cell density at the lesion border (Bardehle et al., 2013; Frik et al., 2018). These astrocytes form a dense cellular border around the lesion site, often referred to as the glial scar, which physically isolates damaged tissue from the surrounding intact cortex and limits the spread of inflammatory signals and blood-derived factors (Buffo et al., 2008; Bush et al., 1999; Cieri & Ramos, 2025).

Notably, reactive astrogliosis is highly heterogenous, as distinct states emerge in a context-dependent manner. For example, astrocytes closer to the lesion display higher proliferative capacity, show robust upregulation of GFAP and vimentin compared to astrocytes located more distally, and form the glial scar (Bardehle et al., 2013; Lange Canhos et al., 2021). In addition to spatial heterogeneity, reactive astrocyte phenotypes are strongly influenced by inflammatory cues. Transcriptomic studies have identified that neurotoxic subset of reactive astrocytes emerges in inflammatory diseases and is induced by microglia-secreted cytokines, including IL-1α, TNF-α and complement component 1q (C1q). These neurotoxic reactive astrocytes are characterized by upregulation of complement 3 (C3) and loss of homeostatic functions, such as trophic support, and secrete a lipid-based factor that promotes neuronal and oligodendroglial death (Guttenplan et al., 2020; Liddelow et al., 2017). While initially described in neuroinflammatory and neurodegenerative contexts, C3-expressing neurotoxic reactive astrocytes have also been detected following traumatic brain injury, indicating that similar inflammatory programs are activated (Cieri et al., 2023; Clark et al., 2019; Yamashita et al., 2025).

Despite the emergence of detrimental reactive states, astrocytes are required for wound stabilization, BBB repair and containment of inflammatory signaling. Genetic and pharmacological ablation of proliferating astrocytes after focal injury increased the

injury size and exacerbated neuronal loss (Bush et al., 1999; Faulkner et al., 2004). Thus, astrocytic responses after cortical injury exert both protective and detrimental effects, with functional outcomes being shaped by inflammatory signals or cellular interactions in the injury milieu (Burda & Sofroniew, 2014; Escartin et al., 2021; Zamanian et al., 2012).

1.1.2.3. Oligodendroglial response:

Oligodendrocytes are highly sensitive to the secondary damage initiated after TBI. Mature, myelinating oligodendrocytes are particularly vulnerable to oxidative stress, excitotoxicity and pro-inflammatory cytokines, which frequently result in widespread apoptosis following the initial insult (Mira et al., 2021). This loss contributes to widespread demyelination and impaired axonal conduction (Amlerova et al., 2024; Huntemer-Silveira et al., 2021).

In response to this damage, resident oligodendrocyte precursor cells (OPCs) undergo activation, characterized by morphological hypertrophy and a dramatic increase in proliferation, positioning them as a major reactive cell population in the injured cortex. Following focal injury, OPCs migrate towards the injury site, rapidly re-enter cell cycle and expand their number within days after injury (Figure 1.2). This proliferative response typically peaks around 2 to 4 days post-injury and persists for several weeks (Franklin & ffrench-Constant, 2008; Hughes et al., 2013; Simon et al., 2011). Moreover, OPC proliferation is spatially restricted to regions surrounding the lesion and is likely coordinated by injury-induced signals including platelet-derived growth factor (PDGF), fibroblast growth factor 2 (FGF2), and cytokines released by damaged tissue and reactive glia (Dimou & Gallo, 2015). While this proliferative response represents an endogenous attempt at remyelination, with some OPCs differentiating into myelinating oligodendrocytes, recent work has demonstrated that myelin repair occurs primarily through constitutive differentiation of OPCs rather than injury-mediated induction, with differentiation attempts remaining relatively constant regardless of oligodendrocyte loss or extent of demyelination (Mironova et al., 2026). However, the injury-induced inflammatory environment can limit OPC differentiation competence and subsequent remyelination, as inflammatory signals can arrest OPCs in a progenitor state or promote reactive phenotypes that contribute to glial scar formation rather than remyelination (Keirstead et al., 1998; Levine et al., 2001; Mironova et al., 2026).

Similarly to reactive astrocytes and microglia, OPC responses are also spatially heterogeneous. OPCs closer to the injury site display transcriptional states that are distinct from those located more distally from the lesion site, showing altered

expression of genes involved in cell cycle regulation, metabolism and stress responses (Koupourtidou et al., 2024). Moreover, while after grey matter injury, such as cortical SWI, OPCs proliferate robustly but show limited differentiation capacity, after white matter injury, OPC proliferation and differentiation contributes to remyelination (Dean et al., 2023; Dimou & Götz, 2014; Mattugini et al., 2018).

Beyond their role as oligodendrocyte precursors, OPCs contribute to wound closure, actively interact with other glial populations and contribute to the inflammatory milieu (Dean et al., 2023). OPCs express cytokine receptors and respond to inflammatory cues from microglia and astrocytes, which modulate their proliferative response and differentiation potential. For example, microglial-derived TNFα and IL-1β can arrest OPC differentiation, while OPC-derived transforming growth factor-beta 2 (TGF-β2) can regulate microglial activation states (Dean et al., 2023; Greenhalgh et al., 2020; Peferoen et al., 2014).

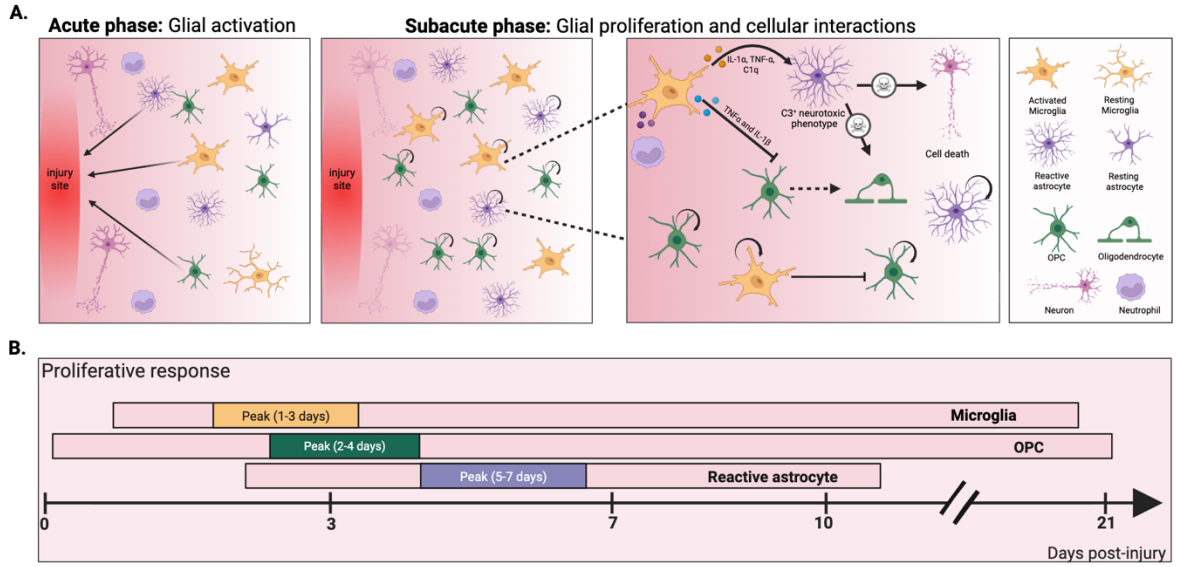

Figure 1.2: Glial responses in acute and subacute phases after TBI. A. During the acute phase, microglia, astrocytes, and OPCs become activated and migrate toward the lesion site. During the subacute phase, glial cells undergo robust proliferation, with OPCs representing a major proliferative population. Activated microglia secrete pro-inflammatory cytokines (IL-1α, TNF-α, C1q), which can induce reactive astrocytes to acquire a C3-expressing neurotoxic phenotype, promoting neuronal and oligodendroglial death and inhibiting OPC differentiation into oligodendrocytes. **B.** Timeline of glial proliferative responses following TBI, showing peak proliferation for microglia (1-3 days post-injury), OPCs (2-4 days post-injury), and reactive astrocytes (5-7 days post-injury). Adapted from Amlerova et al., (2024), created with Biorender (Bardehle et al., 2013; Hughes et al., 2013; Liddelow et al., 2017).

1.1.3. Limited intrinsic regeneration and plasticity in the adult CNS

The long-standing view that the adult mammalian brain is incapable of generating new neurons was first challenged over 50 years ago, following reports of ongoing neurogenesis in the adult rat brain and postnatal hippocampal dentate gyrus (Altman, 1962; Altman & Das, 1965). Despite these early reports, adult neurogenesis was not widely accepted for several decades and thought to be restricted to embryonic development. This view was later revised following evidence of adult neurogenesis in songbirds (Goldman & Nottebohm, 1983), mammals (Kuhn et al., 1996; Reynolds & Weiss, 1992), and humans (Eriksson et al., 1998).

In the adult mammalian brain, constitutive neurogenesis is largely restricted to two brain regions, the subventricular zone (SVZ) lining the lateral ventricles, and the subgranular zone (SGZ) of the hippocampal dentate gyrus (DG; Bonaguidi et al., 2012; Gage et al., 1995; Palmer et al., 1997; Reynolds & Weiss, 1992). In the DG, neural stem cells undergo asymmetric division, generate neuroblasts that migrate into the granule layer, differentiate into glutamatergic granule neurons, and functionally integrate into hippocampal circuits (Kempermann & Kronenberg, 2003). In the SVZ, neural stem cells give rise to neuroblasts that migrate tangentially along the rostral migratory stream toward the olfactory bulb (OB), differentiate predominantly into GABAergic granule cells and integrate into OB circuits (Lois & Alvarez-Buylla, 1994; Ponti et al., 2013). Neurons generated in these regions contribute to specific forms of plasticity, including odor discrimination (Breton-Provencher et al., 2009), spatial/temporal pattern separation, and consolidation of explicit memories (Aimone et al., 2011; Jurkowski et al., 2020; Koehl & Abrous, 2011). In the cortex, the generation of new neurons under physiological conditions is either absent or occurs at extremely low levels that remain controversial (Bhardwaj et al., 2006; La Rosa et al., 2020; Magavi et al., 2000). Additional brain regions have been reported to contain newly generated neurons beyond early development, including the hypothalamus, amygdala, striatum, substantia nigra and cortex (Bernier et al., 2002; Evans et al., 2002; Magavi et al., 2000; Parent et al., 1995; M. Zhao et al., 2003).

Following injury in the adult mammalian brain, proliferation of neural precursors in the DG and SVZ is increased and neuroblasts can migrate toward the injured brain regions such as the striatum, cortex or hippocampus (Arvidsson et al., 2002; Dash et al., 2001; T. Yamashita et al., 2006). While integration into striatum and hippocampal circuits has been reported, adult neurogenesis remains largely insufficient to promote regeneration and instead can contribute to maladaptive outcomes such as hyperexcitability and epilepsy-like states (Butler et al., 2015; Neuberger et al., 2017; Aguilar-Arredondo & Zepeda, 2018). In the cortex, neuronal

regeneration is further constrained by the scarcity of neuronal progenitors (Bhardwaj et al., 2006) and limited neuroblast migration from neurogenic niches (Ohab & Carmichael, 2008), which also undergo ageing-mediated decline in stem cell competence (Obernier & Alvarez-Buylla, 2019). Moreover, the injury environment is actively adverse to neuronal differentiation, with gliogenic transcription factors, such as Olig2, being upregulated, and signaling pathways including the Notch pathway, being activated, both of which suppress neurogenesis (Buffo et al., 2005; Magnusson et al., 2014). Lastly, pro-inflammatory cytokines secreted by reactive glia and infiltrating immune cells inhibit neuronal differentiation from neural precursor cells, while the glial scar prevents the migration and integration of any newly generated neurons (Loane & Kumar, 2016).

In parallel to neuronal loss, brain injury also results in oligodendrocyte death and axonal damage which contribute to demyelination and impaired signal conduction in surviving circuits (Armstrong et al., 2016; Dent et al., 2015). Although the adult brain possesses endogenous capacity for remyelination through differentiation of OPCs into mature myelinating oligodendrocytes, remyelination is often incomplete, particularly under chronic inflammatory conditions that hinder OPC differentiation (Dimou et al., 2008; Kang et al., 2010).

Despite the lack of effective neuronal regeneration, injury induces plasticity in resident glial populations. Among these populations, reactive astrocytes can harbor latent neurogenic programs after injury (Magnusson et al., 2014; Nato et al., 2015). In the injured striatum and cortex, reactive astrocytes were shown to generate proliferative progenitors that can give rise to neuroblasts and, at low frequency, neurons, particularly under conditions of reduced Notch signaling (Magnusson et al., 2014, 2020). Furthermore, astrocytes that initiate neurogenesis become transcriptionally similar to SVZ neural stem cells and progress through a similar neuronal program. Nevertheless, this contribution is limited, as only a minority of Notch-depleted astrocytes can complete the full neurogenic trajectory (Magnusson et al., 2020). Furthermore, reactive astrocytes can reactivate stem cell-like properties, including self-renewal capacity and multipotent differentiation *in vitro*, but *in vivo*, they predominantly remain within the astrocytic lineage and do not spontaneously generate neurons (Götz et al., 2015; Sirko et al., 2013). Notably, injury-specific factors in human cerebrospinal fluid regulate astrocyte plasticity and neurogenic capacity, suggesting that the injury milieu contains signals that could be harnessed to enhance endogenous regeneration (Sirko et al., 2023). Recent work has also demonstrated that after excitotoxic injury, striatal astrocytes can be focally recruited into a neurogenic program at the lesion border, where their continuous, stochastic activation sustains

neurogenesis over extended periods of time after injury (Fogli et al., 2024). However, while these findings demonstrate that astrocytes possess neurogenic competence that can be activated under specific conditions, the injury-induced environment simultaneously reinforces gliogenic programs that limit spontaneous neuronal differentiation (Loane & Kumar, 2016). Therefore, astrocytes represent a population with significant neurogenic potential that is endogenously activated after injury in a context-dependent manner but that remains largely ineffective.

OPCs also display context-dependent lineage plasticity following CNS injury. Beyond their role in remyelination, OPCs can, to a limited extent, generate astrocytes, contributing to glial scar formation in specific injury contexts (Dimou et al., 2008; Hackett et al., 2018; Huang et al., 2021; Kirdajova et al., 2021). This astrocytic differentiation is more pronounced in severe injuries, such as contusive spinal cord injury and permanent ischemia, and is strongly influenced by local inflammatory cues and extracellular matrix signals (Hackett et al., 2018; Huang et al., 2021; Kirdajova et al., 2021). However, OPC-derived astrocytes represent only a minor fraction of the astrocytic population, and their functional contribution remains unclear. In contrast to astrocytes, evidence of spontaneous neuronal differentiation remains limited, as OPCs only exhibit multipotent characteristics *in vitro* and endogenous neuronal conversion is rarely observed after injury (Dimou & Gallo, 2015; Kang et al., 2010; Richardson et al., 2011). Thus, OPCs exhibit a robust but biased form of endogenous plasticity after CNS injury, characterized by pronounced proliferation, partial remyelination, limited astrocytic differentiation and minimal spontaneous neurogenesis.

Altogether, while the adult mammalian brain mounts endogenous neurogenic and remyelinating responses following injury, these processes are spatially restricted and insufficient to restore function. Importantly, the activation of latent plasticity in resident glial populations suggests that failed regeneration reflects regulatory constraints imposed by the injury environment, rather than a lack of responsive cellular substrates. These observations have prompted the development of strategies aimed at enhancing brain repair, including attempts to stimulate endogenous neurogenesis, remyelination and replacement of lost cells.

1.2 Cell replacement strategies for CNS repair: direct lineage reprogramming

Cell replacement strategies have been extensively explored to overcome the limited intrinsic regenerative capacity of the adult CNS. These approaches aim to restore lost neuronal populations and re-establish functional neural circuits by supplying new neurons or glial cells from exogenous sources, or by promoting endogenous generation of new neural cells within the injured or diseased CNS (Götz & Bocchi, 2021).

Early efforts in neural repair focused predominantly on transplantation-based approaches, including grafting of fetal neural tissue. Pioneering clinical studies in Parkinson's disease, demonstrated that fetal dopaminergic neurons could be successfully transplanted into the striatum and partially ameliorated motor symptoms, providing proof-of-principle that neuronal replacement in the adult human brain is achievable (Lindvall et al., 1992; Spencer et al., 1992). However, fetal tissue transplantation faced substantial limitations including ethical concerns, limited tissue availability, heterogeneity of graft composition, and the occurrence of graft-induced dyskinesias in a subset of patients (Björklund et al., 2003; Freed et al., 2001; Olanow et al., 2003). Subsequent approaches shifted toward embryonic stem cell-derived neurons and induced pluripotent stem cells (iPSC)-derived neural populations, which enabled cells expansion *in vitro* and improved control over cell identity. Autologous iPSC-based approaches further reduced ethical concerns and minimized immune rejection risks (Kriks et al., 2011; Lindvall & Kokaia, 2010). More recently, clinical studies have reported survival and phenotypic stability of transplanted iPSC-derived dopaminergic neurons in patients with Parkinson's disease, with modest but encouraging functional improvements (Sawamoto et al., 2025; Schweitzer et al., 2020). Beyond neuronal replacement, transplantation approaches have also been explored for remyelination. Transplanted OPCs and glial progenitors can differentiate into myelinating oligodendrocytes, restore myelin sheaths and improve axonal conduction in experimental models of demyelination and spinal cord injury (Kawabata et al., 2016; Keirstead et al., 1998; Salewski et al., 2015; Wang et al., 2013). However, clinical translation remains challenging due to the injury milieu which constrains OPC differentiation, and promotes graft survival variability (Assinck et al., 2017; Huntemer-Silveira et al., 2021).

Despite these advances, cell transplantation approaches have not yet achieved consistent, long-term functional recovery across CNS disorders. Major challenges include limited survival of grafted cells, incomplete integration into existing neural circuits, risk of tumorigenesis, and variability in clinical outcomes (Lindvall & Kokaia, 2010; Trounson & McDonald, 2015). These limitations have motivated the

development of alternative strategies aimed at generating new neurons or glial cells *in situ*, from endogenous cellular substrates within the injured CNS.

1.2.1 Historical perspective: direct lineage reprogramming

Cell fate, once established, was believed to be constant and irreversible as illustrated by Waddington's epigenetic landscape model. This model depicted cellular differentiation as a marble rolling downhill through branching valleys and ending in one of many valleys surrounded by high hills representing the epigenetic barriers that prevented cells from transitioning between established fates (Waddington, 1957). According to this model, differentiation of pluripotent cells happens through irreversible fate choices, with differentiated cells thought to be locked into stable terminal identities (Amamoto & Arlotta, 2014; Waddington, 1957). This deterministic view of cell fate was first challenged by somatic cell nuclear transfer experiments, which demonstrated that nuclei from differentiated intestinal cells of tadpoles, when transferred into unnucleated eggs, could generate adult frogs (Gurdon, 1962). This groundbreaking work demonstrated that differentiated cells could revert back to pluripotent states. Subsequent work discovered that cell identity could also be altered through the forced expression of lineage-specific transcription factors. Namely, MyoD expression was shown to convert mouse fibroblasts into functional myoblasts, providing the first evidence that cell fate could be reprogrammed across lineages without passing through a pluripotent state (Davis et al., 1987). This discovery established transcription factor-mediated direct lineage conversion and established the concept of "master regulator" transcription factors capable of dictating cell identity.

The field was further advanced by Takahashi and Yamanaka's demonstration that ectopic expression of the transcription factors Oct3/4, Sox2, c-Myc and Klf4 could successfully reprogram adult mouse fibroblasts into iPSCs (Takahashi & Yamanaka, 2006). While iPSCs provided a powerful tool for cell replacement and disease modeling, they also raised concerns including tumorigenic risk, prolonged differentiation protocols, and limited suitability for direct *in vivo* use (Yasuhara et al., 2020). This prompted renewed interest in direct lineage reprogramming or trans-differentiation, whereby a differentiated cell is directly converted into another without reversion to pluripotency, bypassing the risk of tumorigenesis and enabling potential *in situ* fate conversion (Vasan et al., 2021). These advances laid the groundwork for subsequent studies demonstrating the direct conversion of fibroblasts and glial cells into induced neurons (iNs), establishing direct neuronal reprogramming as a promising cell-replacement strategy for CNS repair (Amamoto & Arlotta, 2014).

1.2.2 In vitro direct neuronal reprogramming

Following the establishment of direct lineage reprogramming as an alternative to pluripotency-based approaches, multiple studies demonstrated that neuronal identity can be induced *in vitro* from differentiated somatic cells through forced expression of lineage-instructive transcription factors. These factors were primarily selected based on their roles during embryonic neurogenesis, including their ability to activate neuronal gene programs and, in some cases, access closed chromatin to initiate fate conversion (Amamoto & Arlotta, 2014; Mircea & Semrau, 2021; Vierbuchen et al., 2010).

Early *in vitro* reprogramming studies focused on neural lineage-derived cells, such as astrocytes or OPCs, based on the assumption that cells developmentally closer to neurons would be more permissive to neuronal conversion. Consistent with this view, initial work demonstrated that ectopic expression of the transcription factor Pax6 could induce neuronal features in postnatal glial cells, providing a proof-of-principle that differentiated glial cells retain latent neurogenic competence and can be reprogramming *in vitro* (Heins et al., 2002). Subsequent studies identified proneural basic helix-loop-helix (bHLH) transcription factors as more efficient drivers of neuronal conversion. In particular, Neurogenin 2 (Neurog2) and Achaete-scute homolog 1 (Ascl1) were shown to reprogram postnatal cortical astrocytes into functional iNs that displayed electrophysiological properties and synaptic connectivity (Heinrich et al., 2010). Notably, Neurog2 preferentially instructed a glutamatergic-like fate, while Ascl1 together with Dlx2 generated GABAergic-like iNs (Berninger et al., 2007; Heinrich et al., 2010). These findings demonstrated that proneural factors can impose subtype-specific neuronal programs on glial cells, consistent with their respective roles in neuronal development (Bertrand et al., 2002), and highlighted that the acquisition of functional properties was context-dependent. Subsequent studies expanded these findings by demonstrating that neuronal subtype specification could be further advanced through the use of alternative transcription factors. For example, NeuroD1 was shown to convert postnatal astrocytes and OPCs into functional glutamatergic-like or GABAergic-like iNs, depending on the cellular context (Guo et al., 2014). In addition, combinatorial expression of Ascl1 with Nurr1 and Lmx1a enabled the conversion of postnatal astrocytes into dopaminergic-like iNs, highlighting the capacity to impose subtype-specific neuronal identities through transcription factor cooperation (Addis et al., 2011).

A major conceptual advance in the field occurred with the demonstration that somatic cells lacking shared developmental origin with neurons could undergo neuronal

reprogramming. Mouse fibroblasts were directly converted into iNs through the combined expression of Ascl1, Brn2 and Myt1l, referred to as BAM factors, and these iNs displayed functional properties, with most acquiring a glutamatergic fate (Vierbuchen et al., 2010). Mechanistically, Ascl1 was shown to act as a pioneer transcription factor, capable of binding to and opening closed chromatin at neuronal loci, facilitating the recruitment of Brn2 to activate neuronal gene expression, while Myt1l contributed to repression of non-neuronal programs (Wapinski et al., 2013). Importantly, subtype specification could also be achieved in fibroblast-derived iNs, as co-expression of Ascl1 with Nurr1 and Lmx1a, or BAM factors together with Lmx1a, Lmx1b, Nurr1 and Pitx3, enabled the generation of dopaminergic-like iNs (Caiazzo et al., 2011; Kim et al., 2011). These findings highlighted the dual role of proneural factors in initiating neuronal programs and enabling subtype specification through cooperation with additional transcriptional networks. Furthermore, these studies demonstrated that neuronal identity could be imposed across germ-layer boundaries and, from a translational point of view, iNs could potentially be derived from accessible dermal cells.

Despite neuronal conversion having been achieved in non-neuronal cells with distinct developmental origins, its efficiency and outcome depend strongly on the epigenetic and transcriptional state of the starting cell population. In astrocytes, repression of neuronal gene expression by factors such as RE1-silencing transcription factor (REST) was shown to limit conversion efficiency, and removal of these repressive barriers significantly enhanced Neurog2-mediated reprogramming (Masserdotti et al., 2015). Moreover, fibroblasts generally require multiple transcription factors to achieve neuronal conversion, while astrocytes and OPCs are more permissive and can undergo neuronal reprogramming following expression of a single proneural factor, in most contexts (Guo et al., 2014; Heinrich et al., 2010; Vierbuchen et al., 2010). Genome-wide studies further revealed that the pioneer activity of factors such as Ascl1 is highly context-dependent, with chromatin binding patterns differing between fibroblasts and astrocytes, emphasizing the importance of the starter cell population in shaping reprogramming trajectories (Aydin et al., 2019).

For clinical translation, neuronal reprogramming must ultimately be achievable in human cells. Human fibroblasts were shown to successfully convert into iNs, although they displayed increased resistance to reprogramming and required additional factors such as NeuroD1 or Neurog2, compared to mouse fibroblasts (Son et al., 2011). Strikingly, human pericytes isolated from the adult cerebral cortex could also be reprogrammed into iNs through co-expression of Ascl1 and Sox2. While pericyte-to-neuron conversion proceeded through a transient neural stem cell-like intermediate

state, these findings provided the first evidence that the adult human brain harbors cell populations amenable to fate conversion (Karow et al., 2012, 2018). Human astrocytes were also shown to be amenable to neuronal reprogramming through ectopic expression of NeuroD1 or NeuroD4 alone, with iNs also displaying functional properties (Guo et al., 2014; Masserdotti et al., 2015). Furthermore, subtype-specification has been achieved in human astrocyte-derived iNs, as combinatorial expression of NeuroD1, Ascl1 and Lmx1a together with small molecules and microRNA miR218, promoted dopaminergic features in models of Parkinson's disease (Rivetti Di Val Cervo et al., 2017), and NeuroD4 and Insm1 generated glutamatergic-like iNs (Masserdotti et al., 2015), further demonstrating the potential of this approach for clinical application. Despite these advances, human-derived iNs typically exhibit slower maturation, increased heterogeneity and reduced survival compared to mouse-derived iNs, highlighting species-specific constraints on reprogramming efficiency (Vierbuchen & Wernig, 2012).

Altogether, *in vitro* neuronal reprogramming studies have established that both mouse and human non-neuronal cells can be converted into iNs through defined transcriptional programs. These studies have provided critical insights into the mechanisms underlying fate conversion, the generation of subtype-specific iNs, and the maturation and functional properties of these cells in highly controlled experimental settings.

1.2.3 In vivo direct neuronal reprogramming

While *in vitro* systems have elucidated some of the mechanisms underlying neuronal fate conversion, they fail to recapitulate key features of the injured or diseased CNS, including inflammation, tissue remodeling, and reactive gliosis. These context-dependent factors strongly influence endogenous repair processes, thereby motivating the investigation of direct neuronal reprogramming strategies *in vivo* to determine whether fate conversion can occur within complex environments and pathological conditions (Bocchi et al., 2022; Gascón et al., 2017).

Early *in vivo* neuronal reprogramming efforts focused on resident glial cells, particularly astrocytes and OPCs, given their efficient conversion *in vitro*, their abundance, local availability, and amenability to viral targeting. Since glial cells have also been implicated in maladaptive processes after injury, their conversion offered a dual benefit of neuronal replacement and partial depletion of cellular populations that hinder regeneration (Dimou & Götz, 2014; Gascón et al., 2017). Initial proof-of-principle studies demonstrated that glia-to-neuron conversion could be achieved in the

adult mammalian brain. Inhibition of Olig2 or induction of Pax6 expression in proliferating cells following cortical stab-wound injury promoted the appearance of immature, doublecortin (DCX)-expressing cells in the adult mouse cortex (Buffo et al., 2005). Subsequently, retroviral-mediated expression of Neurog2, and growth factors EGF and FGF2, was shown to induce DCX-positive cells in the injured neocortex, whereas Ascl1 alone was shown ineffective under similar conditions (Grande et al., 2013).

The cellular origin of iNs *in vivo* was next clarified using genetic fate-mapping approaches. Heinrich et al., (2014) demonstrated that OPCs could acquire neuronal features following ectopic expression of Sox2 alone or with Ascl1 after cortical injury, although most iNs remained immature. Using promoter-restricted constructs, Guo et al., (2014) reported that NeuroD1 expression converted reactive astrocytes and OPCs into iNs displaying mature features, such as NeuN expression and electrophysiological properties in both cortical injury and Alzheimer's disease models, providing the first evidence that glia-to-neuron conversion could be achieved in the context of neurodegeneration. Beyond the lesioned cortex, this approach was also induced in the intact or injured adult striatum, with astrocytes or reactive glia undergoing neuronal conversion following ectopic expression of BAM factors, Sox2, or Neurog2 and growth factors (Grande et al., 2013; Torper et al., 2013). While astrocytes and OPCs represent the main cellular substrates for *in vivo* neuronal conversion, microglia-to-neuron conversion was also reported through NeuroD1 expression in the adult striatum, giving rise to mature and functional iNs (Matsuda et al., 2019). Together, these studies demonstrated that the adult mammalian CNS harbors glial populations susceptible to neuronal reprogramming, capable of generating induced cells that exhibit neuronal morphology, express mature neuronal markers and acquire electrophysiological properties consistent with functional neurons (Bocchi et al., 2022).

Despite these achievements, reprogramming efficiency and survival of iNs *in vivo* were markedly lower than *in vitro*. A key mechanistic constraint was identified by Gascón et al., (2016), who demonstrated that the transition from anaerobic glycolytic glial metabolism to neuronal oxidative metabolism triggered excessive ROS production and promoted ferroptotic cell death. Notably, co-expression with the pro-survival factor Bcl2 substantially improved iNs survival, and further supplementation with antioxidants such as calcitriol or α-Tocopherol, promoted and accelerated neuronal differentiation and maturation (Gascón et al., 2016). This study demonstrated that successful *in vivo* neuronal conversion requires not only the activation of neuronal programs but overcoming environmentally imposed metabolic constraints.

Besides neuronal conversion efficiency, the challenge of neuronal subtype specification was also addressed *in vivo*. While initial studies predominantly generated glutamatergic-like iNs, reflecting default programs induced by factors such as NeuroD1 and Neurog2 (Gascón et al., 2016; Guo et al., 2014), combinatorial approaches enabled the generation of broader subtype outcomes. Ascl1, Lmx1a and Nurr1 generated parvalbumin interneuron-like iNs from OPCs in the adult striatum (Pereira et al., 2017), while NeuroD1, Ascl1, Lmx1a and miR218 induced dopaminergic-like iNs from striatal reactive astrocytes in a model of Parkinson's disease (Rivetti Di Val Cervo et al., 2017). Similarly to findings *in vitro*, the subtype-specification of iNs was shown to depend on the reprogramming factors used. Mattugini et al., (2019) demonstrated that Neurog2 and Nurr1 generated pyramidal-like iNs from cortical astrocytes following injury, while Lentini et al. (2021) showed that retroviral-mediated Ascl1 and Dlx2 co-expression converted hippocampal reactive glia into interneuron-like iNs in a model of epilepsy. These studies demonstrated that subtype specification is achievable *in vivo* and that it can be influenced by reprogramming factor choice.

A consistent observation across *in vivo* studies is that reprogramming competence and subtype-specification depends on both the reprogramming factors and the cellular and regional identity of starting glial population. For example, striatal glial cells are more permissive to neuronal reprogramming than cortical glial cells (Grande et al., 2013; Torper et al., 2015). Moreover, while cortical reactive astrocytes give rise to glutamatergic-like iNs, OPCs give rise to both GABAergic and glutamatergic-like iNs following NeuroD1 overexpression in the injured cortex (Guo et al., 2014). Similarly, Sox2-mediated reprogramming generated GABAergic-like iNs in the striatum, but glutamatergic-like iNs in the adult spinal cord (Niu et al., 2015; Wang et al., 2016). In line with this, transcriptomic and epigenomic studies have revealed that induced neurons often retain molecular signatures of their glial origin, which may influence their differentiation and maturation (Carter et al., 2020; Herrero-Navarro et al., 2021; Stricker & Götz, 2021).

Despite these achievements, the field has faced significant controversy regarding the authenticity of *in vivo* glia-to-neuron conversion. Initially, this approach relied on retroviral and lentiviral-mediated approaches to induce expression of reprogramming factors *in vivo*, but these viral vectors were associated with immunoreactivity and exacerbation of injury-induced inflammation (Mattugini et al., 2019). As an alternative, adeno-associated viruses (AAVs) were investigated as delivery method to induce neuronal reprogramming, given their increased safety, low immunogenicity, and common use in clinical studies (Mattugini et al., 2019; Wang et al., 2024). Moreover, AAVs can transduce both mitotic and post-mitotic cells, bypassing the need for prior

injury-induced proliferation, and were rapidly adopted as a favored viral delivery method. Several studies using AAVs reported efficient astrocyte-to-neuron conversion with remarkable regional specificity, improved functional properties and functional integration, predominantly in injury or diseased models (Chen et al., 2020; Liu et al., 2021; Liu et al., 2015; Mattugini et al., 2019; Qian et al., 2020; Zhang et al., 2020). Moreover, studies also reported that neuronal reprogramming improved functional outcomes across different pathological contexts (Chen et al., 2020; Kim et al., 2024; Qian et al., 2020). However, Wang et al., (2021) challenged these findings using lineage-tracing strategies, demonstrating that NeuroD1-mediated iNs could not be traced to astrocytes, suggesting that presumed iNs were endogenous neurons that had been mis-labelled due to promoter leakiness or viral artifacts. Similarly, claims of NeuroD1-mediated microglia-to-neuron conversion have been challenge as evidence of that NeuroD1 induces microglial apoptosis rather than neuronal conversion (Rao et al., 2021). In contrast, retroviral approaches, which enable specific transduction of dividing cells, provided strong evidence of authentic glia-to-neuron conversion by excluding labeling of pre-existing neurons (Gascón et al., 2016; Guo et al., 2014; Heinrich et al., 2014; Lentini et al., 2021; Marichal et al., 2024; Yamashita et al., 2019). Altogether, these studies highlighted the need to use appropriate controls, assess maturation progression and apply rigorous lineage-tracing methods to ensure lineage fidelity in neuronal conversion (Bocchi et al., 2022; Wang et al., 2021; Xie et al., 2023).

Recently, non-viral approaches have been also explored as potential alternatives for inducing neuronal reprogramming *in vivo,* motivated by concerns regarding genomic integration, immunogenicity, and target specificity. Small-molecule cocktails capable of modulating chromatin state and key developmental signaling pathways were shown to induce astrocyte-to-neuron conversion following local delivery in the striatum and injured spinal cord (Ma et al., 2021; Tan et al., 2024). In parallel, antisense oligonucleotide-based strategies targeting post-transcriptional regulators of cell identity, such as PTBP1, have been reported to induce neuronal features in hippocampal GFAP-expressing cells after delivery into the cerebral spinal fluid (Maimon et al., 2021). However, similarly to AAV-based approaches, these methods have faced substantial challenges regarding the authenticity of neuronal conversion (Xie et al., 2023). Beyond pharmacological approaches, transgenic mouse models have provided valuable tools for investigating reprogramming mechanisms while avoiding viral delivery artifacts. Transgenic approaches have demonstrated that combined inhibition of Notch signaling and nuclear factor I factors enables robust reprogramming of Müller glia into retinal-like neurons in the adult mammalian retina (Le et al., 2024), and that developmental transcription factors, including Ascl1, Islet1 and Pou4f2, can reprogram Müller glia into functional retinal ganglion-like cells (Todd et al., 2022).

Similarly, a recent transgenic model demonstrated that in the injured cortex and injured spinal cord, NeuroD1 expression induced astrocyte-to-neuron conversion, with cells transitioning through an intermediate phase, though iNs lacked functional maturity (Chen et al., 2025). Thus, while non-viral strategies offer conceptual and translational potential, their mechanisms, efficacy, lineage authenticity, and the functional maturation capacity of resulting iNs require further exploration.

In summary, neuronal reprogramming progressed from initial proof-of-principle demonstrations to more sophisticated attempts at subtype specification and functional integration within the adult CNS. However, major challenges remain, including limited long-term survival, guaranteeing lineage authenticity, ongoing uncertainty regarding lineage authenticity, particularly with AAV-based approaches, integration of reprogrammed neurons, and ensuring appropriate subtype specification for the targeted pathology. Addressing these challenges will be essential for translating direct neuronal reprogramming into therapeutic strategies for CNS repair.

1.2.4 Hurdles and constraints in the injured brain

The efficiency of *in vivo* neuronal reprogramming is generally limited compared to *in vitro*, not only due to an inability to activate neuronal programs, but also to environmental constraints that transcription factor expression alone may not fully overcome (Gascón et al., 2017). Accordingly, *in vivo* reprogramming outcomes remain variable, particularly in the injured brain (Vignoles et al., 2019). Brain injury is typically accompanied by reactive gliosis, inflammation, tissue remodeling and oxidative stress, which extensively shape the local cellular environment (Burda & Sofroniew, 2014). The magnitude of these responses, as well as the phenotype of reactive glial cells that emerge, varies based on injury type and severity, contributing to distinct reprogramming outcomes (Vignoles et al., 2019; Zamanian et al., 2012). Notably, injury appears necessary to induce reprogramming of specific glial populations, such as OPCs, yet more severe or invasive injuries can limit neuronal conversion and iNs maturation (Chen et al., 2025; Guo et al., 2014; Heinrich et al., 2014). In addition, injury imposes substantial metabolic challenges during the transition from a glial to neuronal identity, rendering iNs more vulnerable to oxidative stress and ferroptosis (Gascón et al., 2016, 2017).

Neuroinflammatory signaling further exerts complex and time-dependent effects on neuronal reprogramming. While pro-inflammatory factors released by peripheral immune cells and resident microglia may transiently increase cellular plasticity, with studies reporting increased conversion efficiency in the injured cortex and striatum, compared to uninjured conditions (Grande et al., 2013; Heinrich et al., 2014; Niu et

al., 2013), sustained inflammation generally hinders neuronal maturation and functional integration (Gascón et al., 2017; Loane & Kumar, 2016). Within the injury context, several *in vivo* studies have reported efficient generation of mature, subtype-specified, and functionally integrated iNs in the adult injured brain. Notably, Gascón et al., (2016) provided one of first demonstrations of robust neuronal conversion, subtype-specification and long-term maturation of iNs following retroviral-mediated expression of Neurog2 and Bcl2 in the injured cortex, combined with antioxidant supplementation. Moreover, some AAV-based approaches have reported robust generation of mature, subtype-specific and functional iNs, with partial synaptic integration, in the injured cortex, without pro-survival factor co-expression or antioxidant supplementation (Mattugini et al., 2019), while others report limited maturation and acquisition of neuronal electrophysiological properties (Puglisi et al., 2024). However, it is important to note that these studies may not accurately represent the true effects of transcription factors on cell identity due to the potential of AAV-based vectors for artifactual labeling of pre-existing neurons.

Overall, the outcomes of *in vivo* reprogramming remain inconsistent across studies, even within similar injury paradigms (Chen et al., 2025; Puglisi et al., 2024; Zhang et al., 2020). This variability likely reflects differences arising from injury severity, choice of reprogramming factors, and metabolic support, in addition to the viral vector choice, as AAV-based approaches carry the risk of artifactual labeling of endogenous neurons (Chen et al., 2021; Xie et al., 2023), but also exhibit slower onset kinetics than retroviruses and may delay conversion to when inflammation has partially resolved (Gascón et al., 2017; Puglisi et al., 2024; Xie et al., 2023). Altogether, reprogramming efficiency, neuronal maturation, long-term survival and functional integration remain inconsistent in injury contexts. Addressing how injury type and severity, inflammatory responses, metabolic constraints, and regional contexts impact reprogramming outcomes will be required to adapt neuronal reprogramming to different pathological contexts, and for its ultimate therapeutic translation.

1.3 OPCs as substrates for repair after cortical injury

1.3.1 OPC development and injury-induced responses

Oligodendrocytes, the myelin-forming cells of the CNS, arise from OPCs, also referred as NG2 glia or polydendrocytes. OPCs were first identified in the early 1990s based on immunohistochemical labeling for the chondroitin sulfate proteoglycan NG2 and the alpha receptor for platelet-derived growth factor (PDGFRα), and are now recognized as a dynamic and abundant population of resident glial progenitor cells present throughout the developing and adult mammalian CNS (Dawson, 2003; Peters, 2004).

In the mouse forebrain, OPC development occurs in three temporally and spatially distinct waves (Figure 2). The first OPCs arise around embryonic day 12.5 (E12.5) from Nkx2.1-expressing progenitors located in the medial ganglionic eminence (MGE) and anterior entopeduncular area (AEP) of the ventral forebrain. These early-born OPCs migrate extensively and initially populate the entire telencephalon, including the developing cortex. The second embryonic wave occurs around E15.5 from Gsh2-expressing progenitors in the lateral and caudal ganglionic eminences (LGE/CGE), further providing OPCs to cortical and subcortical regions. The third wave occurs postnatally, arising locally within the cortex from Emx1-expressing dorsal progenitors. Notably, although early Nkx2.1-derived OPCs dominate the embryonic forebrain, they are largely eliminated during postnatal development and replaced by later-born OPCs (Kessaris et al., 2006). In the spinal cord, OPCs are initially generated from Olig2-expressing progenitors within the ventral motor neuron progenitor domain around E12.5. These progenitors first generate motor neuron progenitors, and subsequently switch fate to produce OPCs, a transition mediated by Sonic hedgehog (Shh) signaling. A second wave emerges around E15.5-E16.5, with OPCs originating from dorsal radial glial progenitors in the dorsal ventricular zone. Dorsal-derived OPCs partially replace ventral-derived OPCs, preferentially populate dorsal regions and contribute to postnatal oligodendrogenesis (Cai et al., 2005; Fogarty et al., 2005). Notably, development studies indicate that temporally and spatially distinct OPCs are functionally equivalent and can compensate their numbers to ensure normal oligodendrocyte production and myelination (Bergles & Richardson, 2016; Emery & Lu, 2015).

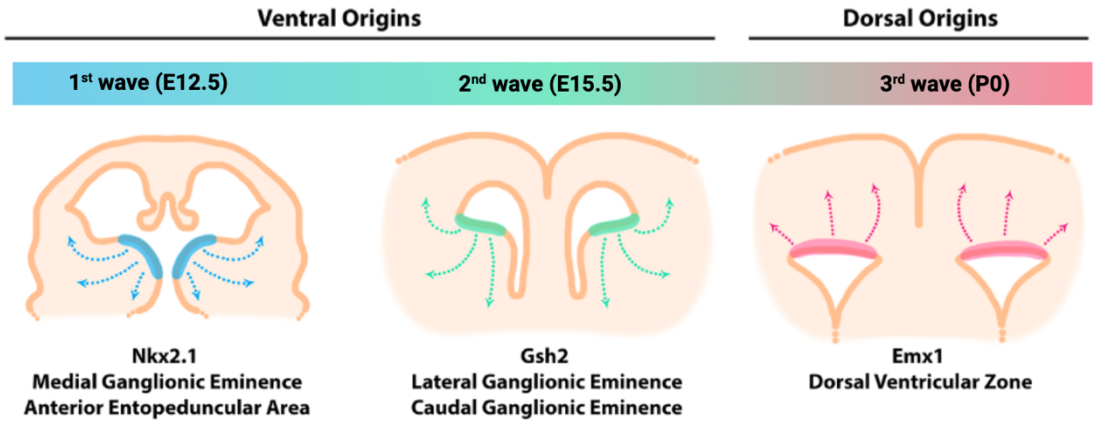

Figure 2: Developmental waves and regional origins of OPCs in the forebrain. OPCs arise in three spatially and temporally distinct waves during forebrain development. In ventral ganglionic regions, the first wave emerges from Nkx2.1-expressing progenitors at E12.5 and the second wave from Gsh2-expressing progenitors at E15.5. This is followed by a third wave arising postnatally from dorsal Emx1-expressing progenitors (adapted from Newville et al., 2017, created in Biorender).

Early specification of OPCs is regulated by key transcription factors, such as Olig2 and Sox10. Olig2 induces Sox10 expression, which marks the commitment to oligodendroglial lineage and enables subsequent expression of the OPC-specific markers PDGFRα and NG2 (Nishiyama et al., 2014). Following specification, OPCs undergo extensive proliferation and migration to populate the CNS, especially during late embryonic and early postnatal development. This phase results in OPC overproduction, and is followed by refinement of their cell numbers through competitive dynamics, as cells compete for space and survival signals from axons and astrocytes and excess OPCs undergo apoptosis (Barres et al., 1992).

OPC differentiation into myelinating mature oligodendrocytes occurs in a multistep process with sequential expression stage-specific markers (Figure 3). This process is typically divided into four successive stages: proliferative OPCs, pre-myelinating oligodendrocytes, immature myelinating oligodendrocytes and mature myelinating oligodendrocytes (Tiane et al., 2019). In mice, the first differentiated oligodendrocytes appear in the spinal cord shortly before birth around E18.5, while forebrain oligodendrocyte differentiation begins around birth and peaks during the first two to three postnatal weeks (Kuhn et al., 2019). This transition requires cell cycle exit, downregulation of the progenitor markers PDGFRα and NG2, and upregulation of myelin genes. Moreover, oligodendrocyte differentiation is controlled by intrinsic

factors, including a transcriptional network involving Sox10 and Olig2, which maintain oligodendroglial lineage identity, and the myelin regulatory factor (Myrf), which drives the expression of myelin genes, including myelin basic protein (MBP) and myelin proteolipid protein (Emery & Lu, 2015). In addition, extrinsic signaling pathways including Wnt/β-catenin, Notch and Bone Morphogenetic Protein (BMP) signaling inhibit differentiation and maintain OPCs in a progenitor state. In contrast, their downregulation promotes oligodendrocyte differentiation and maturation (Bergles & Richardson, 2016; Mayoral & Chan, 2016). These signaling pathways interact with epigenetic mechanisms, including chromatin remodeling to ensure myelination occurs in a spatially and temporally controlled manner (Elbaz & Popko, 2019).

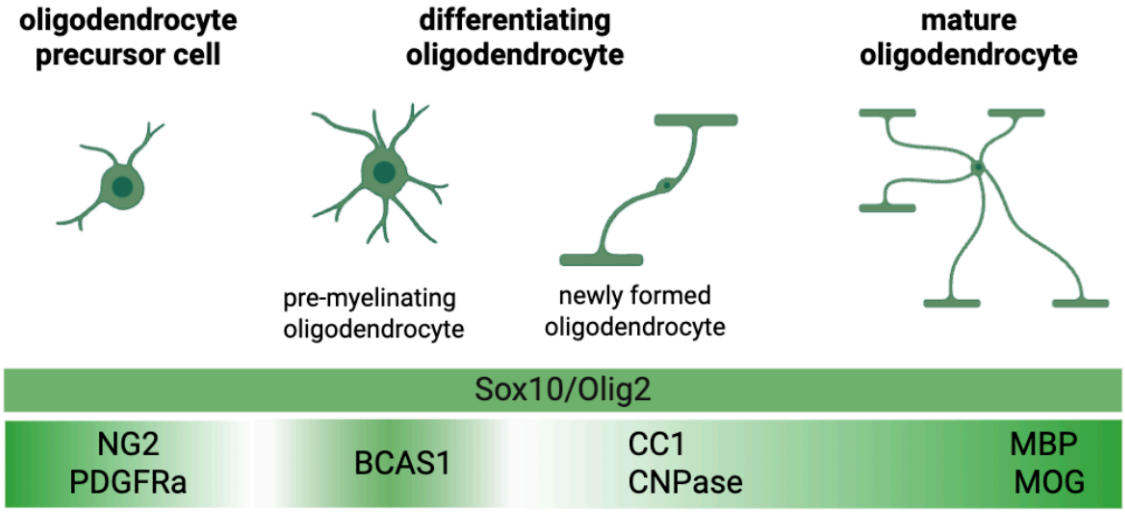

Figure 3: Oligodendroglial lineage progression markers. OPCs differentiate into myelinating oligodendrocytes through sequential stages. Sox10 and Olig2 are maintained throughout the oligodendroglial lineage, while OPCs can be commonly identified by NG2 or PDGFRα expression. Pre-myelinating oligodendrocytes are marked by breast carcinoma amplified sequence 1 (BCAS1), while newly formed oligodendrocytes can be identified by adenomatous polyposis coli clone (CC1) and 2′,3′-cyclic nucleotide 3′-phosphodiesterase (CNPase). Mature myelinating oligodendrocytes express myelin-associated proteins including myelin basic protein (MBP), myelin oligodendrocyte glycoprotein (MOG, adapted from Kamen et al., 2025 , created in Biorender).

In the adult brain, OPCs constitute approximately 2-8% of all cells and are widely distributed in both grey and white matter (Bergles & Richardson, 2016). OPCs represent the largest cycling population outside neurogenic niches in the adult CNS, and are distributed in a grid-like manner, with individual cells maintaining exclusive

territories through self-repulsion mechanisms (Hughes et al., 2013). Homeostasis is maintained through balanced proliferation, migration and differentiation, with OPCs self-renewing following cell death or differentiation into oligodendrocytes. However, recent work demonstrated that myelin repair occurs primarily through the same constitutive differentiation mechanism that operates under homeostatic conditions, as OPC differentiation attempts remain relatively constant and are not significantly increased by oligodendrocyte loss or extensive demyelination (Bergles & Richardson, 2016; Hughes et al., 2013; Mironova et al., 2026). Notably, OPC behavior differs across CNS regions, as white matter OPCs exhibit higher susceptibility to undergo differentiation while grey matter OPCs mostly remain undifferentiated, demonstrating region-specific constraints on oligodendrogenesis (Dimou et al., 2008; Young et al., 2013). With aging, OPC proliferation and differentiation competence decline, in part due to increased activity of inhibitory signaling pathways, including Wnt signaling, which impairs both homeostatic and injury-induced remyelination (Heo et al., 2025; Soomro et al., 2018; Mironova et al., 2026). Beyond their role as myelinating oligodendrocyte progenitors, OPCs display electrophysiological properties, receive direct synaptic input from neurons across different brain regions, including hippocampus and cortex, actively interact with neuronal circuits, as they express neurotransmitter receptors and ion channels, enabling them to sense and respond to neuronal activity (Bergles et al., 2000; Xiao & Czopka, 2023). OPCs can also influence circuit development and plasticity by regulating axonal remodeling and synaptic stability through phagocytosis, and have been shown to sense hypoxia and promote angiogenesis (Buchanan et al., 2022; Xiao & Czopka, 2023).

Following CNS injury, OPCs are rapidly activated, undergo hypertrophy, proliferate and migrate towards the lesion sites, leading to local expansion of OPC pool. Within permissive environments, activated OPCs can differentiate into myelinating oligodendrocytes and contribute to remyelination (Duncan et al., 2020). Although myelin repair occurs through constitutive differentiation of OPCs rather than injury-mediated induction, as differentiation attempts were shown to remain constant despite myelin demand (Mironova et al., 2026). In specific contexts, including severe demyelination, OPCs can also generate Schwann-like myelinating cells, highlighting their lineage plasticity during repair attempts (Franklin & ffrench-Constant, 2017; Zawadzka et al., 2010). In parallel, reactive OPCs can also contribute to lesion remodeling and immune responses. OPCs accumulate at lesion borders and upregulate chondroitin sulfate proteoglycans, including NG2, thereby participating in the formation of the glial scar and creating an inhibitory environment for axonal growth (Petrosyan et al., 2013). Moreover, OPCs respond to inflammatory cues, express cytokines and chemokines, such as IL-17, and participate in antigen presentation under

demyelinating conditions (Kirby et al., 2019; Niu et al., 2019). Disruption of IL-17 signaling in OPCs was shown to attenuate disease severity in experimental models of Multiple Sclerosis, providing evidence that OPC-mediated immune signaling influences the inflammatory response (Kang et al., 2010; Niu et al., 2019). Altogether, these findings position OPCs as multifunctional responders to CNS injury that support remyelination, influence glial scar formation, and modulate immune responses.

1.3.2 OPC competence for neuronal reprogramming

The developmental origin of OPCs, together with their abundance and self-renewal capacity in the adult CNS, makes them an attractive substrate for *in vivo* neuronal reprogramming. A subpopulation of cortical OPCs originates from embryonic ganglionic eminences, the same germinal zones that generate cortical interneurons, supporting the idea that OPCs may retain latent neuronal competence (Kessaris et al., 2006). Consistently, cortical OPCs were shown to exhibit a more permissive chromatin landscape at key interneuron loci compared to fibroblasts and astrocytes, including reduced repressive histone marks, and increased accessibility around key interneuron genes, such as Dlx1/2 (Boshans et al., 2019). In addition, OPCs endogenously express low levels of the proneural factor Ascl1, which has established roles in interneuron development (Battiste et al., 2007; Bertrand et al., 2002; Nakatani et al., 2013), potentially providing an additional advantage for OPC-mediated neuronal fate conversion, especially toward interneuron fate.

Initial *in vitro* studies provided early evidence that OPCs could be reprogrammed toward neuronal lineages (Guo et al., 2014), and subsequent *in vivo* approaches demonstrated that resident OPCs could undergo neuronal reprogramming within the adult CNS. In the adult cortex, Sox2 expression alone or combined with Ascl1 converted NG2 glia into immature iNs following stab-wound injury. Using Sox10-mediated fate-mapping, this study demonstrated that iNs originated from oligodendroglial lineage cells, and that Sox2-mediated neuronal conversion required previous injury (Heinrich et al., 2014). This study suggested that injury-induced signals or reactive states may enhance OPC neurogenic competence. Similarly, in the adult mouse striatum, combinatorial expression of Ascl1, Lmx1a and Nurr1 was reported to efficiently convert NG2 glia into iNs, with converted cells exhibiting mature morphological and electrophysiological properties characteristic of interneurons, though these findings in the striatum were based on AAV-mediated delivery and may be subject to the lineage authenticity concerns discussed above (Pereira et al., 2017; Torper et al., 2015). Nevertheless, NG2-derived iNs predominantly adopted interneuron identities, regardless of the transcription factors used, including factors

intended to specify dopaminergic fate, suggesting the presence of regional constraints, possibly reflecting epigenetic memory (Pereira et al., 2017). More recently, Boshans et al., (2021) demonstrated that Dlx2 alone could convert postnatal OPCs into functional GABAergic-like iNs *in vitro*, with conversion efficiency levels that exceeded what was previously achieved with postnatal astrocytes (Heinrich et al., 2010). In contrast, in the rat cortex, Neurog2 expression reprogrammed OPCs into glutamatergic, pyramidal-like iNs, even in the absence of injury (Bazarek et al., 2023), demonstrating that OPC neurogenic capacity is not restricted to inhibitory neuronal fates or injury contexts.

Altogether, the enhanced neurogenic competence of OPCs for interneuron fates has important implications for therapeutic neuronal replacement strategies, as GABAergic interneurons are lost or functionally impaired in several neurological conditions, including epilepsy and traumatic brain injury (Boshans et al., 2021; Lentini et al., 2021; Zhu et al., 2019). Importantly, the observation that OPCs can acquire subtype-specific interneuron features, including fast-spiking electrophysiological features and parvalbumin-specific marker expression, suggests that OPC reprogramming can generate functionally specialized neuronal subtypes, positioning OPCs as a promising endogenous cellular substrate for brain repair.

1.4 Ascl1 as a context-dependent regulator of lineage fate

1.4.1 Ascl1's role in development: neurogenesis and oligodendrogenesis

Ascl1, also known as Mash1, is a proneural bHLH transcription factor that plays a central role in coordinating progenitor proliferation with subsequent differentiation into neuronal and oligodendroglial lineages. Originally identified as a vertebrate homolog of the *Drosophila* proneural genes of the achaete-scute complex, Ascl1 is transiently expressed in progenitor cells throughout the developing CNS, including the ventral telencephalon, spinal cord and brainstem (Bertrand et al., 2002; Castro et al., 2011; Guillemot, 2007).

During embryonic neurogenesis, Ascl1 functions as a master regulator of neuronal differentiation and subtype specification. In the ventral telencephalon, Ascl1 is required for the specification of interneurons, and loss-of-function studies in mice demonstrated that Ascl1 deletion results in severe deficits in inhibitory neuron production (Casarosa et al., 1999; Parras et al., 2002). In contrast, gain-of-function studies showed that Ascl1 overexpression is sufficient to drive progenitors toward neuronal differentiation, promoting cell cycle exit and activation of downstream neuronal programs, underlining its neurogenic role (Berninger et al., 2007; Castro et al., 2006; Parras et al., 2002).

Ascl1 functions as a pioneer transcription factor, capable of binding to closed chromatin regions and promoting chromatin accessibility at its target sites. This pioneering activity enables Ascl1 to initiate neuronal differentiation programs, even in progenitors that are not yet committed to differentiation, and facilitates the temporal progression of neurogenesis (Raposo et al., 2015). Ascl1 directly activates expression of proneural target genes including the Notch ligand Delta-like 1, which mediates lateral inhibition to coordinate progenitor differentiation, and downstream transcription factors such as NeuroD1 and NeuroD4, which help consolidate neuronal identity (Castro et al., 2011).

Notably, the neurogenic activity of Ascl1 is tightly regulated by expression dynamics. In neural progenitors, Ascl1 is expressed in an oscillatory manner, coordinated out-of-sync with Hes1 oscillations downstream of Notch signaling, as Hes1 represses Ascl1 activity. Oscillatory Ascl1 expression contributes to progenitor maintenance and proliferative competence, as it directly activates cell cycle regulating genes, such as Cyclin-dependent kinase 1 (Cdk1) and Cdk2, without promoting terminal differentiation. As development progresses, sustained and high Ascl1 expression promotes cell cycle exit and stabilization of neuronal identity (Castro et al.,

2011; Imayoshi et al., 2013; Vasconcelos & Castro, 2014). Thus, Ascl1 participates in both progenitor maintenance and in neuronal differentiation, depending on its expression dynamics and cellular contexts.

Beyond its canonical neurogenic function, Ascl1 plays important roles in oligodendroglial lineage specification. As embryonic neurogenesis declines and the developing CNS transitions toward gliogenesis, Ascl1 continues to be expressed in progenitors that contribute to OPC generation. Namely, Ascl1-expressing progenitors initially contribute to neuronal populations, but later generate OPCs, particularly in the ventral forebrain and spinal cord (Battiste et al., 2007; Nakatani et al., 2013; Sugimori et al., 2008). During gliogenic stages, Ascl1 interacts with oligodendroglial determinants such as Olig2 to promote OPC specification and expansion. In the presence of Shh signaling, which induces Olig2 expression in the ventral progenitor domains, Ascl1 and Olig2 act synergistically to promote oligodendrocyte lineage commitment rather than astrocytic fates, contributing to expansion and differentiation of oligodendrocyte lineage cells (Parras et al., 2007; Sugimori et al., 2008). Importantly, Ascl1 expression persists in proliferative OPC populations and is downregulated upon differentiation, and in the postnatal brain, Ascl1 was shown to regulate the balance between OPC proliferation and differentiation. Conditional deletion of Ascl1 favored proliferative over differentiative OPC divisions, leading to a reduction in oligodendrocyte numbers and impaired remyelination following demyelinating injury (Nakatani et al., 2013).

1.4.2 Post-translational regulation of Ascl1 by phosphorylation

The proneural activity of Ascl1 is not only determined by its expression level, but is also tightly regulated by post-translational modifications. Among these, phosphorylation has emerged as a central mechanism controlling the context-dependent functions of Ascl1 (Ali et al., 2014; Li et al., 2014). Murine Ascl1 contains six conserved serine-proline (SP) motifs, located outside of the DNA binding bHLH domain, which are phosphorylated by proline-directed kinases, including CDKs (Ali et al., 2014). CDK-mediated phosphorylation of Ascl1 was associated with the maintenance of progenitor identity and continued proliferation, whereas reduced CDK activity during cell cycle exit led to decreased Ascl1 phosphorylation and promoted a shift toward differentiation programs (Ali et al., 2014). This phosphorylation-mediated regulation was first established in *Xenopus* embryos, where multi-site phosphorylation of Ascl1 was shown to reduce its proneural activity. Preventing Ascl1 phosphorylation by mutating serine residues to alanine in all six SP sites (Ascl1SA6) enhanced neuronal

differentiation. The phospho-deficient Ascl1 mutant was also resistant to both Notch-mediated and CDK-mediated inhibition of neurogenesis, which normally limit proneural activity in progenitors. Notably, this phosphorylation-mediated modulation of Ascl1's neurogenic capacity was also demonstrated in human-derived fibroblasts, where phospho-deficient Ascl1 promoted neuronal maturation following neuronal reprogramming (Ali et al., 2014).

Ascl1 proneural activity is also modulated by RAS/Extracellular signal-regulated kinase (ERK) signaling pathway. In mouse cortical progenitors, elevated RAS levels promoted ERK-mediated phosphorylation of Ascl1 and biased cell fate towards a proliferative and gliogenic fate, including astrocytic and oligodendroglial fates. In contrast, low RAS levels reduced ERK-mediated Ascl1 phosphorylation and favored neuronal differentiation, particularly toward GABAergic neuronal lineages (Li et al., 2014).

Phosphorylation-dependent regulation of Ascl1 is especially relevant in pathological contexts characterized by sustained kinase activity. In *Xenopus* models of neuroblastoma, Ascl1 is maintained in a hyperphosphorylated state, which prevents neuronal differentiation and sustains proliferation. Conversely, expression of phosphomutant Ascl1 restored neurogenesis (Wylie et al., 2015). Similarly, in glioblastoma stem cells Ascl1 is highly phosphorylated and promotes proliferation, whereas preventing phosphorylation promoted cell cycle exit and neuronal differentiation (Azzarelli et al., 2022).

Although unphosphorylated Ascl1 shows increased protein stability compared to wild-type Ascl1, this only contributes partially to its enhanced neurogenic activity (Ali et al., 2014; Woods et al., 2022). Studies have begun to elucidate how phosphorylation alters Ascl1 function, particularly at the chromatin level (Figure 4). During S/G2/M phases, when CDK activity is high, phosphorylated Ascl1 preferentially occupies promoters of pro-mitotic genes, supporting cell cycle progress. In contrast, during G1 phase, CDK activity decreases and leads to reduced Ascl1 phosphorylation. Consequently, Ascl1 preferentially binds to neuronal enhancers and primes them for activation. Consistently, phosphomutant Ascl1 was shown to enhance binding at neuronal enhancers, increase chromatin accessibility and expression of neuronal genes (Woods et al., 2022).

Together, these studies establish that phosphorylation determines whether Ascl1 supports proliferation or neuronal differentiation in response to cell cycle or growth factor signaling. These mechanisms provided a framework for understanding how Ascl1 regulates cell identity, and importantly how its function may be modulated

to promote specific lineage fates, having direct implications for regeneration or lineage reprogramming.

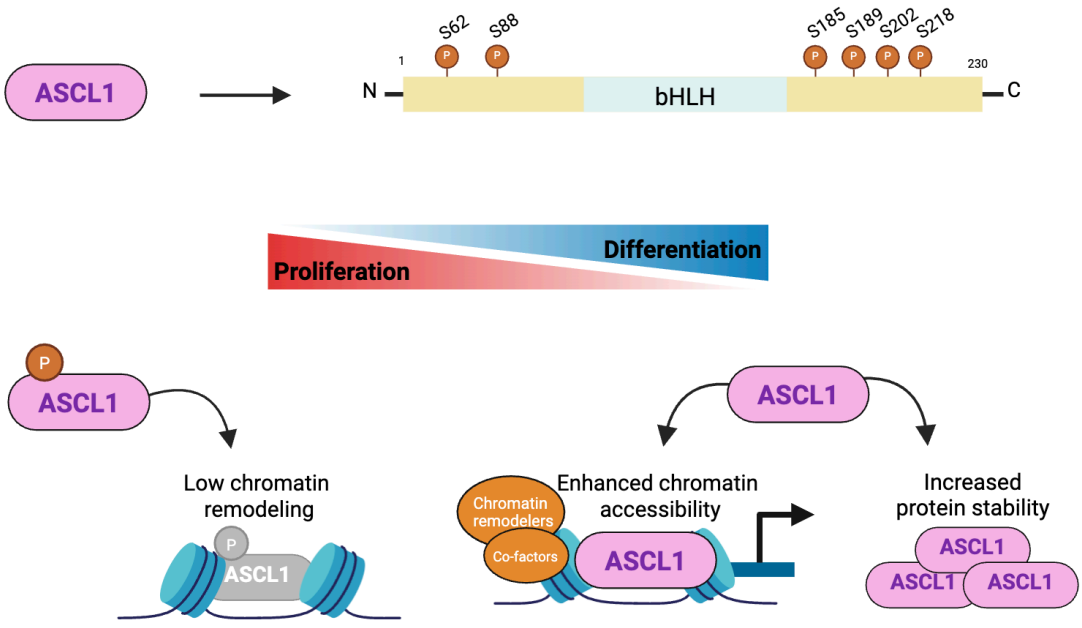

Figure 4: Model of phosphorylation-dependent regulation of Ascl1. Mouse Ascl1 contains six conserved serine-proline (SP) phosphorylation sites located outside of bHLH DNA-binding domain. Increased phosphorylation of Ascl1 biases its function toward proliferative programs and limits chromatin remodeling at neuronal regulatory elements. In contrast, reduced Ascl1 phosphorylation enhances protein stability and binding at neuronal enhancers and chromatin accessibility through recruitment of chromatin remodelers and co-factors, and promotes neuronal differentiation (adapted from Lundie-Brown et al., 2025; Woods et al., 2022, created in Biorender).

1.4.3 Ascl1-mediated lineage reprogramming

Ascl1 has been extensively explored as a driver of neuronal reprogramming, given its role as a master regulator of neurogenesis during development. Accordingly, ectopic Ascl1 expression was shown capable of inducing conversion of postnatal cortical astrocytes into GABAergic-like iNs *in vitro* (Berninger et al., 2007; Heinrich et al., 2010). Despite this neurogenic capacity *in vitro*, the efficiency of Ascl1-mediated neuronal conversion *in vivo* has been mostly limited and context-dependent. In the injured adult cortex, Ascl1 alone failed to convert reactive glia into iNs (Heinrich et al., 2014), suggesting possible environmental constraints that hinder glial cell susceptibility to undergo Ascl1-mediated reprogramming, either due to injury or regional setting. In contrast, other studies demonstrated efficient neuronal conversion

of adult or postnatal astrocytes in the intact striatum, dorsal midbrain or cortex following Ascl1 overexpression (Liu et al., 2015). However, these studies used AAV-vectors, and as discussed in subsection 1.2.3, questions remain about lineage authenticity. If confirmed, these findings would support the notion that injury may hinder Ascl1's neurogenic capacity.

While in injury contexts Ascl1's limited neurogenic capacity likely reflects inhibitory mechanisms, such as inflammatory signaling and elevated CDK activity, which promote Ascl1 phosphorylation (Ali et al., 2014), Ascl1's limitations are not restricted to injury settings. As described in subsection 1.4.2, phosphorylation biases Ascl1 toward progenitor maintenance and gliogenic outcomes, rather than neuronal differentiation (Ali et al., 2014; Li et al., 2014). Consistently, in the intact postnatal cortex, Ascl1 overexpression was recently shown to promote OPC proliferation rather than glia-to-neuron conversion (Galante et al., 2022b), demonstrating that Ascl1 activity sustains proliferation and promotes progenitor expansion *in vivo*, instead of directly driving neuronal fate acquisition.

To overcome phosphorylation-mediated fate bias, phospho-deficient Ascl1 (Ascl1SA6) was introduced as a reprogramming factor. Consistently, Ascl1SA6 overexpression improved neuronal conversion compared to wild-type Ascl1 in the postnatal cortex (Marichal et al., 2024). Given the reported metabolic vulnerability of young iNs and the alleviation of ROS-induced ferroptosis by Bcl2 co-expression (Gascón et al., 2016), Marichal et al., (2024) tested whether co-expression of Ascl1 or Ascl1SA6 with Bcl2 would yield higher reprogramming efficiency in the postnatal cortex. Strikingly, Ascl1SA6 and Bcl2 co-expression substantially improved reprogramming efficiency and enabled the generation of astrocyte-derived iNs with molecular and electrophysiological hallmarks of fast-spiking parvalbumin interneurons. However, while Bcl2 co-expression enhanced Ascl1-mediated neuronal conversion, overall efficiency remained limited, suggesting that Ascl1's neurogenic activity remains intrinsically constrained in the postnatal cortex even when metabolic constraints are addressed (Marichal et al., 2024).

These findings establish that Ascl1 function *in vivo* is highly context-dependent, with wild-type Ascl1 predominantly promoting OPC proliferation in the postnatal cortex instead of inducing neuronal conversion. While preventing its phosphorylation increased its neurogenic capacity, it remains unclear whether phosphorylation similarly governs Ascl1's neurogenic activity in the adult injured brain, where inflammation, elevated kinase activity, and reactive gliosis may impose additional constraints on both neuronal conversion and glial responses. Determining whether modulation of Ascl1's phosphorylation can unlock its neurogenic potential, and whether wild-type Ascl1 can

robustly expand OPCs while preserving their differentiation competence in this context, will advance our understanding of the mechanisms constraining regeneration after brain injury. Moreover, it will reveal whether Ascl1 phosphorylation status can be strategically harnessed for distinct therapeutic outcomes, including neuronal replacement through unphosphorylated Ascl1 or enhanced OPC expansion and remyelination through phosphorylated Ascl1, representing alternative avenues for brain repair.

2 Aims of the study

In vivo reprogramming of non-neuronal cells into neurons or oligodendrocytes, offers a promising strategy to replace cells lost after injury and restore functionality. In the intact postnatal cortex, overexpression of the proneural transcription factor Ascl1 was shown to be ineffective at driving glia-to-neuron reprogramming (Galante et al., 2022a), and instead, it enhanced OPC proliferation (Galante et al., 2022b). By contrast, a phospho-deficient mutant of Ascl1 (Ascl1SA6), combined with the pro-survival factor Bcl2, was shown to successfully convert astrocytes into induced neurons with hallmarks of parvalbumin fast-spiking interneurons (Marichal et al., 2024). While these findings suggest potential strategies for neuronal replacement or oligodendrocyte expansion, the injured adult brain presents a vastly different environment, characterized by reactive gliosis, inflammation, neuronal loss and glial scar formation, which both support and hinder regenerative responses (Burda & Sofroniew, 2014). Understanding how the injury-induced inflammatory milieu influences the efficiency and outcome of reprogramming is essential for translating this approach toward therapeutic applications. Therefore, in this study I aimed to investigate how Ascl1 phosphorylation status shapes glial lineage responses in the injured adult mouse cortex, where the cellular environment recapitulates hurdles to regeneration.

This study had two specific objectives:

- **To determine whether Ascl1 phosphorylation status influences neuronal reprogramming in the injured adult mouse cortex.** Using retroviral-mediated gene delivery to express Ascl1 or Ascl1SA6 alone, or with Bcl2 in proliferating reactive glia, I assessed neuronal conversion efficiency, characterized the iNs maturation state, and identified their cellular origins using genetic fate-mapping.

- **To assess the proliferative response induced by Ascl1 overexpression and its potential for oligodendroglial lineage cell expansion in the injured adult mouse cortex.** I examined whether this response is restricted to oligodendroglial lineage cells, analyzed its temporal dynamics, and evaluated the ability of proliferating OPCs to exit the cell cycle and undergo differentiation into oligodendrocytes.

3 Materials and Methods

3.1 Production of retroviruses

Replication-deficient Moloney Murine Leukemia Virus (MMLV)-based retroviruses were used for specific transduction of dividing reactive glial cells in the injured adult mouse cortex. Classical γ-retroviruses such as MMLV preferentially integrate into dividing cells, since they lack an active nuclear import mechanism, and therefore rely on nuclear envelope breakdown during mitosis to access the host genome for integration (Roe et al., 1993). In this study, retroviral particles were pseudotyped with vesicular stomatitis virus glycoprotein (VSV-G), which enables broad tropism and efficient transduction of mammalian cells (Yang et al., 1995). Gene expression was driven by the ubiquitous CAG promoter, which combines the chicken β-actin promoter with the cytomegalovirus (CMV) enhancer element for strong and sustained expression (Hitoshi et al., 1991). Constructs also included an internal ribosome entry site (IRES) followed by a fluorescent reporter (DsRed or eGFP) for visualization of transduced cells, and a Woodchuck Hepatitis Virus Posttranscriptional Regulatory Element (WPRE) downstream to enhance transgene expression (Zufferey et al., 1999). Retroviral constructs encoding two genes were linked by a self-cleaving T2A peptide to ensure equimolar co-expression (Goedhart et al., 2011).

All retroviral expression plasmids used in this study were produced in the laboratory by former members (Heinrich et al., 2014; Galante et al., 2022; Marichal et al., 2024), except for the retrovirus encoding human B-cell lymphoma 2 (5'LTR-hBcl2-IRES-GFP), containing a 5'LTR promoter instead of CAG, which was provided by Prof. Sergio Gascón (Gascón et al., 2016). A list of all retroviral constructs used in this study is provided in Table 1.

Table 1: Retroviral constructs used in this study.

pCAG-IRES-DsRed	Control retrovirus expressing DsRed under the CAG promoter via an IRES
pCAG-Ascl1-IRES-DsRed	Wild-type Ascl1 under the CAG promoter with DsRed via an IRES
pCAG-Ascl1SA6-IRES-DsRed	Phospho-deficient Ascl1 mutant (Ascl1SA6) under the CAG promoter with DsRed via an IRES
5'LTR-hBcl2-IRES-GFP	Human Bcl2 under 5'LTR promoter with GFP via an IRES
pCAG-Ascl1-T2A-Bcl2-IRES-DsRed	Ascl1 and Bcl2 linked by T2A peptide under the CAG promoter with DsRed via an IRES
pCAG-Ascl1SA6-T2A-Bcl2-IRES-DsRed	Ascl1SA6 and Bcl2 linked by T2A peptide under the CAG promoter with DsRed via an IRES

Retroviruses were produced using 1F8 cells, a monoclonal cell line derived from 293GPG cells, which stably express the retroviral gag and pol genes, while the expression of VSV-G is inducible and controlled by a tetracycline-repressible (tet-off) promoter (Ory et al., 1996). 1F8 cells were cultured in growth medium (Table 2) at 37ºC with humidified air containing 5% CO_2 and passaged at a 1:2 ratio upon reaching 70-80 % confluence. Prior to transfection, 10^7 1F8 cells were seeded in plating medium (Table 2) containing a reduced tetracycline concentration to limit VSV-G expression-mediated cytotoxicity. The following day, transfection was performed using polyethyleneimine (PEI) at a 3:1 mass ratio of PEI to DNA, with 25 µg of plasmid DNA per plate, diluted in Opti-MEM (ThermoFisher Scientific #10149832). After overnight incubation, the plating medium was replaced with packaging medium lacking tetracycline to induce VSV-G expression.

Viral particles were harvested three days after transfection. Namely, supernatants were collected, and fresh packaging medium was added to the cells for additional viral particle harvests. Supernatants containing the viral particles were cleared of cellular debris by centrifugation at 3000 rpm for 15 min at room temperature (RT), then filtered through a 0.45 µm low-protein binding filter PVDF syringe filter (StarLab #E4780-1451) and subjected to ultracentrifugation at 24000 rpm for 2 hours at 4ºC. The resulting viral pellet was resuspended in 100 µL of Tris-buffered saline-5 (TBS-5) and stored overnight at 4ºC. The harvest was repeated twice, namely two and four days after the first harvest. Viral particles from the first and second harvests were combined, while the third harvest was kept separate. Aliquots of 5 µL were prepared and stored at -80ºC until use. Viral preparations used for retroviral injection had titers ranging between 10^6- 10^8 transducing units/ml.

Table 2: Medium used for retroviral production

Growth medium	DMEM/F12 (Gibco #21331-020,) 1x Glutamine (Gibco #25030081) 10% Fetal Bovine Serum (Invitrogen #10270-106) 2 µg/ml Puromycin (Merck #P9620) 2 µg/ml Tetracycline (Merck # T7660) 0.3 mg/ml G418 Sulfate (InvivoGen #ant-gn-5)
Plating medium	DMEM (Gibco #21969-035) 1x Glutamine (Gibco #25030081) 10% Fetal Bovine Serum (Invitrogen #10270-106) 1x NEAA (Thermo Fisher Scientific #11140050) 1x Na-Pyruvate (Merck #P2256) 0.5 µg/ml Tetracycline (Merck # T7660)
Packaging medium	DMEM (Gibco #21969-035) 1x Glutamine (Gibco #25030081) 10% Fetal Bovine Serum (Invitrogen #10270-106) 1x NEAA (Thermo Fisher Scientific #11140050) 1x Na-Pyruvate (Merck #P2256)

3.2 Animal experiments

3.2.1 Mice

All animal experiments were conducted in accordance with institutional and governmental animal care guidelines. Experiments in wild-type animals were approved by the ethical committee of the state of Rhineland-Palatinate State (permit 23 177-07/ G22-1-007). Lineage-tracing experiments in transgenic mice were approved by the ethical committee of King's College London and conducted under the United Kingdom Home Office project license PP8849003. Mice were housed under standard laboratory conditions in a 12-hour light/dark cycle and with *ad libitum* access to food and water.

Wild-type C57BL/6J adult mice (7 weeks old) were purchased from Janvier Labs (Le Genest-Saint-Isle, France). Transgenic mouse lines were obtained from Jackson Laboratories. Aldh1l1-Cre/ERT2 mice (#JAX031008, Srinivasan et al., 2016) in which Cre recombinase expression is driven by the aldehyde dehydrogenase 1 family member L1 locus, or NG2-CreERTM (#JAX008538, Zhu et al., 2011), expressing Cre under the mouse Neuron/Glial Antigen-2 promoter, and the RCE:loxP EGFP reporter line (#JAX032037, (Sousa et al., 2009). The Cre transgenic lines were crossed with

the RCE:loxP to generate Aldh1l1-CreERT2/RCE:loxP or NG2-CreERTM/RCE:loxP double-transgenic mice.

3.2.2 Genotyping

Genotyping was performed on offspring prior to fate-mapping experiments to identify animals carrying the desired transgenic alleles. To this aim, ear biopsies were collected from mice from P10 onwards for genomic DNA extraction. Tissue samples were digested in 75 µl lysis buffer (250 mM NaOH, Sigma #S5881, and 0.2mM ethylenediaminetetraacetic acid, EDTA, Merck #E8008) for 1h at 95^{o}C. Following digestion, 75 µl of 1X neutralization buffer (0.4M Trizma® hydrochloride, HCl, Sigma-Aldrich #T15760) was added, and the sample was centrifuged for 1 min, to remove debris.

PCR amplification was performed using GoTaq DNA Polymerase (Promega), according to the manufacturer's protocol. Each 20 µl reaction consisted of 1 µl extracted DNA and 19 µL of PCR reaction mix which contained 1X PCRBIO Taq Mix Red (PCR Biosystems, #PB10.23) and primer mix at a 10 µM concentration (Table 3). The reaction was run in a thermocycler (Eppendorf nexus X2) with cycling programs listed in Table 3.

PCR products were run in an electrophoresis chamber (Bio-Rad, Sub-Cell GT Cell) at 100V in a 2% agarose gel (Invitrogen #16500) prepared with 1X Tris-acetate-EDTA (TAE) derived from a 50X stock solution (50 mM EDTA disodium salt, Sigma-Aldrich #E5134; 2M Tris, Invitrogen #15504-020; 1M acetic acid, Sigma-Aldrich #ARK2183, and 1X SYBRTM Safe DNA Gel Stain, ThermoFisher #S33102). Bands were visualized with Syngene^{TM} NuGenius Gel Documentation System.

Table 3: Transgenic mouse lines, corresponding primers and expected band sizes.

Transgenic line	**Targeted allele**	**Primers (5'- 3')**	**Band size**
Aldh1l1-CreERT2/RCE	Aldh1l1	**F**: GGCAAACGGACAGAAGCA **R**: CTTCAACAGGTGCCTTCCA	198 bp
NG2-CreERTM/RCE	Cre	**F:** TCCATAAAGGCCCTGACATC **R:** TGCGAACCTCATCACTCGT	100bp

Table 4: PCR programs used for genotyping

		Aldh1l1-CreERT2/RCE	NG2-CreERTM/RCE
Initial Denaturalization	1x	94°C 2 min	94°C 2 min
Denaturalization		94°C 20 sec	94°C 15 sec
Annealing	10x	60°C 15 sec	65°C 15 sec
Extension		68°C 15 sec	68°C 30 sec
Denaturalization		94°C 15 sec	94°C 15 sec
Annealing	28x	60°C 15 sec	60°C 15 sec
Extension		72°C 10 sec	72°C 30 sec
Final Extension	1x	72°C 2 min	72°C 2 min

3.2.3 Drug administration

a) Tamoxifen administration:

Tamoxifen (ApexBio Technology #B5965) was dissolved in corn oil (Sigma-Aldrich #C8267) at 37 °C to achieve a final concentration of 6 mg/ml. Adult (8-12 weeks old) NG2-CreERTM/RCE or Aldh1l1-CreERT2/RCE mice received daily intraperitoneal injections (150 mg/kg) for five consecutive days prior to surgical procedures. This aimed to induce Cre-mediated recombination and EGFP expression in oligodendrocyte precursor cells (NG2-expressing) or astrocytes (Aldh1l1-expressing).

b) 5-ethynyl-2'-deoxyuridine (EdU) administration:

EdU (Sigma #900584) was dissolved in sterile 0.9 % NaCl (Biotecnhologies #7647-14-5) containing 0.25 % dimethyl sulfoxide (DMSO, Invitrogen #2896561) and administered via intraperitoneal injection at 50 mg/kg. To detect proliferating cells in S-phase at the time of viral injection, adult mice (8-12 weeks old) received a single injection 4 hours prior to perfusion (subsection 4.3.4). To evaluate proliferating cells at 4-, 12-, 28- and 70 days after retroviral injection, mice received two EdU injections during the 24 hours prior to sacrifice.

3.2.4 Cortical stab-wound injury

Adult mice (8-12 weeks old) received a single subcutaneous dose of Rimadyl (Carprofen, 4 mg/kg) 30 min prior to surgery. Mice were anesthetized with an intraperitoneal injection of 0.5 mg/kg Medetomidine, 5 mg/kg Midazolam, and 0.025 mg/kg Fentanyl. Bepanthen® (Bayer #01578681) was applied to the eyes to prevent desiccation. Muscular relaxation and lack of pedal withdrawal reflex were confirmed before the procedure to ensure deep anesthesia. Adult mice were placed on a heating pad (World Precision Instruments #ATC-2000) set at 37°C with the head secured in a stereotaxic apparatus (Stoelting #51925). A midline incision was made with a surgical blade (Swann-Morton #0203), and with a micro driller (Stoelting #581610V) a ~1.5 mm diameter circular craniotomy was drilled into the skull on the right hemisphere, posterior to bregma, taking care to avoid major blood vessels. A stab wound was performed as previously described (Buffo et al., 2005; Gascón et al., 2016; Heinrich et al., 2014), by inserting an ophthalmic surgical knife (Alcon, #8065912001) through the craniotomy to a depth of 0.5 mm from the dura. The knife was moved approximately 1 mm along the anteroposterior axis to producing a lesion of ~1 mm in length. After the injury, the skin was sutured with a non-absorbable suture (Dafilon #624495), and anesthesia was reversed with an intraperitoneal injection of 2.5 mg/kg Atipamezole, 0.5 mg/kg Flumazenil, and 0.1 mg/kg Buprenorphine. Once awake, animals were returned to their cage, which was kept on a heating pad set to 37°C. Animals were monitored until recovery and then daily for three consecutive days.

3.2.5 Retroviral injection

Three days after the injury (Heinrich et al., 2014), mice were submitted to a second surgery for viral injection. Animals were anesthetized as described above, and the suture was opened. A glass capillary (Hirschmann ring caps® #9600105) was pulled by a vertical micropipette puller (Narishige PC-10, heater level 67.4) and the glass pipette (tip diameter of around 20 µm) was loaded with 1.5 µl of viral suspension. For injection, the pipette was connected to a three-way stopcock (B. Braun # 1050001285) via PE20 tubing, with a 10 ml syringe attached (B. Braun # 157269), allowing for manually controlled delivery of the viral suspension. The pipette was mounted on the stereotaxic arm, aligned with the center of the injury site and lowered to a depth of 0.5 mm. A total 1 µl of viral suspension was manually injected in 0.2 µl increments every 2 min. Before retraction, the pipette was left in place for 5 min to prevent leakage and ensure appropriate diffusion. The skin was then sutured, and anesthesia was reversed as previously described. Animals were monitored until recovery and then daily for three consecutive days.

3.2.6 Perfusion

Animals were anesthetized with a lethal dose of 120 mg/kg Ketamine and 16 mg/kg Xylazine diluted in 0.9% NaCl administered by intraperitoneal injection. Once deep anesthesia was confirmed, mice were transcardially perfused with 80 ml of 0.9% NaCl, followed by 50 ml of ice-cold 4% paraformaldehyde (PFA, Sigma Aldrich # P6148) dissolved in 0.1M phosphate buffer (PB; 30 mM Na2HPO4·12H2O, Merck #10039; 33 mM NaH2PO4·2H2O, Merck #13472; pH 7.4). After fixation, brains were dissected, post-fixed in 4% PFA overnight at 4ºC and stored in phosphate-buffered saline (PBS; Gibco #14190-250) prior to slicing. Brains were sliced on a vibratome (Leica HM650V) into 40 µm thick coronal sections, distributed in six consecutive series and stored in a cryoprotective solution (20% glucose, Sigma #G8270; 40% ethylene glycol, Sigma #324558; 0.025% sodium azide, Sigma #S2202, and 0.05M PB pH 7.4) at -20ºC.

3.3 Histology

3.3.1 Immunohistochemistry

Immunohistochemistry was performed on free-floating sections from one of the six series per brain. Sections were washed three times for 15 min in filtered 1X Tris-buffered saline (TBS, 50mM Tris-Cl, Invitrogen #15504-020; 150mM NaCl, Amresco #0241, pH 7.6). For PDGFRa, BCAS1 and Sox9, antigen retrieval was performed, consisting of a 3 min incubation at 95ºC in 10 mM citrate buffer (trisodium citrate dihydrate, Merck #71405, and 0.05% Tween 20, Merck #P9416; pH 6), followed by three additional 15 min washes in 1X TBS. Sections were then incubated for 1.5 hours at RT in blocking solution (5% Donkey serum, Sigma #D9663; 0.3% Triton X-100, Sigma #T8787 in 1X TBS). Primary antibodies (Table 5), diluted in blocking solution, were added to the sections for a 2-hour incubation at RT, and then overnight, or for 72 hours at 4ºC when staining for Sox10. The following day, sections were washed three times for 15 min in 1X TBS and incubated with species-specific secondary antibodies (Table 6) diluted in blocking solution, for 1.5 hours at RT. For EdU detection, the Click-iT ™ EdU Cell Proliferation Imaging Kit (Thermo Fisher Scientific #C10340) was used according to the manufacturer's protocol. Sections were incubated in the reaction mix for 30 min at RT, and washed three times in 1X TBS. For NeuroTrace staining, the manufacturer's protocol was followed. Briefly, sections were washed in PBS with 0.1% Triton X-100 for 10 min at RT, followed by two PBS washes for 5 min. Sections were next incubated with NeutroTrace ™ (Invitrogen # N21479;

1:100) for 30 min at RT, washed once in PBS with 0.1% Triton X-100 for 10 min, and two more times with PBS for 5 min. Next, sections were incubated with 5µM 4',6-diamidino-2-phenylindole (DAPI, Sigma #D9542) diluted in PBS for 5 min at RT. DAPI was removed with three additional washes with 1X TBS, followed by two 15 min washes with 0.1M PB prior to mounting. Sections were mounted on Superfrost™ microscope slides (Thermo Fisher Scientific), allowed to dry and Prolong Gold Antifade Mountant (Invitrogen #P36930) was added before covering sections with a glass coverslip.

3.3.2 Single molecule fluorescence in situ hybridization

Single-molecule fluorescence *in situ* hybridization (smFISH) was performed using the RNAscope Multiplex Fluorescent v2 assay (ACDBio #323110) according to the manufacturer's protocol. All solutions were prepared with Diethyl Pyrocarbonate-treated water (DEPC, Sigma).
Sections were washed twice with PB 0.1M for 15 min, mounted on Superfrost™ microscope slides (Thermo Fisher Scientific), and air-dried overnight at RT. The following day, sections were dried in the HybEZTM II Oven (PN 321710/321720) at 60°C for 1 hour and sequentially dehydrated in 50%, 70%, and 100% ethanol for 5 min each. Sections were next treated with hydrogen peroxide for 10 min at RT and washed three times with DEPC-treated water for 5 min. Next, sections were incubated with RNAscope Multiplex FL v2 Target Retrieval Solution at 90°C for 10 min, rinsed in water, briefly dipped in 100% ethanol, and air-dried. A hydrophobic barrier was drawn around the tissue using an ImmEdge Hydrophobic Barrier Pen (Vector Labs #310018) and allowed to dry. Protease III was added for 15 min at 40°C, followed by three washes with water. Sections were then hybridized with Mm-C3-C1 (ACDBio #1116038) probe at 40°C for 2 hours, washed with 1X Wash Buffer, and stored overnight at 4°C. The next day, sections were washed three times for 15 min with 1X Wash Buffer, incubated with RNAscope Multiplex FL v2 HRP for signal amplification and development, and stained with the fluorophore dye Opal690 (AkoyaBio #FP1487A) for detection. Three 5 min washes with 1X Wash Buffer were performed between each step, according to the manufacturer's protocol.

Following smFISH, immunohistochemistry was performed to detect the reporter gene expressed by transduced cells. Primary and secondary antibodies were used at twice the concentration listed in Table 5 and 6. Sections were incubated in blocking solution for 30 min at RT, followed by incubation with primary antibodies (Table 5) diluted in blocking solution overnight at 4°C. Afterwards, sections were washed three times with 1X TBS for 5 min at RT, incubated with secondary antibodies (Table 6)

for 1.5 hours at RT, and washed three more times with 1X TBS for 5 min. Lastly, sections were incubated with DAPI for 5 min, washed twice with 1X TBS and twice with 0.1PB for 5 min each, allowed to dry, and mounted in Prolong Gold Antifade medium

Table 5: Primary antibodies

Antigen	Host species	Dilution	Source
BCAS1	Guinea pig	1:250	Synaptic System (445004)
C3d	Rabbit	1:500	DAKO (A0063)
CC1	Mouse	1:250	Calbiochem (OP80)
CD45	Rat	1:1000	BD Pharmigen (557659)
DCX	Guinea pig	1:250	Millipore (AB2253)
GFAP	Mouse	1:300	Sigma (G3893)
GFAP	Goat	1:300	ABCam (ab535554)
GFP	Chicken	1:1000	AvesLab (GFP-1020)
Iba1	Rat	1:250	Synaptic System (HS234017)
NeuN	Mouse	1:500	Millipore (MAB377)
PDGFRa	Mouse	1:250	R&D Systems (AF1062)
RFP	Rabbit	1:500	Rockland (600401379)
Sox10	Goat	1:250	R&D Systems (AF2864)
Sox9	Rabbit	1:500	ABCam (ab185966)

Table 6: Secondary antibodies

Species specificity	Fluorescence	Dilution	Source
Donkey anti-chicken	488	1:250	Jackson Immuno (703-545-155)
Donkey anti-goat	488	1:250	Invitrogen (A11055)
Donkey anti-goat	Cy3	1:500	Dianova (705-165-147)
Donkey anti-goat	Cy5	1:500	Dianova (705-175-147)
Donkey anti-guinea pig	Alexa 488	1:250	Jackson Immuno (706-545-148)
Donkey anti-guinea pig	Cy5	1:500	Dianova (706-166-148)
Donkey anti-mouse	Alexa 647	1:500	Invitrogen (A31571)
Donkey anti-mouse	Cy3	1:300	Invitrogen (A10037)
Donkey anti-rabbit	Cy3	1:500	Dianova (711-165-152)
Donkey anti-rat	Alexa 647	1:500	FluoProbes (FSSC6120)
Donkey anti-rat	Alexa 547	1:500	Dianova (FP-SB6120)

3.4 Image acquisition, image analysis and quantification

3.4.1 Image acquisition

Maximum-intensity projections were generated in ZEN (Zeiss) software for Apotome-acquired images or in ImageJ/FIJI (National Institute of Health) for confocal images.

Tile scans of regions containing reporter-positive cells (DsRed or GFP) were used for analysis of marker expression or EdU incorporation. All quantifications were performed on maximum-intensity projections in ImageJ/FIJI.

3.4.2 Image analysis and quantification

a) **Quantification of marker expression in transduced cells:** the total number of reporter-positive cells ($DsRed^+$ or GFP^+) and reporter-positive cells co-expressing glial (GFAP, Sox10, and Iba1) or neuronal markers (DCX, NeuN, and Neurotrace) were manually counted across all sections of one completed series per brain. Percentages of marker-expressing cells were calculated by dividing the number of double-positive cells by the total number of reporter-positive cells. For EdU quantification, the number of cells co-expressing EdU, the reporter gene, and/or the specific marker was divided by the total number of transduced cells or by the total number of marker-expressing transduced cells. Quantifications included all transduced cells within the analyzed series.

b) **Quantification of glial activation and immune response:** CD45-, GFAP-, and Iba1-expressing cells were quantified in five coronal sections per animal, spaced 240 µm apart. Sections were selected to span the region surrounding the injection core, defined as the section containing the highest density of reporter-positive cells, together with two anterior and two posterior sections. This strategy was chosen to capture the spatial extent of lesion- and/or viral-induced glial responses. Images were acquired as tile scans combined with 1.25 µm spaced Z-stacks on both the ipsilateral and contralateral hemispheres. Automated quantification was performed in ImageJ/FIGI and adapted from Young & Morrison (2018). Images were converted to 8-bit and processed with the median filter ("Despeckle"), which replaces each pixel with the median of its 3x3 neighborhood (Young & Morrison, 2018). Thresholds were manually set using Otsu's method (Otsu, 1979), with marker-specific intensity ranges (15-35 for Iba1; 10-25 for GFAP). Particles were detected by the "Analyze particles" function with defined area sizes and a circularity range of 0.00 and 0.50. Threshold settings were selected by manually

counting Iba1- and GFAP-expressing cells in at least three representative sections and selecting values that resulted in <5% deviation from manual counts.

c) **Quantification of C3 mRNA signal (smFISH):** C3 mRNA signal was quantified on maximum-intensity projections of Z-stacks acquired at 0.8µm intervals using a TCS SP5 confocal with a 40x oil-immersion objective (NA 1.3). For each brain, three representative coronal sections were selected for analysis. In the reprogramming condition, sections were selected based on the presence of reporter-positive cells at the injury site, whereas in the injury-only condition sections were selected based on anatomical correspondence to the injury site identified by DAPI staining. Images were acquired from the reprogramming site (injury+retrovirus), contralateral hemisphere, and injury-only region. Subsequently, images were converted to 8-bit, processed with the median filter ("Despeckle"), the background was subtracted (rolling-ball radius 300 pixels), and Otsu's threshold was applied (ranging between 110 and 121). Two regions of interest (ROIs) were then defined: i) the total tissue area within the field of view, and ii) the threshold-positive mRNA signal. The C3-positive area was measured and expressed as a percentage of the total tissue area.

d) **Quantification of Sox10 and EdU cell density:** Sox10 and EdU cell density were quantified using the automatic cell-count workflow described previously. Otsu's threshold ranged between 60-100, and circularity was set to 0.50-1.00. Threshold and particle-size values were defined by manually counting Sox10- and EdU-expressing cells in three representative sections and selecting values that differed by <5% from the manual counts. Cell density was calculated by dividing the number of marker-positive cells by the ROI area (mm^2) and expressed as the number of marker-positive cells per mm^2.

e) **Quantification of labeling efficiency for fate-mapping experiments:** The total number of marker-positive cells (PDGFRa or Sox9) and the number of cells co-expressing GFP and the corresponding marker were manually counted in a 2048 x 2048-pixel ROI. Labeling efficiency was presented as the percentage of marker-positive cells that co-expressed GFP.

f) **Quantification for characterization of fate-mapped cells:** The total number of transduced cells and the number of transduced cells that co-expressed GFP and/or neuronal markers, glial markers, or EdU were manually quantified. In subsection 4.2.6, the proportions of cells expressing GFP (fate-mapped cells), GFP and neuronal markers (fate-mapped induced neurons), or neuronal markers alone were

calculated relative to the total number of transduced cells. For EdU analysis, the number of EdU-incorporating transduced fate-mapped cells was counted and divided by the total number of fate-mapped transduced cells.

3.5 Statistical analysis

Statistical analyses were performed in GraphPad Prism 10 (GraphPad, San Diego, USA). Normality of data distribution was assessed by the Shapiro-Wilk test. For the comparison between two groups with normally distributed data (Shapiro-Wilk test $p>0.05$), parametric tests were applied. An unpaired two-tailed t-test was applied to independent groups or a paired two-tailed t-test for paired measurements, e.g., within-animal measurements. For data that did not display a normal distribution, comparisons between two independent groups were performed by the Mann-Whitney U-test. For comparisons among multiple experimental groups, one-way analysis of variance (ANOVA) followed by Tukey's multiple-comparison test was used for normally distributed data. Non-normally distributed data were analyzed using the Kruskal-Walli's test followed by Dunn's multiple comparisons test. Two-way ANOVA with Šídák's multiple comparisons test was applied to data with two independent variables.

Data were presented as mean ± standard deviation (SD). Statistical significance was defined as p-value <0.05 for all tests, and non-significant comparisons ($p>0.05$) were indicated as "ns". The number of biological replicates (n) and the statistical tests used were indicated in each figure legend.

4 Results

Chapter I: Ascl1SA6 and Bcl2 co-expression induces limited neuronal conversion in the injured adult mouse cortex

The proneural transcription factor Ascl1 is a master regulator of neurogenesis and neuronal differentiation during development (Castro et al., 2011). Accordingly, Ascl1 successfully converted postnatal cortical astrocytes into induced neurons (iNs) *in vitro* (Berninger et al., 2007). However, when tested *in vivo,* Ascl1 failed to induce glia-to-neuron conversion in the postnatal cortex (Galante et al., 2022a). In contrast, the co-expression of a phospho-deficient Ascl1 mutant (Ascl1SA6), in which six serine residues were mutated to alanine (Ali et al., 2014), together with the pro-survival factors Bcl2, enabled robust conversion of postnatal astrocytes into iNs *in vivo* (Marichal et al., 2024). Altogether, these findings suggest that neuronal reprogramming efficiency is context-dependent.

Despite the robust neuronal conversion in the intact postnatal cortex, it remains unknown whether Ascl1SA6-Bcl2 can induce neuronal reprogramming in the context of an injury. Therefore, Ascl1SA6-Bcl2-mediated neuronal reprogramming was tested in injured adult mouse cortex, where the local environment is characterized by pronounced inflammation and glial activation, with the emergence of distinct detrimental reactive glial subtypes that can contribute to neuronal loss (Bardehle et al., 2013; Buffo et al., 2008; Liddelow et al., 2017). Importantly, previous studies have demonstrated that reactive glia can be reprogrammed into iNs after cortical injury, for example through Ascl1 and Sox2 overexpression (Heinrich et al., 2014), or co-expression of Neurogenin 2 and Bcl2 (Gascón et al., 2016). Given that neuronal reprogramming can be achieved in the injured cortex and that Ascl1SA6 and Bcl2 co-expression is highly effective in the intact postnatal cortex, this chapter investigates the potential of Ascl1SA6 and Bcl2 to promote glia-to-neuron in the injured adult mouse cortex.

4.1 Retroviral injection results in transduction of proliferating reactive glial cells in the injured adult cortex

Cortical stab-wound injury induces a localized and robust proliferative response of resident glial cells, which peaks between 2-4 days post-injury (Bardehle et al., 2013; Buffo et al., 2008). These proliferating glial cells can be selectively targeted using replication-deficient retrovirus, which integrates in the genome of dividing cells,

thereby excluding post-mitotic neurons. Following integration, transgene expression is expected to persist unless actively silenced by the host cell. This provides a reliable method to deliver reprogramming factors to induce glia-to-neuron conversion in the injured adult cortex (Gascón et al., 2016; Heinrich et al., 2014).

To establish this experimental model, a stab-wound injury was performed in the somatosensory cortex of adult mice. Three days later, at the peak of injury-induced glial proliferation (Buffo et al., 2008), a control retrovirus encoding a fluorescent reporter gene DsRed (CAG-IRES-DsRed) was injected at the injury site to label dividing glial cells. At 4 days post-injection (dpi, corresponding to 7 days post-stab wound injury), the identity of transduced cells was assessed by immunostaining to determine which glial populations would be targeted for subsequent reprogramming experiments (Figure 5A).

At 4 dpi, expression of cell-type specific markers was assessed to determine the identity of transduced cells. Marker expression was analyzed in adjacent brain sections from the same animals, with each marker detected in independent immunostainings. Sox10 was used to label oligodendroglial lineage cells, GFAP to identify reactive astrocytes, which upregulated it after injury (Buffo et al., 2008), Iba1 for microglia and DCX for neuronal progenitors. Quantitative analysis revealed that most transduced cells expressed Sox10 (Sox10: 52.9 ± 11.4%). Smaller fractions of transduced cells expressed GFAP (31.6 ± 8.02%) or Iba1 (Iba1: 13.8 ± 6.23%). These results indicate that oligodendroglial lineage cells constitute the main starter population targeted by retroviral transduction, followed by reactive astrocytes, and microglia. No DCX-expressing cells were detected, (0 ± 0%), indicating that there is no induction of neurogenesis in the absence of reprogramming (Figure 5B, C).

A.

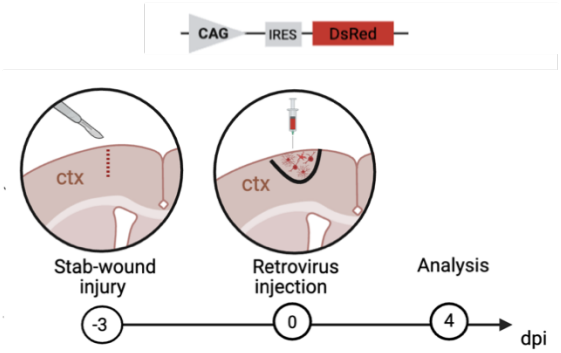

B.

Markers	Total transduced cells (n=3)	Total marker+ cells (n=3)	% of marker+ transduced cells
Sox10	590	310	52.9 ± 11.4 %
GFAP	440	138	31.6 ± 8.02 %
Iba1	468	68	13.8 ± 6.23 %
DCX	374	0	0 ± 0 %

C.

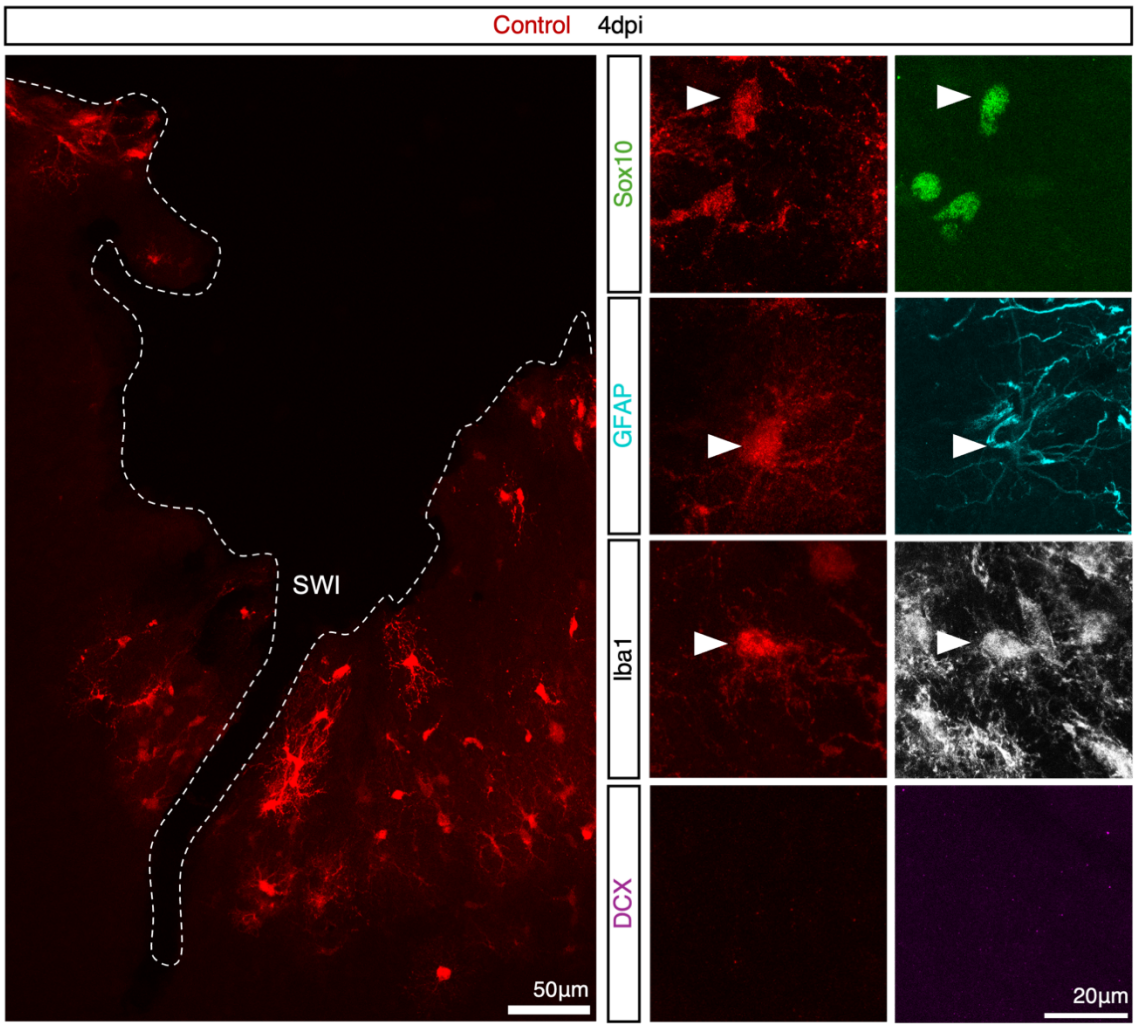

Figure 5: Retrovirus-mediated specific transduction of reactive glia in the injured adult cortex at 4 days post-injection (dpi). A. Schematic representation of experimental approach. A stab-wound injury was performed in the somatosensory cortex of adult mice (day -3). Retrovirus encoding DsRed alone (as control) was injected three days later (day 0). At 4 dpi the identity of transduced cells was assessed by immunostaining against Sox10 (oligodendroglial marker), GFAP (reactive astroglia marker), Iba1 (microglia marker) and DCX (immature neuronal marker). **B.** Quantification of lineage marker expression among transduced cells 4 dpi. **C.** Representative confocal images of the injured adult mouse cortex showing transduced cells (in red) and their expression of lineage markers: Sox10 (in green), GFAP (in cyan), Iba1 (in white), or DCX (in magenta). Dashed lines delineate stab-wound injury (SWI). White arrowheads indicate marker-positive cells. Data shown as mean ± SD. n=3 mice, 374-590 cells analyzed in total.

4.2. *In vivo* reprogramming of reactive glia by forced expression of Ascl1SA6 and Bcl2

4.2.1. Ascl1SA6 overexpression induces early downregulation of glial markers in the injured adult cortex

To assess early effects of Ascl1 or Ascl1SA6 overexpression on transduced glial cells, retroviruses encoding DsRed (CAG-IRES-DsRed, as control), Ascl1 (CAG-Ascl1-IRES-DsRed), Ascl1SA6 (CAG-Ascl1SA6-IRES-DsRed) were injected at three days post-injury, and immunostaining against glial markers Sox10 (for oligodendroglial lineage cells) or GFAP (for reactive astrocytes) was performed at 4 dpi. Analysis focused on Sox10 and GFAP as these markers correspond to the primary glial populations targeted by retroviral transduction (subsection 4.1).

At this early stage, the proportion of Sox10-expressing transduced cells in the Ascl1 group was similar to control (control: 53.0 ± 11.4%, Ascl1: 56.7 ± 5.0%, Figure 6B, C), indicating that Ascl1 overexpression does not alter oligodendroglial identity at 4 dpi. In contrast, Ascl1SA6 overexpression significantly reduced the proportion of transduced cells that expressed Sox10, compared to both control and Ascl1 (Ascl1SA6: 16.3 ± 7.5%, p=0.017 for Ascl1SA6 vs control, and p=0.013 for Ascl1SA6 vs Ascl1, Figure 6B, C). This finding suggests that Ascl1SA6 initiates a lineage fate transition from oligodendroglial identity at 4 dpi.

Next, GFAP expression was evaluated in transduced cells. The proportion of GFAP-expressing cells was reduced in both Ascl1 and Ascl1SA6 groups compared to control, but only Ascl1SA6 group reached statistical significance (control: 23.5 ± 14.4%, Ascl1: 6.52 ± 4.72%, Ascl1SA6: 0.54 ± 0.94%, p=0.042 for Ascl1SA6 vs control, Figure 6B, C). This reduction may reflect changes in astrocytic identity or reactive state, and suggests distinct influences of Ascl1 and Ascl1SA6 on astrocytic states.

Altogether, these findings indicate that Ascl1 and Ascl1SA6 induce distinct effects on reactive glia as early as 4 dpi. More importantly, Ascl1SA6 overexpression rapidly downregulates both Sox10 and GFAP expression in transduced cells, consistent with initiation of lineage conversion away from glial identity.

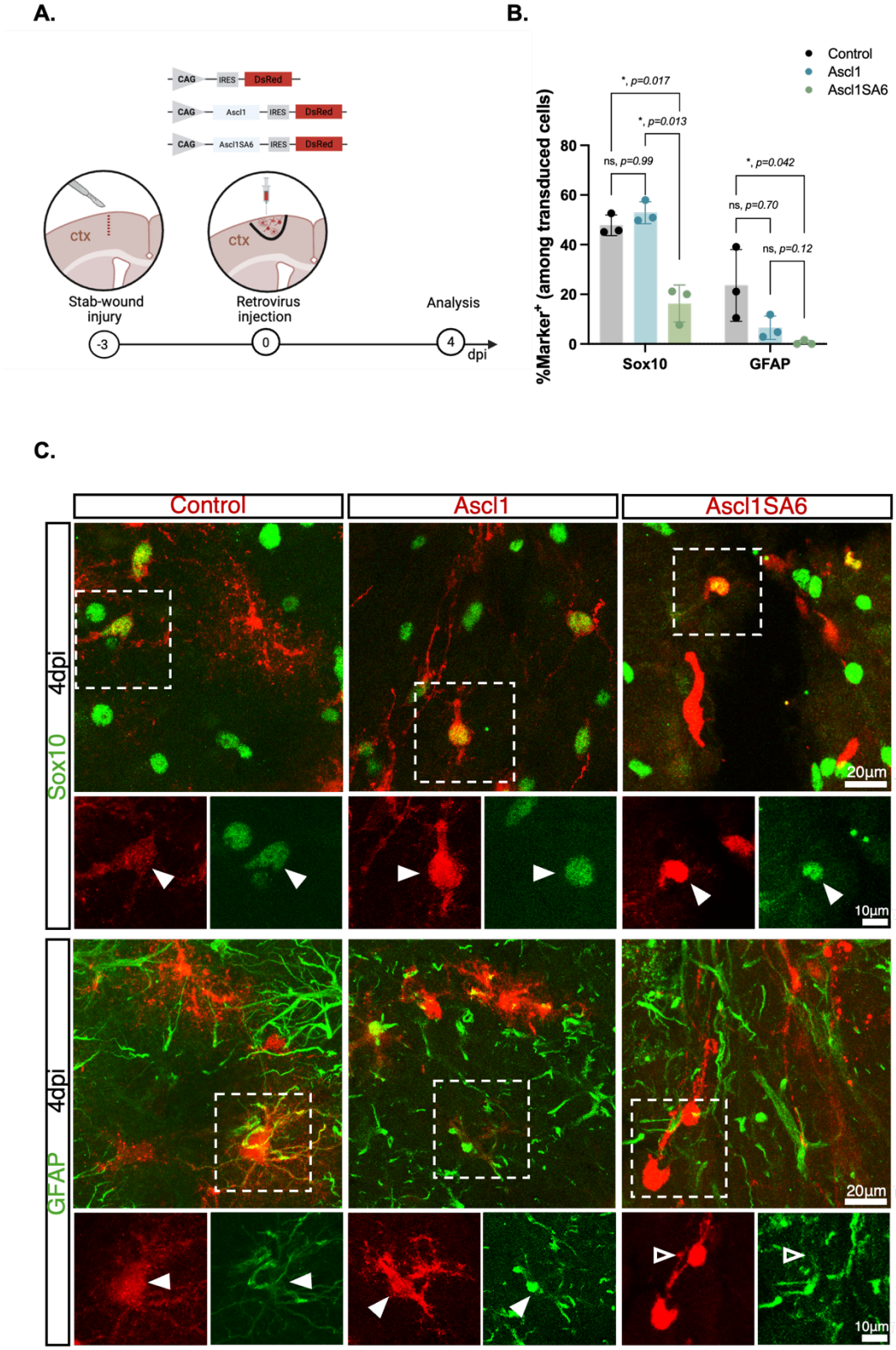
A.
CAG
IRES
DsRed
CAG
Ascl1
IRES
DsRed
CAG
Ascl1SA6
IRES
DsRed
ctx
ctx
Stab-wound injury
Retrovirus injection
Analysis
-3
0
4
dpi
B.
Control
Ascl1
Ascl1SA6
%Marker+ (among transduced cells)
*, p=0.017
*, p=0.013
ns, p=0.99
*, p=0.042
ns, p=0.70
ns, p=0.12
Sox10
GFAP
C.
Control
Ascl1
Ascl1SA6
Sox10 4dpi
GFAP 4dpi
20µm
10µm
20µm
10µm

Figure 6: Ascl1SA6 overexpression induces downregulation of glial markers in the injured adult cortex at 4 days post-injection (dpi). A. Schematic representation of experimental approach. Cortical stab-wound injury was performed in the somatosensory cortex of adult mice (day -3). Retrovirus encoding DsRed only (control), Ascl1 or Ascl1SA6 was injected three days following cortical stab-wound injury (day 0). At 4 dpi the identity of transduced cells was assessed by immunostaining against Sox10 (oligodendroglial marker) or GFAP (reactive astroglia marker). **B.** Quantification of the relative proportion of transduced cells that expressed Sox10 or GFAP at 4 dpi. **C.** Representative confocal images highlighting Sox10 (in green, first panel), GFAP (in green, second panel) expression in transduced cells (in red). White arrowheads indicate marker-positive cells and empty arrowheads indicate marker-negative cells. Data shown as mean ± SD. Statistical tests: one-way ANOVA followed by Tukey's multiple comparison test (% Sox10) or Kruskal Wallis test followed by Dunn's multiple comparison test (% GFAP). n=3 mice/group, control: 590 cells analyzed, Ascl1: 1337 cells analyzed; Ascl1SA6: 167 cells analyzed.

4.2.2. *Ascl1 overexpression fails to induce glia-to-neuron conversion while Ascl1SA6 alone induces limited neuronal marker expression*

To determine whether the early loss of Sox10 and GFAP expression in Ascl1SA6-transduced cells leads to acquisition of neuronal identity, the expression of neuronal markers was assessed at a later stage, namely at 12 dpi. At this time point, immunostaining against doublecortin (DCX, immature neuronal marker) and neuronal nuclear protein (NeuN, mature neuronal marker) was performed in cells transduced with control, Ascl1 and Ascl1SA6 (Figure 7A).

DCX expression was found absent in transduced cells across conditions (control: $0 \pm 0\%$, Ascl1: $0 \pm 0\%$, Ascl1SA6: $0 \pm 0\%$, Figure 7C, D), indicating that transduced cells do not express this immature neuronal marker, or that DCX expression may be transient and undetectable at this stage. Interestingly, NeuN expression was limited but detectable in Ascl1SA6-transduced cells, while control- and Ascl1-transduced cells showed no expression (control: $0 \pm 0\%$, Ascl1: $0 \pm 0\%$, Ascl1SA6: $1.49 \pm 1.30\%$, Figure 7C, D). In addition, Ascl1SA6-transduced cells displayed an immature neuronal-like morphology, with smaller somata and one elongated process. This suggests that Ascl1SA6 yields higher neurogenic competency than Ascl1 in the injured adult cortex, though its expression alone is insufficient to drive efficient glia-to-neuron conversion.

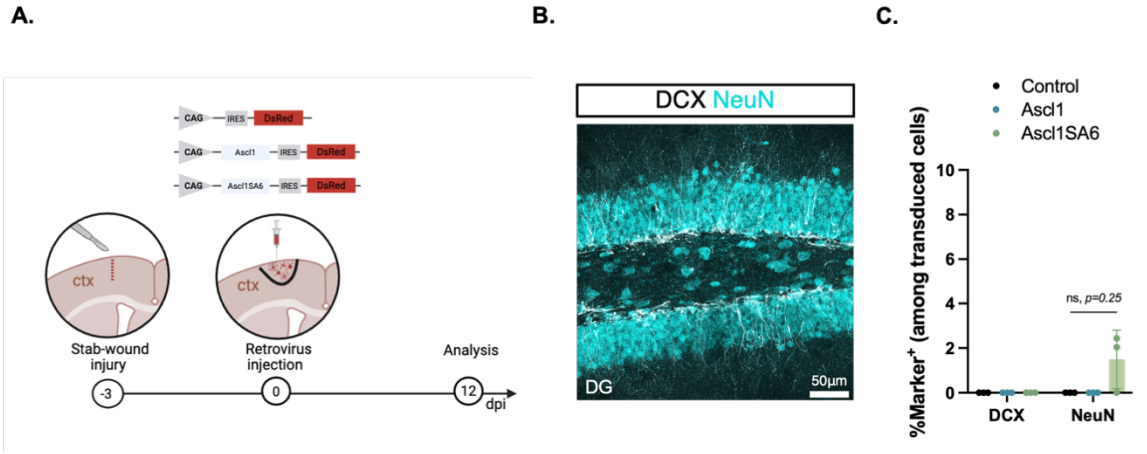
A.
B.
C.
CAG
IRES
DsRed
Ascl1
Ascl1SA6
ctx
Stab-wound injury
Retrovirus injection
Analysis
-3
0
12
dpi
DCX NeuN
DG
50µm
Control
Ascl1
Ascl1SA6
%Marker+ (among transduced cells)
ns, p=0.25
DCX
NeuN

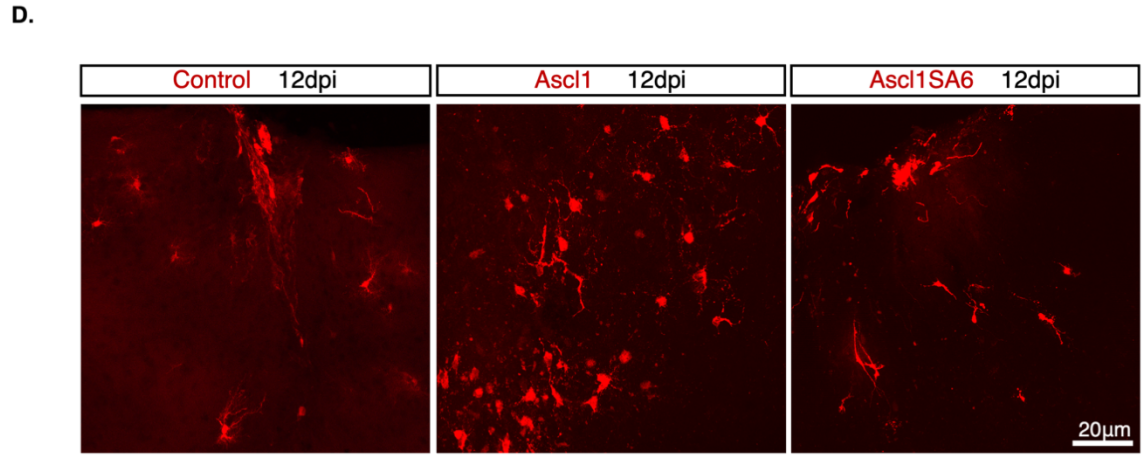
D.
Control 12dpi
Ascl1 12dpi
Ascl1SA6 12dpi
20µm

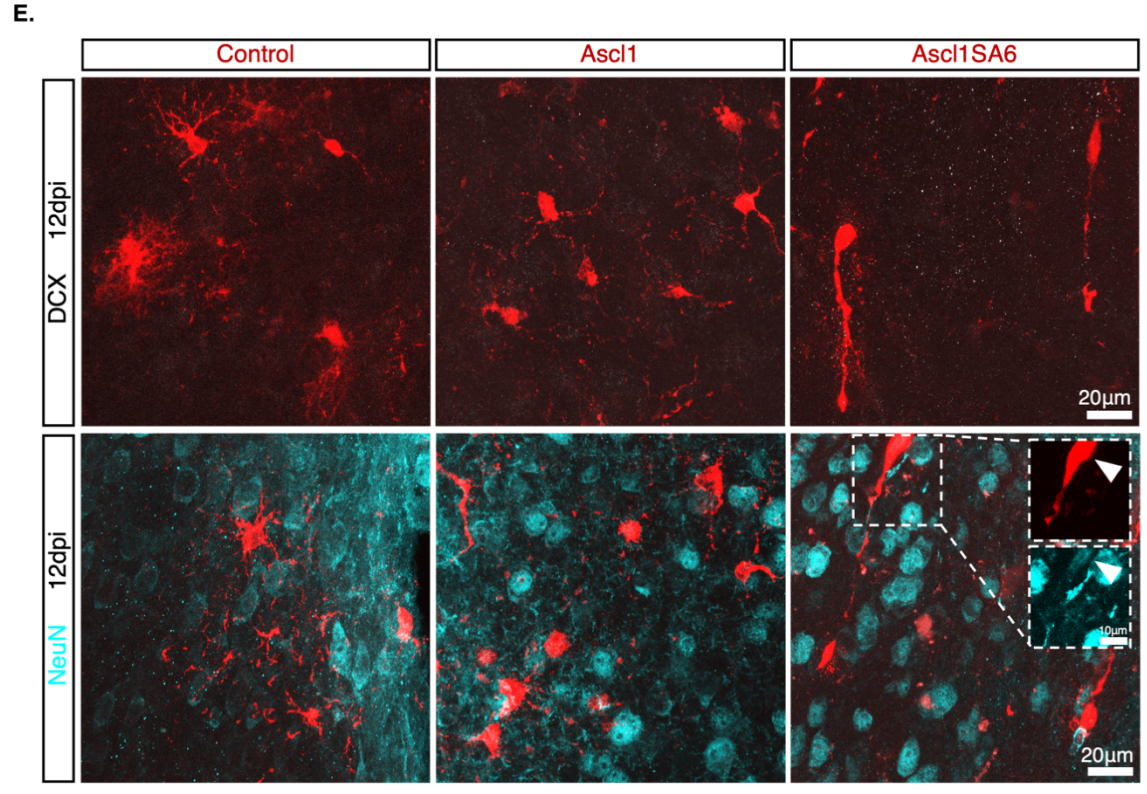
E.
Control
Ascl1
Ascl1SA6
DCX 12dpi
NeuN 12dpi
20µm
10µm

Figure 7: Ascl1SA6 alone induces minimal neuronal marker expression at 12 days post-injection (dpi). A. Schematic representation of experimental approach. Cortical stab-wound injury was performed in the somatosensory cortex of adult mice (day -3). Retrovirus encoding DsRed only (control), Ascl1 or Ascl1SA6 was injected three days following cortical stab-wound injury (day 0). At 12 dpi the identity of transduced cells was assessed by immunostaining against DCX (immature neuronal marker) and NeuN (mature neuronal marker). **B.** Representative confocal images displaying NeuN and DCX expression in the dentate gyrus (used as reference endogenous DCX expression). **C.** Quantification of the relative proportion of transduced cells that expressed DCX or NeuN at 12 dpi. **D.** Representative confocal images highlighting DCX- (in white, first panel) or NeuN- (in cyan, second panel) expression in transduced cells (in red). White arrowheads indicate marker-positive cells and empty arrowheads indicate marker-negative cells. Data shown as mean ± SD. Statistical tests: Kruskal Wallis test followed by Dunn's multiple comparison test. n=3 mice/group, control: 171 cells analyzed, Ascl1: 446 cells analyzed; Ascl1SA6: 160 cells analyzed.

4.2.3. Co-expression of Ascl1SA6 and Bcl2 enhances conversion of reactive glia into neuronal-like cells in the injured adult cortex

The very low proportion of Ascl1SA6-transduced cells that expressed neuronal markers suggests that Ascl1SA6 alone is insufficient to achieve efficient neuronal conversion in the injured adult cortex. Previous work by Gascón et al. (2016) demonstrated that Bcl2 co-expression with reprogramming factors drastically enhances reprogramming efficiency by preventing ferroptosis-mediated death of induced neurons (iNs). Furthermore, Marichal et al. (2024) demonstrated that co-expression of Bcl2 with Ascl1SA6 induced robust neuronal conversion in the postnatal intact brain, thus, prompting the co-expression of Ascl1SA6 and Bcl2 to test whether it could improve neuronal conversion efficiency in the injured adult cortex.

To test the effect of Bcl2 co-expression, retroviruses encoding either DsRed only (as control), Ascl1-Bcl2 (CAG-Ascl1-T2A-Bcl2-IRES-DsRed) or Ascl1SA6-Bcl2 (CAG-Ascl1SA6-T2A-Bcl2-IRES-DsRed) were injected three days after cortical stab-wound injury. The expression of neuronal markers, DCX and NeuN, was assessed by immunostaining at 12 dpi (Figure 8A). At this stage, morphological changes were evident across groups. While most Ascl1-Bcl2-transduced cells largely retained glial-like features with small somata and multiple short and thin processes, most Ascl1SA6-Bcl2 transduced cells exhibited more rounded somata with one or two elongated processes extending from the cell body, resembling neuronal morphology (Figure 8C).

Quantification of marker expression revealed minimal DCX expression with no significant differences between groups (control: 0 ± 0%, Ascl1-Bcl2: 1.30 ± 2.24%, Ascl1SA6-Bcl2: 0 ± 0%, Figure 8B, D). DCX-expressing cells were detected only sporadically in the Ascl1-Bcl2 group (observed in one animal, n=3 total), suggesting that co-expressing Bcl2 may enhance survival or persistence of rare immature neuron-like cells generated by Ascl1 overexpression, which is consistent with the limited neuronal conversion reported for Ascl1 and Bcl2 in the postnatal intact cortex (Marichal et al., 2024). In contrast, NeuN expression was detected exclusively in cells transduced with Ascl1SA6-Bcl2-transduced (control: 0 ± 0%, Ascl1-Bcl2: 0 ± 0%, Ascl1SA6-Bcl2: 11.1 ± 6.13%, Figure 8B, D). Comparing these results with AsclSA6 alone (1.49 ± 1.30%, subsection 4.2.2), Bcl2 co-expression increased the proportion of NeuN-expressing transduced cells (from 1.49% to 11.1%), demonstrating that Bcl2 substantially enhanced the reprogramming efficiency, likely due to improved cell survival.

Notably, a striking discrepancy was observed between the relatively low proportion of NeuN-expressing transduced cells (11.1%) and the high proportion

Ascl1SA6-Bcl2-transduced cells that displayed neuronal morphology at 12 dpi (Figure 8C). These cells that undergo morphological conversion without acquiring detectable neuronal marker expression are hereafter referred to as "neuronal-like cells" to distinguish them from iNs. The abundance of neuronal-like cells suggests that either most Ascl1SA6-Bcl2-transduced cells remain in a partially converted state at this stage, or alternatively, that NeuN detection may underestimate neuronal conversion efficiency in the injured cortex.

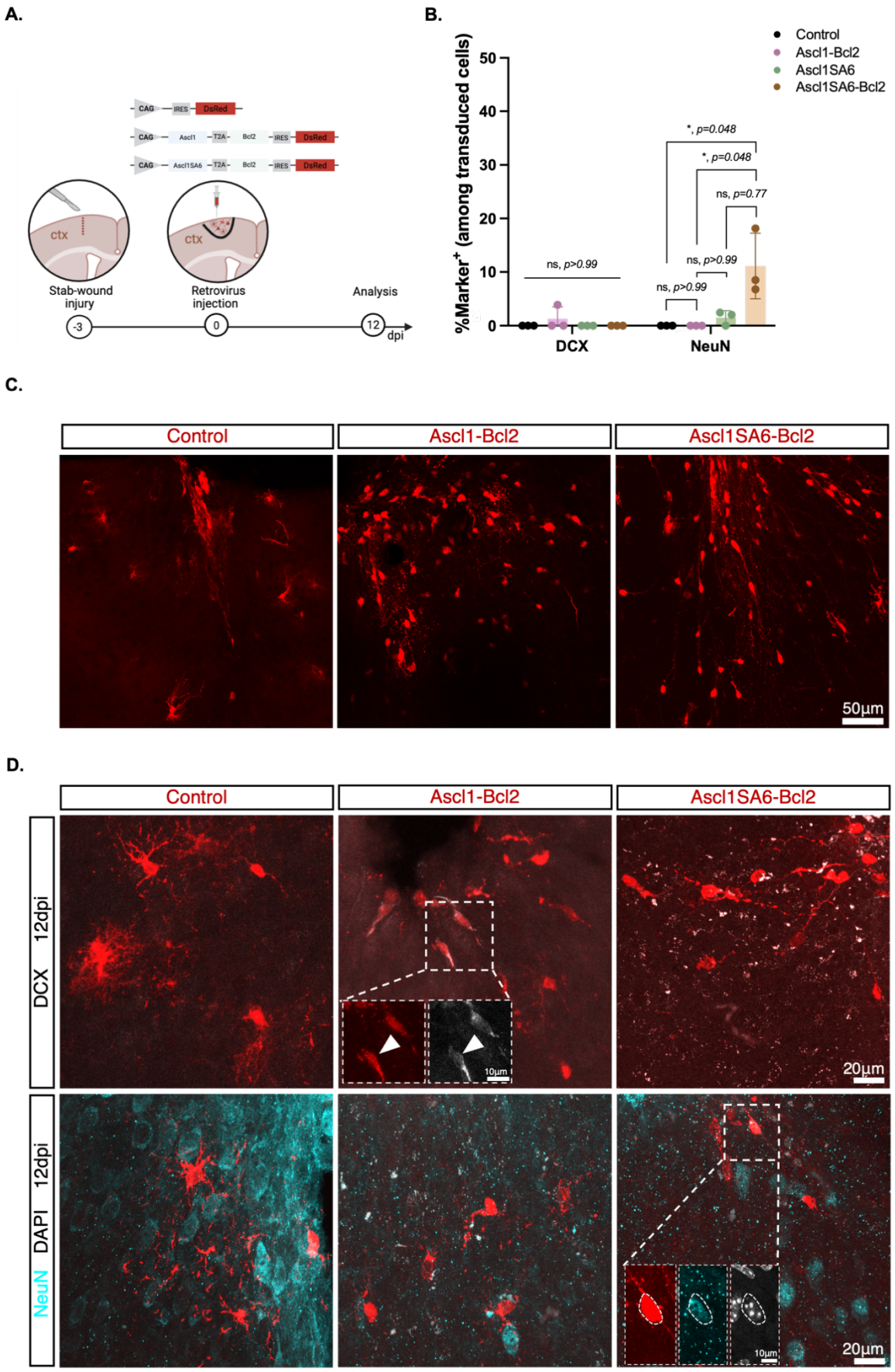
A.
CAG
IRES
DsRed
Ascl1
T2A
Bcl2
Ascl1SA6
ctx
Stab-wound injury
Retrovirus injection
Analysis
-3
0
12
dpi
B.
Control
Ascl1-Bcl2
Ascl1SA6
Ascl1SA6-Bcl2
%Marker+ (among transduced cells)
ns, p>0.99
*, p=0.048
*, p=0.048
ns, p=0.77
ns, p>0.99
ns, p>0.99
DCX
NeuN
C.
Control
Ascl1-Bcl2
Ascl1SA6-Bcl2
50µm
D.
Control
Ascl1-Bcl2
Ascl1SA6-Bcl2
DCX 12dpi
NeuN DAPI 12dpi
10µm
20µm
10µm
20µm

Figure 8: Co-expression of Ascl1SA6 and Bcl2 enhances conversion of reactive glia into neuronal-like cells in the injured adult cortex at 12 days post-injection (dpi). A. Schematic representation of experimental approach. Retrovirus encoding DsRed only (as control), Ascl1-Bcl2 or Ascl1SA6-Bcl2 were injected three days following cortical stab-wound injury. At 12 dpi immunostaining against DCX (immature neuronal marker) or NeuN (mature neuronal marker) was performed to assess expression of neuronal markers in transduced cells. **B.** Quantification of the proportion of transduced cells expressing DCX or NeuN at 12 dpi. **C.** Representative confocal images showing transduced cells (in red) in the injured cortex. **D.** Representative confocal images highlighting DCX (in white) or NeuN (in cyan) and DAPI (in white) expression in transduced cells. White arrowheads indicate marker-positive cells. Data shown as mean ± SD. Statistical tests: Kruskal Wallis test followed by Dunn's multiple comparison test. n=3 mice per group, control: 171 cells analyzed, Ascl1-Bcl2: 103 cells analyzed and Ascl1SA6-Bcl2: 285 cells analyzed.

4.2.4. Ascl1SA6-Bcl2-mediated neuronal conversion may be underestimated due to loss of NeuN antigenicity in the injured adult cortex.

The detection of NeuN expression in Ascl1SA6-Bcl2-transduced cells (11.1%, subsection 4.2.3), represents a significant improvement over Ascl1SA6 alone (1.15%, subsection 4.2.2). However, the overall proportion remained lower than expected given that most transduced cells exhibited neuronal-like morphology. This raised the question of whether the limited NeuN detection reflected incomplete neuronal conversion or technical limitation in marker detection.

Brain injury has been shown to cause transient or progressive loss of NeuN immunoreactivity due to protein degradation or loss of antigenicity (Hernandez et al., 2019; Munoz-Ballester et al., 2022). Despite reduced NeuN signal, neurons remain identifiable using Nissl-based stains, which bind to ribosomal RNA in the rough endoplasmic reticulum of neuronal cell bodies (Munoz-Ballester et al., 2022). Therefore, NeuroTrace (a fluorescence Nissl dye) was used as an alternative neuronal marker to test whether NeuN immunoreactivity underestimates neuronal conversion in the injured adult cortex.

At 12 dpi, NeuN and NeuroTrace expression was accessed in the injured adult cortex. In regions distant to the injury site, NeuN and Neurotrace co-localized, confirming that both marker label neuronal population (Figure 9B). However, NeuN signal was largely reduced or absent within and closely surrounding the injury site, corresponding to the region containing most transduced cells (Figure 9D). In contrast, NeuroTrace labeling remained robust (Figure 9B), which supports that regional loss of NeuN immunoreactivity occurs specifically at the reprogramming site (injury + retrovirus injection). Moreover, many Ascl1SA6-Bcl2-transduced cells displaying neuronal-like morphology lacked NeuN expression (Figure 9D). In contrast, analysis of Neurotrace expression revealed a significantly higher proportion of NeuroTrace-expressing transduced cells compared to the NeuN-expressing fraction (Ascl1SA6-Bcl2: 11.1 ± 6.13% NeuN vs 32.2 ± 11.5% Neurotrace, p=0.04, Figure 8C, D, E), indicating that neuronal identity of transduced cells was underestimated with NeuN immunolabeling. In addition, Neurotrace labeling was also evaluated in cells transduced with control and Ascl1-Bcl2. Analysis revealed no detectable expression in control group (control: 0 ± 0%, vs Ascl1SA6-Bcl2 p=0.043, Figure 9F, G) and minimal labeling of Ascl1-Bcl2-transduced cells (Ascl1-Bcl2: 1.30 ± 2.25%, Figure 9F, G), indicating limited reprogramming competency of Ascl1 and Bcl2 in the injured adult cortex.

In summary, these results suggest that Ascl1SA6-Bcl2 can induce neuronal conversion in the injured adult cortex. However, the maturation state of the iNs remains unclear due to a) potential injury-induced loss of NeuN signal, b) inability to distinguish between immature or mature states with Neurotrace labeling, and c) absence of DCX expression (subsection 4.2.3).

4.2.5. Most Ascl1SA6-Bcl2-transduced cells do not retain glial identity in the injured adult cortex

The persistent discrepancy between the proportion of transduced cells that displayed neuronal-like morphology and those that expressed neuronal markers prompted the important question of whether Ascl1SA6-Bcl2-transduced cells retain their initial glial identity or remain in an intermediate state between neuronal and glial fate.

To determine whether Ascl1SA6-Bcl2-transduced cells achieve complete neuronal reprogramming, expression of glial markers was assessed at 12 dpi. Given that most control-transduced cells are oligodendroglial cells or reactive astrocytes, Sox10 and GFAP expression was analyzed in transduced cells. Moreover, overexpression of Ascl1SA6 alone reduced both Sox10- (from 56% to 16%, subsection 4.2.1) and GFAP-(from 23.5% to 0.54%, subsection 4.2.1) expression at 4 dpi. Thus, it was next examined whether this effect persists at 12 dpi in Ascl1SA6-Bcl2-transduced cells.

Retroviruses encoding control, Ascl1-Bcl2 or Ascl1SA6-Bcl2 were injected in the injured adult cortex and immunostaining against Sox10 and GFAP was performed at 12 dpi (Figure 10A). Quantification revealed a significant decrease in Sox10 expression in cells transduced with Ascl1SA6-Bcl2 compared to Ascl1-Bcl2 (control: 52.2 ± 10.4%, Ascl1-Bcl2: 69.2 ± 4.17%, Ascl1SA6-Bcl2: 6.27 ± 2.33%, p=0.02, Figure 10B, C), highlighting the distinct effect between the two phosphorylation states of Ascl1 in lineage fate and that Ascl1SA6-Bcl2 further downregulated oligodendroglial identity markers by 12 dpi. Additionally, in the Ascl1SA6-Bcl2 group, Sox10-expressing transduced cells lacked neuronal-like morphology (Figure 10C), indicating that these cells likely failed to undergo neuronal conversion.

In contrast, GFAP expression was not detected in Ascl1-Bcl2 or Ascl1SA6-Bcl2-transduced cells (control: 14.5 ± 8.53%, Ascl1-Bcl2: 0 ± 0%, Ascl1SA6-Bcl2: 0 ± 0%, Figure 10B, C). The absence of GFAP expression may reflect loss of astroglial identity or suppression of astrocytic reactivity. Together, these findings demonstrate that

Ascl1SA6-Bcl2 downregulates glial marker expression in the injured cortex, consistent with progression away from glial states.

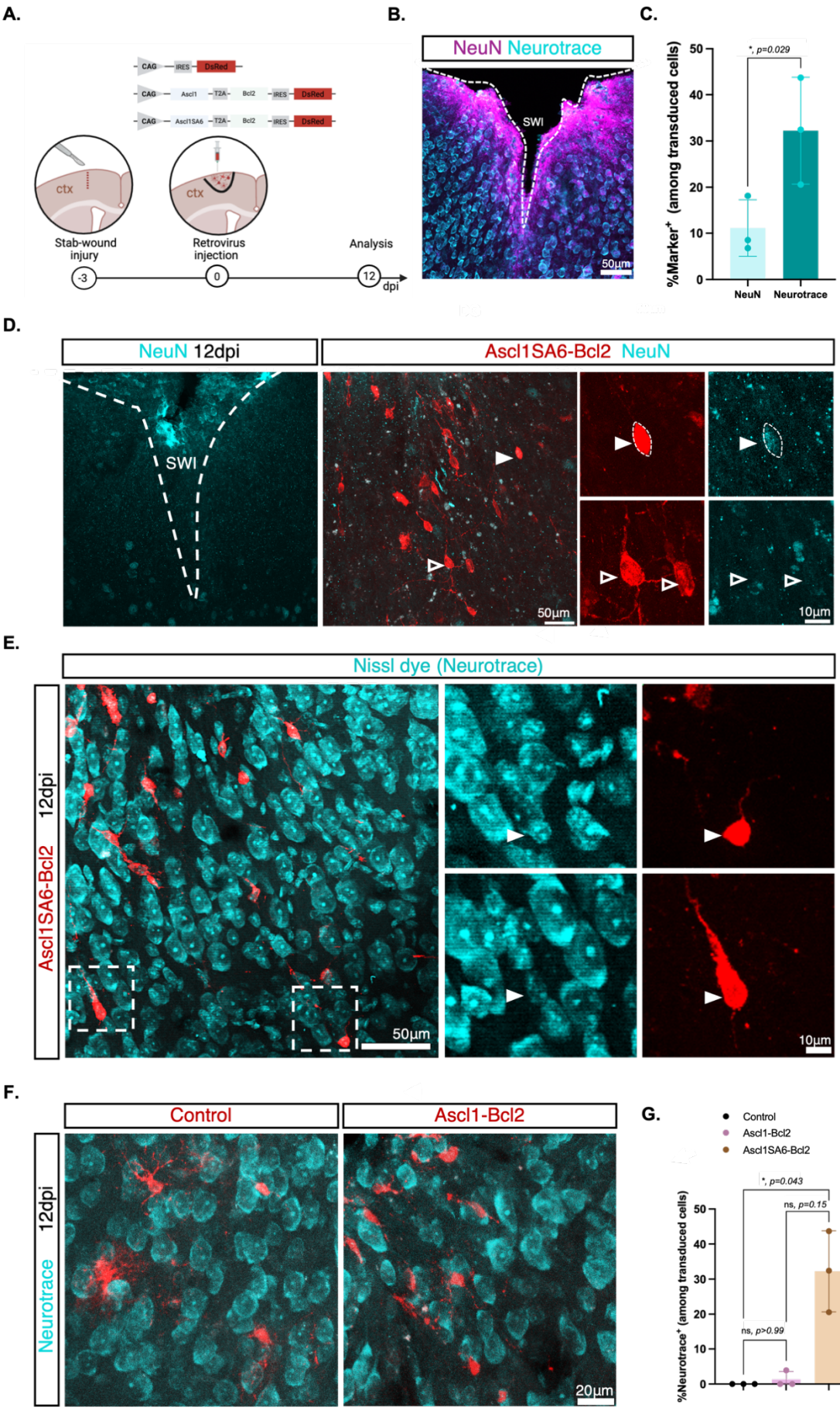
A.
CAG IRES DsRed
CAG Ascl1 T2A Bcl2 IRES DsRed
CAG Ascl1SA6 T2A Bcl2 IRES DsRed
ctx
ctx
Stab-wound injury
Retrovirus injection
Analysis
-3
0
12
dpi
B.
NeuN Neurotrace
SWI
50µm
C.
*, p=0.029
%Marker+ (among transduced cells)
NeuN
Neurotrace
D.
NeuN 12dpi
Ascl1SA6-Bcl2 NeuN
SWI
50µm
10µm
E.
Nissl dye (Neurotrace)
Ascl1SA6-Bcl2 12dpi
50µm
10µm
F.
Control
Ascl1-Bcl2
Neurotrace 12dpi
20µm
G.
Control
Ascl1-Bcl2
Ascl1SA6-Bcl2
*, p=0.043
ns, p=0.15
ns, p>0.99
%Neurotrace+ (among transduced cells)

Figure 9: Ascl1SA6-Bcl2-mediated neuronal conversion may be underestimated due to loss of NeuN antigenicity in the injured adult cortex. A. Schematic representation of experimental approach. Retrovirus encoding control, Ascl1-Bcl2 or Ascl1SA6-Bcl2 was injected three days following cortical stab-wound injury. At 12 dpi immunostaining against NeuN (mature neuronal marker) and Neurotrace (fluorescent Nissl dye) was performed to compare neuronal marker detection in transduced cells. **B.** Representative confocal images demonstrating co-localization of NeuN (in cyan) and Neurotrace (in magenta) in the injured cortex. **C.** Quantification of the proportion of Ascl1SA6-Bcl2-transduced cells expressing NeuN or Neurotrace at 12 dpi. **D.** Representative confocal images showing NeuN (in cyan) expression in the injured cortex and in transduced cells (in red) **E.** Representative confocal images highlighting Neurotrace (in cyan) labeling in Ascl1SA6-Bcl2-transduced cells (in red). **F.** Representative confocal images showing Neurotrace (in cyan) expression in control or Ascl1-Bcl2-transduced cells (in red). **G.** Quantification of the proportion of transduced cells expressing Neurotrace at 12 dpi. White arrowheads indicate marker-positive cells and empty arrowheads indicate marker-negative cells. Data shown as mean ± SD. Statistical tests: paired t-test (% marker positive cells) or Kruskal Wallis test followed by Dunn's multiple comparison test (% Neurotrace$^+$). n=3 mice per group, control: 171 cell analyzed, Ascl1-Bcl2: 103 cells analyzed and Ascl1SA6-Bcl2: 285 cells analyzed.

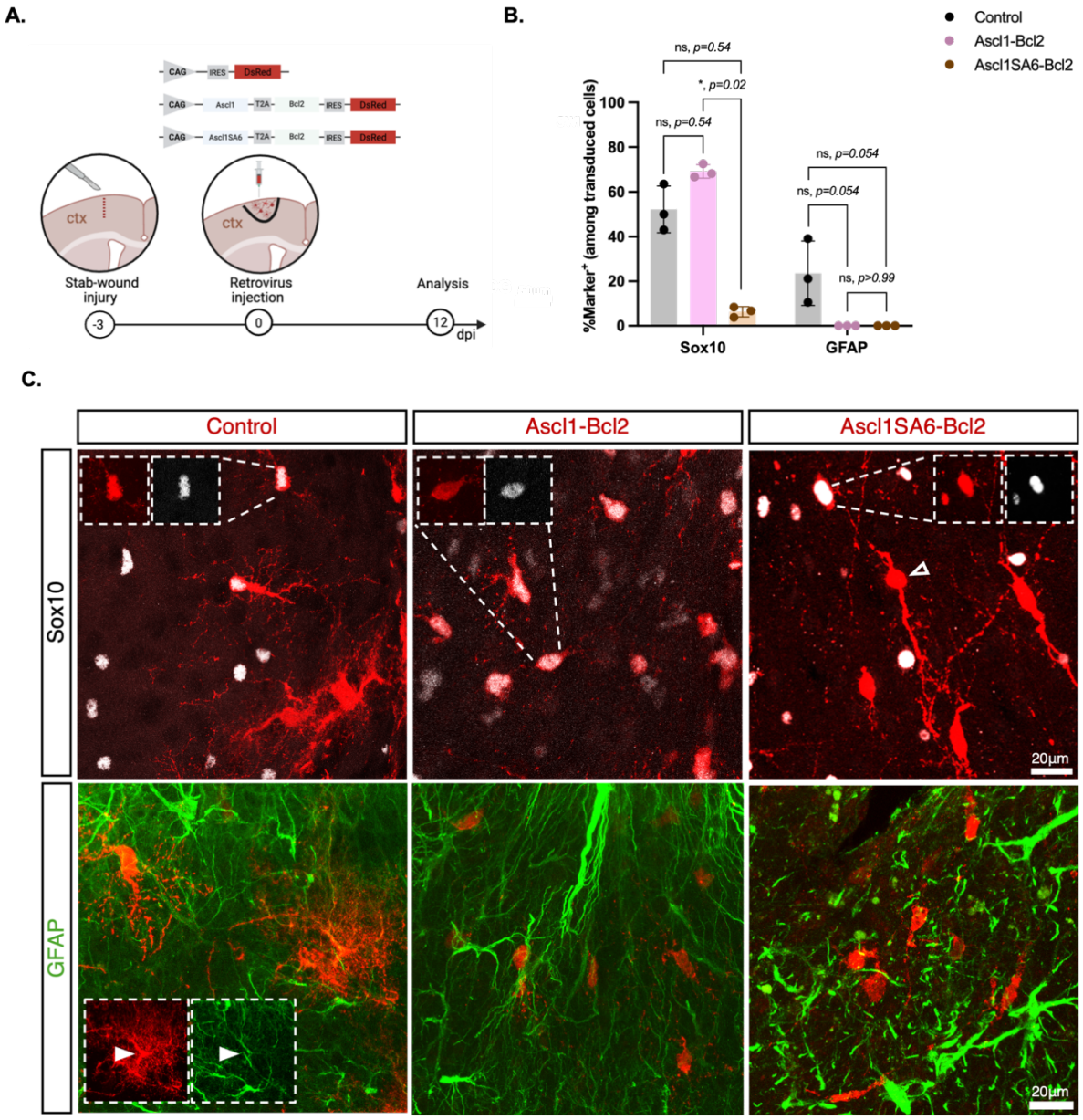

Figure 10: Most Ascl1SA6-Bcl2-transduced cells do not retain glial identity in the injured adult cortex. A. Schematic representation of experimental approach. Retrovirus encoding control, Ascl1-Bcl2 or Ascl1SA6-Bcl2 was injected three days after cortical stab-wound injury. At 12 dpi immunostaining against Sox10 (oligodendroglial marker) and GFAP (reactive astrocyte marker) was performed to assess expression of glial markers in transduced cells. **B.** Quantification of the proportion of transduced cells expressing Sox10 or GFAP at 12 dpi. **C.** Representative confocal images showing Sox10 (in white) or GFAP (in green) expression in transduced cells (in red) in the injured cortex. White arrowheads indicate marker-positive cells. Data shown as mean ± SD. Statistical tests: paired t-test (% Sox10$^+$) or Kruskal Wallis test followed by Dunn's multiple comparison test (% GFAP$^+$). n=3 mice per group, control: 240 cells analyzed; Ascl1-Bcl2: 283 cells analyzed; Ascl1SA6-Bcl2: 285 cells analyzed cells analyzed.

4.2.6. Genetic fate-mapping reveals that induced neuron-like cells do not derive from reactive astrocytes in the injured adult cortex

The marked loss of Sox10 expression in Ascl1SA6-Bcl2-transduced cells, together with the observation that oligodendroglial lineage cells constitute the majority of the initially transduced population (53%, subsection 4.1.1), suggests that OPCs represent a major cellular substrate for neuronal conversion in the injured adult cortex. Additionally, the near-complete loss of GFAP expression suggests that reactive astrocytes either do not persist after Ascl1SA6-Bcl2 transduction or contribute minimally to the reprogrammed population. Nevertheless, in the postnatal intact cortex, astrocytes were shown to be the primary cellular source of Ascl1SA6-Bcl2-derived iNs (Marichal et al., 2024), raising the question of whether astrocytes also contribute to neuronal conversion in the injured adult cortex despite the overall lack of GFAP expression.

To determine the cellular origin of the Ascl1SA6-Bcl2 induced neuronal-like cells, genetic fate-mapping was performed using transgenic mouse lines that specifically label distinct glial populations. First, to reveal if iNs originate from astrocytes, Aldh1l1-CreER^{T2} transgenic mice (Srinivasan et al., 2016) were crossed with RCE:loxP reporter mice (Sousa et al., 2009) to generate Aldh1l1-CreER^{T2}/RCE mice, in which astrocytes were endogenously labeled with GFP. To induce Cre recombination and GFP expression in astrocytes, tamoxifen (150mg/kg) was administered daily for five consecutive days. This was then followed by cortical injury and retroviral injection encoding of Ascl1SA6-Bcl2 (Figure 11A).

Astrocyte labeling efficiency was first evaluated at 12 dpi by assessing co-expression of GFP with the astrocytic marker Sox9. Analysis revealed most Sox9-expressing cells co-expressed GFP in the injured adult cortex (GFP$^+$/Sox9$^+$: 57.5 ± 16.3%, GFP$^-$/Sox9$^+$: 42.5 ± 16.3%, Figure 11B, C), indicating robust astrocyte labeling in Aldh1l1-CreER^{T2}/RCE mice.

To determine whether Ascl1SA6-Bcl2-iNs derive from reactive astrocytes, GFP co-expression with neuronal markers (NeuN or NeuroTrace) was analyzed in transduced cells at 12 dpi. Strikingly, none of the NeuN- or Neurotrace-expressing transduced cells co-expressed GFP (RFP$^+$/GFP$^+$/NeuN$^+$: 0 ± 0%, RFP$^+$/GFP$^+$/Neurotrace$^+$: 0 ± 0%, Figure 11D, E). However, a small fraction of transduced cells that lacked neuronal marker expression were fate-mapped to astrocytes (RFP$^+$/GFP$^+$/NeuN$^-$: 5.65 ± 1.85%, Figure 11D, E). Importantly, fate-mapped cells exhibited neuronal-like morphology, including altered soma shape and elongated processes, suggesting that transduced reactive astrocytes initiate fate

conversion. Despite this morphology shift, none of the fate-mapped cells with neuronal-like morphology expressed NeuN or Neurotrace (Figure 11D, E), indicating incomplete or arrested neuronal reprogramming of reactive astrocytes to Ascl1SA6-Bcl2 by 12 dpi.

In summary, these findings demonstrate that in the injured adult cortex, reactive astrocytes are largely refractory to Ascl1SA6-Bcl2-mediated neuronal reprogramming. In contrast, transduced cells that acquire both neuronal morphology and neuronal markers expression seem to derive from non-astrocytic cells.

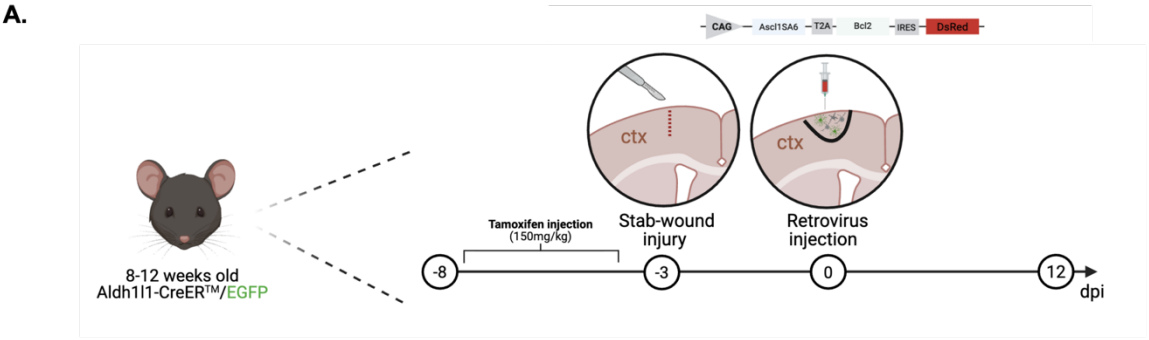
A.
CAG
Ascl1SA6
T2A
Bcl2
IRES
DsRed
ctx
ctx
8-12 weeks old
Aldh1l1-CreER™/EGFP
Tamoxifen injection
(150mg/kg)
Stab-wound
injury
Retrovirus
injection
-8
-3
0
12
dpi

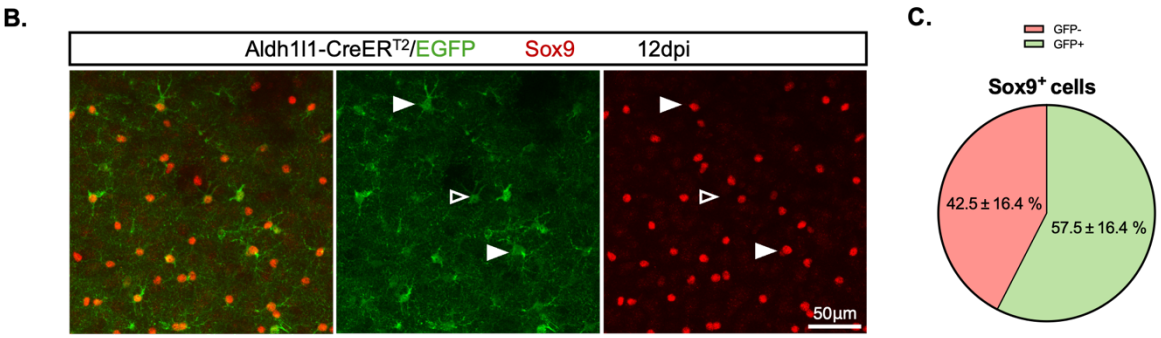
B.
Aldh1l1-CreER^T2/EGFP Sox9 12dpi
50μm
C.
GFP-
GFP+
Sox9+ cells
42.5 ± 16.4 %
57.5 ± 16.4 %

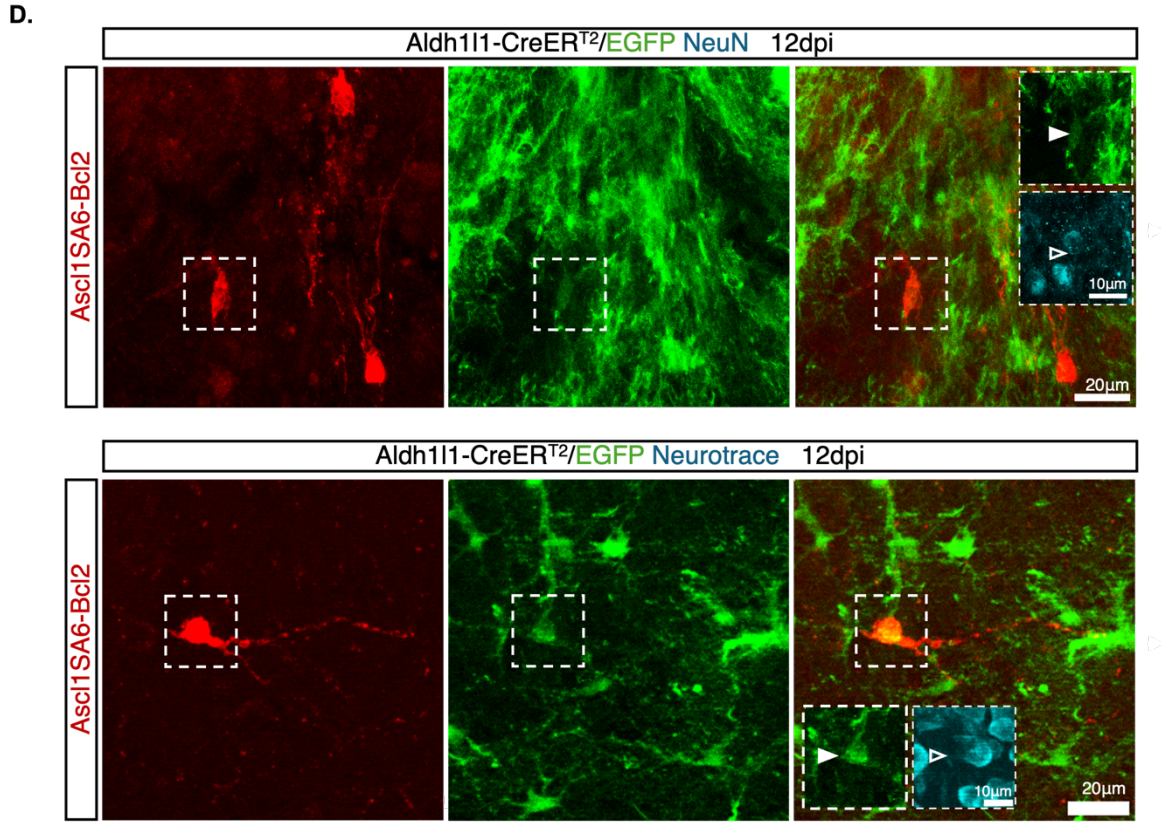
D.
Aldh1l1-CreER^T2/EGFP NeuN 12dpi
Ascl1SA6-Bcl2
10μm
20μm
Aldh1l1-CreER^T2/EGFP Neurotrace 12dpi
Ascl1SA6-Bcl2
10μm
20μm

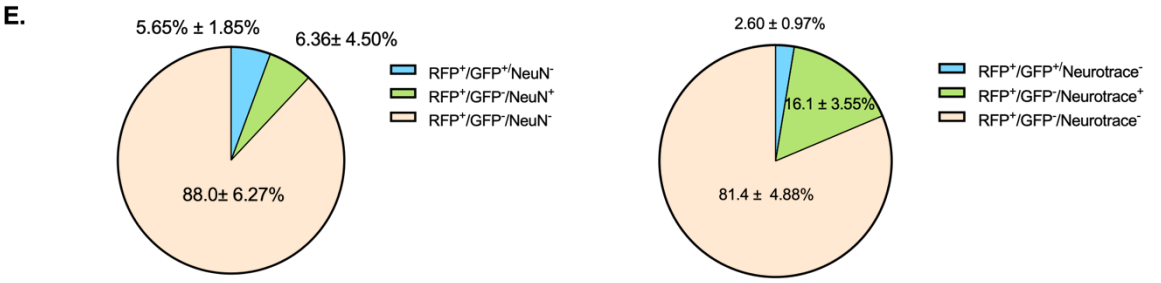
E.
5.65% ± 1.85%
6.36± 4.50%
88.0± 6.27%
RFP+/GFP+/NeuN-
RFP+/GFP-/NeuN+
RFP+/GFP-/NeuN-
2.60 ± 0.97%
16.1 ± 3.55%
81.4 ± 4.88%
RFP+/GFP+/Neurotrace-
RFP+/GFP-/Neurotrace+
RFP+/GFP-/Neurotrace-

Figure 11: Genetic fate-mapping revealed that induced neurons do not derive from reactive astrocytes in the injured cortex. A. Schematic representation of experimental approach. Retrovirus encoding Ascl1SA6-Bcl2 was injected in Aldh1l1-CreER^{T2}/RCE mice three days following cortical stab-wound injury. To induce Cre-recombination for the labeling of astrocytes with GFP, mice received one intraperitoneal injection of tamoxifen daily for five consecutive days. **B.** Representative confocal images displaying labeling efficiency in Aldh1l1-CreER^{T2}/RCE mice at 12 dpi. **C.** Quantification of the percentage of Sox9-expressing cells that co-express GFP in the cortex at 12 dpi. **D.** Representative confocal images showing GFP and neuronal markers (NeuN or NeuroTrace, in cyan) expression in Ascl1SA6-Bcl2-transduced cells (in red) **E.** Pie-chart with the relative proportion of transduced cells that express GFP, GFP and NeuN/NeuroTrace or NeuN/Neurotrace that are GFP negative at 12 dpi. White arrowheads indicate marker-positive cells. Data shown as mean ± SD. n=3 mice per group, Ascl1SA6-Bcl2: 120 transduced cells analyzed.

4.2.7. Genetic fate-mapping reveals that a subset of induced neuronal-like cells derived from oligodendrocyte precursor cells in the injured adult cortex

Given that astrocytes do not appear to be the cellular origin of Ascl1SA6-Bcl2-induced neuronal-like cells, and that oligodendroglial lineage cells constitute the majority of the initial transduced population (53%, subsection 4.1.1), it was next tested iNs derive from OPCs. For this, NG2-CreER^{TM} (Zhu et al., 2011) were crossed with RCE:loxP (Sousa et al., 2009) reporter mice to generate NG2-CreER^{TM}/RCE mice, enabling the endogenous labeling of OPCs with GFP. GFP expression was induced by daily administration tamoxifen (150mg/kg) for five consecutive days, followed by cortical injury and Ascl1SA6-Bcl2 retroviral injection (Figure 12A).

OPC labeling efficiency was evaluated at 12 dpi by assessing co-expression of GFP and the OPC marker platelet-derived growth factor receptor alpha (PDGFRα). Analysis revealed that most PDGFRa-expressing cells co-expressed GFP in the injured cortex (GFP$^+$/PDGFRα$^+$: 56.1 ± 17.1%, GFP$^-$/ PDGFRα $^+$: 43.9 ± 17.1%, Figure 12B, C), indicating robust labeling of OPCs in NG2-CreER^{TM}/RCE mice.

To determine whether Ascl1SA6-Bcl2-induced neuronal-like cells originate from OPCs, co-expression of neuronal markers (NeuN and Neurotrace) and GFP were detected in transduced cells at 12 dpi. A subset of transduced cells co-expressed both GFP and NeuN or Neurotrace (RFP$^+$/GFP$^+$/NeuN$^+$: 4.08 ± 3.92%, RFP$^+$/GFP$^+$/ Neurotrace$^+$: 11.6 ± 4.35%, Figure 12E), demonstrating that a subset of OPCs can successfully convert into Neurotrace or NeuN-expressing cells in the injured adult cortex. These OPC-derived iNs also displayed neuronal morphology with elongated processes and rounded somata (Figure 12D).

In addition, fate-mapped cells that did not express any neuronal marker (RFP$^+$/GFP$^+$/NeuN$^-$: 27.9 ± 4.99%, RFP$^+$/GFP$^+$/Neurotrace$^-$: 28.5 ± 8.80%, Figure 12D, E), predominantly displayed a neuronal-like morphology, suggesting that not all transduced OPCs that initiate morphological changes can successfully progress in their conversion into iNs by 12 dpi. This finding parallels observations in astrocyte fate-mapping (subsection 4.2.6), in which fate-mapped cells also displayed neuronal-like morphology without expressing neuronal markers. Despite the differences in proportion of fate-mapped transduced cells (astrocytes: 5.65% ± 1.85%, OPCs: 27.9 ± 4.99%, Figure 11E, 12E), it suggests that most Ascl1SA6-Bcl2-transduced cells fails to acquire neuronal molecular identity at this stage, thus, raising the question of whether this effect reflects hurdles in the local environment that limit efficient neuronal conversion in the injured adult cortex.

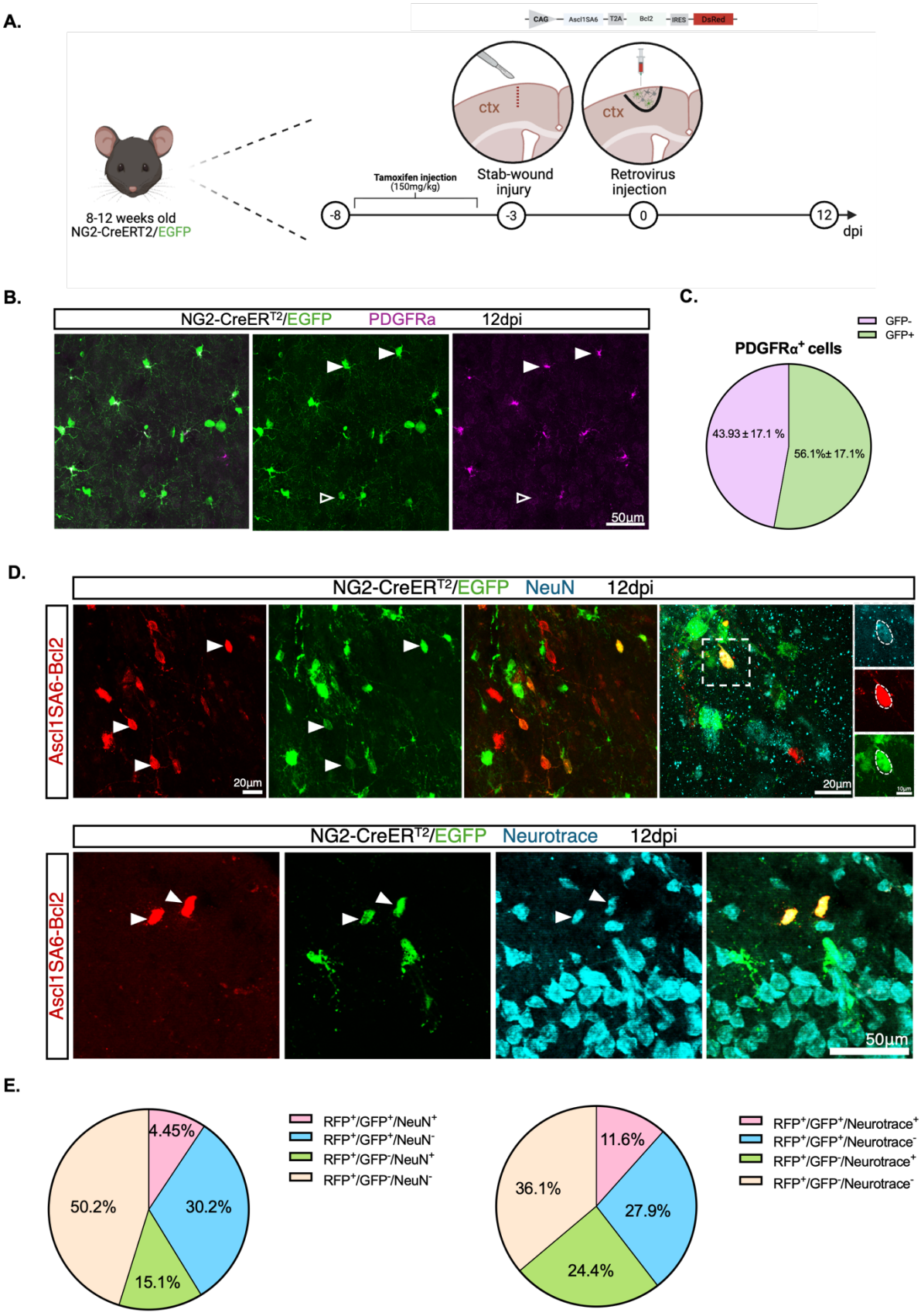
A.
CAG
Ascl1SA6
T2A
Bcl2
IRES
DsRed
ctx
ctx
8-12 weeks old
NG2-CreERT2/EGFP
Tamoxifen injection
(150mg/kg)
Stab-wound
injury
Retrovirus
injection
-8
-3
0
12
dpi
B.
NG2-CreER^{T2}/EGFP PDGFRa 12dpi
50µm
C.
GFP-
GFP+
PDGFRα^{+} cells
43.93 ± 17.1 %
56.1%± 17.1%
D.
NG2-CreER^{T2}/EGFP NeuN 12dpi
Ascl1SA6-Bcl2
20µm
20µm
10µm
NG2-CreER^{T2}/EGFP Neurotrace 12dpi
Ascl1SA6-Bcl2
50µm
E.
4.45%
30.2%
15.1%
50.2%
RFP^{+}/GFP^{+}/NeuN^{+}
RFP^{+}/GFP^{+}/NeuN^{-}
RFP^{+}/GFP^{-}/NeuN^{+}
RFP^{+}/GFP^{-}/NeuN^{-}
11.6%
27.9%
24.4%
36.1%
RFP^{+}/GFP^{+}/Neurotrace^{+}
RFP^{+}/GFP^{+}/Neurotrace^{-}
RFP^{+}/GFP^{-}/Neurotrace^{+}
RFP^{+}/GFP^{-}/Neurotrace^{-}

Figure 12: Genetic fate-mapping reveals that some induced neuronal-like cells derive from oligodendrocyte precursor cells in the injured cortex. A. Schematic representation of experimental approach. Retrovirus encoding Ascl1SA6-Bcl2 was injected in NG2-CreER^{TM}/RCE mice three days following cortical stab-wound injury. To induce Cre-recombination for the labeling of astrocytes with GFP, mice received one intraperitoneal injection of tamoxifen daily for five consecutive days. **B.** Representative confocal images displaying labeling efficiency in NG2-CreER^{TM}/RCE mice at 12 dpi. **C.** Quantification of the percentage of PDGFRα-expressing cells that co-express GFP in the cortex at 12 dpi. **D.** Representative confocal images showing GFP and neuronal markers (NeuN or NeuroTrace, in cyan) expression in transduced cells (in red) **E.** Pie chart with relative proportion of transduced cells that express GFP and NeuN/NeuroTrace or NeuN/Neurotrace but are GFP negative at 12 dpi. White arrowheads indicate marker-positive cells. Data shown as mean ± SD. n=3 mice per group, Ascl1SA6-Bcl2: 120 cells analyzed.

4.3. Environmental hurdles for neuronal reprogramming following Ascl1SA6 and Bcl2 overexpression in the injured adult cortex

Genetic fate-mapping experiments revealed that cellular competence for Ascl1SA6-Bcl2-mediated neuronal conversion is context-dependent. In the intact postnatal cortex, astrocytes serve as the primary cellular source for successful reprogramming and achieve robust neuronal conversion (Marichal et al., 2024). In contrast, observations in the injured adult cortex demonstrated that Ascl1SA6-Bcl2 failed to efficiently convert reactive astrocytes but instead achieved partial conversion of OPCs (subsections 4.2.6 and 4.2.7). Moreover, the limited neuronal conversion efficiency by Ascl1SA6-Bcl2 in the injured adult cortex, together with the high proportion of partially reprogrammed cells characterized by neuronal-like morphology without marker expression, suggests that the local environment may be restricting complete neuronal conversion. Since neuronal conversion was induced in the injured cortex, where the cellular environment is pro-inflammatory, the surrounding milieu was investigated as a potential barrier to reprogramming.

4.3.1 Characterization of the reactive environment induced by cortical stab-wound injury and retroviral injection in the adult cortex

Cortical injury induces alterations of the local environment, characterized by infiltration of peripheral immune cells, recruitment and activation of glial cells (Bardehle et al., 2013; Buffo et al., 2008; Lucin & Wyss-Coray, 2009). At 12 dpi NeuN antigenicity was found reduced and neuronal conversion efficiency remained limited in the injured adult cortex (subsection 4.2.4), suggesting that environmental constrains may still hinder reprogramming at this stage. To assess this, the cellular environment at the reprogramming site was characterized by evaluating the glial response at 12 dpi following cortical stab-wound injury and retroviral injection. The retrovirus encoding Ascl1SA6 was selected for this characterization because it induces early morphological changes and downregulation of glial marker expression consistent with reprograming initiation (subsection 4.2.1), while failing to drive efficient neuronal conversion in the injured adult cortex (subsection 4.2.2). Thus, enabling analysis of the cellular environment under conditions in which reprogramming is initiated but does not efficiently progress. To distinguish the specific contribution of the retroviral injection from the lesion alone, an "injury-only" condition (without retrovirus injection) was analyzed in parallel (Figure 13A). Expression of the leukocyte common antigen CD45, Iba1 (for microglia) and GFAP (for reactive astrocytes) was assessed to evaluate immune infiltration, microglial recruitment and astrocytic activation, respectively in both conditions (Figure 13C). Cell densities were quantified within a ROI defined as

the cortical area surrounding the injury site, and in the reprogramming condition, the ROI additionally encompassed the area containing reporter-positive cells.

At 12 dpi, a pronounced accumulation of reactive glia (GFAP- and Iba1-expressing cells) and infiltration of peripheral leukocytes (CD45-expressing cells) were detected in both injury only and reprogramming site (Figure 13C). In the injured-only cortex, astrocytes and microglia displayed hypertrophic morphology characteristic of reactive states. This reactive phenotype appeared exacerbated at the reprogramming site, where reactive glia formed dense clusters surrounding transduced cells (Figure 13C). Quantification of marker-expressing cells confirmed a significant increase in Iba1-expressing cells at the reprogramming site compared with injury only (SWI only: 797.2 ± 178.1 $Iba1^+/mm^2$; reprogramming site: 1143.6 ± 232.3 $Iba1^+/mm^2$, p=0.03 Figure 9C, Figure 13B, C). A similar trend toward higher densities of CD45- and GFAP-expressing cells was also detected following retroviral injection (SWI only: 161.1 ± 32.9 $CD45^+/mm^2$, 1012.5 ± 433.6 $GFAP^+/mm^2$; reprogramming site: 638.6 ± 234.5 $CD45^+/mm^2$, 1753.1 ± 208.0 $GFAP^+/mm^2$) though this difference did not reach significance.

Together, these findings demonstrate that retroviral injection aggravates the injury-induced inflammatory and reactive glial response and that glia-to-neuron conversion is induced in a highly reactive milieu.

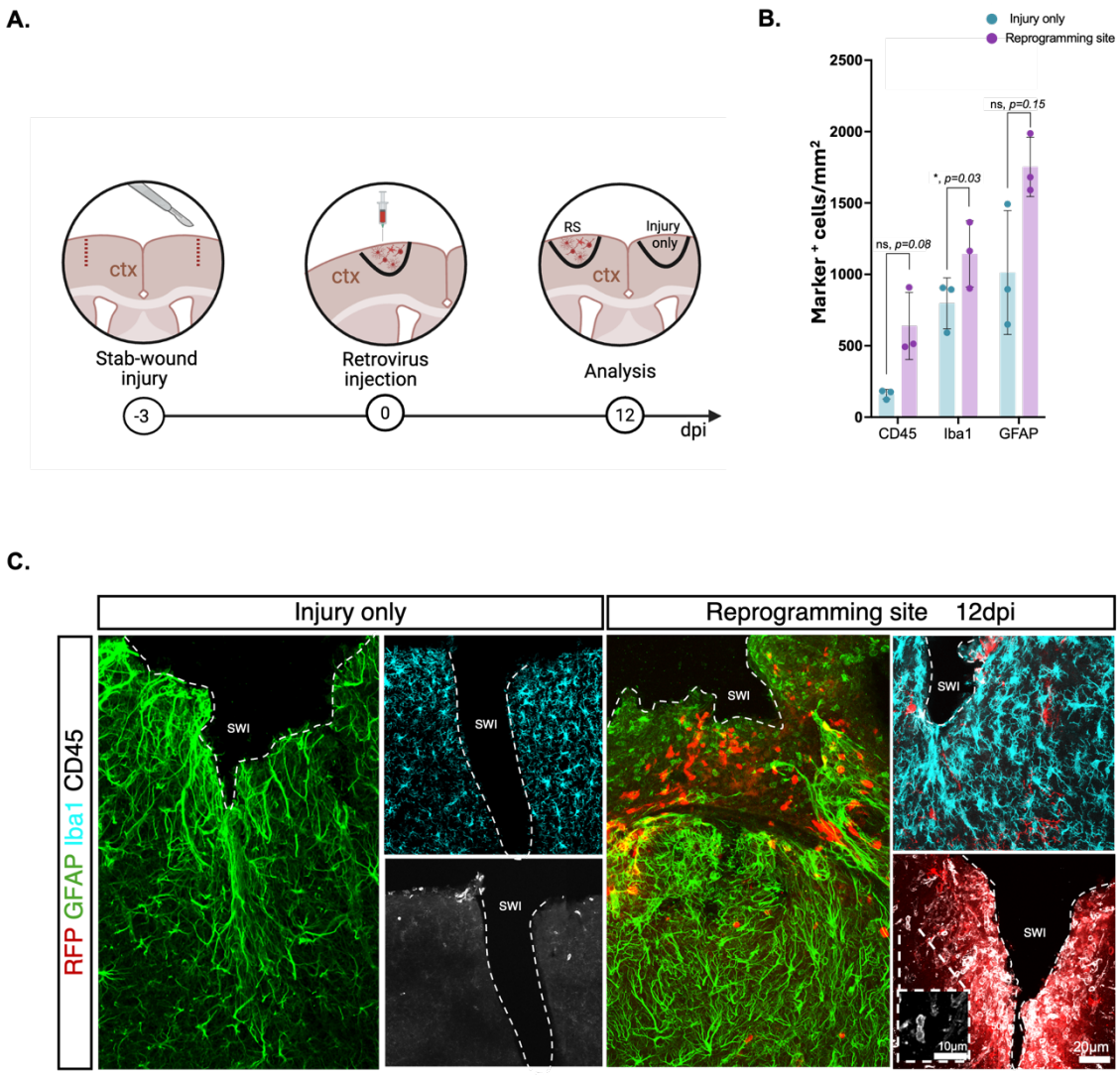

Figure 13: Retrovirus injection exacerbates glial reactivity and immune cell infiltration at the reprogramming site following cortical injury. A. Schematic representation of experimental approach. Cortical stab-wound injury was performed in the somatosensory cortex (injury only condition) and retrovirus encoding Ascl1SA6 was injected three days later. At 12 dpi immunostaining against GFAP (reactive astrocyte marker), Iba1 (microglial marker) and CD45 (leukocyte marker) was performed to assess expression of inflammatory hallmarks in the injured-only, and at the reprogramming site (injury and retroviral injection). **B.** Quantification of CD45-, Iba1- or GFAP-expressing cell density at 12 dpi in injury-only and reprogramming site. **C.** Representative confocal images showing CD45 (in white), GFAP (in green) or Iba1 (cyan) expression in both conditions (injury only vs reprogramming site). Data shown as mean ± SD. Statistical test: unpaired t-test. n=3 mice per group.

4.3.2 Complement 3 expression identifies neurotoxic reactive astrocytes within the reprogramming milieu

Since the reactive glial response was enhanced at the reprogramming site compared to injury alone (subsection 4.3.1), and brain injuries can trigger reactive astrocytes to adopt a neurotoxic phenotype that contributes to neuronal death (Guttenplan et al., 2020; Liddelow et al., 2017), it was next investigated whether such reactive astrocytes were present at the reprogramming site. This neurotoxic subtype of reactive astrocytes is characterized by the expression of complement 3 (C3), a key effector of the complement cascade and an essential component of the innate immune response (Lian et al., 2016; Stevens et al., 2007) C3-expressing reactive astrocytes secrete lipid-based factors that are toxic to neurons and oligodendrocytes *in vitro* and *in vivo* (Guttenplan et al., 2020; Liddelow et al., 2017), and their presence at the reprogramming site could represent a major environmental hurdle limiting neuronal conversion efficiency in the injured adult cortex.

To determine whether neurotoxic reactive astrocytes arise in the reprogramming site, C3 expression was assessed by immunostaining at 12 dpi, comparing injury-only (stab-wound injury) to the reprogramming site (injury and retroviral injection, Figure 14A). Analysis revealed robust C3 expression at both injury only and reprogramming site conditions (injury only: 452 ± 220 $C3^+/mm^2$, reprogramming site: 637 ± 145 $C3^+/mm^2$, p=0.29, Figure 14B, C), indicating that cortical injury induces C3 expression, and retrovirus expression or reprogramming induction does not significantly alter C3 cell density. C3-expressing cells displayed highly ramified, hypertrophic morphology which is characteristic of reactive astrocytes (Figure 14C).

To confirm the identity of C3-expressing cells, co-expression with GFAP (reactive astrocyte marker) was firstly assessed at the reprogramming site at 12 dpi. Strikingly, the majority C3-expressing cells co-expressed GFAP ($C3^+/GFAP^+$: 71.4 ± 1.62%, Figure 14B, C) confirming that C3-expressing cells are predominantly reactive astrocytes and indicating their abundant presence in the injured cortex at this stage.

Given that the neurotoxic phenotype acquired by astrocytes is activated by microglia-secreted pro-inflammatory cytokines including IL-1α, TNFα and C1q (Liddelow et al., 2017), C3 expression was next evaluated in Iba1-expressing cells to determine whether microglia express C3 or if C3 expression is astrocytes-specific. Quantification exposed that C3 expression was absent in microglia ($C3^+/Iba1^+$: 0 ± 0% Figure 14B, C), indicating that at 12 dpi, mainly reactive astrocytes express C3 in the reprogramming milieu.

Altogether, these findings demonstrate that a neurotoxic subtype of reactive astrocytes, characterized by C3 expression, is present and abundant at the reprogramming site at 12 dpi.

4.3.3 C3 mRNA expression is increased at the reprogramming site and detected in transduced cells

C3 immunostaining revealed that neurotoxic reactive astrocytes are present at similar densities in both injury-alone and reprogramming site conditions at 12 dpi, suggesting C3-expressing cells arise from the cortical injury alone. To determine whether transcriptional activity of C3 differs between conditions despite similar protein levels, C3 mRNA was assessed by *in situ* hybridization using RNAscope at 12 dpi (15 days post-injury). Three conditions were compared: uninjured cortex (contralateral hemisphere to the reprogramming site), injured-only cortex (stab-wound alone), and reprogramming site (Figure 15A).

Quantification of C3 mRNA signal, expressed as $C3^+$ area per field and comprised of measuring the relative area covered by C3 mRNA puncta, revealed condition-dependent differences (Figure 15B, C). Namely, C3 mRNA expression was completely absent in the uninjured brain (uninjured: 0 ± 0%, Figure 15B, C), confirming that C3 expression is rare in the healthy adult cortex. In the injured cortex at 12 dpi, sparse C3 mRNA signal was detected (injury only: 2.21 ± 0.79%, Figure 15B, C), confirming that cortical injury induces C3 transcriptional activity. At the reprogramming site, C3 signal was markedly increased relative to the uninjured condition (reprogramming site: 15.93 ± 11.38%, p=0.02, Figure 15B, C), suggesting that the combination of injury and retroviral injection or reprogramming induction increases C3 transcriptional activity beyond injury-induced levels. While C3 mRNA levels at the reprogramming site showed a trend toward increase compared to injury alone, this difference did not reach statistical significance (reprogramming site vs injury only p=0.52), suggesting that injury is the primary inducer of C3 transcriptional activity, with retroviral injection contributing to, but not substantially altering, C3 mRNA expression levels at the reprogramming site.

Furthermore, RNAscope was combined with immunostaining to detect Ascl1SA6-transduced cells in the reprogramming site at 12 dpi (Figure 15A). Notably, C3 mRNA signal was found to overlap spatially with a fraction of transduced cells (%$C3^+$: 29.8 ± 4.48 %, $C3^-$: 70.2 ± 4.48%, p= 0.02, Figure 15B, C), demonstrating that a subset of transduced cells actively expressed C3 mRNA at this stage.

Together, these findings indicate that C3-expressing neurotoxic reactive astrocytes are present in the reprogramming milieu, and that a subset of Ascl1SA6-transduced cells express C3 mRNA. Whether C3-expressing transduced cells represent reactive astrocytes that failed to undergo neuronal reprogramming or cells that transiently express C3 during conversion remains to be determined. Nevertheless, the presence of C3 at the reprogramming site suggests that transduced cells are exposed to a neurotoxic inflammatory environment that may constrain successful neuronal conversion.

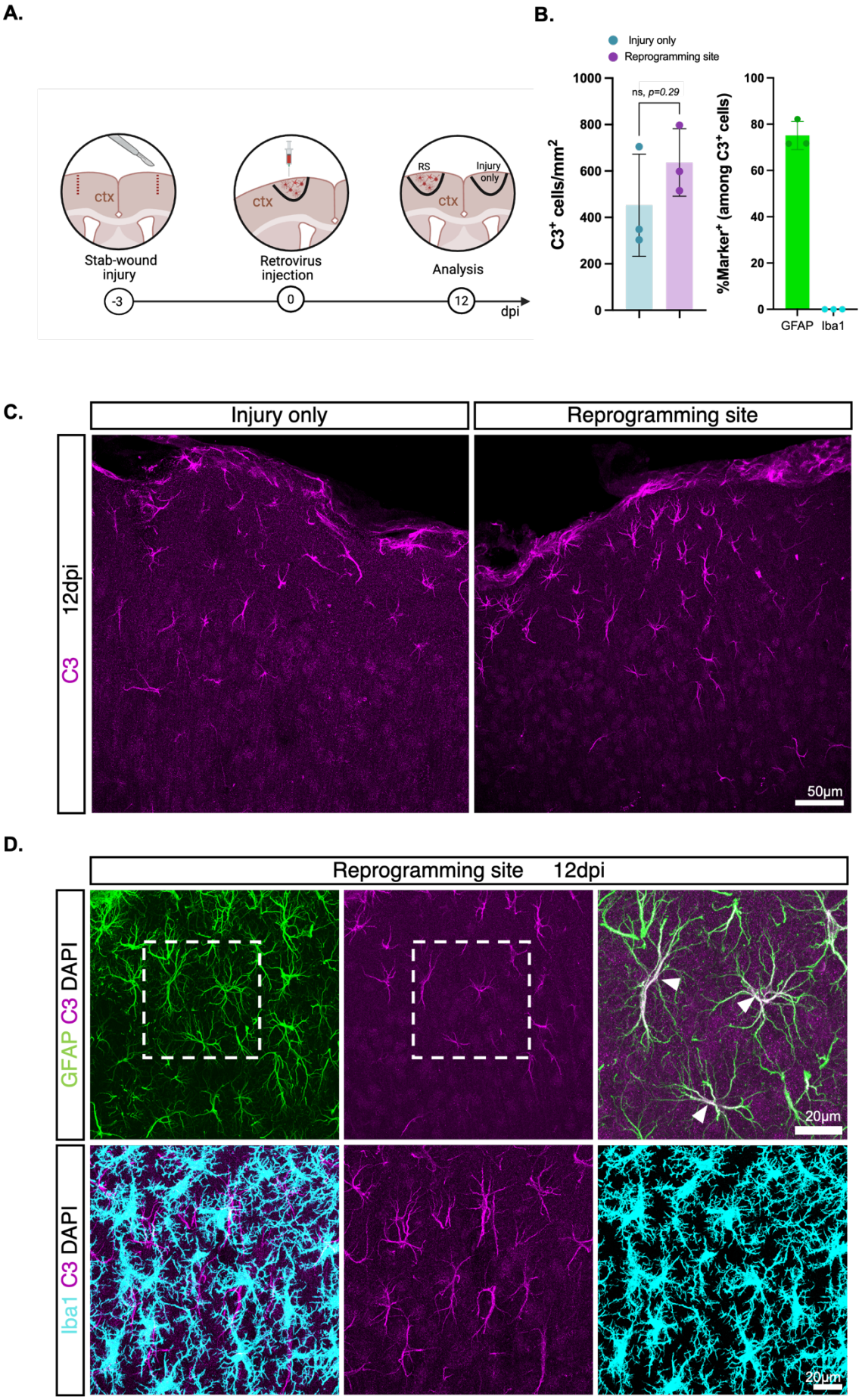
A.
ctx
Stab-wound injury
-3
ctx
Retrovirus injection
0
RS
Injury only
ctx
Analysis
12
dpi
B.
Injury only
Reprogramming site
ns, p=0.29
C3+ cells/mm2
1000
800
600
400
200
0
%Marker+ (among C3+ cells)
100
80
60
40
20
0
GFAP
Iba1
C.
Injury only
Reprogramming site
C3 12dpi
50µm
D.
Reprogramming site 12dpi
GFAP C3 DAPI
20µm
Iba1 C3 DAPI
20µm

Figure 14: Complement 3 expression identifies neurotoxic reactive astrocytes at the reprogramming site. A. Schematic representation of experimental approach. Retrovirus encoding Ascl1SA6 was injected three days after stab-wound injury in the adult cortex. At 12 dpi immunostaining against Complement 3 (C3) was performed to assess co-expression in GFAP (reactive astrocyte marker) and Iba1 (microglial marker) in the injured-only, and at the reprogramming site (injury and retroviral injection). **B.** Quantification of number of C3-expressing cells in the injury only or reprogramming site conditions and relative proportion of C3-expressing cells that co-express GFAP or Iba1 at 12 dpi **C.** Representative confocal images showing C3 (in magenta) in the injury only, and reprogramming site conditions. **D.** Representative confocal images showing C3 (in magenta), GFAP (in green) or Iba1 (cyan) expression. White arrowheads indicate marker positive cells. Data shown as mean ± SD. Statistical test: unpaired t-test. n=3 mice per group. 1910 cells analyzed.

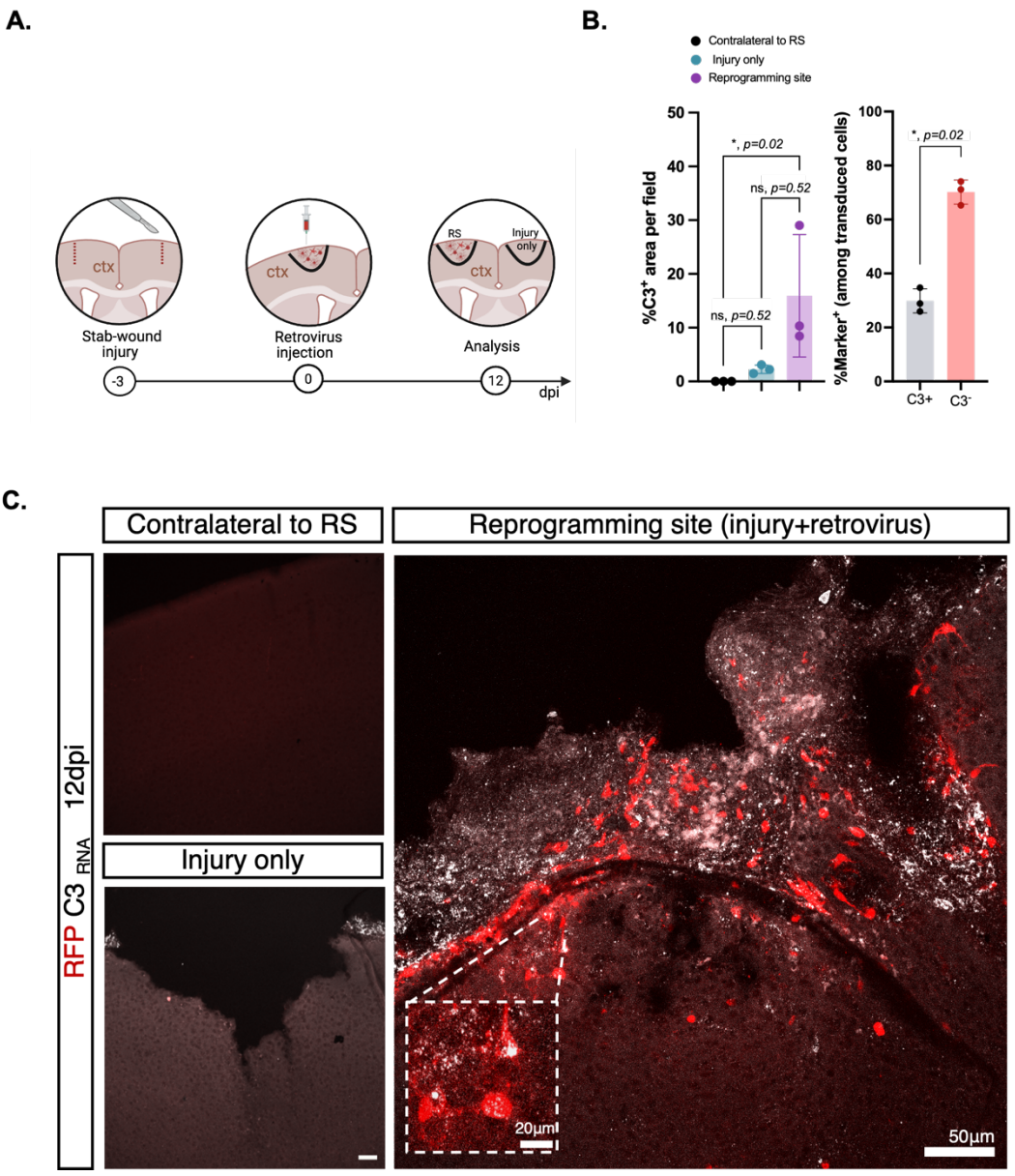

Figure 15: C3 mRNA expression is increased at the reprogramming site and detected in transduced cells. A. Schematic representation of experimental approach. Cortical stab-wound injury was performed in the somatosensory cortex (injury only condition) and retrovirus encoding Ascl1SA6 was injected three days after. The contralateral hemisphere (uninjured cortex) served as negative control. At 12 dpi, C3 mRNA expression was assessed in the adult cortex by RNAscope *in situ* hybridization combined with immunostaining. **B.** Quantification of relative C3-expressing area in the uninjured adult cortex, injury-only, and reprogramming site conditions (left), and percentage of transduced cells that express C3 mRNA (right). **C.** Representative confocal images showing C3 mRNA (in white) and transduced cells (in red). Data shown as mean ± SD. Statistical test: Kruskal-Wallis followed by Dunn's multiple comparisons test. n=3 mice per group. Ascl1SA6: 207 cells analyzed.

4.3.4 C3-expressing neurotoxic reactive astrocytes proliferate at the time of retroviral injection

The observation that reactive astrocytes do not successfully reprogram into induced neurons, despite initiating morphological changes in the injured cortex, contrasts with findings in the postnatal intact cortex, where astrocytes are the primary cellular origin of Ascl1SA6-Bcl2-induced neurons (Marichal et al., 2024). Additionally, given that C3-expressing neurotoxic reactive astrocytes were identified at the reprogramming site, and that C3 mRNA signal co-localized with a subset of transduced cells at 12 dpi, it was next examined whether C3-expressing astrocytes are proliferating at the time of retroviral delivery, and thus accessible for retroviral transduction.

To address this, 5-ethynyl-2′-deoxyuridine (EdU) was used to label cells in active S-phase. Animals received a single intraperitoneal injection of EdU (50mg/kg) 4 hours before sacrifice at three days after injury, corresponding to the time-point of the retroviral injection (Figure 16A) This short-pulse labeling paradigm was chosen to capture actively proliferating cells at the peak of injury-induced proliferation (Buffo et al., 2008).

EdU incorporation was first confirmed in the uninjured brain, where labeled cells were mostly confined to neurogenic areas, such as the subventricular zone (SVZ), serving as a positive control (Figure 16B). Immunostaining at 3 days post-lesion revealed EdU incorporation in reactive astrocytes identified by GFAP expression as well as in C3-expressing cells (Figure 16C). Among all EdU-incorporating cells, a significantly larger fraction corresponded to reactive astrocytes that co-expressed C3 ($GFAP^+/C3^{+)}$ compared to $GFAP^+/C3^-$ astrocytes ($GFAP^+/C3^+$: 9.04 ± 2.55%, $GFAP^+/C3^-$: 1.39 ± 0.10%, p=0.006, Figure 16B, C). These results indicate that, among proliferating cells at the time of retroviral delivery, C3 expression is enriched in EdU-incorporating reactive astrocytes.

Altogether, these findings suggest that C3-expressing neurotoxic reactive astrocytes are present within the proliferating cell population accessible for retroviral transduction, and raise the hypothesis that acquisition of the neurotoxic phenotype may limit their ability to undergo Ascl1SA6-Bcl2-mediated neuronal conversion in the injured adult cortex.

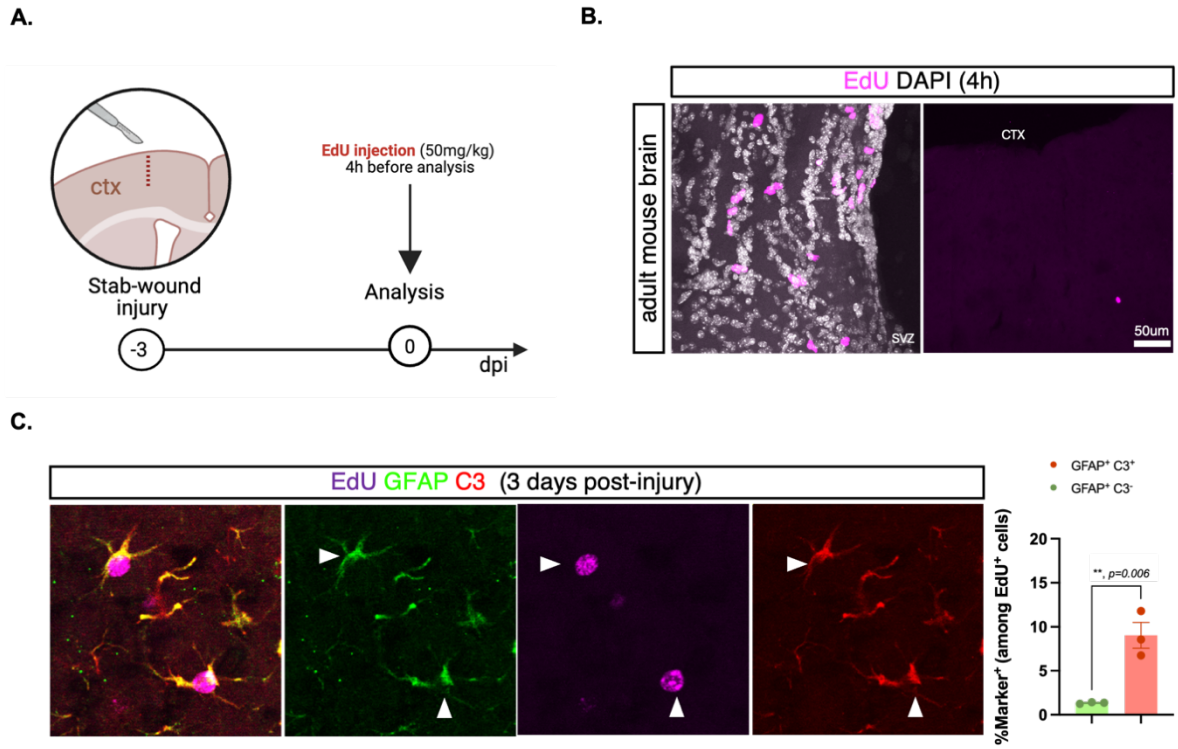

Figure 16: C3-expressing reactive astrocytes proliferate at the time of retroviral injection in the injured adult cortex A. Schematic representation of experimental approach. Cortical stab-wound injury was performed in the somatosensory cortex. To label proliferating cells, animals received an intraperitoneal injection of EdU (50mg/kg) 4 hours before sacrifice at 3 days post-injury, corresponding to the time-point when retrovirus is delivered to induce neuronal reprogramming. **B.** Representative confocal images showing EdU labeling in the subventricular zone (SVZ) of the uninjured adult brain (positive control), and in the adult uninjured cortex. **C.** Representative confocal images of the injured adult cortex displaying EdU (in magenta), GFAP (in green) and C3 (in red) expression at 3 days post-injury. **D.** Quantification of the percentage of marker-positive EdU-incorporating cells. White arrowheads indicate marker-positive cells. Data shown as mean ± SD. Statistical test: paired t-test. n=3 mice per group. 604 cells analyzed.

4.4. Ascl1SA6-Bcl2-induced neurons persist and undergo maturation in the injured adult cortex

While Ascl1SA6-Bcl2-iNs can be detected at 12 dpi, the proportion of transduced cells that express neuronal markers was limited compared to general neuronal morphology acquisition at this stage, suggesting that complete neuronal conversion may be delayed or partial in the injured adult cortex. This contrasts with the high conversion efficiency reported in the intact postnatal cortex (Marichal et al., 2024) and points to environmental barriers to neuronal conversion in the injured cortex. These observations prompted the examination of whether Ascl1SA6-Bcl2 transduced cells continue to undergo neuronal identity acquisition and survive within the previously characterized inflammatory milieu.

To determine whether iNs undergo maturation and survive over time in the injured adult cortex, namely in an environment characterized by immune cell infiltration, reactive gliosis and the presence of C3-expressing neurotoxic reactive astrocytes, NeuN expression was assessed at 28 dpi (Figure 17A). At this stage, most of injury-induced alterations in NeuN (mature marker) antigenicity have largely resolved, enabling reliable evaluation of mature neuronal marker expression.

Retroviruses encoding Ascl1-Bcl2 or Ascl1SA6-Bcl2 were injected three days after cortical stab-wound injury and analysis was performed at 28 dpi. Immunostaining for NeuN revealed an increase in Ascl1SA6-Bcl2-derived iNs at this time-point ($NeuN^+$: 32.1 ± 3.23%, Figure 17B, C). In contrast, NeuN expression remained rare in Ascl1-Bcl2 -transduced cells ($NeuN^+$: 1.01 ± 0.99%, p=0.0002, Figure 17B, C), confirming the limited reprogramming capacity of this combination in the injured cortex.

Importantly, the proportion of Ascl1SA6-Bcl2-transduced cells expressing NeuN at 28 dpi was significantly higher than at 12 dpi (32.05% vs 11.1%, p=0.02, Figure 17E), suggesting progressive gain of mature neuronal identity. To confirm the increase in neuronal identity acquisition, Neurotrace labeling was assessed at 28 dpi and compared to 12 dpi. Consistently, the proportion of Neurotrace-expressing transduced cells increased significantly over time (12 dpi: 32.3 ± 11.5% vs 28 dpi: 58.5 ± 6.38%, p=0.02, Figure 17D, E), indicating that additional cells acquired neuronal features or that neuronal marker-negative cells were selectively lost between time-points. However, while iNs displayed robust, elongated and complex processes at 12 dpi, by 28 dpi these structures appeared markedly simplified (Figure 17D), suggesting either actual deterioration of neuronal processes or reduced reporter gene expression at later time-points. Nevertheless, the progressive increase in mature neuronal marker expression suggests that at least a subset of Ascl1SA6-Bcl2-iNs continue to undergo maturation

over time in the injured adult cortex, even if full morphological maturation remains limited.

Together, these findings indicate that Ascl1SA6-Bcl2-mediated neuronal conversion progresses over time in the injured adult cortex, as revealed by increased mature neuronal marker expression.

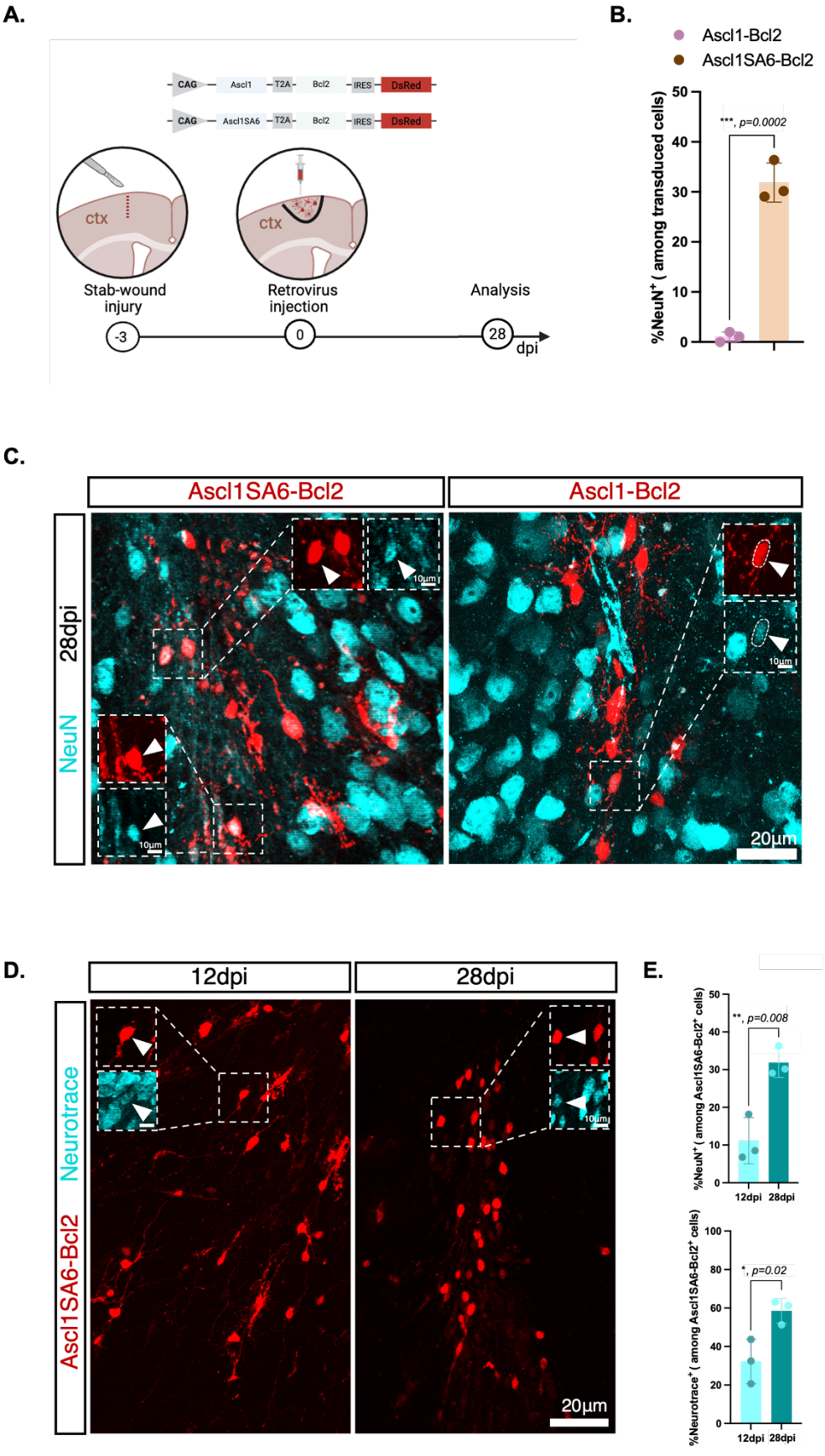
A.
CAG
Ascl1
T2A
Bcl2
IRES
DsRed
CAG
Ascl1SA6
T2A
Bcl2
IRES
DsRed
ctx
ctx
Stab-wound injury
Retrovirus injection
Analysis
-3
0
28
dpi
B.
Ascl1-Bcl2
Ascl1SA6-Bcl2
%NeuN+ (among transduced cells)
***, p=0.0002
C.
Ascl1SA6-Bcl2
Ascl1-Bcl2
28dpi
NeuN
10µm
20µm
D.
12dpi
28dpi
Ascl1SA6-Bcl2
Neurotrace
20µm
E.
%NeuN+ (among Ascl1SA6-Bcl2+ cells)
**, p=0.008
12dpi
28dpi
%Neurotrace+ (among Ascl1SA6-Bcl2+ cells)
*, p=0.02
12dpi
28dpi

Figure 17: Ascl1SA6-Bcl2-transduced cells acquire mature neuronal marker expression in the injured adult cortex at 28 days post-injection (dpi). A. Schematic representation of experimental approach. Retrovirus encoding Ascl1-Bcl2 or Ascl1SA6-Bcl2 was injected three days following cortical stab-wound injury. At 28 pi immunostaining against NeuN and Neurotrace was performed to assess neuronal marker expression in transduced cells. **B.** Quantification of the proportion of transduced cells expressing NeuN at 28 dpi. **C.** Representative confocal images showing NeuN (in cyan) expression in transduced cells. **D.** Representative confocal images showing transduced cells at 12 dpi vs 28 dpi and Neurotrace (in cyan) expression in transduced cells. **E.** Quantification of the proportion of transduced cells expressing NeuN or Neurotrace at 12 dpi vs 28 dpi. White arrowheads indicate marker-positive cells. Data shown as mean ± SD. Statistical test: unpaired t-test (graph in **B**.) or paired t-test (graphs in **E**.). n=3 mice per group. Ascl1-Bcl2: 387 cells analyzed; Ascl1SA6-Bcl2: 550 cells analyzed

In this chapter, I demonstrated that Ascl1SA6 and Bcl2 can induce neuronal reprogramming in the injured adult cortex, whereas Ascl1 and Bcl2 show minimal neurogenic capacity, confirming that Ascl1's phosphorylation state critically influences its neurogenic potential. Although Ascl1SA6-Bcl2-mediated reprogramming efficiency is initially low, characterized by incomplete neuronal marker expression, most Ascl1SA6-Bcl2-transduced cells acquire neuronal-like morphology. Genetic fate-mapping revealed that OPCs represent a major contributing source of iNs, while reactive astrocytes showed limited contribution to neuronal conversion. Environmental characterization revealed a pro-inflammatory milieu in which C3-expressing neurotoxic astrocytes emerge and may compromise neuronal survival and reprogramming efficiency. Despite this inflammatory reprogramming milieu and limited early conversion, iNs survive and show progressive acquisition of mature neuronal marker expression over time. Altogether, these findings indicate that Ascl1SA6-Bcl2-mediated neuronal conversion can be achieved in the injured adult cortex, but is likely constrained by both environmental barriers and intrinsic cellular competence.

Chapter II: Ascl1 overexpression enhances and sustains oligodendrocyte precursor cell proliferation in the injured adult cortex

Chapter I demonstrated that Ascl1SA6 and Bcl2 co-expression induces glia-to-neuron conversion in the injured adult cortex, with OPCs identified as a major cellular source of iNs. This finding contrasts with reports in the postnatal intact cortex, where astrocytes efficiently undergo neuronal conversion (Marichal et al., 2024), suggesting that the injury milieu impacts cellular competence for reprogramming.

Ascl1 is a key regulator of both neurogenesis and oligodendrocyte development (Castro et al., 2011; Nakatani et al., 2013). While Ascl1 shows very limited ability to drive neuronal conversion in the postnatal intact brain (Galante et al., 2022a) and in the injured adult cortex (see Chapter I), its overexpression instead enhanced OPC proliferation in the postnatal cortex (Galante et al., 2022b) These observations raise the question of whether Ascl1-mediated OPC proliferation is preserved in the injured cortex or constrained by the injury-induced environment.

This chapter investigates the effect of Ascl1, alone or in combination with Bcl2, on reactive glia in the injured adult cortex, with a particular focus on the proliferative response of OPCs.

4.5. Ascl1 overexpression promotes oligodendrocyte precursor cell proliferation in a sustained and cell-autonomous manner

4.5.1. OPC proliferative behavior under homeostatic conditions and following cortical injury

Prior to assessing Ascl1-mediated effects on proliferation, the baseline proliferative behavior of OPCs and their endogenous response to cortical injury were characterized. Sox10 expression was used to identify cells of oligodendroglial lineage, encompassing OPCs and more differentiated oligodendrocytes. Given that proliferative activity is largely confined to OPCs in the adult and injured cortex, and that retrovirus preferentially target proliferating cells, Sox10-expressing transduced or EdU-incorporating cells are hereafter referred to as OPCs or oligodendroglial lineage cells (Galante et al., 2022; Heinrich et al., 2014; Hughes et al., 2013).

To characterize the baseline proliferative behavior of OPCs, EdU incorporation was detected in cells expressing the pan-oligodendroglial marker Sox10 in the uninjured cortex (contralateral hemisphere) and following stab-wound injury across multiple time-points. A cortical stab-wound injury was performed and a retrovirus encoding

DsRed alone (CAG-IRES-DsRed, as control) was injected at the injury site three days later. Since the control virus was injected for subsequent assessment of Ascl1-mediated effects on OPC proliferation, potential effects on injury-induced response cannot be excluded. Animals received two i.p. EdU injections (50mg/kg) during the 24 hours preceding sacrifice, and analyses were performed at 4-, 12-, 28- and 70 dpi, to capture subacute and chronic phases of the injury response. This labeling window was selected to provide broader detection of proliferating cells compared to the previously used paradigm (single injection, 4 hours prior to sacrifice, subsection 4.3.4). EdU incorporation was quantified in Sox10-expressing cells in the contralateral hemisphere and among non-transduced Sox10-expressing cells in the injured cortex (Figure 18A).

In the uninjured contralateral adult cortex, Sox10-expressing cells exhibited minimal EdU incorporation across all examined time-points (4 dpi: 0.88 ± 0.24%, 12 dpi: 0.94 ± 0.85%, 28 dpi: 0.98 ± 0.82%, 70 dpi: 0.58 ± 0.51%; Figure 18B, C). These values established a low and stable baseline OPC proliferation rate after short-pulse EdU labeling in the adult cortex and suggest that the contralateral hemisphere maintains homeostatic conditions.

In contrast, Sox10-expressing cells in the injured cortex displayed a robust increase in EdU incorporation at 4 dpi compared to the contralateral uninjured side (11.4 ± 1.41%; p=0.02; Figure 18B, C), aligning with the previously described injury-induced proliferative response of OPCs (Simon et al., 2011; Sirko et al., 2013). Notably, this proliferative response was transient, as the fraction of EdU-incorporating Sox10-expressing cells declined substantially by 12 dpi (12 dpi: 0.94 ± 0.83%; 4 dpi vs 12 dpi: p=0.03; Figure 18B, C) and was no longer significantly different from contralateral levels. At later time-points (28 and 70 dpi), EdU incorporation remained low and comparable to baseline levels (28 dpi: 0.61 ± 0.47%, 70 dpi: 0.40 ± 0.22%; Figure 18B, C).

Together, these findings defined the baseline proliferative behavior of endogenous OPCs under homeostatic conditions and showed a transient injury-induced response in the adult cortex. This temporal baseline provides a reference framework for evaluating the impact of Ascl1 overexpression on OPC proliferation.

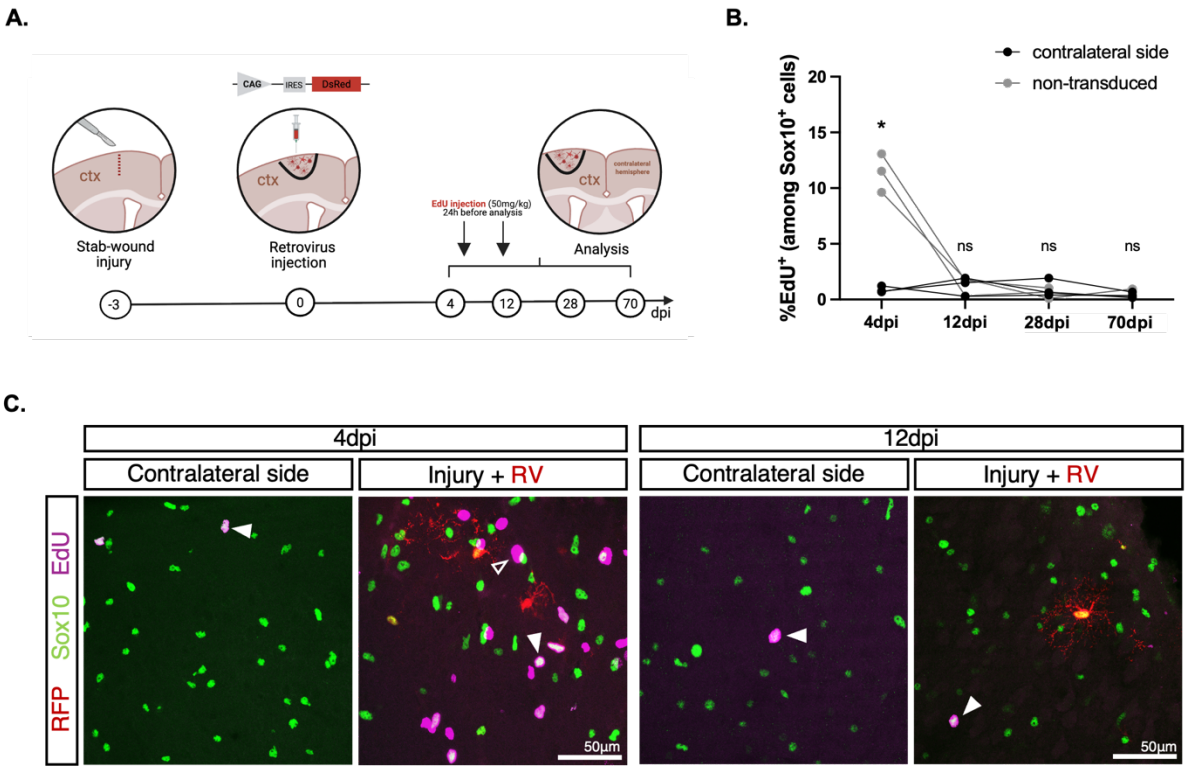

Figure 18: Homeostatic and injury-induced OPC proliferation across time in the injured adult cortex. A. Schematic representation of experimental approach. A cortical stab-wound injury was performed, followed by retroviral injection encoding DsRed only (as control) three days later. EdU was administered twice via i.p. injection 24h prior to sacrifice. At 4-, 12-, 28- and 70 dpi immunostaining against Sox10 and EdU was performed to access EdU incorporation in Sox10$^+$ cells in the uninjured contralateral cortex (homeostatic condition) and among non-transduced cells (injury condition). **B.** Quantification of the percentage of Sox10-expressing cells that incorporate EdU across time. **C.** Representative confocal images highlighting Sox10-expressing (in green) and EdU incorporating (in cyan) cells. White/empty arrowheads indicate marker-positive or marker-negative cells, respectively. Data shown as mean ± SD. Statistical tests: one-way ANOVA test followed by Tukey's multiple comparison test, *=0.02, n=3 mice/time-point. Sox10$^+$: 1200-1700 cells analyzed per animal. RV: Retrovirus

4.5.2. Ascl1-Bcl2 increased the proportion of Sox10-expressing cells in the injured adult cortex at 4 dpi

To determine whether Ascl1 overexpression alters the proportion of oligodendroglial lineage cells population in the injured adult cortex, Sox10 expression was assessed in transduced cells. Retroviruses encoding DsRed only (as control), Ascl1 (CAG-Ascl1-IRES-DsRed), Ascl1-Bcl2 (CAG-Ascl1-T2A-Bcl2-IRES-DsRed), Ascl1SA6 (CAG-Ascl1SA6-IRES-DsRed), or Bcl2 (CAG-Bcl2-IRES-GFP) were injected into the injury site three days after a cortical stab-wound injury, and analysis was conducted at 4 dpi to capture initial effects following transduction (Figure 19A). The same cohort of animals described in subsections 4.1 and 4.2.1 were used for this analysis.

At this stage, the proportion of Sox10-expressing transduced cells was similar between Ascl1 and control groups (control: 53.0 ± 11.4%, Ascl1: 56.7 ± 5.0%, Figure 19B, C), indicating that Ascl1 overexpression does not influence the proportion of Sox10-expressing cells among the transduced population at early stages. In contrast, co-expression of Ascl1 and Bcl2 significantly increased the fraction of Sox10-expressing transduced cells relative to control (Ascl1-Bcl2: 80.7 ± 13.3%, control: 53.0 ± 11.4%, p=0.03, Figure 19B, C), suggesting that Bcl2 co-expression enhances oligodendroglial lineage cell survival in the injured cortex. Similarly, Bcl2 overexpression alone increased the fraction of Sox10-expressing transduced cells compared to control and Ascl1, but this effect did not reach statistical significance (Bcl2: 62.5 ± 8.0%, Figure 19B, C), suggesting that the pro-survival factor alone may promote survival of transduced OPCs at this stage. In contrast, Ascl1SA6 overexpression markedly reduced the proportion of Sox10-expressing cells compared to all other groups (Ascl1SA6: 16.3 ± 7.5%, p<0.05 vs all groups, Figure 19B, C), indicating early downregulation of Sox10 expression in transduced cells, which aligns with its neurogenic potential demonstrated in Chapter I (subsection 4.2.2).

Together, these findings indicate that overexpression of Ascl1 alone does not impact the proportion of oligodendroglial lineage cells at this early stage, whereas an increased fraction is observed upon co-expression with Bcl2, potentially reflecting enhanced OPC survival following injury.

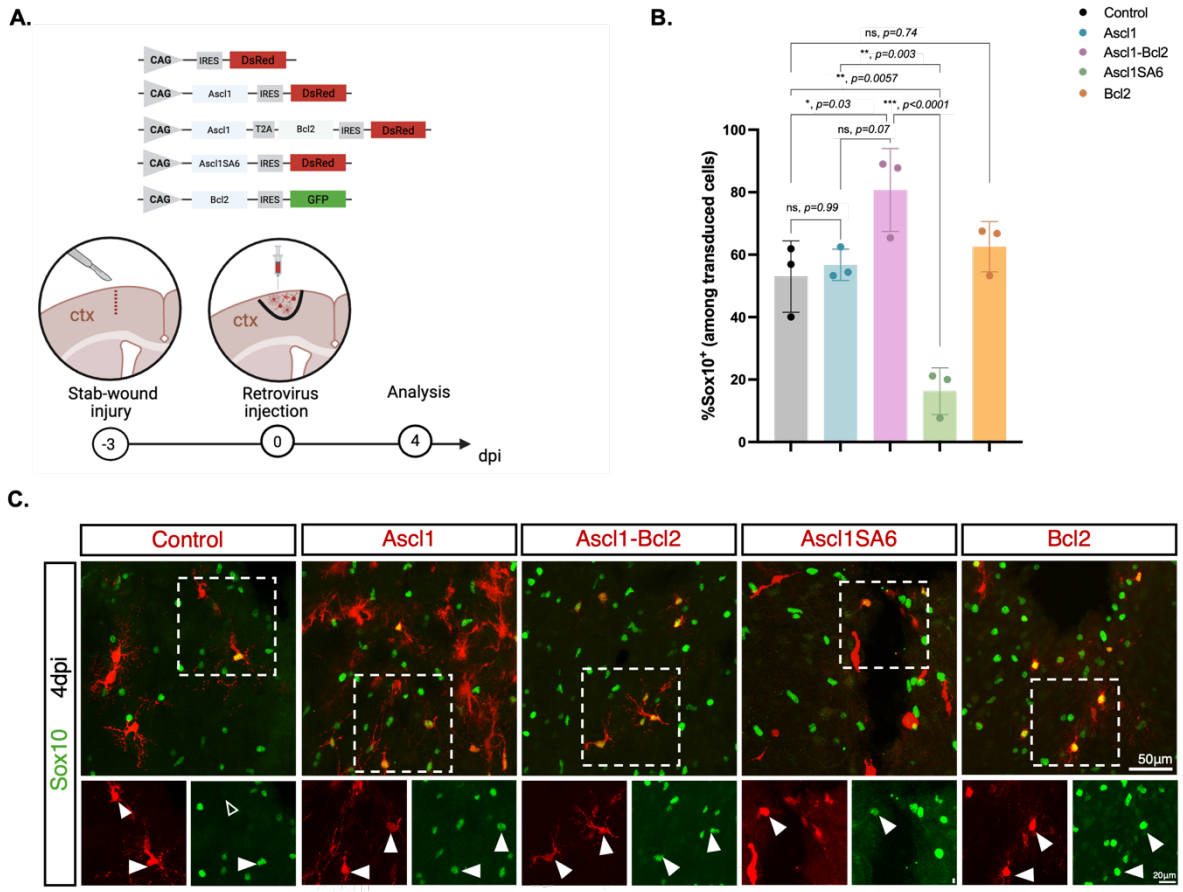

Figure 19: Ascl1 and Bcl2 overexpression increases proportion of oligodendrocyte lineage cells in the injured adult cortex at 4 days post-injection (dpi). A. Schematic representation of experimental approach. Retroviruses encoding DsRed only (control), Ascl1, Ascl1 and Bcl2, Ascl1SA6, or Bcl2 were injected three days following cortical stab-wound injury. At 4 dpi immunostaining against Sox10 was performed to assess its expression in transduced cells. **B.** Quantification of the percentage of transduced cells that express Sox10 at 4 dpi. **C.** Representative confocal images highlighting Sox10 expression (in green) in transduced cells with control, Ascl1, Ascl1-Bcl2, Ascl1SA6 or Bcl2 (in red, Bcl2-transduced cells are also displayed in red for consistency). White/empty arrowheads indicate marker-positive or marker-negative cells, respectively. Data shown as mean ± SD. Statistical tests: one-way ANOVA test followed by Tukey's multiple comparison test. n=3 mice per group, control: 590 cells analyzed; Ascl1: 1337 cells analyzed; Ascl1-Bcl2: 281 cells analyzed; Ascl1SA6: 167 cells analyzed; Bcl2: 595 cells analyzed.

4.5.3. *Ascl1 alone or with Bcl2 enhances OPC proliferation in the injured adult cortex at 4 dpi*

The observation that Ascl1-Bcl2 overexpression increased the fraction of transduced Sox10-expressing cells prompted the question of whether this effect reflects enhanced proliferation of transduced OPCs. To test this, EdU labeling was used to identify actively proliferating cells. Animals received two intraperitoneal injections of EdU (50mg/kg), 24 hours before sacrifice at 4 dpi (Figure 20A). EdU-incorporation was detected in transduced across all conditions, and the proportion of proliferating transduced cells (% EdU^+ among transduced cells) was significantly higher following Ascl1 and Ascl1-Bcl2 overexpression compared to control, Bcl2 alone and Ascl1SA6 (control: 5.42 ± 2.88%, Ascl1: 30.2 ± 7.22%; Ascl1-Bcl2: 29.6 ± 14.5%; Ascl1SA6: 3.03 ± 3.00%, Bcl2: 2.62 ± 2.06%, p=0.03, Figure 20B, C). These findings suggest that Ascl1 alone or combined with Bcl2 enhances proliferation in transduced cells. Notably, no significant differences were detected between Ascl1 alone and Ascl1-Bcl2, indicating that Bcl2 co-expression does not further increase the Ascl1-mediated proliferative effect (Figure 20B, C). In contrast, cells transduced with Ascl1SA6 or Bcl2 alone showed minimal EdU incorporation (Ascl1SA6: 3.03 ± 3.00%, Bcl2: 2.62 ± 2.06%, Figure 20B, C), possibly reflecting cell cycle exit or alternative cell fate transitions.

To determine if the Ascl1-mediated proliferative effect was induced in oligodendroglial lineage cells, EdU incorporation was assessed specifically in Sox10-expressing transduced cells (% EdU^+ among $Sox10^+$ transduced cells). Similar to the overall transduced population, overexpression of Ascl1 or Ascl1-Bcl2 resulted in a substantial increase of proliferating Sox10-positive transduced cells relative to control, Bcl2 alone and Ascl1SA6 (control: 11.2 ± 5.70%, Ascl1: 30.1 ± 4.93%, Ascl1-Bcl2: 30.4 ± 10.9%, Ascl1SA6: 0 ± 0%, Bcl2: 3.75 ± 2.97%, p<0.05, Figure 20B, C), indicating that Ascl1 and Ascl1-Bcl2 enhance proliferation of oligodendroglial lineage cells. In striking contrast, Ascl1SA6 group showed absence of EdU-incorporation in Sox10-expressing transduced cells (Ascl1SA6: 0 ± 0%, Figure 20B, C), which combined with the low fraction of transduced cells that express Sox10, further corroborates that Ascl1SA6 shifts cells towards a neuronal fate. Notably, Ascl1 overexpression did not increase the proportion of Sox10-expressing transduced cells and yet yielded a similar percentage of proliferating transduced cells and proliferating transduced Sox10-positive cells as Ascl1-Bcl2, suggesting a primary proliferative effect of Ascl1. To reveal whether increased proliferation of transduced OPC leads to an increase in oligodendroglial lineage cell numbers, Sox10-expressing cell density was measured across all groups by quantifying the total number of Sox10-positive cells within the reprogramming site across all groups. At 4 dpi no significant differences in Sox10-

expressing cell density were observed among groups (control: 877.9 ± 203.1 $Sox10^+/mm^2$, Ascl1: 1055.7 ± 343.9 $Sox10^+/mm^2$, Ascl1-Bcl2: 923.6 ± 297.9 $Sox10^+/mm^2$, Ascl1SA6: 836.1 ± 190.7 $Sox10^+/mm^2$, Bcl2: 820.9 ± 189.7 $Sox10^+/mm^2$, Figure 20D, E). Given that retroviral transduction targets only a subset of cells within the lesion site, the Ascl1-mediated increase in transduced OPC proliferation may be insufficient to measurably alter Sox10-expressing cell density around the reprogramming site at this time-point. Alternatively, the absence of changes in surrounding oligodendroglial lineage cells could indicate that Ascl1 overexpression does not influence neighboring OPCs.

To corroborate whether the Ascl1-induced increase in proliferation reflects a cell-autonomous effect or instead results from indirect, non-cell-autonomous influence within the injured environment, EdU-incorporation was quantified in surrounding non-transduced Sox10-expressing cells (Figure 20F, G). No differences in the proportion of EdU-incorporating non-transduced oligodendroglial lineage cells were observed among groups (control: 8.62 ± 3.29%, Ascl1: 10.5 ± 2.89%, Ascl1-Bcl2: 7.75 ± 4.95%, Ascl1SA6: 12.1 ± 5.72%, Bcl2: 5.27 ± 1.22%, Figure 20F, G), suggesting that Ascl1-mediated proliferative effect is restricted to transduced cells and does not propagate to surrounding cells, consistent with a cell-autonomous effect.

Altogether, these findings suggest that Ascl1 overexpression, alone or with Bcl2, enhances OPC proliferation in a cell-autonomous manner, without influencing the overall oligodendroglial lineage cell density at this stage.

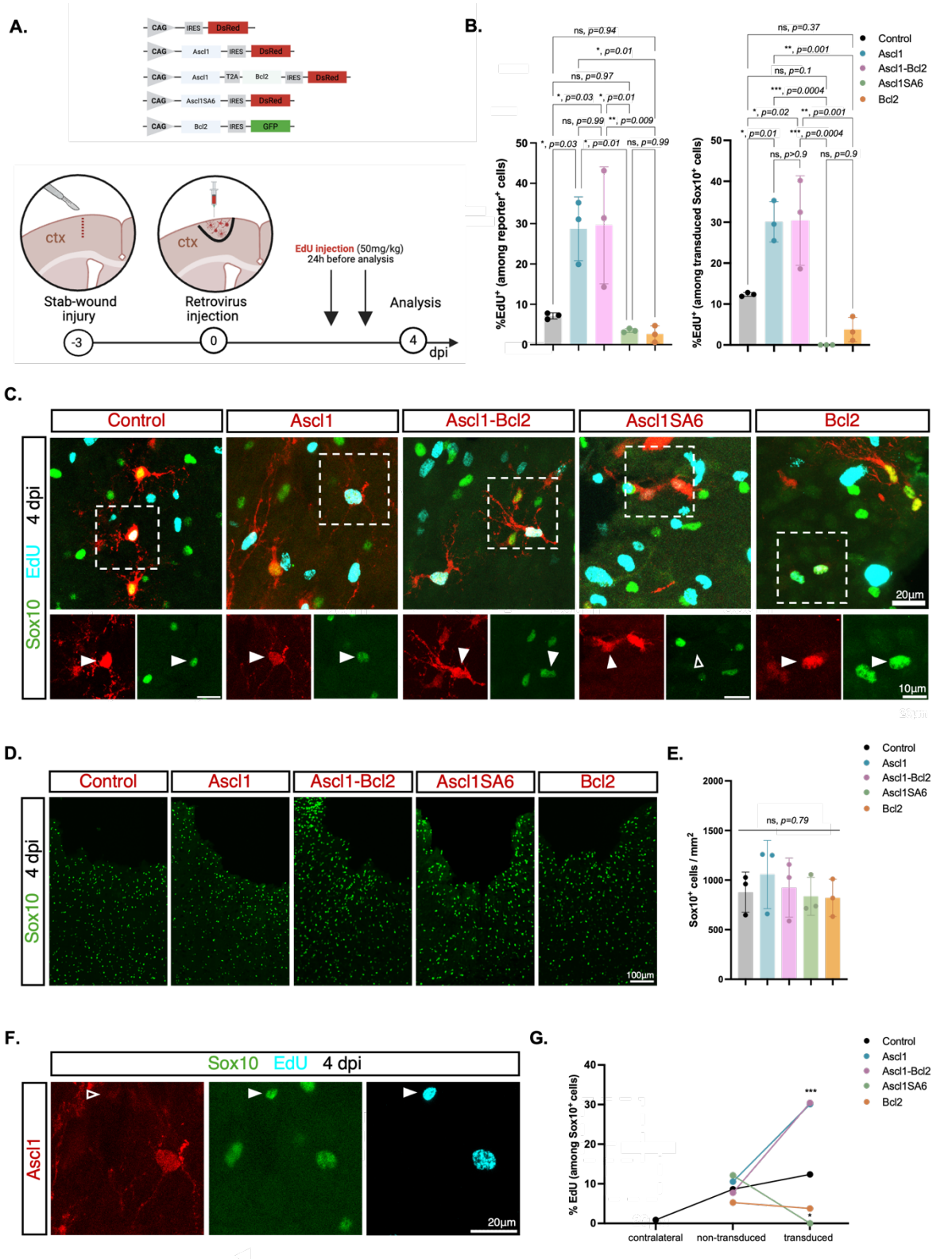
A.
CAG IRES DsRed
CAG Ascl1 IRES DsRed
CAG Ascl1 T2A Bcl2 IRES DsRed
CAG Ascl1SA6 IRES DsRed
CAG Bcl2 IRES GFP
ctx
ctx
Stab-wound injury
Retrovirus injection
EdU injection (50mg/kg) 24h before analysis
Analysis
-3
0
4
dpi
B.
%EdU+ (among reporter+ cells)
%EdU+ (among transduced Sox10+ cells)
Control
Ascl1
Ascl1-Bcl2
Ascl1SA6
Bcl2
C.
Control
Ascl1
Ascl1-Bcl2
Ascl1SA6
Bcl2
Sox10 EdU 4 dpi
20µm
10µm
D.
Control
Ascl1
Ascl1-Bcl2
Ascl1SA6
Bcl2
Sox10 4 dpi
100µm
E.
Sox10+ cells / mm2
ns, p=0.79
F.
Sox10 EdU 4 dpi
Ascl1
20µm
G.
% EdU (among Sox10+ cells)
contralateral
non-transduced
transduced

Figure 20: Overexpression of Ascl1 alone or with Bcl2 increases proportion of proliferating oligodendrocyte lineage cells in the injured adult cortex at 4 days post-injection (dpi). A. Schematic representation of experimental approach. Retroviruses encoding DsRed only (as control), Ascl1, Ascl1 and Bcl2, Ascl1SA6 or Bcl2 were injected three days following cortical stab-wound injury. To label proliferating cells, animals received two intraperitoneal injections of EdU 24 hours before sacrifice (4 dpi). **B.** Quantification of the percentage of transduced cells that incorporated EdU and of cells that incorporated EdU among Sox10-expressing transduced cells at 4 dpi. **C.** Representative confocal images showing EdU incorporation (in cyan) and Sox10 expression (in green) in transduced cells (red) with control, Ascl1, Ascl1-Bcl2, Ascl1SA6 or Bcl2 (also displayed in red, for consistency). **D.** Representative confocal images showing Sox10-expressing cell density (in green) at the injection site across groups. **E.** Quantification of total number of Sox10-expressing cell density (cells/mm^2). **F.** Representative confocal images showing EdU incorporation in non-transduced Sox10-expressing cells. **G.** Quantification of percentage of EdU incorporation among non-transduced Sox10 cells to assess potential non-cell-autonomous effects of Ascl1 overexpression. White arrowheads indicate marker-positive and empty arrows indicate marker-negative cells. Data shown as mean ± SD. Statistical tests: one-way ANOVA test followed by Tukey's (left graph in **B.**, left graph in **E.**, and **G.**), Kruskal Wallis' test and Dunn's multiple comparison test (right graph in **B.**, or two-way ANOVA and Šídák's multiple comparisons test (right graph in **E.**) n=3 mice per group. Data shown as mean ± SD. Statistical tests: one-way ANOVA test followed by Tukey's multiple comparison test. Significance: Ascl1 (p=0.004), Ascl1-Bcl2 (p<0.0001), n=3 mice per group. control: 590 cells analyzed; Ascl1: 1337 cells analyzed; Ascl1-Bcl2: 281 cells analyzed; Ascl1SA6: 167 cells analyzed; Bcl2: 595 cells analyzed.

4.5.4. *Ascl1-induced proliferation does not extend to reactive astrocytes or microglia in the injured adult cortex at 4dpi*

Given the increased OPC proliferation observed after Ascl1 or Ascl1-Bcl2 overexpression, it was next investigated whether this effect was restricted to OPCs or extended to other glial cell types in the injured adult cortex, namely reactive astrocytes or microglia, which are also targeted by retroviruses following cortical injury (subsection 4.1.1).

To determine whether Ascl1 overexpression alters the proportion of transduced reactive astrocytes, GFAP was evaluated in cells transduced with control, Ascl1, Ascl1-Bcl2, Ascl1SA6 or Bcl2 at 4 dpi (Figure 21A). Quantification revealed a lower proportion of GFAP-expressing transduced cells in Ascl1, Ascl1-Bcl2 and Ascl1SA6 groups compared to control and Bcl2 (control: 31.6 ± 8.02%, Ascl1: 6.52 ± 4.72%, Ascl1-Bcl2: 4.32 ± 4.49%, Ascl1SA6: 0.54 ± 0.94%, Bcl2: 14.6 ± 14.3%, Figure 21B, C). However, only control and Ascl1SA6 groups differed significantly (control vs Ascl1SA6 p=0.021, Figure 21B, C). This marked reduction in GFAP expression in transduced cells in the Ascl1SA6 group is consistent with its enhanced neurogenic activity described in Chapter I. Overall, these findings indicate a reduction of GFAP expression among transduced cells following Ascl1 or Ascl1-Bcl2 overexpression.

To test whether Ascl1 overexpression enhances proliferation of transduced reactive astrocytes, EdU incorporation was evaluated in GFAP-expressing transduced cells. At 4 dpi, EdU-incorporating transduced reactive astrocytes were rare across all groups (control: 0 ± 0%, Ascl1: 6.50 ± 8.91%, Ascl1-Bcl2: not determined due to insufficient number of GFAP-expressing transduced cells, Ascl1SA6: 0 ± 0%, Bcl2: 0 ± 0%, Figure 21B, C). Although the Ascl1 group showed a small fraction of proliferating GFAP-expressing transduced cells, this did not reach statistical significance, suggesting that Ascl1 overexpression does not enhance proliferation of reactive astrocytes in the injured adult cortex at this stage.

Next, the effect of Ascl1 overexpression on microglia was investigated by evaluating Iba1 expression in transduced cells (Figure 22A). Quantification revealed a significantly lower proportion of Iba1-expressing cells within the transduced population in the Ascl1 and Ascl1-Bcl2 groups compared to control (control: 13.8 ± 6.23 %, Ascl1: 6.10 ± 3.19%, Ascl1-Bcl2: 1.28 ± 3.85%, p>0.05, Figure 22B, C), while Ascl1SA6 and Bcl2 groups showed proportions similar to control (Ascl1SA6: 10.6 ± 5.30%, Bcl2: 15.0 ± 8.37%, Figure 22B, C). These findings indicate a reduction of Iba1 expression in Ascl1- or Ascl1-Bcl2-transduced cells in the injured adult cortex at 4 dpi. Finally, to reveal whether Ascl1 promotes microglial proliferation, EdU incorporation was

detected in Iba1-expressing transduced cells. Consistent with observations in EdU-incorporating transduced reactive astrocytes, EdU incorporation was rare across all groups (control: 0 ± 0%, Ascl1: 0 ± 0%, Ascl1-Bcl2: 0 ± 0%, Ascl1SA6: 0 ± 0%, Bcl2: not determined, due to insufficient number of transduced Iba1-expressing cells, Figure 22B, D), indicating that Ascl1 does not induce microglial proliferation.

Together, these findings suggest that Ascl1-mediated enhancement of proliferation is restricted to cells of oligodendroglial lineage and does not extend to reactive astrocytes or microglia in the injured adult cortex at 4 dpi.

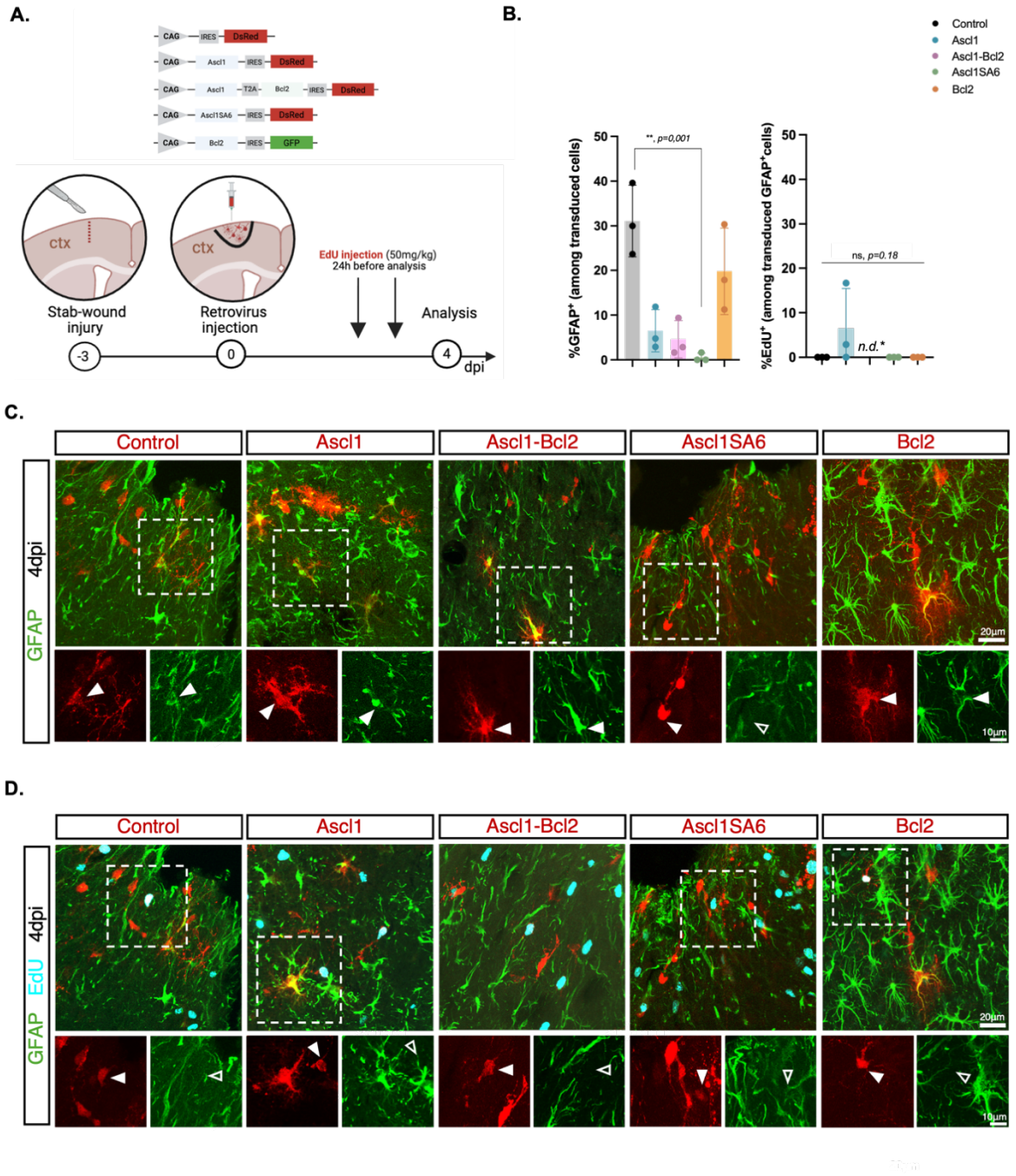
A.
CAG IRES DsRed
CAG Ascl1 IRES DsRed
CAG Ascl1 T2A Bcl2 IRES DsRed
CAG Ascl1SA6 IRES DsRed
CAG Bcl2 IRES GFP
ctx
ctx
Stab-wound injury
Retrovirus injection
EdU injection (50mg/kg) 24h before analysis
Analysis
-3
0
4
dpi
B.
Control
Ascl1
Ascl1-Bcl2
Ascl1SA6
Bcl2
%GFAP+ (among transduced cells)
**, p=0,001
%EdU+ (among transduced GFAP+cells)
ns, p=0.18
n.d.*
C.
Control
Ascl1
Ascl1-Bcl2
Ascl1SA6
Bcl2
4dpi
GFAP
20µm
10µm
D.
Control
Ascl1
Ascl1-Bcl2
Ascl1SA6
Bcl2
4dpi
EdU
GFAP
20µm
10µm

Figure 21: Overexpression of Ascl1 alone or with Bcl2 does not promote proliferation in reactive astrocytes in the injured adult cortex at 4 days post-injection (dpi). A. Schematic representation of experimental approach. Retroviruses encoding DsRed only (control), Ascl1, Ascl1 and Bcl2, Ascl1SA6 or Bcl2 were injected three days following cortical stab-wound injury. To label proliferating cells, animals received two intraperitoneal injections of EdU 24 hours before sacrifice (4 dpi). **B.** Quantification of the percentage of transduced cells that express GFAP or of $GFAP^+$ transduced cells that incorporated EdU cells at 4 dpi. **C.** Representative confocal images showing GFAP expression (in green) in transduced cells (red) with control, Ascl1, Ascl1-Bcl2, Ascl1SA6 or Bcl2 (also displayed in red, for consistency). **D.** Representative confocal images showing EdU incorporation (in cyan) in transduced GFAP-expressing cells. White arrowheads indicate marker-positive and empty arrowheads indicate marker-negative cells. Data shown as mean ± SD. Statistical tests: Kruskal-Wallis's test followed by Dunn's multiple comparison test. n=3 mice per group, control: 239 transduced cells analyzed; Ascl1: 1458 cells analyzed; Ascl1-Bcl2: 268 cells analyzed; Ascl1SA6: 210 cells analyzed; Bcl2: 420 cells analyzed. *n.d*:* not determined due to insufficient number of GFAP-expressing transduced cells.

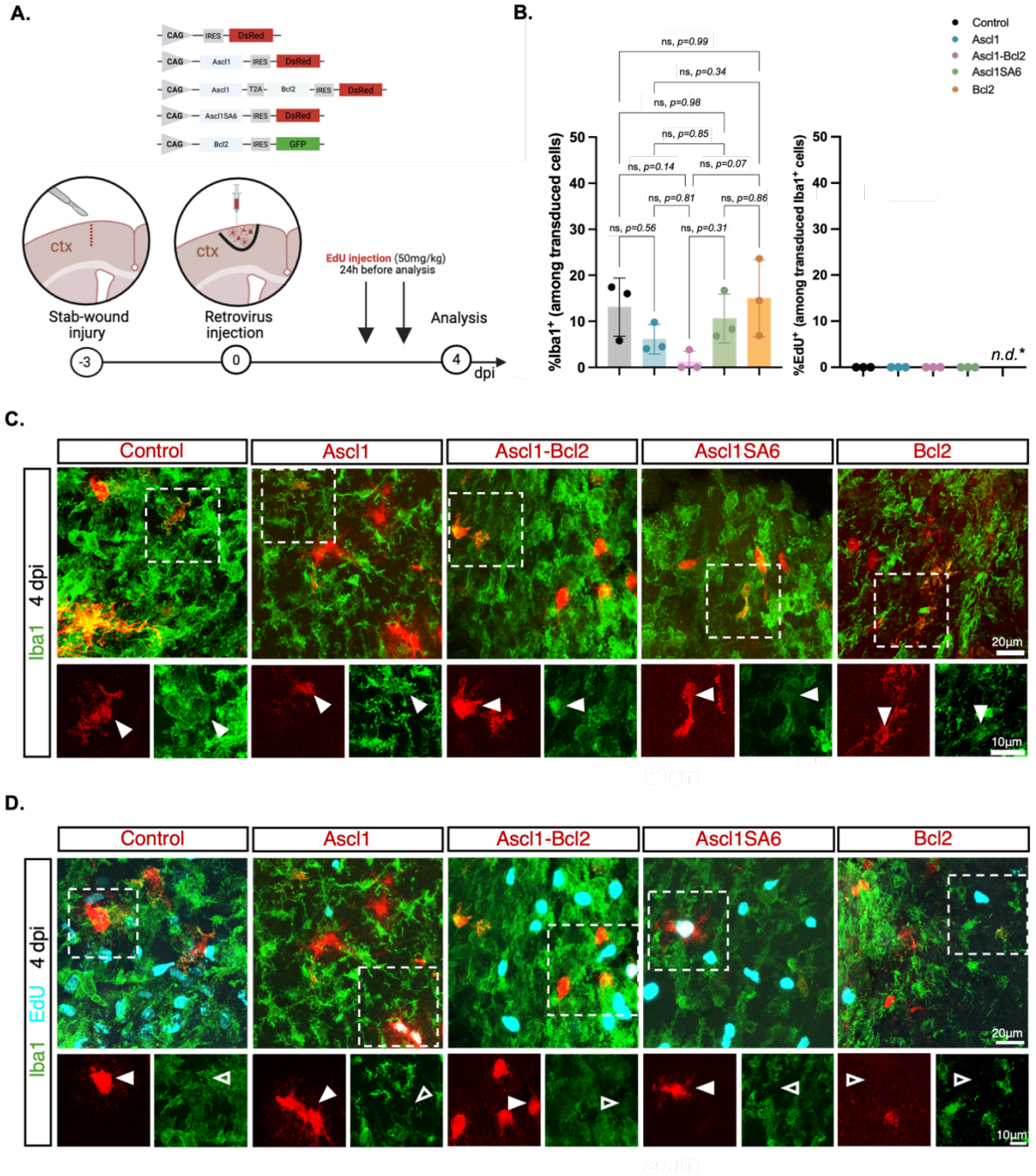
A.
CAG IRES DsRed
CAG Ascl1 IRES DsRed
CAG Ascl1 T2A Bcl2 IRES DsRed
CAG Ascl1SA6 IRES DsRed
CAG Bcl2 IRES GFP
ctx
ctx
Stab-wound injury
Retrovirus injection
EdU injection (50mg/kg) 24h before analysis
Analysis
-3
0
4
dpi
B.
Control
Ascl1
Ascl1-Bcl2
Ascl1SA6
Bcl2
ns, p=0.99
ns, p=0.34
ns, p=0.98
ns, p=0.85
ns, p=0.14
ns, p=0.07
ns, p=0.81
ns, p=0.86
ns, p=0.56
ns, p=0.31
%Iba1+ (among transduced cells)
%EdU+ (among transduced Iba1+ cells)
n.d.*
C.
Control
Ascl1
Ascl1-Bcl2
Ascl1SA6
Bcl2
Iba1 4 dpi
20µm
10µm
D.
Control
Ascl1
Ascl1-Bcl2
Ascl1SA6
Bcl2
Iba1 EdU 4 dpi
20µm
10µm

Figure 22: Overexpression of Ascl1 alone or with Bcl2 does not promote proliferation in microglia in the injured adult cortex at 4 days post-injection (dpi). A. Schematic representation of experimental approach. Retroviruses encoding DsRed only (control), Ascl1, Ascl1 and Bcl2, Ascl1SA6 or Bcl2 were injected three days following cortical stab-wound injury. To label proliferating cells, animals received two intraperitoneal injections of EdU 24 hours before sacrifice (4 dpi). **B.** Quantification of the percentage of transduced cells that express Iba1 or of Iba1-transduced cells that incorporated EdU cells at 4 dpi. **C.** Representative confocal images showing Iba1 expression (in green) in transduced cells (red) with control, Ascl1, Ascl1-Bcl2, Ascl1SA6 or Bcl2 (also displayed in red, for consistency). **D.** Representative confocal images showing EdU incorporation (in cyan) in transduced Iba1-expressing cells. White arrowheads indicate marker-positive and empty arrowheads indicate marker-negative cells. Data shown as mean ± SD. Statistical tests: Kruskal-Wallis's test followed by Dunn's multiple comparison test. n=3 mice per group, control: 171 cells analyzed; Ascl1: 1048 cells analyzed; Ascl1-Bcl2: 244 cells analyzed; Ascl1SA6: 152 cells analyzed; Bcl2: 170 cells analyzed. *n.d**: not determined due to insufficient number of Iba1-expressing transduced cells.

4.5.5. *Ascl1 increases the proportion of oligodendroglial lineage cells in the injured adult cortex at 12 dpi*

To determine whether the Ascl1-induced effect on OPCs persists beyond the early post-injury phase, I analyzed Sox10 expression in cells transduced with control, Ascl1 alone, Ascl1 and Bcl2, or Bcl2 at a later time point, i.e., 12 dpi (Figure 23A). Given that Ascl1SA6 overexpression induced early downregulation of Sox10 and reduced proliferation, this condition was not evaluated at this later time-point.

At 12 dpi, the proportion of transduced cells that expressed Sox10 did not differ between control, Ascl1-Bcl2 and Bcl2 conditions (control: 52.2 ± 10.42%, Ascl1-Bcl2: 69.1 ± 3.01%, Bcl2: 64.5 ± 6.84%, Figure 18B, C). In striking contrast, this proportion was significantly increased following Ascl1 overexpression (Ascl1: 92.1 ± 2.80 %, Ascl1 vs all other conditions $p<0.05$, Figure 18B, C), indicating Ascl1 increases the proportion of transduced OPCs at this stage.

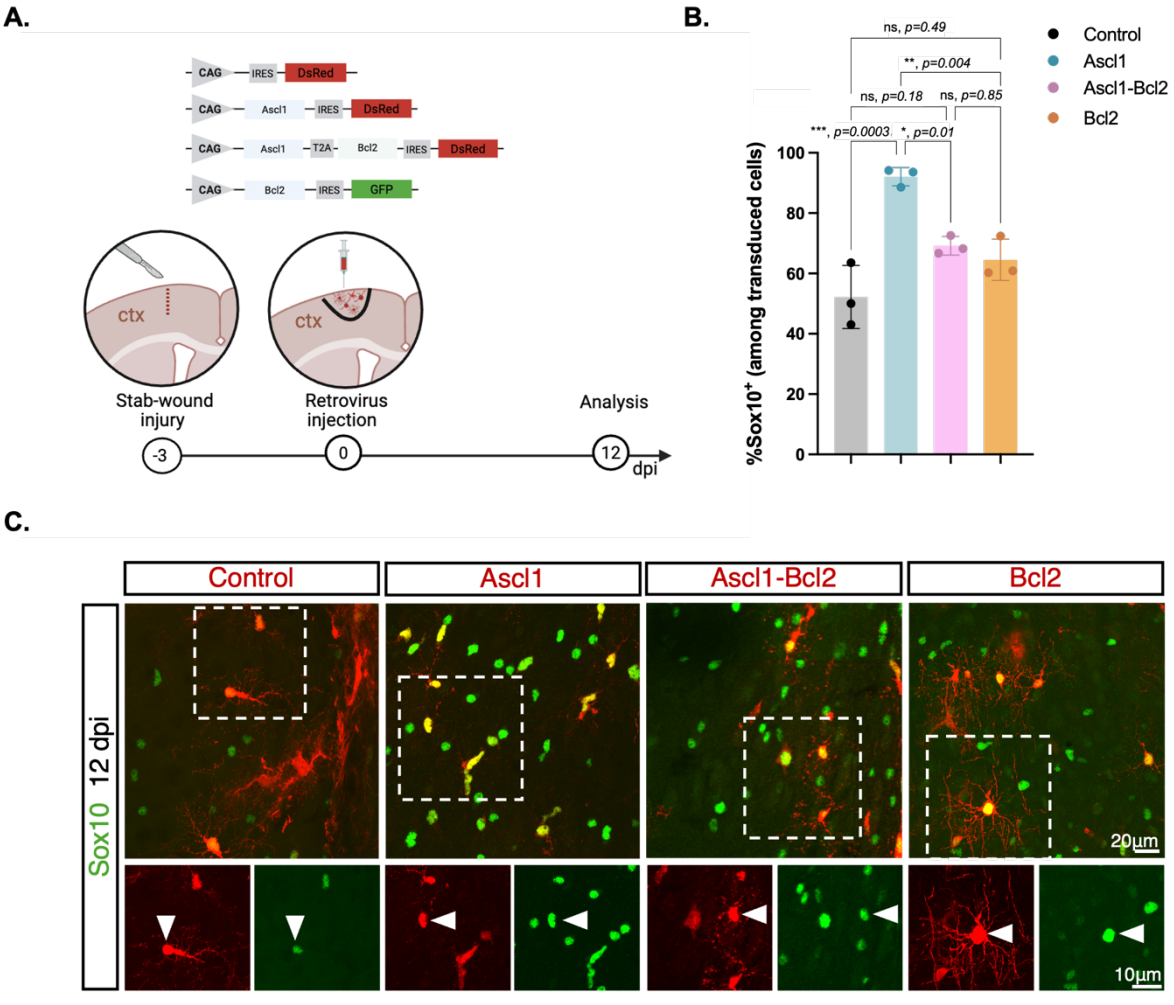

Figure 23: Ascl1 overexpression increases proportion of oligodendroglial lineage cells in the injured adult cortex at 12 days post-injection (dpi). A. Schematic representation of experimental approach. Retroviruses encoding DsRed only (control), Ascl1, Ascl1 and Bcl2 or Bcl2 were injected three days following cortical stab-wound injury. At 12 dpi, Sox10 expression was assessed in transduced cells. **B.** Quantification of the percentage of transduced cells that express Sox10 cells at 12 dpi. **C.** Representative confocal images highlighting Sox10 expression (in green) in transduced cells with control, Ascl1, Ascl1-Bcl2, or Bcl2 (in red). White arrowheads indicate marker-positive cells. Data shown as mean ± SD. Statistical tests: one-way ANOVA test followed by Tukey's multiple comparison test. n=3 mice per group, control: 240 cells analyzed; Ascl1: 989 cells analyzed; Ascl1-Bcl2: 283 cells analyzed; Bcl2: 835 cells analyzed.

4.5.6. *Ascl1-induced proliferation of oligodendrocyte precursor cells is sustained in the injured adult cortex at 12 dpi*

Most likely, the increased proportion of transduced Sox10-expressing cells at 12 dpi reflects sustained proliferation of Ascl1-transduced OPCs beyond the early post-injury phase. To test this, EdU incorporation was assessed in transduced cells at 12 dpi (Figure 24A).

At this stage, the percentage of EdU-incorporating transduced cells was significantly higher following Ascl1 overexpression compared to control and Bcl2 alone groups (control: 2.54 ± 1.50%, Ascl1: 16.9 ± 1.75%, Ascl1-Bcl2: 7.99 ± 4.48%, Bcl2: 0.70 ± 0.41%, p=0.01, Figure 24B, C), indicating that Ascl1-induced proliferation persists at 12 dpi. While Ascl1-Bcl2 overexpression promoted only moderate EdU-incorporation, it did not differ significantly from the effect induced by Ascl1 (Ascl1 vs Ascl1-Bcl2 p=0.08, Figure 24B, C). In contrast, Bcl2-transduced cells rarely incorporated EdU, suggesting that Bcl2 has a limited proliferative effect. Analysis of the proportion of proliferating transduced OPCs (Sox10 and EdU-double positive cells) revealed a striking increase following Ascl1 overexpression compared to control, Ascl1-Bcl2 and Bcl2 alone (control: 4.63 ± 1.80%, Ascl1: 18.3 ± 1.46%, Ascl1-Bcl2: 8.93 ± 3.63%, Bcl2: 1.09 ± 0.68%, p=0.003, Figure 24B, C). These results indicate that Ascl1 overexpression maintains enhanced OPC proliferation at 12 dpi, with no additional proliferative effect of Bcl2. Instead, co-expression of Bcl2 with Ascl1 appears to attenuate this effect at this timepoint.

To determine whether sustained Ascl1-induced proliferation renders increased oligodendroglial cell numbers, Sox10-expressing cell density (cells/mm^2) was quantified at 12 dpi. In contrast to 4 dpi, Ascl1 overexpression resulted in a striking increase of Sox10-expressing cell density compared to other conditions (control: 523.2 ± 119.1 Sox10$^+$/mm^2, Ascl1: 1046.9 ± 229.8 Sox10$^+$/mm^2, Ascl1-Bcl2: 637.7 ± 81.7 Sox10$^+$/mm^2, Bcl2: 687.2 ± 67.9 Sox10$^+$/mm^2, Figure 24D, E), suggesting that Ascl1-mediated proliferative effect expands oligodendroglial population in the injured cortex.

In summary, these findings suggest that Ascl1-mediated enhancement of OPC proliferation persists beyond the early post-injury phase, resulting in the expansion of oligodendroglial cells by 12 dpi.

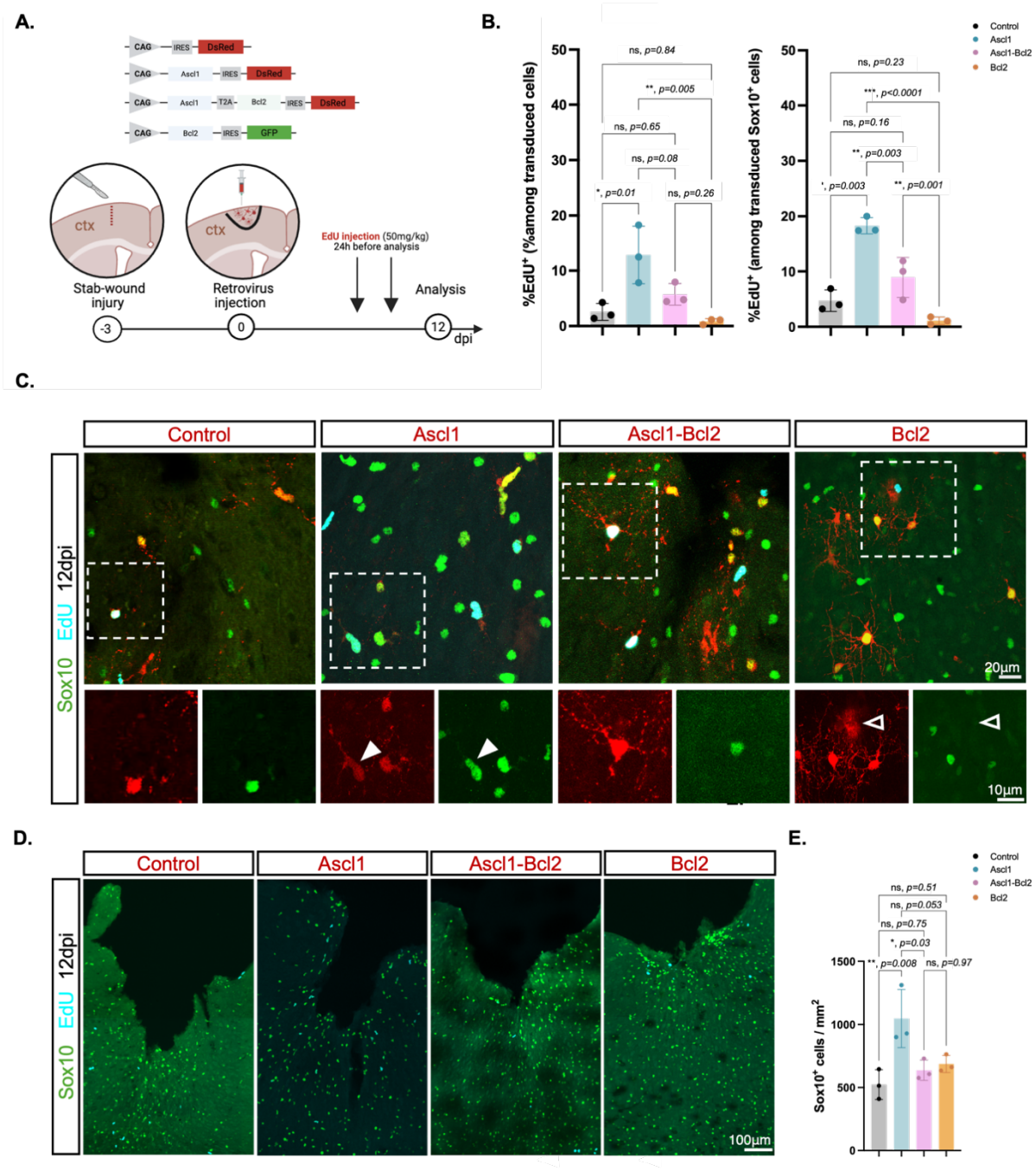
A.
CAG IRES DsRed
CAG Ascl1 IRES DsRed
CAG Ascl1 T2A Bcl2 IRES DsRed
CAG Bcl2 IRES GFP
ctx
ctx
Stab-wound injury
Retrovirus injection
EdU injection (50mg/kg) 24h before analysis
Analysis
-3
0
12
dpi
B.
%EdU+ (%among transduced cells)
%EdU+ (among transduced Sox10+ cells)
ns, p=0.84
**, p=0.005
ns, p=0.65
ns, p=0.08
*, p=0.01
ns, p=0.26
ns, p=0.23
***, p<0.0001
ns, p=0.16
**, p=0.003
', p=0.003
**, p=0.001
Control
Ascl1
Ascl1-Bcl2
Bcl2
C.
Control
Ascl1
Ascl1-Bcl2
Bcl2
Sox10 EdU 12dpi
20µm
10µm
D.
Control
Ascl1
Ascl1-Bcl2
Bcl2
Sox10 EdU 12dpi
100µm
E.
Sox10+ cells / mm2
ns, p=0.51
ns, p=0.053
ns, p=0.75
*, p=0.03
**, p=0.008
ns, p=0.97
Control
Ascl1
Ascl1-Bcl2
Bcl2

Figure 24: Ascl1 overexpression increases proliferation of cells of oligodendroglial lineage in the injured adult cortex at 12 days post-injection (dpi). A. Schematic representation of experimental approach. Retroviruses encoding DsRed only (control), Ascl1, Ascl1 and Bcl2, or Bcl2 were injected three days following cortical stab-wound injury. 24 hours before sacrifice, animals received two intraperitoneal injections of EdU to label proliferating cells at 12 dpi. **B.** Quantification of the percentage of transduced cells that incorporate EdU and of cells that incorporate EdU among Sox10-expressing transduced cells at 12 dpi. **C.** Representative confocal images displaying EdU incorporation (in cyan) and Sox10 expression (in green) in transduced cells. **D.** Representative confocal images showing Sox10-expressing cell density (in green) and EdU-incorporating cells (in cyan) at the injection site across groups. **E.** Quantification of total number of Sox10-expressing cell density (cells/mm^2). White arrowheads indicate marker-positive and empty arrowheads indicate marker-negative cells. Data shown as mean ± SD. Statistical tests: Kruskal-Wallis' test followed by Dunn's multiple comparison test (B) or one-way ANOVA followed by Tukey's multiple comparison test (E). n=3 mice per group, control: 240 cells analyzed; Ascl1: 989 cells analyzed; Ascl1-Bcl2: 283 cells analyzed; Bcl2: 835 cells analyzed.

4.5.7. *Ascl1-induced proliferation does not extend to reactive astrocytes in the injured adult cortex at 12 dpi*

The sustained effect of Ascl1 on OPC proliferation at 12 dpi prompted assessment to reveal whether this proliferative effect remains restricted to OPCs or extends to other glial cell types, such as reactive astrocytes, at this time-point.

To address this, GFAP expression was evaluated in cells transduced with control, Ascl1, Ascl1-Bcl2 or Bcl2 at 12 dpi (Figure 25A). The proportion of transduced reactive astrocytes was decreased in Ascl1 and Ascl1-Bcl2 groups compared to control and Bcl2 (control: 14.5 ± 8.52%, Ascl1: 1.38 ± 1.37%, Ascl1-Bcl2: 0 ± 0%, Bcl2: 11.75 ± 5.94%, p=0.03, Figure 25B, C), indicating minimal contribution of reactive astrocytes to the Ascl1-transduced population. Furthermore, the proportion of transduced reactive astrocytes at 12 dpi decreased compared to 4 dpi (4 dpi - Ascl1: 6.52 ± 4.72%, Ascl1-Bcl2: 4.32 ± 4.49%), suggesting either limited survival of reactive astrocytes, GFAP downregulation or fate transition following Ascl1 or Ascl1-Bcl2 overexpression.

Next, to determine the effect of Ascl1 on reactive astrocyte proliferation, EdU-incorporation was analyzed in transduced GFAP-expressing cells 12 dpi. Notably, no EdU-incorporating reactive astrocytes were detected following transduction with control, Ascl1, Ascl1-Bcl2 or Bcl2 (control: 0 ± 0%, Ascl1: 0 ± 0%, Ascl1-Bcl2: 0 ± 0%, Bcl2: 0 ± 0%, Figure 25B, D), suggesting that transduced reactive astroglia do not proliferate under any condition, including following Ascl1 expression.

Together, these findings demonstrate that Ascl1-mediated effect remains restricted to cells of oligodendroglial lineage in the injured adult cortex at 12 dpi.

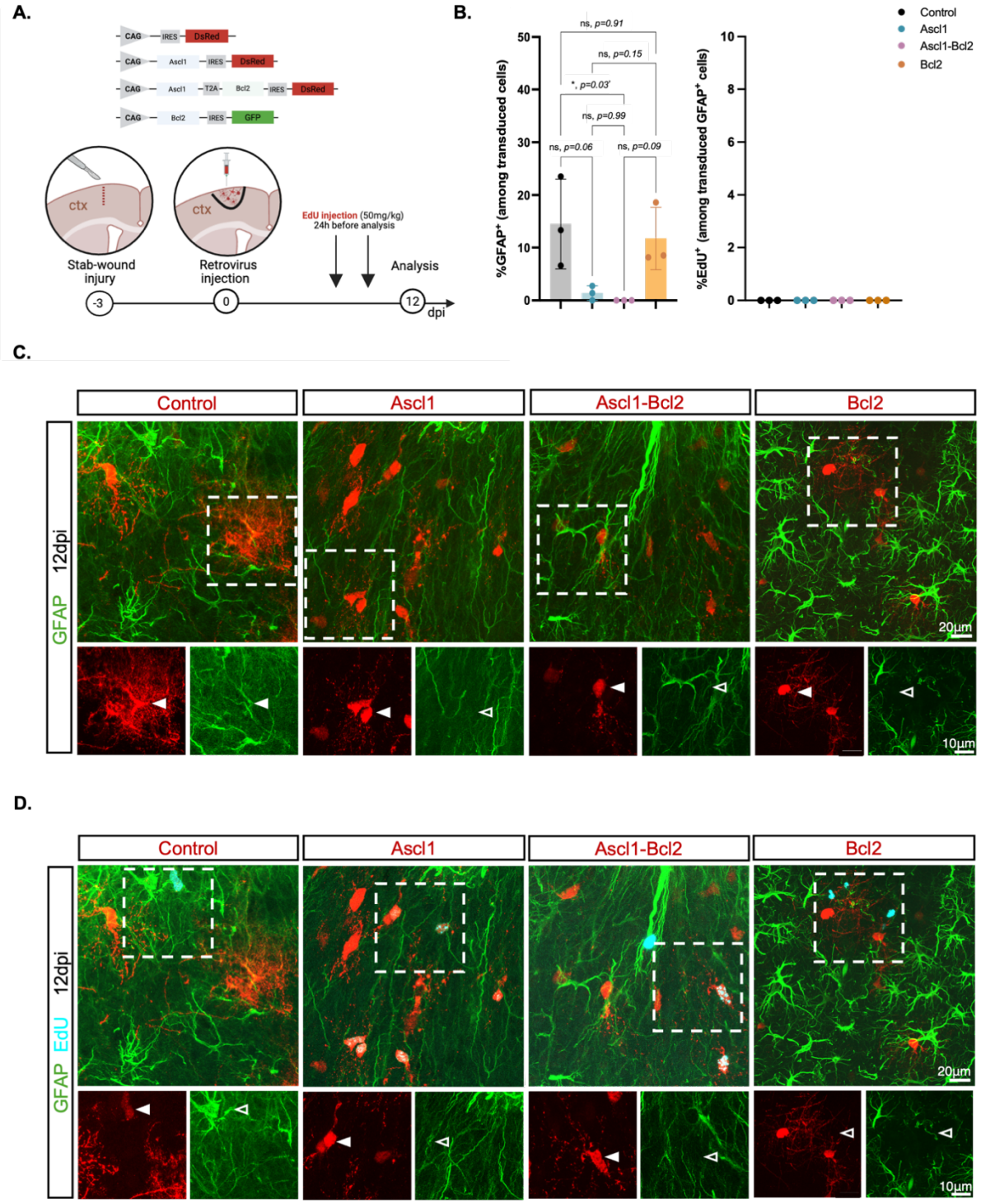
A.
CAG IRES DsRed
CAG Ascl1 IRES DsRed
CAG Ascl1 T2A Bcl2 IRES DsRed
CAG Bcl2 IRES GFP
ctx
ctx
Stab-wound injury
Retrovirus injection
EdU injection (50mg/kg) 24h before analysis
Analysis
-3
0
12
dpi
B.
Control
Ascl1
Ascl1-Bcl2
Bcl2
ns, p=0.91
ns, p=0.15
*, p=0.03
ns, p=0.99
ns, p=0.06
ns, p=0.09
%GFAP+ (among transduced cells)
%EdU+ (among transduced GFAP+ cells)
C.
Control
Ascl1
Ascl1-Bcl2
Bcl2
GFAP 12dpi
20µm
10µm
D.
Control
Ascl1
Ascl1-Bcl2
Bcl2
GFAP EdU 12dpi
20µm
10µm

Figure 25: Ascl1 overexpression does not affect proportion or proliferation of reactive astrocytes in the injured adult cortex at 12 days post-injection (dpi). A. Schematic representation of experimental approach. Retroviruses encoding DsRed only (control), Ascl1, Ascl1 and Bcl2, or Bcl2 were injected three days following cortical stab-wound injury. 24 hours before sacrifice, animals received two intraperitoneal injections of EdU to label proliferating cells at 12 dpi. **B.** Quantification of the percentage of transduced cells that incorporate EdU and of cells that incorporate EdU among GFAP-expressing transduced cells at 12 dpi. **C.** Representative confocal images showing GFAP expression (in green) in transduced cells with across groups (in red) **D.** Representative confocal images displaying EdU incorporation (in cyan) and GFAP expression (in green) in transduced cells. White arrowheads indicate marker-positive and empty arrowheads indicate marker-negative cells. Data shown as mean ± SD. Statistical tests: Kruskal-Wallis' test followed by Dunn's multiple comparison test, n=3 mice per group, control: 244 cells analyzed; Ascl1: 992 cells analyzed; Ascl1-Bcl2: 140 cells analyzed; Bcl2: 751 cells analyzed.

4.5.8. Ascl1-transduced proliferating cells do not derive from astrocytes in the injured adult cortex

Ascl1 overexpression increased the proportion of Sox10-expressing cells at 4- and 12 dpi in the injured adult cortex. While this effect may primarily reflect enhanced proliferation of transduced OPCs, it also raised the question of whether the observed shift toward oligodendroglial identity could also result from conversion of other glial cells, particularly reactive astrocytes, into oligodendroglial cells. Moreover, ectopic expression Sox10 has been shown to convert astrocytes into oligodendroglial-like cells *in vivo* (Mokhtarzadeh Khanghahi et al., 2018) and given Ascl1's role in oligodendrocyte specification and differentiation during development (Nakatani et al., 2013), it was next examined whether astrocyte-to-oligodendroglia reprogramming occurs in the injured cortex following Ascl1 overexpression.

To determine the cellular origin of proliferating Ascl1-transduced cells, genetic fate-mapping was conducted using Aldh1l1-CreER^{T2}/RCE mice, in which astrocytes are endogenously labeled with GFP (Marichal et al., 2024; Sousa et al., 2009; Srinivasan et al., 2016). Tamoxifen (150mg/kg, daily for five consecutive days) was administered to induce GFP expression, followed by cortical injury, and retroviral injection (Figure 22A). Astrocyte labelling efficiency was evaluated by assessing co-expression of GFP with the pan-astrocytic marker Sox9 at 12 dpi (Figure 26A). Analysis revealed that a substantial proportion of astrocytes was successfully labeled with GFP (GFP$^+$/Sox9$^+$: 66.3 ± 5.0%, GFP$^-$/Sox 9$^+$: 33.7 ± 5.0%, Figure 26B, C), demonstrating robust astrocyte labeling in Aldh1l1-CreER^{T2}/RCE mice.

GFP expression was next assessed in cells transduced with control, Ascl1 or Ascl1-Bcl2 to determine their astrocytic origin. The control group showed the highest proportion of transduced cells co-expressing GFP, indicating a greater fraction of astrocyte-derived cells compared to Ascl1 or Ascl1-Bcl2 groups (control: 23.6 ± 4.70%, Ascl1: 14.8 ± 2.73%, Ascl1-Bcl2: 5.01 ± 2.55%, $p<0.003$, Figure 26D, E). Furthermore, the lower proportion of traced cells detected in Ascl1 and Ascl1-Bcl2 groups did not differ significantly, demonstrating minimal contribution of astrocytes to Ascl1- and Ascl1-Bcl2-transduced populations. Next, to reveal whether proliferating transduced cells originated from astrocytes, EdU-incorporation was analyzed in GFP-expressing transduced cells at 12 dpi. Notably, no EdU-incorporating cells were detected in any group (control: 0 ± 0%, Ascl1: 0 ± 0%, Ascl1-Bcl2: 0 ± 0%, Figure 26F, G), indicating that proliferating transduced cells do not originate from astrocytes.

Lastly, whether astrocyte-derived transduced cells acquire oligodendroglial identity was examined by assessing Sox10 expression in fate-mapped cells (GFP-

expressing). Sox10 expression was absent in astrocyte-derived transduced cells across groups (control: 0 ± 0%, Ascl1: 0 ± 0%, Ascl1-Bcl2: 0 ± 0%, Figure 26F, G), suggesting that astrocyte-to-oligodendroglia conversion does not contribute to the Ascl1-mediated increase in oligodendroglial cells observed in the injured adult cortex.

4.5.9. Ascl1 enhances proliferation of pre-existing OPCs in a cell-autonomous manner in the injured adult cortex

The absence of astrocyte-derived proliferating cells suggested that Ascl1-transduced proliferating cells originate from pre-existing OPCs. To test this, genetic fate-mapping was conducted using NG2-CreER^{TM}/RCE mice, in which OPCs are endogenously labelled with GFP (Marichal et al., 2024; Sousa et al., 2009; X. Zhu et al., 2011). Tamoxifen was administered, as previously described, prior to cortical injury and retroviral injection (Figure 27A). Labeling efficacy was assessed by quantifying GFP-expressing cells co-expressing the OPC marker, PDGFRα. At 12 dpi, OPCs that co-expressed GFP were detected in the injured adult cortex (GFP$^+$/ PDGFRα$^+$: 61.5 ± 17.9%, GFP$^-$/ PDGFRα$^+$: 38.5 ± 17.9% in control, GFP$^+$/ PDGFRα$^+$: 43.7 ± 12.73%, GFP$^-$/ PDGFRα$^+$: 56.3 ± 12.73% in Ascl1, GFP$^+$/ PDGFRα$^+$: 51.3 ± 9.43%, GFP$^-$/ PDGFRα$^+$: 48.7 ± 12.73% in Ascl1-Bcl2, Figure 27B, C), indicating an overall robust OPC labeling in NG2-CreER^{TM}/RCE mice, despite variability among groups.

GFP expression was next assessed in transduced cells across groups to determine their cellular origin (Figure 27D). Quantification revealed GFP co-expression across groups, with no significant differences in the proportion of OPC-derived transduced cells (control: 28.2 ± 3.31%, Ascl1: 23.5 ± 9.42%, Ascl1-Bcl2: 40.7 ± 4.81%, Figure 27E), indicating that an important fraction of the transduced population could be traced back to pre-existing OPCs.

To further characterize OPC-derived transduced cells, Sox10 expression was evaluated in GFP and DsRed co-expressing cells to confirm their oligodendroglial identity (Figure 27E). A substantial fraction of fate-mapped transduced cells expressed Sox10 across all groups, with an increased proportion observed in Ascl1 and Ascl1-Bcl2 groups compared to control (control: 63.9 ± 6.42%, Ascl1: 93.6 ± 5.59%, Ascl1-Bcl2: 85.4 ± 1.79%, $p<0.03$, Figure 27E), indicating a higher fraction of fate-mapped cells transduced with Ascl1 or Ascl1-Bcl2 are of oligodendroglial lineage. Notably, Sox10-expressing cells were among the non-fate-mapped transduced population in all groups (control: 23.8 ± 17.1%, Ascl1: 59.0 ± 21.6%, Ascl1-Bcl2: 43.5 ± 4.22%), which is consistent with the partial recombination efficiency observed in NG2-CreER^{TM}/RCE mice (~ 50-60%, Figure 27B, C). These results further support an OPC origin of a

substantial fraction of transduced cells and indicate that OPC-derived cells largely retain oligodendroglial lineage identity at 12 dpi.

The cellular origin of proliferating transduced cells was identified next by assessing EdU incorporation in OPC-derived cells. Analysis revealed a significantly higher proportion of proliferating OPC-derived cells in the Ascl1 group compared to the control group (control: 0.88 ± 1.52%, Ascl1: 13.6 ± 5.15%, p=0.003, Figure 27F, G). In contrast, the fraction observed in the Ascl1-Bcl2 group (Ascl1-Bcl2: 6.36 ± 3.55%, Figure 27F, G) did not differ significantly from either control or Ascl1 conditions. These results indicate that Ascl1 overexpression enhances proliferation of pre-existing OPCs.

Lastly, to determine if the Ascl1-mediated effect extends beyond transduced cells over time, EdU labeling in non-transduced but genetically fate-mapped OPCs (GFP-expressing only) was analyzed. No differences in the proportion of non-transduced, fate-mapped proliferating OPCs were observed among groups (control: 0.83 ± 0.72%, Ascl1: 0.98± 0.41%, Ascl1-Bcl2: 0 ± 0%, Figure 23G), indicating that the effect of Ascl1 is restricted to transduced cells in the injured adult cortex and therefore cell-autonomous.

Altogether, these findings suggest that proliferating Ascl1-transduced cells arise from pre-existing OPCs, that OPC-derived Ascl1-transduced cells maintain their oligodendroglial identity, and that Ascl1-mediated proliferative effect remains cell-autonomous.

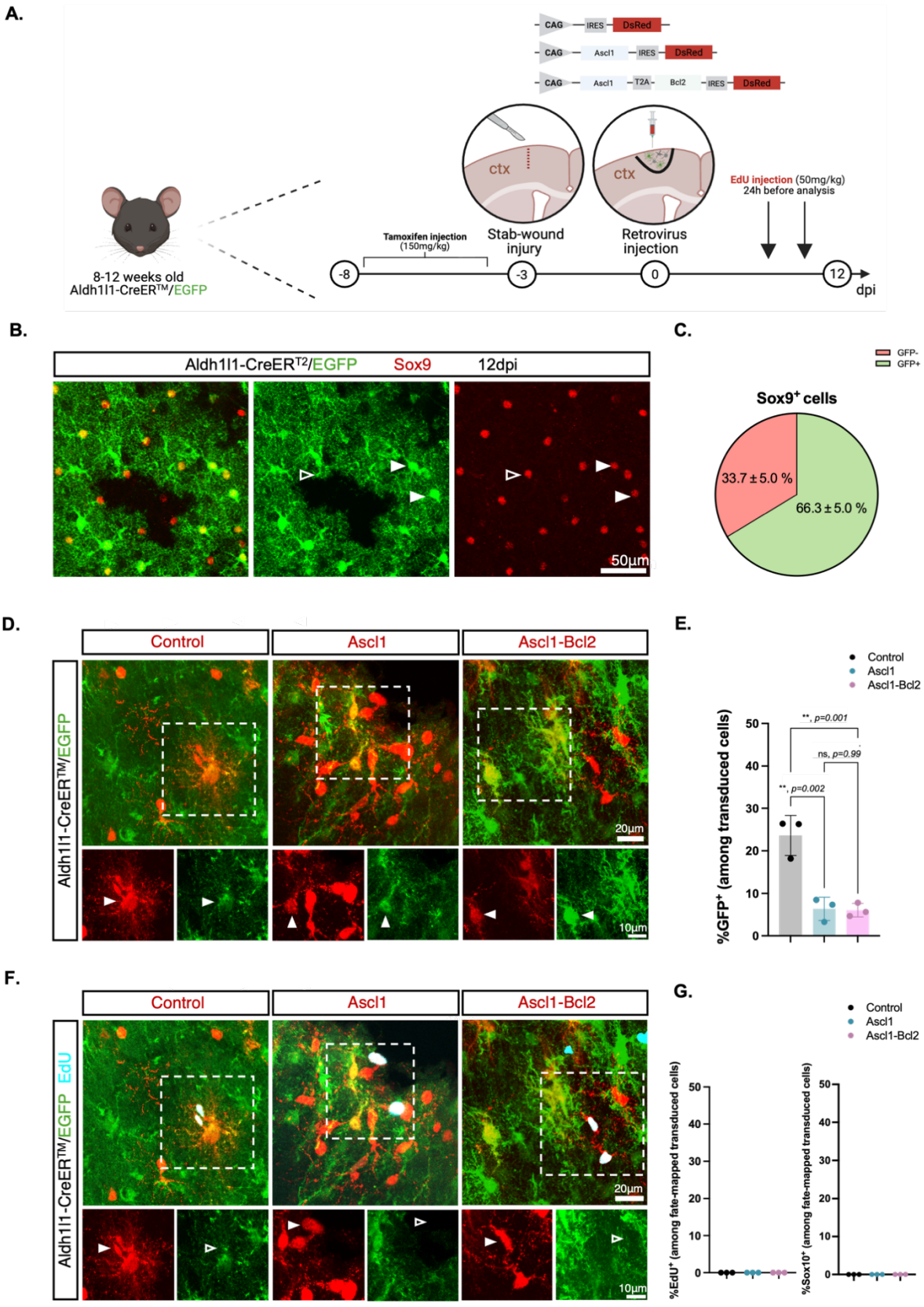
A.
CAG IRES DsRed
CAG Ascl1 IRES DsRed
CAG Ascl1 T2A Bcl2 IRES DsRed
ctx
ctx
8-12 weeks old
Aldh1l1-CreER™/EGFP
Tamoxifen injection
(150mg/kg)
Stab-wound
injury
Retrovirus
injection
EdU injection (50mg/kg)
24h before analysis
-8
-3
0
12
dpi
B.
Aldh1l1-CreER^T2/EGFP Sox9 12dpi
50µm
C.
GFP-
GFP+
Sox9+ cells
33.7 ± 5.0 %
66.3 ± 5.0 %
D.
Control
Ascl1
Ascl1-Bcl2
Aldh1l1-CreER™/EGFP
20µm
10µm
E.
Control
Ascl1
Ascl1-Bcl2
%GFP+ (among transduced cells)
**, p=0.001
ns, p=0.99
**, p=0.002
F.
Control
Ascl1
Ascl1-Bcl2
Aldh1l1-CreER™/EGFP EdU
20µm
10µm
G.
Control
Ascl1
Ascl1-Bcl2
%EdU+ (among fate-mapped transduced cells)
%Sox10+ (among fate-mapped transduced cells)

Figure 26: Genetic fate-mapping revealed that Ascl1-transduced proliferating cells do not derive from astrocytes in the injured adult cortex. A. Schematic representation of experimental approach. Retroviruses encoding DsRed only (control), Ascl1, Ascl1 and Bcl2 were injected in Aldh1l1-CreER^{T2}/RCE mice three days following cortical stab-wound injury. To induce Cre-recombination for the labeling of astrocytes with GFP, mice received one intraperitoneal injection of tamoxifen daily for five consecutive days. To label proliferating cells at 12 dpi, mice received two intraperitoneal injections of EdU 24 hours before sacrifice. **B.** Representative confocal images displaying labeling efficiency in Aldh1l1-CreER^{T2}/RCE mice at 12 dpi. **C.** Quantification of the percentage of Sox9-expressing cells that co-express GFP in the cortex at 12 dpi. **D.** Representative confocal images showing GFP expression in transduced cells with across groups (in red) **E.** Quantification of the percentage of transduced cells that derive from astrocytes at 12 dpi. **F.** Representative confocal images showing GFP expression (in green) and EdU incorporation (in cyan) in transduced cells with across groups (in red). **G.** Quantification of the percentage of transduced fate-mapped cells that incorporate EdU or express Sox10. White arrowheads indicate marker-positive and empty arrowheads indicate marker-negative cells. Data shown as mean ± SD. Statistical tests: Kruskal-Wallis' test followed by Dunn's multiple comparison test, n=3 mice per group, control: 289 cells analyzed; Ascl1: 2236 cells analyzed; Ascl1-Bcl2: 647 cells analyzed.

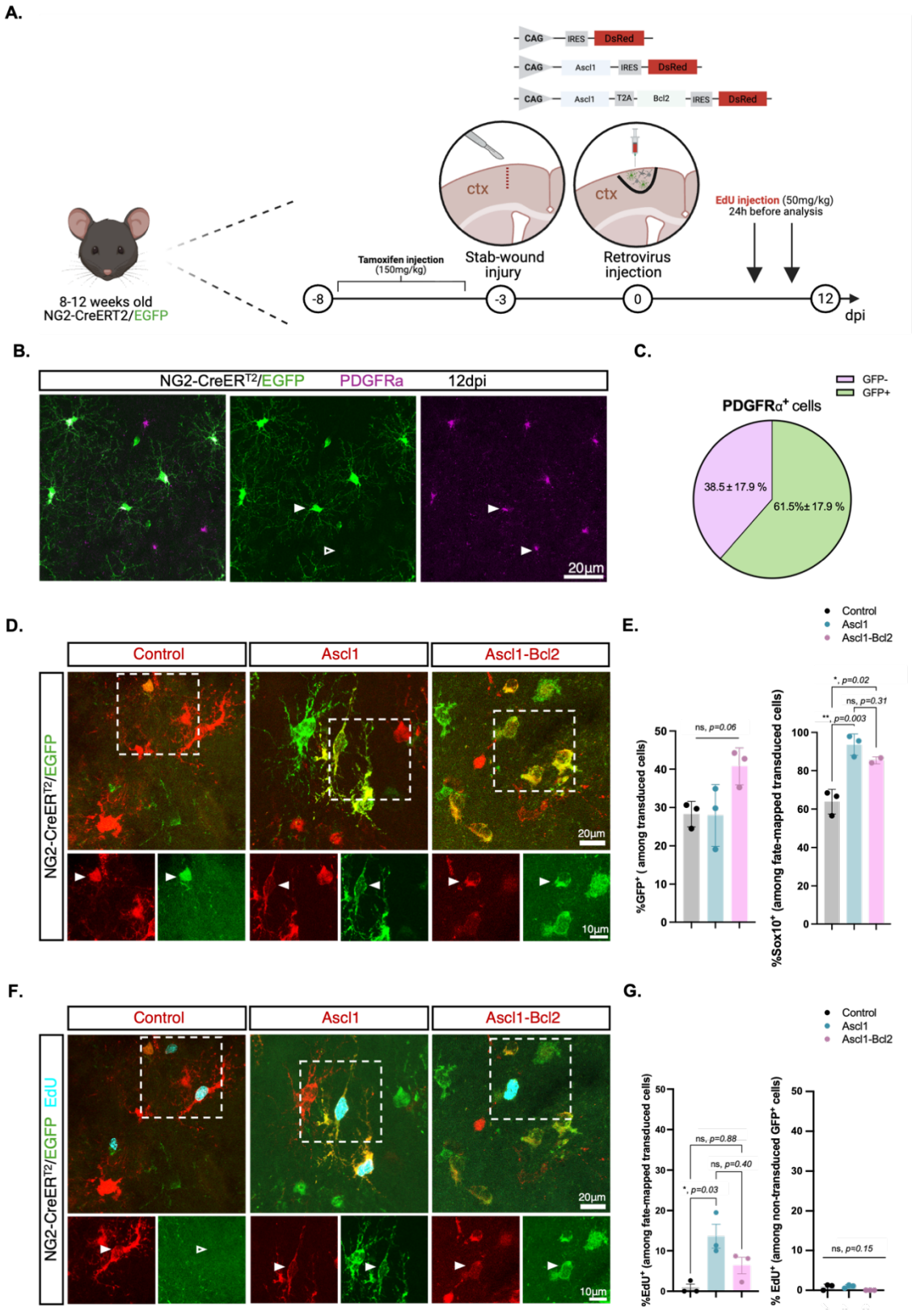
A.
CAG IRES DsRed
CAG Ascl1 IRES DsRed
CAG Ascl1 T2A Bcl2 IRES DsRed
ctx
ctx
EdU injection (50mg/kg)
24h before analysis
8-12 weeks old
NG2-CreERT2/EGFP
Tamoxifen injection
(150mg/kg)
Stab-wound
injury
Retrovirus
injection
-8
-3
0
12
dpi
B.
NG2-CreERT2/EGFP PDGFRa 12dpi
20µm
C.
GFP-
GFP+
PDGFRα+ cells
38.5 ± 17.9 %
61.5%± 17.9 %
D.
Control
Ascl1
Ascl1-Bcl2
NG2-CreERT2/EGFP
20µm
10µm
E.
Control
Ascl1
Ascl1-Bcl2
%GFP+ (among transduced cells)
ns, p=0.06
%Sox10+ (among fate-mapped transduced cells)
*, p=0.02
ns, p=0.31
**, p=0.003
F.
Control
Ascl1
Ascl1-Bcl2
NG2-CreERT2/EGFP EdU
20µm
10µm
G.
Control
Ascl1
Ascl1-Bcl2
%EdU+ (among fate-mapped transduced cells)
ns, p=0.88
ns, p=0.40
*, p=0.03
% EdU+ (among non-transduced GFP+ cells)
ns, p=0.15

Figure 27: Genetic fate-mapping revealed that Ascl1 overexpression enhances proliferation of pre-existing OPCs in the injured adult cortex. **A.** Schematic representation of experimental approach. Retroviruses encoding DsRed only (control), Ascl1, Ascl1 and Bcl2 were injected in NG2-CreER^{TM}/RCE mice three days following cortical stab-wound injury. To induce Cre-recombination for the labeling of astrocytes with GFP, mice received one intraperitoneal injection of tamoxifen daily for five consecutive days. To label proliferating cells at 12 dpi, mice received two intraperitoneal injections of EdU 24 hours before sacrifice. **B.** Representative confocal images displaying labeling efficiency in NG2-CreER^{TM}/RCE mice at 12 dpi. **C.** Quantification of the percentage of PDGFRα-expressing cells that co-express GFP in the cortex at 12 dpi. **D.** Representative confocal images showing GFP expression in transduced cells with across groups (in red) **E.** Quantification of the percentage of transduced cells that derived from OPCs and of fate-mapped cells that express Sox10 at 12 dpi. **F.** Representative confocal images showing GFP expression (in green) and EdU incorporation (in cyan) in transduced cells with across groups (in red). **G.** Quantification of the percentage of transduced fate-mapped cells and non-transduced OPCs that incorporate EdU. White arrowheads indicate marker-positive and empty arrowheads indicate marker-negative cells. Data shown as mean ± SD. Statistical tests: one-way ANOVA and Tukey's multiple comparison test (graph in **E**.), or Kruskal-Wallis' test followed by Dunn's multiple comparison test (graph in **G**.), n=3 mice per group, control: 259 cells analyzed; Ascl1: 515 cells analyzed; Ascl1-Bcl2: 416 cells analyzed.

4.5.10. Ascl1-induced proliferation of oligodendrocyte precursor cells is maintained long-term in the injured adult cortex

Having established that Ascl1 induces sustained OPC proliferation at 12 dpi (subsection 4.5.5 and 4.5.8), it was next investigated whether this proliferative effect persists long-term or declines over time. Given that retrovirus-mediated transgene expression is expected to persist unless actively silenced, Sox10 expression and EdU incorporation were examined in transduced cells at 28 and 70 dpi to assess the long-term maintenance of the Ascl1-mediated effect on oligodendroglial identity and proliferation.

At 28 dpi, Sox10 expression was evaluated in cells transduced with control, Ascl1, Ascl1-Bcl2 or Bcl2 (Figure 28A). Quantification revealed that the proportion of Sox10-expressing cells was significantly higher in Ascl1 and Ascl1-Bcl2 groups compared to control and Bcl2 alone (control: 57.9 ± 5.94%, Ascl1: 86.2 ± 4.86%, Ascl1-Bcl2: 85.7 ± 8.20%, Bcl2: 72.7 ± 3.61%, p=0.002, Figure 28B, C), indicating that the shift towards oligodendroglial identity observed at earlier stages (4 and 12 dpi) persists at 28 dpi. Next, EdU-labeling was conducted as described previously and analysis showed that the fraction of EdU-incorporating transduced cells remained elevated in the Ascl1 group compared to control and Bcl2 alone (control: 0 ± 0 %, Ascl1: 14.2 ± 1.62%, Ascl1-Bcl2: 9.29 ± 1.21%, Bcl2: 0.44 ± 0.43%, p=0.02, Figure 28B, D), indicating that Ascl1-induced proliferation is maintained at 28 dpi. Similarly, EdU-incorporation among Sox10-expressing transduced cells showed sustained proliferation of Ascl1-transduced OPCs (control: 0 ± 0%, Ascl1: 14.2 ± 2.98%, Ascl1-Bcl2: 9.18 ± 2.15%, Bcl2: 0.63 ± 0.60%, p=0.02, Figure 28B, D), confirming that proliferation occurs specifically within oligodendroglial lineage cells at this stage. No significant differences were observed between Ascl1 and Ascl1-Bcl2, consistent with observations at earlier stages. To determine whether sustained proliferation results in changes in oligodendroglial lineage cell density, the total number of Sox10-expressing cells was quantified around the lesion site at 28 dpi. Sox10-expressing cell density ($Sox10^+$ cells/mm^2) did not change significantly between groups (control: 612.9 ± 123.5 cells/mm^2, Ascl1: 868.7 ± 262.1 cells/mm^2, Ascl1-Bcl2: 577.6 ± 115.4 cells/mm^2, Bcl2: 792.4 ± 185.4 cells/mm^2, n=3/group, p>0.05; data not shown), indicating the Ascl1-mediated increase in Sox10-expressing cell density observed at 12 dpi (subsection 4.5.6) is not maintained at 28 dpi. Altogether, these findings suggest that Ascl1 alone is sufficient to induce OPC proliferation, that this effect is sustained over time, and that the addition of Bcl2 does not further enhance this proliferative response.

To investigate whether Ascl1-mediated proliferative effect on OPCs persists even longer, Sox10 expression and EdU incorporation expression was evaluated at 70

dpi (Figure 29A). The proportion of Sox10-expressing cells remained increased in Ascl1 and Ascl1-Bcl2 groups compared to control (control: 62.1 ± 1.27%, Ascl1: 96.3 ± 0.83%, Ascl1-Bcl2: 96.7 ± 1.80%, p=0.0001, Figure 29B, C), indicating that Ascl1 or Ascl1-Bcl2 sustained oligodendroglial marker expression long-term. Strikingly, EdU-incorporation also remained significantly increased in Ascl1-transduced cells compared to control (control: 0.64 ± 1.11%, Ascl1: 12.7 ± 2.69%, Ascl1-Bcl2: 3.47 ± 2.39%, p=0.03, Figure 29B, D) as well as in transduced OPCs (control: 1.01 ± 1.74%, Ascl1: 13.5 ± 3.18%, Ascl1-Bcl2: 4.17 ± 2.63%, p=0.03, Figure 29B, D), indicating long-term sustained OPC proliferation by Ascl1.

In summary, these findings demonstrate that Ascl1-induced OPC proliferation persists for up to 10 weeks post-transduction (70 dpi) in the injured adult cortex and that oligodendroglial identity is maintained long-term in transduced cells.

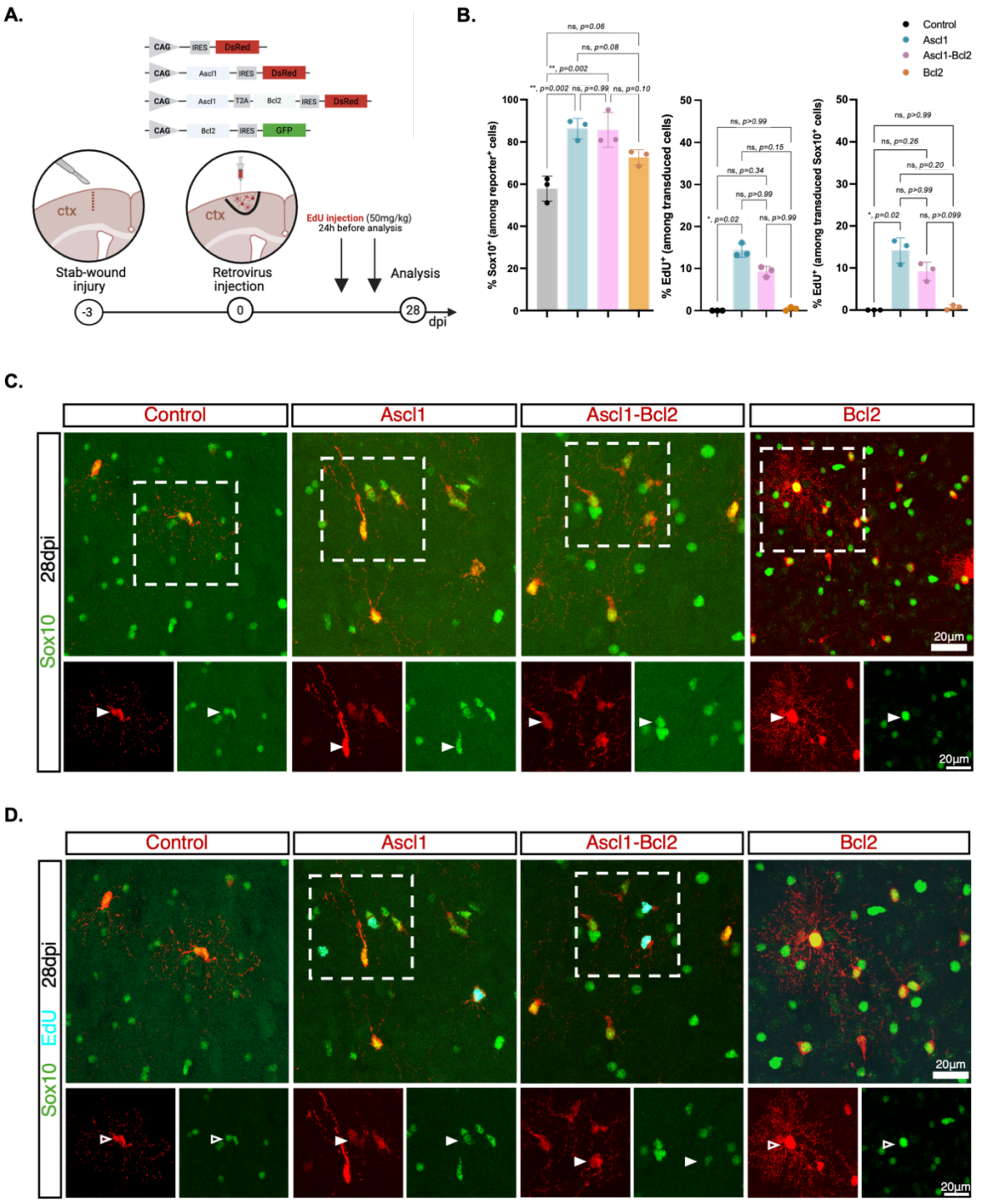
A.
CAG IRES DsRed
CAG Ascl1 IRES DsRed
CAG Ascl1 T2A Bcl2 IRES DsRed
CAG Bcl2 IRES GFP
ctx
ctx
Stab-wound injury
Retrovirus injection
EdU injection (50mg/kg) 24h before analysis
Analysis
-3
0
28
dpi
B.
Control
Ascl1
Ascl1-Bcl2
Bcl2
% Sox10+ (among reporter+ cells)
% EdU+ (among transduced cells)
% EdU+ (among transduced Sox10+ cells)
C.
Control
Ascl1
Ascl1-Bcl2
Bcl2
28dpi
Sox10
20µm
D.
Control
Ascl1
Ascl1-Bcl2
Bcl2
28dpi
EdU
Sox10
20µm

Figure 28: Ascl1-mediated increase of OPC proliferation in the injured adult cortex is maintained at 28 days post-injection (dpi). A. Schematic representation of experimental approach. Retroviruses encoding DsRed only (control), Ascl1, Ascl1 and Bcl2, or Bcl2 were injected three days following cortical stab-wound injury. 24 hours before sacrifice, animals received two intraperitoneal injections of EdU to label proliferating cells at 28 dpi. **B.** Quantification of the percentage of transduced cells that express Sox10, incorporate EdU, and of cells that incorporate EdU among Sox10-expressing transduced cells at 28 dpi. **C.** Representative confocal images displaying Sox10 expression (in green) in transduced cells (in red). **D.** Representative confocal images displaying EdU incorporation (in cyan) and Sox10 expression (in green) in transduced cells. White arrowheads indicate marker-positive and empty arrowheads indicate marker-negative cells. Data shown as mean ± SD. Statistical tests: one-way ANOVA followed by Tukey's multiple comparison test (%Sox10) or Kruskal-Wallis' test followed by Dunn's multiple comparison test (%EdU). n=3 mice per group, control: 187 transduced cells analyzed; Ascl1: 466 cells analyzed; Ascl1-Bcl2: 1043 cells analyzed; Bcl2: 693 cells analyzed.

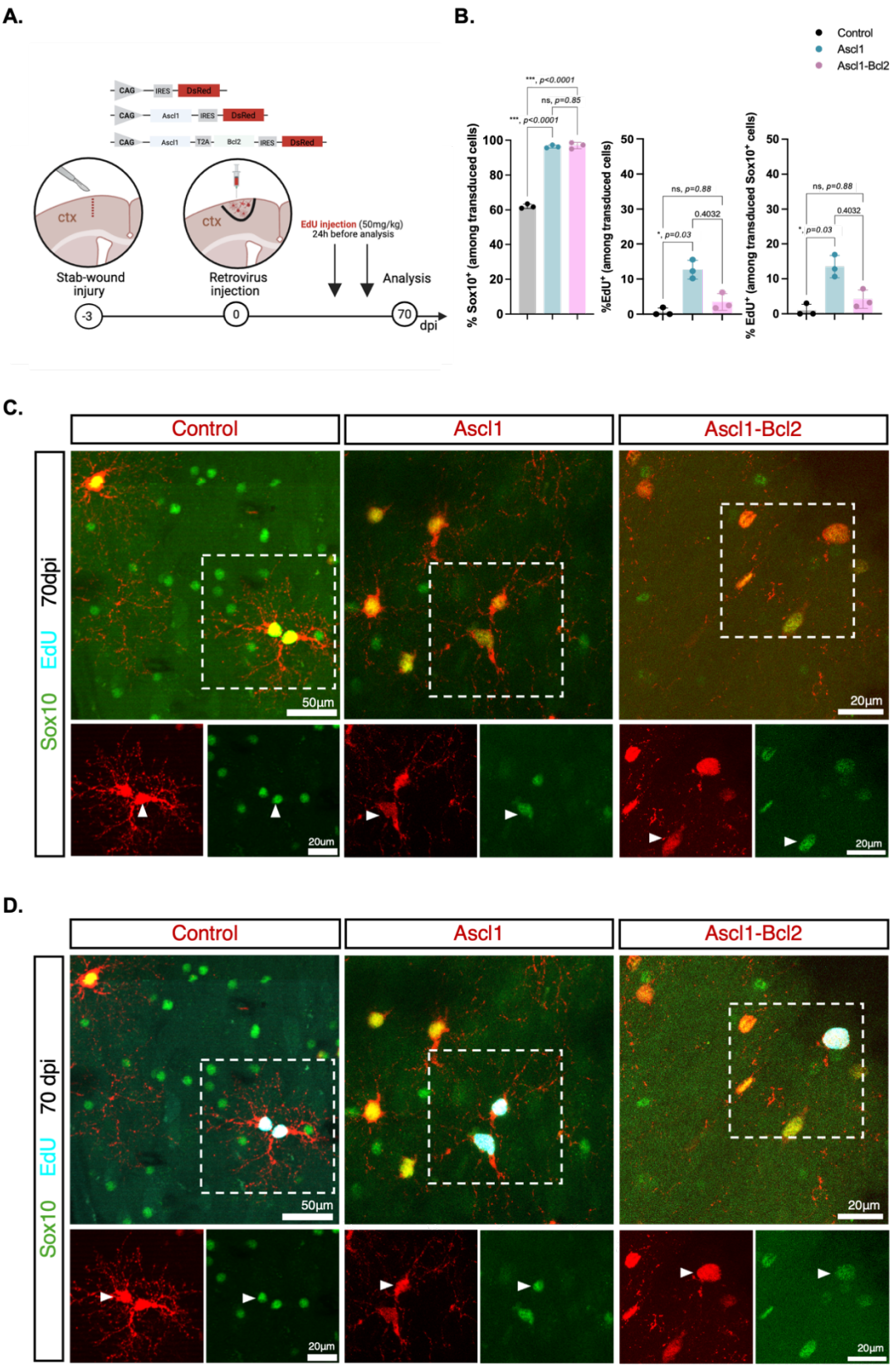
A.
CAG
IRES
DsRed
Ascl1
T2A
Bcl2
ctx
Stab-wound injury
Retrovirus injection
EdU injection (50mg/kg) 24h before analysis
Analysis
-3
0
70
dpi
B.
Control
Ascl1
Ascl1-Bcl2
% Sox10+ (among transduced cells)
%EdU+ (among transduced cells)
% EdU+ (among transduced Sox10+ cells)
***, p<0.0001
ns, p=0.85
ns, p=0.88
0.4032
*, p=0.03
C.
Control
Ascl1
Ascl1-Bcl2
Sox10 EdU 70dpi
50µm
20µm
D.
Control
Ascl1
Ascl1-Bcl2
Sox10 EdU 70 dpi
50µm
20µm

Figure 29: Ascl1-mediated increase of OPC proliferation in the injured adult cortex is sustained at 70 days post-injection (dpi). A. Schematic representation of experimental approach. Retroviruses encoding DsRed only (control), Ascl1, Ascl1 and Bcl2 were injected three days following cortical stab-wound injury. 24 hours before sacrifice, animals received two intraperitoneal injections of EdU to label proliferating cells at 70 dpi. **B.** Quantification of the percentage of transduced cells that express Sox10, incorporate EdU, and of cells that incorporate EdU among Sox10-expressing transduced cells at 70 dpi. **C.** Representative confocal images displaying Sox10 expression (in green) in transduced cells (in red). **D.** Representative confocal images displaying EdU incorporation (in cyan) and Sox10 expression (in green) in transduced cells. White arrowheads indicate marker-positive and empty arrowheads indicate marker-negative cells. Data shown as mean ± SD. Statistical tests: one-way ANOVA followed by Tukey's multiple comparison test (% Sox10) or Kruskal-Wallis' test followed by Dunn's multiple comparison test (%EdU). n=3 mice per group, control: 255 cells analyzed; Ascl1: 382 cells analyzed; Ascl1-Bcl2: 616 cells analyzed.

4.6. Transduced oligodendroglial lineage cells can undergo differentiation into oligodendrocytes in the injured adult cortex

4.6.1. Ascl1 overexpression does not prevent differentiation of oligodendroglial lineage cells into pre-myelinating oligodendrocytes in the injured adult cortex

Since Ascl1 overexpression promotes sustained OPC proliferation in the injured adult cortex, it was next investigated whether this proliferative effect impacts the ability of OPC to undergo maturation and differentiation into oligodendrocytes. To investigate whether OPC differentiation is hindered by Ascl1, expression of the pre-myelinating oligodendrocyte marker breast carcinoma amplified sequence 1 (BCAS1) was evaluated in cells transduced with control, Ascl1, Ascl1-Bcl2, or Bcl2 at 28 dpi (Figure 30A).

At this stage, BCAS1 expression was detected in transduced cells across all groups (Figure 30C). Notably, the proportion of BCAS1-expressing transduced cells was significantly higher in the Ascl1-Bcl2 group compared to control (control: 11.02 ± 1.61%, Ascl1: 20.67 ± 4.41%, Ascl1-Bcl2: 27.2 ± 2.13%, Bcl2: 17.7 ± 8.60%, p=0.02, Figure 30B, C), suggesting that co-expression of Ascl1 and Bcl2 may promote differentiation of OPCs into pre-myelinating oligodendrocytes.

Altogether, these findings demonstrate that Ascl1 does not prevent OPC differentiation, but co-expression with Bcl2 may facilitate OPCs progression toward pre-myelinating oligodendrocytes at 28 dpi.

4.6.2. Subset of Ascl1-transduced oligodendroglia can undergo further differentiation into mature oligodendrocytes in the injured adult cortex

To determine whether transduced cells expressing pre-myelinating markers at 28 dpi maintain this identity or continue to differentiate into mature oligodendrocytes over time, BCAS1 expression was evaluated in cells transduced with control, Ascl1, or Ascl1-Bcl2 at 70 dpi (Figure 31A). For this time-point, Bcl2-alone condition was not included.

BCAS1 expression was detected across all groups, with no significant differences in the proportion of BCAS1-expressing transduced cells between groups at 70 dpi (control: 17.07 ± 2.13%, Ascl1: 17.01 ± 1.62%, Ascl1-Bcl2: 10.6 ± 3.66%, p>0.05, Figure 31B, C). Compared to 28 dpi, the proportion of BCAS1-expressing cells was reduced in both Ascl1 and Ascl1-Bcl2 groups (28 dpi - Ascl1: 20.67 ± 4.41%, Ascl1-

Bcl2: 27.2 ± 2.13%, Figure 30B, C), suggesting that pre-myelinating transduced cells may progress in their differentiation towards mature oligodendrocytes.

To determine whether the reduced proportion of BCAS1-expressing transduced cells reflects their progression to mature oligodendrocytes, CC1 expression, a marker enriched in mature oligodendrocytes, was assessed at 70 dpi. Analysis revealed a fraction of CC1-expressing transduced cells across all groups, but this proportion did not differ significantly between conditions (control: 4.40 ± 3.81%, Ascl1: 4.43 ± 2.96%, Ascl1-Bcl2: 7.43 ± 1.26%, p=0.39, Figure 31B, D), suggesting that a fraction of transduced cells differentiates into mature oligodendrocytes by 70 dpi.

Altogether these results indicate that while Ascl1 overexpression promotes sustained OPC proliferation, it does not impair OPC differentiation competence. This suggests that the expanded OPC population retains the capacity to generate mature oligodendrocytes in the injured adult cortex.

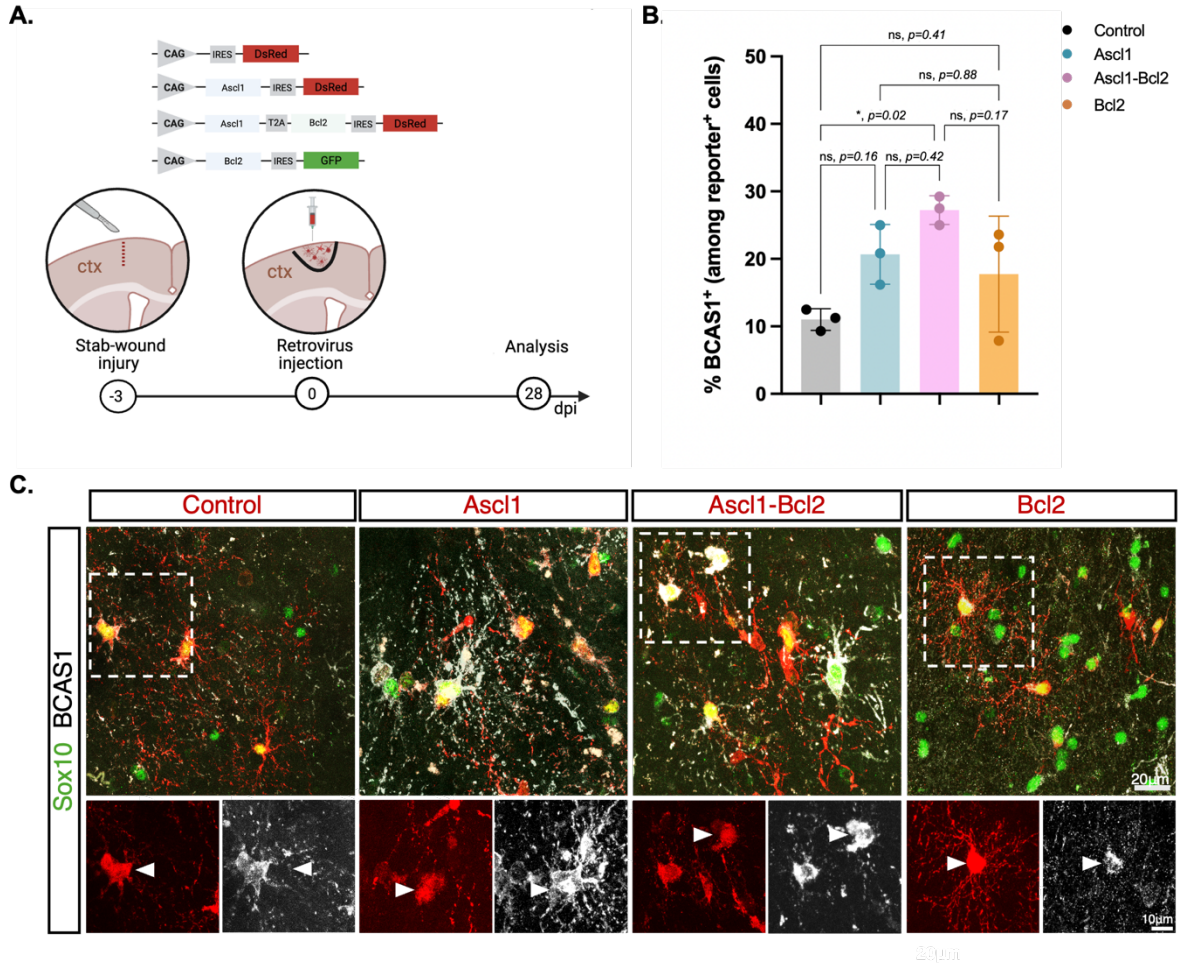

Figure 30: Transduced oligodendroglial lineage cells express markers of pre-myelinating oligodendrocytes at 28 days post-injection (dpi). A. Schematic representation of experimental approach. Retroviruses encoding DsRed only (control), Ascl1, Ascl1 and Bcl2, or Bcl2 were injected three days following cortical stab-wound injury. At 28 dpi, BCAS1 expression was assessed in Sox10-expressing transduced cells. **B.** Quantification of the percentage of transduced cells that express Sox10 and BCAS1 at 28 dpi. **C.** Representative confocal images displaying Sox10 (in green) and BCAS1 (in white) expression in transduced cells (in red). White arrowheads indicate marker-positive and empty arrowheads indicate marker-negative cells. Data shown as mean ± SD. Statistical tests: one-way ANOVA followed by Tukey's multiple comparison test. n=3 mice per group, control: 281 transduced cells analyzed; Ascl1: 276 cells analyzed; Ascl1-Bcl2: 603 cells analyzed; Bcl2: 693 cells analyzed.

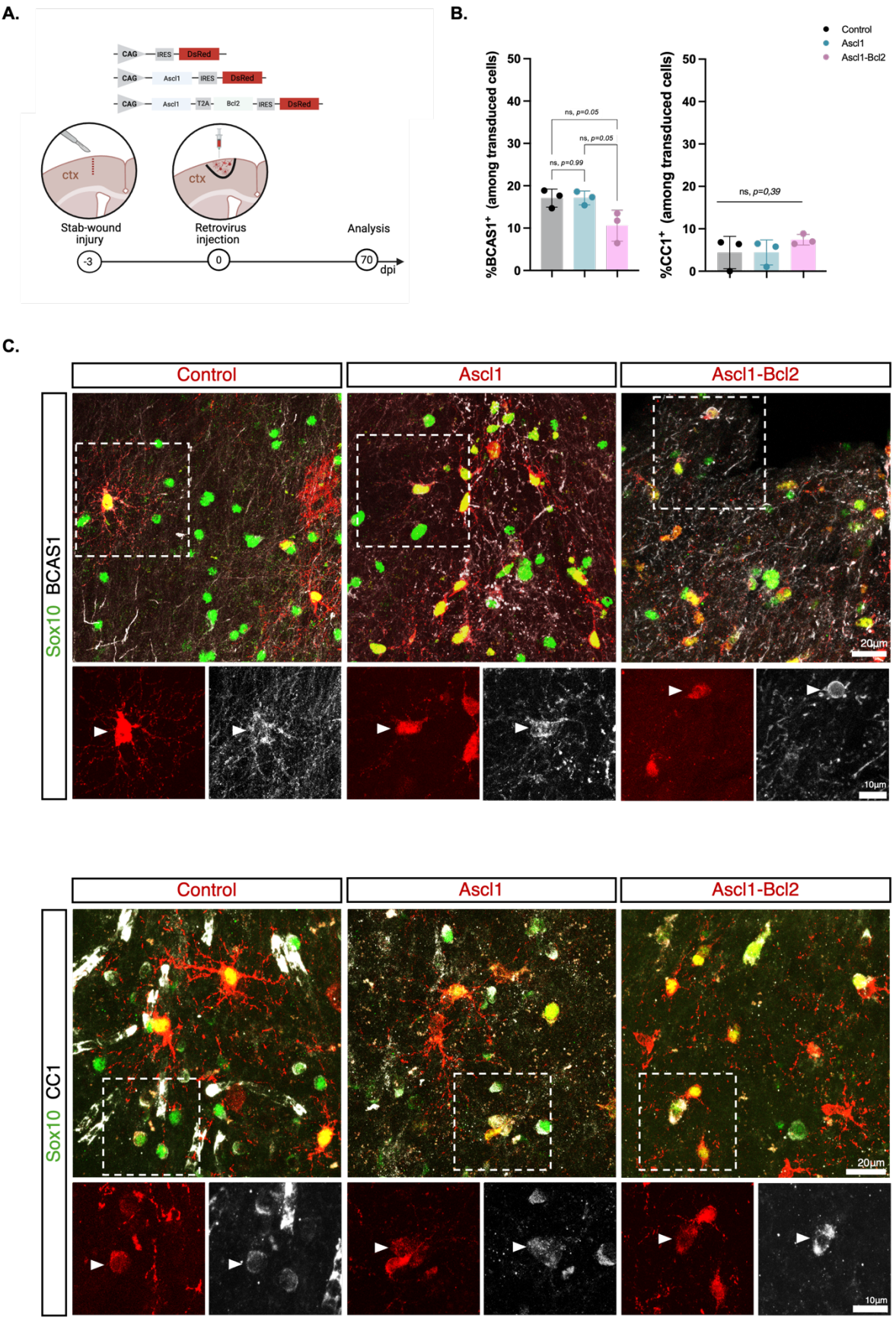
A.
CAG
IRES
DsRed
CAG
Ascl1
IRES
DsRed
CAG
Ascl1
T2A
Bcl2
IRES
DsRed
ctx
ctx
Stab-wound injury
Retrovirus injection
Analysis
-3
0
70
dpi
B.
Control
Ascl1
Ascl1-Bcl2
%BCAS1+ (among transduced cells)
%CC1+ (among transduced cells)
ns, p=0.05
ns, p=0.05
ns, p=0.99
ns, p=0,39
C.
Control
Ascl1
Ascl1-Bcl2
Sox10 BCAS1
20µm
10µm
Control
Ascl1
Ascl1-Bcl2
Sox10 CC1
20µm
10µm

Figure 31: Transduced oligodendroglial lineage cells express markers of pre-myelinating oligodendrocytes and mature oligodendrocytes at 70 days post-injection (dpi). A. Schematic representation of experimental approach. Retroviruses encoding DsRed only (control), Ascl1, Ascl1 and Bcl2 were injected three days following cortical stab-wound injury. At 70 dpi, BCAS1 or CC1 expression was assessed in Sox10-expressing transduced cells. **B.** Quantification of the percentage of transduced cells that express Sox10 and BCAS1 or Sox10 and CC1 at 70 dpi. **C.** Representative confocal images displaying Sox10 (in green) and BCAS1 (in white) expression in transduced cells (in red). **D.** Representative confocal images displaying Sox10 (in green) and CC1 (in white) expression in transduced cells (in red). White arrows indicate marker-positive and empty arrows indicate marker-negative cells. Data shown as mean ± SD. Statistical tests: one-way ANOVA followed by Tukey's multiple comparison test. n=3 mice per group, control: 118 cells analyzed; Ascl1: 396 cells analyzed; Ascl1-Bcl2: 522 cells analyzed.

In conclusion, this chapter demonstrated that Ascl1 overexpression induced robust, sustained and cell-autonomous OPC proliferation in the injured adult cortex. Genetic fate-mapping revealed that the expanded oligodendroglial population mainly derived from pre-existing OPCs, with no detectable contribution from reactive astrocytes. Ascl1-mediated proliferative response was marginally influenced by Bcl2 co-expression at early stages, but this effect declined over time, suggesting that Ascl1 is the primary driver of OPC proliferation in this context. Importantly, despite their sustained proliferative activity, Ascl1-transduced OPCs exhibited potential for subsequent differentiation, with a fraction progressing toward pre-myelinating stages. Thus, Ascl1 does not appear to prevent OPC maturation and may hold therapeutic potential for remyelination approaches in the injured brain.

5. Discussion

Brain injury and neurodegenerative disorders lead to irreversible loss of neurons and oligodendrocytes, resulting in permanent functional deficits due to the limited regenerative capacity of the adult mammalian brain (reviewed in Zhao et al., 2023). Moreover, loss or dysfunction of myelinating oligodendrocytes and associated myelin abnormalities are features of several pathological conditions, including TBI and demyelinating disorders, such as multiple sclerosis (Festa et al., 2025). In demyelinating disorders, an additional challenge is the arrest of OPC differentiation into mature oligodendrocytes due to inhibitory environmental cues (Tepavčević & Lubetzki, 2022).

In vivo direct reprogramming of endogenous glial cells into neurons or myelinating oligodendrocytes offers a promising strategy for brain repair, aiming to replace lost cells and restore function. *In vivo* glia-to-neuron conversion has been extensively investigated across different pathological contexts (reviewed in Vignoles et al., 2019), and more recently, astrocyte-to-oligodendrocyte lineage cell conversion has also been demonstrated following demyelination (Mokhtarzadeh Khanghahi et al., 2018). While direct reprogramming may bypass arrested OPC differentiation, alternative remyelination approaches have focused on expanding and sustaining the progenitor pool, as reduced local OPC availability and impaired OPC function have been reported in chronic demyelinating contexts (reviewed in Tepavčević & Lubetzki, 2022).

The proneural transcription factor Ascl1 has been explored as a potential reprogramming factor to induce neuronal conversion *in vitro* (Berninger et al., 2007; Chanda et al., 2014). However, efficient Ascl1-mediated glia-to-neuron conversion remains limited *in vivo*, especially in the cerebral cortex (Galante et al., 2022a; Marichal et al., 2024). Ascl1's reprogramming capacity is strongly influenced by its phosphorylation state, as its phospho-deficient mutant, Ascl1SA6, has been reported to yield higher neuronal reprogramming capacity compared to wild-type Ascl1 in the postnatal cortex (Galante et al., 2022a; Marichal et al., 2024). In contrast, in the same model, Ascl1 overexpression predominantly promoted oligodendrocyte precursor cell (OPC) proliferation rather than glia-to-neuron conversion (Galante et al., 2022b). Whether similar effects occur in the injured cortex remained unexplored.

In this study, I investigated the reprogramming potential of Ascl1 and Ascl1SA6 in the injured adult cortex and how their activity is influenced by the hostile inflammatory environment induced by cortical stab-wound injury. I also assessed

whether Ascl1 enhances OPC proliferation, whether this effect is sustained long-term (up to 2.5 months post-transduction), and whether sustained Ascl1-induced proliferation is compatible with OPCs undergoing differentiation. To address this, Ascl1 and Ascl1SA6, alone or in combination with Bcl2, were overexpressed after cortical stab-wound injury, and the identity and proliferative activity of transduced cells were analyzed over time.

In Chapter I, I demonstrated that Ascl1SA6 and Bcl2 induced limited but persistent neuronal reprogramming in the injured cortex, with OPCs constituting a major cellular source of induced neurons (iNs). I also identified potential environmental barriers that likely restrict neuronal conversion and hinder iNs maturation, including the presence of C3-expressing neurotoxic reactive astrocytes at the reprogramming site, and showed that despite these barriers, iNs survived and progressively expressed mature neuronal markers at later stages.

In Chapter II, I showed that Ascl1 enhances OPC proliferation in a sustained and cell-autonomous manner, and that this effect does not extend to other glial cell types, such as reactive astrocytes or microglia. Notably, despite sustained Ascl1-induced proliferation, a subset of transduced OPCs remained capable of differentiating into pre-myelinating oligodendrocytes and mature oligodendrocytes, suggesting that Ascl1-driven proliferation does not preclude OPC differentiation. Altogether, these findings indicate that the phosphorylation state of Ascl1 determines distinct glial responses in the injured cortex and that the local environment influences cellular competence and reprogramming outcomes.

This work provides insights into the limitations and opportunities of Ascl1-mediatedc lineage decisions, which may help improve its efficiency and translation into therapeutic approaches for brain injury.

5.1 Ascl1 phosphorylation state mediates distinct reprogramming outcomes in the injured cortex

In the present study, the effects of Ascl1 or its phospho-deficient mutant Ascl1SA6 overexpression in reactive glia were investigated in the injured adult cortex. Although Ascl1 overexpression efficiently induces neuronal conversion of postnatal cortical astrocytes *in vitro* (Berninger et al., 2007), it fails to reprogram cortical glia into neurons *in vivo* (Galante et al., 2022a; Heinrich et al., 2014; Marichal et al., 2024). Consistent with these reports, Ascl1 overexpression in the injured adult cortex failed to induce neuronal marker expression in transduced cells, which largely retained glial morphology (Figure 6B, C; 3B, C), suggesting that in the injured cortex, Ascl1 overexpression does not promote neuronal conversion. In contrast, Ascl1SA6 overexpression induced rapid downregulation of both glial markers, resulting in a marked decrease in the fraction of transduced OPCs (~37% decrease) and reactive astrocytes (~23% decrease; Figure 6B). This loss of glial marker expression is consistent with a shift away from non-neuronal identity and suggests initiation of lineage conversion.

To determine whether the early loss of glial marker expression reflected the initiation of neuronal conversion, neuronal identity was evaluated at an intermediate stage (12 dpi). Despite the early reduction of Sox10 and GFAP expression and the acquisition of an immature neuronal-like morphology by most transduced cells, Ascl1SA6-transduced cells did not express the immature neuronal marker DCX, and only ~ 1% acquired mature marker, NeuN, expression (Figure 7B, C). In contrast, Ascl1-transduced cells retained glial-like morphology and did not express DCX or NeuN (Figure 7B, C). Together, these findings are consistent with previous reports showing that Ascl1 overexpression alone is insufficient to drive neuronal conversion in the injured adult cortex (Heinrich et al., 2014). While Ascl1SA6 exhibits enhanced neurogenic capacity compared to wild-type Ascl1 (Cooper et al., 2026; Galante et al., 2022a; Marichal et al., 2024), its overexpression alone in the injured adult cortex resulted in limited neuronal conversion, suggesting that additional factors are required to achieve efficient glia-to-neuron conversion in this context.

These discrepancies in reprogramming outcomes between Ascl1 and Ascl1SA6 are consistent with their distinct neurogenic abilities reported in previous studies. Specifically, multi-site phosphorylation has been shown to regulate Ascl1's ability to drive neuronal differentiation in a cell cycle dependent manner, as Cdk-mediated phosphorylation limited its neurogenic function and unphosphorylated Ascl1 promoted neuronal differentiation in *Xenopus* embryos (Ali et al., 2014). In parallel, Ascl1's

phosphorylation and neurogenic activity were also shown to be modulated by RAS/ERK signaling in neural progenitors, with high RAS levels favoring proliferation and gliogenesis, and lower RAS levels suppressing proliferation and promoting neurogenesis (Li et al., 2014). Notably, elevated RAS signaling has been reported in injury models, raising the possibility that injury-associated signaling may bias Ascl1 away from neuronal programs *in vivo* (Liu et al., 2015). Beyond developmental contexts, unphosphorylated Ascl1 was also demonstrated to promote neuronal differentiation and induce cell cycle exit in cancer cells, thereby reducing tumorigenic potential (Ali et al., 2014; Wylie et al., 2015).

In this study, the reprogramming outcomes of Ascl1 and Ascl1SA6 overexpression in the injured adult brain, suggest that Ascl1 becomes phosphorylated in transduced reactive cortical glial cells. While direct evidence for Ascl1 phosphorylation in OPCs or astrocytes is lacking, one hypothesis would be that active kinase pathways in reactive glia maintain Ascl1 in a phosphorylated state. Candidate pathways include Cdk-mediated phosphorylation or RAS/ERK signaling, both of which have been shown to regulate Ascl1 activity in other cellular contexts (Ali et al., 2014; Li et al., 2014). Whether alternative kinases could contribute to Ascl1 phosphorylation in reactive glial cells remains to be determined.

Alternatively, the enhanced capacity of Ascl1SA6 may not solely result from preventing phosphorylation, as serine-to-alanine mutations could alter protein conformation or modulate interactions with binding partners, thereby rendering Ascl1SA6 more neurogenic (Ali et al., 2014; Azzarelli et al., 2024). Post-translational phosphorylation has been linked to accelerated Ascl1 degradation, whereas unphosphorylated Ascl1 exhibits increased protein stability (Ali et al., 2014; Azzarelli et al., 2024; Liu et al., 2024). Similarly, Ascl1SA6-transduced cells were reported to exhibit higher levels of Ascl1 protein than Ascl1-transduced cells (Marichal et al., 2024). While increased protein stability and delayed degradation may prolong Ascl1 availability at neuronal loci and enhance its ability to activate neuronal programs, no direct correlation has been established between the increased stability of unphosphorylated Ascl1 and its enhanced neurogenic competence (Azzarelli et al., 2024). Notably, unphosphorylated Ascl1 also exhibits increased chromatin opening at neuronal loci during reprogramming, potentially facilitating chromatin remodeling required for neuronal conversion (Azzarelli et al., 2024).

Finally, Ascl1 expression dynamics may further influence reprogramming outcomes. In neural stem cells, oscillatory Ascl1 expression maintains cells in a proliferative state, whereas sustained Ascl1 expression promotes neuronal differentiation (Imayoshi et al., 2013). In the context of retroviral-mediated expression,

Ascl1 levels are expected to remain constitutively high in transduced reactive glia, a condition that would be predicted to favor neuronal conversion. However, rapid Ascl1 phosphorylation in reactive glial cells could counteract this effect and direct Ascl1 activity towards proliferative or gliogenic programs.

Altogether, these results indicate that preventing Ascl1 phosphorylation enhances its neurogenic potential and accelerates loss of glial marker expression. However, this modification alone is insufficient to drive efficient neuronal conversion in the injured adult cortex, highlighting the that the injury milieu may constrain reprogramming efficiency.

5.2. Co-expression of Ascl1SA6 with Bcl2 enhances neuronal reprogramming efficiency

5.2.1. Bcl2-mediated effect on neuronal reprogramming in the injured adult cortex

Newly generated iNs are highly vulnerable to cell death during reprogramming, largely due to conversion-induced cellular stress. In particular, reprogrammed cells undergo a metabolic transition from gliogenic glycolysis to neuronal oxidative phosphorylation, which is accompanied by increased mitochondrial activity and excessive ROS production (Gascón et al., 2016, 2017). Co-expression of neurogenic transcription factors with the anti-apoptotic protein Bcl2 was shown to substantially increase conversion efficiency and iNs survival, as Bcl2 co-expression alleviated ferroptosis, an iron-dependent programmed cell death driven by excessive ROS production (Dixon et al., 2012; Gascón et al., 2016; Marichal et al., 2024).

To assess whether promoting cell survival could enhance reprogramming efficiency in the injured adult cortex, Ascl1 and Ascl1SA6 were co-expressed with Bcl2 (Figure 8A). Ascl1-Bcl2 overexpression resulted in low neuronal conversion efficiency, with minimal morphological changes and limited expression of neuronal markers (DCX and NeuN) in transduced cells (Figure 8B, C). While some neuronal conversion was observed, these findings indicate that Ascl1 exhibits limited neurogenic potential in the injured adult cortex, with Bcl2 co-expression providing a modest enhancement of this outcome. This finding is consistent with reports from the postnatal intact cortex, in which Ascl1 and Bcl2 overexpression similarly resulted in limited glia-to-neuron conversion (Marichal et al., 2024).

In contrast, Ascl1SA6-Bcl2 overexpression led to an increase in the proportion of NeuN-expressing transduced cells (~10%) in the injured adult cortex and most transduced cells displayed immature neuronal-like morphology, characterized by a rounded soma and one to two elongated processes (Figure 8B, C). However, overall NeuN expression remained low, and no DCX-expressing cells were detected (Figure 8B, C), suggesting delayed maturation or incomplete acquisition of neuronal identity. This contrasts with findings in the postnatal intact cortex, where Ascl1SA6 and Bcl2 gave rise to both NeuN-, and DCX-expressing iNs at comparable time-points (Marichal et al., 2024). The absence of DCX expression in this study also differs from previous reports in the injured adult cortex, which reported the generation of DCX-expressing iNs using different reprogramming factors, including Ascl1 and Sox2 (Heinrich et al., 2014) or Neurog2 and Bcl2 (Gascón et al., 2016). Similarly, Lentini et al., (2021), reported DCX expression in converted cells following Ascl1 and Dlx2 overexpression

in the epileptic hippocampus, where reactive glia were also targeted. These discrepancies could reflect environmental constraints in the injured cortex that Ascl1SA6 and Bcl2 may not overcome, contrasting with Sox2 or Neurog2 and Bcl2, which yielded higher efficiency in the same injury model (Gascón et al., 2016; Heinrich et al., 2014). Alternatively, Ascl1SA6-Bcl2-iNs may bypass the canonical DCX-expressing intermediate state. Altogether, the absence of DCX expression, together with the low fraction of NeuN-expressing iNs detected, is consistent with delayed or altered neuronal identity acquisition or iN maturation following Ascl1SA6-Bcl2-mediated neuronal reprogramming in the injured milieu.

Additional metabolic support, including ectopic expression of neuronal mitochondrial genes (Russo et al., 2021) or antioxidant treatments, such as α-tocopherol, have been shown to accelerate neuronal conversion and improve neuronal maturation (Gascón et al., 2016). Whether similar antioxidant or metabolic interventions could improve the outcome of Ascl1- and Ascl1SA6-mediated reprogramming by alleviating metabolic constraints and promoting iNs maturation remains to be tested.

Altogether, these findings suggest that while Bcl2 improves conversion efficiency by enhancing iNs survival, potentially rescuing cells undergoing conversion that would otherwise succumb to ferroptosis, additional supplementation or factor co-expression may be required to overcome intrinsic and environmental barriers that limit iNs maturation in the injured adult cortex.

5.2.2. Technical limitations: injury-induced loss of NeuN antigenicity

Neuronal identity and maturation assessment commonly rely on the detection of NeuN expression (reviewed in Bocchi et al., 2022). NeuN, encoded by the *Rbfox3* gene, is a neuron-specific RNA-binding protein involved in the regulation of alternative splicing programs (Kim et al., 2009). Notably, brain injury can alter NeuN expression and immunoreactivity through changes at the transcriptional and post-transcriptional level, as well as by inducing protein degradation (Munoz-Ballester et al., 2022; Ogino et al., 2022). In addition, both the injury-induced inflammatory response (Gusel'Nikova & Korzhevskiy, 2015; Hernandez et al., 2019) and oxidative stress have been associated with reduced NeuN immunoreactivity in the injured brain (Sugawara et al., 2004). These findings highlight the limitations of using NeuN expression alone as a reliable marker of neuronal identity in the injury-induced milieu. Consistent with these observations, NeuN expression was markedly reduced around the injury site, corresponding to the area containing most transduced cells (Figure 9C), suggesting

that newly generated iNs are exposed to the same environmental cues that reduce NeuN immunoreactivity in pre-existing mature neurons.

As an alternative, neuronal identity was assessed using Nissl dye labeling (NeuroTrace), which labels neuronal somata by binding to Nissl substance in the rough endoplasmic reticulum and is considered less susceptible to injury-mediated degradation (Hernandez et al., 2019). In the present study, Nissl staining revealed a ~21% increase in labeled iNs compared to NeuN immunostaining, indicating that NeuN underestimates neuronal populations in the injured cortex (Figure 9B, D). While NeuN is highly specific for mature neurons, Nissl dyes do not distinguish between immature and mature neurons and can, to a lesser extent, label non-neuronal cells such as pericytes (Damisah et al., 2017). However, no glial marker expression was detected in Nissl-stained cells (data not shown), and the small fraction of Nissl-stained transduced cells displaying non-neuronal morphology were excluded from quantifications (~ 1%). Notably, no Nissl-stained transduced cells were detected with control and Ascl1-Bcl2, further supporting the specificity of Nissl dye labeling in the present context (Figure 9F, G). Additional markers, such as MAP2 or βIII-tubulin, can also be used to assess neuronal identity, but their predominantly dendritic and axonal localization can make expression assessment challenging in converted cells that lack fully developed processes. Therefore, a combinatorial approach using NeuN, Nissl staining, and morphology evaluation was applied in this study to obtain a more robust estimate of neuronal conversion efficiency in the injured adult cortex.

5.3. Context-dependent competence of glial cells for neuronal reprogramming

In this study, neuronal reprogramming was induced in the injured adult cortex using MMLV-based retroviruses for gene delivery. MMLV retroviruses infect both non-proliferating and proliferating cells, but only transduce dividing cells, as integration of viral DNA depends on dissolution of the nuclear envelope during mitosis (Roe et al., 1993; Salas-Briceno et al., 2024). This strategy enables the specific target of proliferating reactive glia rather than postmitotic endogenous neurons (Gascón et al., 2016; Heinrich et al., 2014). Consistently, early characterization of control virus-transduced cells (DsRed only) showed that the majority were OPCs (~53%, Figure 5B, C), followed by reactive astrocytes (~32%, Figure 5B, C) and microglia (~14%). Moreover, no DCX expression was detected in transduced cells, indicating that neuronal progenitors were not targeted in the injured adult cortex (Figure 5B, C), although injury-induced effects on DCX expression cannot be fully excluded.

5.3.1. OPCs are the main cellular source for retrovirus-mediated neuronal reprogramming in the injured adult cortex

Brain injury triggers OPCs to undergo alterations, including migration towards the lesion site and an enhanced proliferative response (Dean et al., 2023; Hughes et al., 2013). Studies have shown that OPC proliferation peaks between 2- and 4-days post-injury (Hughes et al., 2013; Simon et al., 2011). Consistent with this, retrovirus-mediated gene delivery, performed at 3 days post-injury, predominantly transduced OPCs (>50%, Figure 5B, C), matching previous reports using retroviral vectors in the same injury model (Heinrich et al., 2014). Together, this finding confirms that OPCs constitute the primarily targeted population for neuronal reprogramming.

Genetic fate-mapping experiments using a NG2-CreERTM/RCE mouse line (Sousa et al., 2009; Zhu et al., 2011), which specifically labels OPCs, revealed that more than 30% of Ascl1SA6-Bcl2-transduced cells derived from OPCs and that 5-12% expressed NeuN or NeuroTrace in the injured adult cortex, respectively (Figure 12D, E). Considering the OPC labeling efficiency achieved with this transgenic line (~ 56%, Figure 12B, C), the proportion of OPC-derived iNs likely underestimates the contribution of OPCs to neuronal conversion. Optimization of tamoxifen delivery could increase recombination efficiency and reveal additional fate-mapped cells. Nevertheless, these observations align with previous work demonstrating that OPCs-derived iNs arise in the injured adult cortex (Heinrich et al., 2014). In addition, successful OPC-to-neuron conversion has also been reported in different brain regions and conditions, including the striatum (Pereira et al., 2017; Torper et al., 2015) and

injured spinal cord (Tai et al., 2021), further supporting their susceptibility for neuronal reprogramming

Beyond their abundance and elevated proliferative activity, which facilitates their target by retroviral vectors, OPCs display intrinsic properties that may render them more competent for neuronal reprogramming in the injured cortex. During forebrain development, a subset of OPCs arises from ventral neural progenitors in the embryonic ganglionic eminences and share a proximal origin with cortical interneurons and migrate tangentially through the telencephalon (Kessaris et al., 2006). Furthermore, chromatin profiling studies demonstrated that OPCs exhibit increased chromatin accessibility around key interneuron genes compared with astrocytes, suggesting that OPCs may retain a more permissive chromatin landscape at interneuron loci despite their commitment to the oligodendrocyte lineage (Boshans et al., 2019), possibly facilitating reactivation of interneuron programs during reprogramming. Notably, this hypothesis is not supported by observations in the postnatal intact cortex, where Ascl1SA6 and Bcl2-generated interneuron-like iNs arise predominantly from astrocytes rather than OPCs (Marichal et al., 2024). This discrepancy highlights the strong influence of environmental context on cellular reprogramming competence and raising the possibility that cortical injury may enhance OPC susceptibility to neuronal reprogramming.

In addition, OPCs are highly heterogeneous, including in their response to cortical stab wound injury (Koupourtidou et al., 2024). Such heterogeneity may also contribute to differential competence for neuronal reprogramming. This study shows that only a fraction of retrovirus-targeted OPCs underwent neuronal conversion, suggesting variability in intrinsic competence among OPC subsets. Transcriptomic profiling of converting versus non-converting OPCs will be essential to identify specific transcriptional or epigenetic signatures associated with increased neurogenic potential, thus, providing insights into how to improve OPC-mediated neuronal conversion in the injured cortex.

5.3.2. Astrocytes are refractory to retrovirus-mediated neuronal conversion in the injured adult cortex

Astrocytes were the second major population targeted with retroviral vectors for Ascl1SA6-Bcl2-mediated neuronal conversion in the injured model (~32%; Figure 5B, C). This proportion was expected since retroviruses were delivered at 3 days post-injury, whereas reactive astrocyte proliferation has been shown to peak later, around 5-7 days post-injury (Bardehle et al., 2013; Sirko et al., 2013). Strikingly, genetic fate-mapping using Aldh1l1-CreERT2/RCE (Sousa et al., 2009; Srinivasan et al., 2016),

which endogenously labels astrocytes, revealed that Ascl1SA6-Bcl2-derived iNs did not originate from reactive astrocytes in the injured adult cortex (Figure 11D, E). Although recombination efficiency with this line reached ~58%, it may still underestimate the astrocytic contribution to reprogramming. In this study, the fraction of Ascl1SA6-Bcl2 transduced cells that were fate-mapped to reactive astrocytes was low (~2-6%), and none of these cells expressed NeuN or Neurotrace (Figure 11). This finding contrasts with observations in the postnatal intact cortex, where Ascl1SA6 and Bcl2 predominantly converted astrocytes into iNs (Marichal et al., 2024).

Notably, while more studies have reported successful neuronal reprogramming of reactive astrocytes in the lesioned cortex using alternative neurogenic factors, such as Neurog2 and Nurr1 or NeuroD1 (Chen et al., 2020; Mattugini et al., 2019; Zhang et al., 2020), the authenticity of astrocyte-to-neuron conversion in these paradigms has been questioned due to the use of AAV-based vectors. In these studies, AAVs transduced both dividing and non-dividing astrocytes, thereby targeting a broader astrocytic population than retroviral vectors, but accumulating evidence suggests that astrocytic-specific promoters (e.g., *Gfap*) can show non-specific expression in pre-existing neurons, leading to artefactual labeling of endogenous neurons rather than genuine generation of iNs (Wang et al., 2021; Xie et al., 2023). By contrast, studies employing retroviral vectors have provided more robust evidence of authentic astrocyte-to-neuron conversion, demonstrating that cortical reactive astrocytes can be converted by NeuroD1 (Guo et al., 2014; Xiang et al., 2024) or a phospho-deficient form of Neurog2, Neurog2SA (Puglisi et al., 2024). Altogether, these findings suggest that reactive astrocytes in the injured adult cortex may be refractory to retroviral Ascl1SA6-mediated reprogramming.

Following cortical injury, astrocytes undergo extensive transcriptional and morphological remodeling, including hypertrophy, upregulation of GFAP, and cell cycle re-entry (Bardehle et al., 2013; Buffo et al., 2008; Lange Canhos et al., 2021). Notably, reactive astrocytes can acquire neural stem cell-like properties, such as the ability to form neurospheres *in vitro* (Sirko et al., 2013; Zamboni et al., 2020), and injury-specific factors in cerebrospinal fluid have been shown to regulate astrocyte plasticity and neurogenic capacity (Sirko et al., 2023), suggesting that injury-induced plasticity may render them a permissive substrate for neuronal reprogramming. Similarly, in the striatum, astrocytes demonstrated sustained neurogenic competence following excitotoxic injury (Fogli et al., 2024). However, despite this latent neurogenic capacity, cortical reactive astrocytes in this study remained largely refractory to Ascl1SA6-Bcl2-mediated conversion, suggesting that additional regional or context-specific constraints limit their reprogramming in the injured adult cortex. Moreover,

proliferation has emerged as a determinant of reprogramming efficiency, as hyperproliferative cells displayed increased susceptibility to neuronal conversion (Wang et al., 2025). In this study, retroviral injection was administered at 3 days post-injury, whereas astrocyte proliferation peaks around 5-7 days post-injury (Bardehle et al., 2013; Sirko et al., 2013), potentially limiting the transduction of reactive astrocytes in an optimally permissive proliferative state. Nevertheless, injury-induced reactive astrocytes can also adopt a neurotoxic phenotype, activated by microglia-secreted pro-inflammatory cytokines (IL-1α, TNFα, and C1q) and characterized by C3 expression (Clark et al., 2019; Liddelow et al., 2017). Consistently, C3-expressing reactive astrocytes were present in the reprogramming milieu, and C3 mRNA was detected in a subset of transduced cells (Figure 14B, C; Figure 15B, C). Given that neurotoxic reactive astrocytes lose their homeostatic functions and acquire neuroinflammatory features, it is hypothesized that this limits their ability to undergo Ascl1SA6-Bcl2-mediated conversion. Nevertheless, some neurogenic transcription factors, such as NeuroD1, appear to overcome the potentially low reprogramming competency of C3-expressing neurotoxic reactive astrocytes. AAV-mediated NeuroD1 expression in astrocytes not only induced astrocyte-to-neuron conversion but also reduced the proportion of C3-expressing reactive astrocytes (Zhang et al., 2018), yet its authenticity remains to be confirmed. By contrast, in this study the proportion of C3-expressing cells (Figure 14B, C) or C3 mRNA levels (Figure 15B, C) did not differ between injury-only or reprogramming conditions, suggesting that Ascl1SA6 does not reduce the neurotoxic reactive astrocyte population in the injured adult cortex. Whether this would be affected by Bcl2 co-expression remains to be investigated.

Moreover, EdU labeling revealed that proliferating reactive astrocytes at the time of retroviral injection expressed C3 (Figure 16B, C), suggesting that the reactive astrocytes that are accessible to retroviral transduction are predominantly neurotoxic. This supports the hypothesis that the acquisition of a C3-expressing neurotoxic phenotype may diminish the susceptibility of reactive astrocytes to Ascl1SA6-Bcl2-mediated reprogramming in the injured adult cortex. However, whether C3-expressing neurotoxic reactive astrocytes are directly targeted for neuronal reprogramming, and the extent of their contribution to the Ascl1SA6-Bcl2-transduced cell population, will require further validation, for example through genetic fate-mapping approaches.

Future experiments combining Ascl1SA6-Bcl2-mediated neuronal reprogramming with strategies that prevent neurotoxic phenotype induction, including genetic ablation of microglial-secreted activating cytokines (IL-1α, TNFα, and C1q, Liddelow et al., 2017), or pharmacological suppressors (e.g., NLY01, Yun et al., 2018)),

would reveal whether non-neurotoxic reactive astrocytes exhibit higher reprogramming competence.

Together, these findings suggest that Ascl1SA6-Bcl2 does not efficiently convert reactive astrocytes in the injured adult cortex, and that this may be due to the injury-induced transcriptional and inflammatory state of reactive astrocytes, as well as the reprogramming factors used.

5.4. Impact of the local environment to Ascl1SA6-mediated reprogramming in the injured adult cortex

Reprogramming efficiency is highly context-dependent as the same transcription factors can induce distinct outcomes *in vitro* versus *in vivo*, across brain regions, between young and aged brains, and under healthy or injured conditions (Grande et al., 2013; Herrero-Navarro et al., 2021; Vignoles et al., 2019). These discrepancies can arise from both cell-intrinsic properties, such as starting cell identity, and extrinsic factors, including the surrounding environment.

In the adult cortex, injury has been reported to increase reprogramming susceptibility. For example, Sox2-mediated OPC-to-neuron conversion requires that the injury precede viral delivery (Heinrich et al., 2014), and Neurog2 and Nurr1 overexpression shows higher reprogramming efficiency near the lesion site (Mattugini et al., 2019) although this study employed AAV-based vectors whose specificity has been questioned (see subsection 5.3.2). This enhanced competence is hypothesized to result from injury-induced proliferation and subsequent increase in cellular plasticity, as discussed above (subsection 5.3.2), suggesting the notion that injury may transiently render reactive glia more permissive to lineage conversion.

However, the same injury environment that may prime reactive glia for initial conversion also imposes barriers throughout the reprogramming process. Several studies have demonstrated that injury can delay iNs maturation, limit long-term survival, and restrict the acquisition of specific subtypes (Gascón et al., 2016; Grande et al., 2013; Guo et al., 2014; Heinrich et al., 2014). A striking example is the robust astrocyte-to-neuron conversion induced by Ascl1SA6 and Bcl2 in the intact postnatal brain (Marichal et al., 2024). In contrast, in the present study, the same combination seems to promote partial OPC-to-neuron conversion and rare reprogramming of reactive astrocytes. These observations further support the hypothesis that the local milieu can either facilitate or restrict neuronal conversion of glial cells, depending on the cellular source, developmental stage, and injury conditions.

5.4.1. *Injury- and retrovirus-induced inflammatory response at the reprogramming site*

Traumatic cortical injury leads to extensive remodeling of the local environment, triggering an inflammatory response characterized by microglial activation, reactive gliosis, and peripheral immune cell infiltration (Bardehle et al., 2013; Boulton & Al-Rubaie, 2025; Buffo et al., 2005). Consistently, in this study, injury-induced environment exhibited robust leukocyte infiltration and accumulation of activated microglia and reactive astrocytes weeks after injury (Figure 12B, C).

Additionally, retroviral delivery further amplified this inflammatory signature by enhancing microglia recruitment and leukocyte infiltration (Figure 12B, C). This finding agrees with reports showing that retroviral vectors elicit stronger immunoreactivity than AAVs in the injured adult cortex (Mattugini et al., 2019). However, MMLV retroviruses provide a more reliable tool for transgene delivery to induce neuronal reprogramming, as they preferentially transduce dividing cells, thereby reducing the risk of artefactual labelling of endogenous neurons than has been reported with AAV-based vectors (reviewed in Leaman et al., 2022; Wang et al., 2021; Xiang et al., 2021). Nevertheless, this specificity may come at the cost of a stronger inflammatory response, which may further hinder reprogramming efficiency.

Among injury-induced changes, activated microglia secrete pro-inflammatory cytokines that can impair dendritic development and synaptogenesis and promote excessive synaptic pruning (Witcher et al., 2021; Yu et al., 2022). Notably, depleting microglia has been shown to improve Ascl1-mediated neurogenesis in the retina (Todd et al., 2019), suggesting that transiently reducing microglial activation during reprogramming may create a more permissive environment for neuronal conversion. Furthermore, microglia-released pro-inflammatory cytokines can also trigger reactive astrocytes to acquire a neurotoxic phenotype, and their presence in the injury milieu may represent a potential barrier to efficient neuronal reprogramming (Liddelow et al., 2017). Consistently, C3-expressing reactive astrocytes and elevated C3 mRNA were detected around the reprogramming site, as detailed in section 5.3.2 (Figure 14; Figure 15). Activated microglia are also a major source of ROS in the injured and diseased brain (reviewed in Haslund-Vinding et al., 2017). Moreover, neuronal conversion increases ROS levels and increases iNs vulnerability to ROS-mediated ferroptotic cell death (Dixon et al., 2012; Gascón et al., 2016), thus, injury-driven oxidative stress and conversion-induced metabolic stress may synergistically increase iN vulnerability to ferroptosis.

Notably, different injury models can trigger distinct inflammatory responses. For example, ischemic stroke was shown to induce anti-inflammatory or neuroprotective microglial and astrocytic states (Zamanian et al., 2012), and a higher NeuroD1-mediated conversion efficiency was demonstrated after ischemic stroke than after cortical stab-wound injury (Chen et al., 2025). This finding suggests that the type of injury and the reactive glial states it induces may influence the reprogramming outcome. Future studies testing Ascl1SA6-Bcl2-mediated reprogramming in an ischemic model would help determine the extent to which the injury context shapes reprogramming efficiency.

Altogether, injury-specific inflammatory environment, the presence of detrimental glial phenotypes, and ROS-associated metabolic stresses pose substantial barriers to efficient neuronal reprogramming, particularly affecting iNs maturation and survival.

5.4.2 Local environment hinders neuronal maturation in the injured cortex

The adult injured cortex imposes significant constraints not only on initial conversion efficiency, but also on the subsequent maturation and survival of iNs. Heinrich et al. (2014) showed that Ascl1- and Sox2-derived iNs remain morphologically immature and lack NeuN expression at early time-points, suggesting delayed iN maturation. In the present study, Ascl1SA6-Bcl2 overexpression resulted in a progressive increase in NeuN-expressing iNs from 12 dpi to 28 dpi (11% to 32%) and NeuroTrace labelling increased similarly (22% to 60%; Figure 17E), suggesting that iNs can undergo maturation within the injured cortex.

Despite iNs acquiring mature neuronal marker expression, this was accompanied by apparent morphological simplification characterized by fewer processes and reduced complexity. This observation could reflect either actual morphology deterioration or progressive downregulation of reporter expression, a phenomenon that has been observed in MMLV-based vectors, due to transcriptional silencing during cellular differentiation (Pannell & Ellis, 2001), thereby concealing the actual morphology of surviving iNs. Notably, even in the intact postnatal brain, Ascl1SA6 and Bcl2-derived iNs remain smaller than endogenous neurons at comparable time-points (Marichal et al., 2024), suggesting full morphological maturation may be limited with this reprogramming combination. Moreover, in the postnatal brain, Ascl1SA6 and Bcl2 overexpression achieved a conversion efficiency of ~80% (% of NeuN-expressing iNs), with iNs displaying molecular, morphological, and electrophysiological features of fast-spiking PV-like interneurons (Marichal et al., 2024), strikingly contrasting with the

findings in this study (~32%, no detected PV expression, data not shown). The outcome observed also contrasts with others using the same injury model, in which Neurog2 and Bcl2 co-expression generated iNs that displayed deep-layer pyramidal neuron features, mature morphology and electrophysiological properties (Gascón et al., 2016). The high conversion rate and maturation observed required additional support beyond the neurogenic transcription factor and Bcl2 co-expression, namely by antioxidant treatments such as α-Tocotrienol, suggesting that overcoming metabolic and survival hurdles is necessary for iN maturation in the injury context (Gascón et al., 2016). Whether similar antioxidant treatments or alternative approaches such as co-expression of neuron-enriched mitochondrial genes to facilitate metabolic adaptation (Russo et al., 2021) would rescue morphological deterioration and support maturation of Ascl1SA6-Bcl2-iNs in the injured adult cortex remains to be tested. Together, these observations suggest that using only Ascl1SA6-Bcl2 may be insufficient to generate mature subtype-specific iNs in the injured cortex.

Notably, the injury milieu imposes additional constraints on neuronal maturation, as described previously. Moreover, given the presence of C3 neurotoxic astrocytes, activated microglia, and the susceptibility of iNs to metabolic stress and ferroptotic cell death, it is hypothesized that environmental factors may be hindering iNs maturation and survival. Neurotoxic reactive astrocytes release factors that not only induce neuronal death but also inhibit neurogenesis (Liddelow et al., 2017). While not directly tested in this study, reducing neurotoxic reactive astrocytes either by blocking their activation or transiently depleting the environment of activated microglia during critical periods of iNs maturation, or providing sustained trophic support may promote a more permissive milieu for efficient neuronal conversion, iNs maturation, and long-term survival.

Another factor that may influence reprogramming outcome is the timing of transgene delivery and expression relative to the injury response. In this study, retroviral vectors were delivered 3 days post-injury, resulting in transgene expression during the acute phase of the injury. In contrast, AAV-based reprogramming studies often reported robust neuronal conversion and maturation in the injured cortex without requiring antioxidant support (Chen et al., 2020; Kim et al., 2024; Mattugini et al., 2019; Zhang et al., 2020). While this discrepancy may largely reflect artefactual labelling of endogenous neurons, AAVs also exhibit slower expression kinetics, with peak expression occurring 7-10 days post-transduction (Zincarelli et al., 2008). Therefore, AAV-mediated neuronal reprogramming, if genuine, is likely initiated after the acute inflammatory phase has begun to resolve (Gascón et al., 2017). Consistent with this notion, delayed transplantation of embryonic-derived motor neurons into the

injured cortex resulted in improved graft survival and integration compared to immediate transplantation (Péron et al., 2017), suggesting that the timing of cellular interventions relative to injury response can influence outcome.

In the present model, delaying retroviral delivery (e.g., 5- or 7 days post-injury) or using inducible systems to shift Ascl1SA6-Bcl2 expression to later stages of injury could help test whether the timing of neuronal conversion induction impacts the reprogramming outcome. Such temporal modulation would also alter the starting cell population, as reactive astrocyte proliferation peaks between 5 and 7 days post-injury (Bardehle et al., 2013; Simon et al., 2011), potentially increasing their availability for reprogramming. Future studies will be required to determine whether aligning reprogramming induction with later injury phases enhances conversion efficiency, iNs maturation, and survival.

Together, these observations indicate that while Ascl1SA6-Bcl2 initiates neuronal conversion in the injured cortex, progression to morphological and functional maturation remains limited. This limitation likely reflects a combination of the restrictive injury environment and the intrinsic constraints of reprogramming factors used. Identifying strategies to overcome these maturation barriers and ensure long-term survival, whether through direct modulation of the local environment or additional metabolic and trophic support, will be essential for advancing this approach toward therapeutic application in injury and disease contexts.

5.5. Ascl1 reinforces oligodendroglial identity and promotes OPC proliferation after cortical injury

In this study, Ascl1 overexpression in the injured adult cortex did not induce neuronal reprogramming. Instead, Ascl1, either alone or co-expressed with Bcl2, markedly increased OPC proportion and proliferation. This proliferative effect persisted beyond early post-injury phase and was restricted to transduced OPCs, with no detectable effect on reactive astrocytes and microglia. In contrast, the phospho-deficient mutant Ascl1SA6 reduced OPC proliferation and Sox10 expression, consistent with previous observations that it promotes transition towards neuronal fate. These findings suggest that in the injured cortex, Ascl1 primarily reinforces oligodendroglial identity and promotes OPC proliferation, whereas preventing Ascl1 phosphorylation drives OPCs toward neuronal conversion.

5.5.1 OPC proliferation dynamics in the adult brain during homeostasis and injury

OPCs represent one the few glial populations in the adult brain that retain proliferative capacity under physiological conditions, undergoing low self-renewal to maintain homeostasis (Hughes et al., 2013; Young et al., 2013). In contrast, traumatic brain injury induces marked changes in OPC behavior, rapidly accelerates their proliferation by shortening the G1-phase and increasing cycling rates (Buffo et al., 2008; Hughes et al., 2013; Simon et al., 2011). Therefore, defining OPC proliferative dynamics in the uninjured adult cortex and following injury was essential to distinguish between endogenous injury-induced responses and non-endogenous proliferative alterations.

In the uninjured contralateral adult cortex, OPCs displayed minimal EdU incorporation following a 24 hours short-pulse labelling, with the proportion of EdU incorporating cells among Sox10-expressing cells ranging from ~0.6 to 1.0%. Importantly, this proliferation rate remained stable across all time points (4 - 70 dpi; Figure 18B, C), reflecting the slow baseline cycling of OPCs in the adult cortex. These findings are consistent with previous reports demonstrating that adult OPCs retain lifelong proliferative capacity while exhibiting slow cycling kinetics, with an average cell cycle length raging between 10 to 37 days under homeostatic conditions, depending on age and brain regions (Hughes et al., 2013; Simon et al., 2011; Young et al., 2013).

Cortical stab-wound injury induced a substantial but transient increase in OPC proliferative activity (Figure 18B, C). During the early post-injury phase (4 dpi), the proportion of EdU-incorporation among Sox10-expressing cells increased ~10% relative

to the contralateral side, reflecting an enhancement of OPC proliferation. This response agrees with reported cytokine-mediated activation of OPCs in the injured environment (reviewed in Dimou & Gallo, 2015). By 12 dpi, corresponding to a time-point beyond the early post-injury phase (Figure 18B, C), OPC proliferation rate had returned to baseline levels, in agreement with previous studies showing that injury-induced OPC proliferation initiates within 24 hours, peaks between 2-4 days and resolves around 10 days post-injury (Hughes et al., 2013).

Together these findings highlight distinct OPC proliferative behavior under homeostatic and injury conditions in the adult cortex, thereby establishing an endogenous baseline for assessing Ascl1-mediated effects on proliferation.

5.5.2 Ascl1's established role in oligodendrogenesis and progenitor proliferation

Besides its role as a master regulator of neurogenesis, Ascl1 is also critically involved in oligodendroglial lineage development. During development, Ascl1 is expressed in neural progenitors that give rise to oligodendroglial lineage cells, where it promotes OPC specification and early differentiation (Battiste et al., 2007; Kim et al., 2007; Sugimori et al., 2008). Ascl1 ablation was shown to reduce OPC numbers in both forebrain and spinal cord and impair their generation from neural progenitors (Nakatani et al., 2013; Parras et al., 2007).

In this study, the proportion of Sox10-expressing transduced cells was increased shortly after Ascl1-Bcl2 overexpression (4 dpi; Figure 18B, C) and later following Ascl1 alone (12 dpi; Figure 22B, C). While these observations suggest that Ascl1 promotes or sustains oligodendroglial identity, the increase in Sox10-expressing cells could also reflect preferential survival or proliferation of pre-existing OPCs rather than lineage conversion from other glial types. Similarly, overexpression of Ascl1 enhanced the proportion of transduced OPCs in the postnatal intact cortex (Galante et al., 2022b), consistent with developmental studies showing that Ascl1 promotes OPC specification. Evidence from the adult CNS further supports this interpretation. In demyelinating models, conditional deletion of Ascl1 impairs the proliferative response of OPCs and delays subsequent remyelination. Conversely, retroviral-mediated Ascl1 expression in the same model, increased the number of proliferating OPCs, and at later time-points, the density of CC1-expressing mature oligodendrocytes (Nakatani et al., 2013), suggesting that Ascl1 can enhance OPC expansion and their subsequent differentiation into oligodendrocytes. Ascl1 similarly enhances oligodendrogenesis in ischemic injury models (Zhang et al., 2011). Altogether, these observations, together with findings from

this study, demonstrate that Ascl1 maintains or reinforces OPC lineage commitment in developmental and injury contexts.

In neural progenitors Ascl1 is required for progenitor expansion by activating cell cycle genes while suppressing differentiation programs (Ali et al., 2014; Castro et al., 2011). In the oligodendroglial lineage, Ascl1 is transiently expressed in mitotic OPCs, where its oscillatory expression supports progenitor expansion and regulates the balance between proliferation and differentiation during oligodendrocyte formation (Kelenis et al., 2018; Sueda & Kageyama, 2021). Accordingly, Ascl1 alone or with Bcl2 significantly increased the proportion of EdU-incorporating Sox10-positive transduced cells in the injured cortex. At 4 dpi, Ascl1 alone or with Bcl2 led to a ~ 25% increase in the proportion of EdU-incorporating transduced cells, and this proliferative activity was restricted to transduced Sox10-positive cells, demonstrating that Ascl1 enhances OPC proliferation in the injured adult cortex in a cell-autonomous manner. This effect did not result in increased Sox10-expressing cell density at the reprogramming site at this early time-point, which may reflect early injury-induced cell death (Horky et al., 2006) or indicate that proliferating OPCs require more time to reach detectable densities.

Ascl1-mediated proliferative effect persisted beyond the early post-injury phase. At 12 dpi, Ascl1-transduced OPCs maintained elevated EdU-incorporation (~ 14%; Figure 23B, C), consistent with observations in the postnatal intact cortex, where Ascl1 overexpression similarly enhanced OPC proliferation (Galante et al., 2022b). Moreover, sustained Ascl1-induced OPC proliferation was accompanied by an increase in oligodendroglial cell density within Ascl1-expressing regions (Figure 23D, E), suggesting that Ascl1 promotes OPC expansion in the injured adult cortex. These findings align with Ascl1's established developmental role, as endogenous Ascl1 is upregulated in proliferating OPCs, but becomes downregulated as cells exit cell cycle and progress toward mature oligodendrocytes (Kelenis et al., 2018; Nakatani et al., 2013).

Importantly, Ascl1 function is context-dependent and strongly influenced by post-translational modification. As discussed earlier (see subsection 5.1), multi-site phosphorylation by cyclin-dependent kinases promotes cell cycle gene activation and suppresses neuronal differentiation programs, while preventing phosphorylation promotes neuronal differentiation (Ali et al., 2014). Following injury, signaling pathways capable of maintaining Ascl1 in a phosphorylated state, including RAS/ERK signaling are upregulated (Liu et al., 2015; Wang et al., 2025). In addition, growth factors such as FGF2 are released at the injury site further stimulating RAS-ERK signaling (Santiago et al., 1999). Accordingly, overexpression of the phospho-deficient

mutant Ascl1SA6 markedly reduced EdU-incorporation and downregulated Sox10, suggesting that preventing Ascl1 phosphorylation suppresses OPC proliferation and favors neuronal fate acquisition.

Together, these findings suggest that Ascl1 reinforces oligodendroglial lineage identity and enhances OPC proliferation in the injured adult cortex.

5.5.3 OPC-specific responsiveness to Ascl1 in the injured adult cortex

In this study, Ascl1 overexpression increased the proportion of transduced oligodendroglial cells and enhanced OPC proliferation in the injured cortex. Despite Ascl1's role in promoting progenitor proliferation (Castro et al., 2011), its effects were restricted to oligodendroglial lineage cells. Namely, Ascl1 overexpression reduced the proportion of transduced reactive astrocytes and microglia, and did not enhance their proliferative activity (Figure 21B, C; Figure 22B, C), suggesting that Ascl1-driven proliferation is constrained to OPCs in the injured adult cortex.

OPCs are the main population targeted with retroviruses after cortical stab-wound injury, followed by reactive astrocytes and microglia, consistent with their cycling dynamics in this model (Bardehle et al., 2013; Buffo et al., 2008; Simon et al., 2011; Sirko et al., 2013). Accordingly, OPCs represented a major cellular source for Ascl1SA6-Bcl2-derived iNs (see Chapter I) and were the main population undergoing Ascl1-induced proliferation. Given that Ascl1 is upregulated in demyelination models and promotes OPC expansion (Nakatani et al., 2013), it is hypothesized that the cortical stab-wound injury may provide an environment in which OPCs are naturally primed for Ascl1-mediated proliferative responses. Together, these findings suggest that the injury milieu offers a cellular context in which Ascl1 activity is directed toward oligodendroglial lineage programs.

Although higher OPC availability may contribute to the lineage-restrictive proliferative effect, the limited number of Ascl1-transduced astrocytes and microglia suggests that OPCs are more responsive to Ascl1 activity. In support of this hypothesis, OPCs exhibit a distinct epigenetic signature, with permissive chromatin at specific neurogenic and interneuron gene loci, which could facilitate their response to proneural transcription factors (Boshans et al., 2019). In addition, Ascl1 is endogenously expressed in proliferating OPCs (Nakatani et al., 2013), potentially priming OPCs for rapid transcriptional activation after ectopic Ascl1 expression. In contrast, astrocytes and microglia are characterized by more restrictive identity-stabilizing chromatin states (Lavin et al., 2014; Pavlou et al., 2019). Recent work revealed that astrocytes display methylation patterns that stabilize astrocytic gene expression while silencing

neuronal genes, reinforcing astrocytic identity. Notably, in the striatum, injury can induce demethylation in neural stem cell and neurogenic loci, enabling the acquisition of a neural stem cell-like methylome (Kremer et al., 2024). Similarly, in striatal astrocytes, Notch depletion is sufficient to trigger a neurogenic program, whereas in the cortex, this process was stalled unless injury is induced (Magnusson et al., 2020; Zamboni et al., 2020). Altogether, this suggests that cortical astrocytes may require additional signals to undergo Ascl1-mediated lineage modulation, and that the cortical environment imposes barriers that are not readily overcome by injury alone.

The finding that Ascl1 reduces the proportion of transduced reactive astrocytes and microglia raised several interpretations. One possibility is that ectopic Ascl1 expression downregulates astrocytic or microglial lineage markers, leading to apparent loss of these populations through lineage conversion. This aligns with reports indicating that Ascl1 rapidly suppresses astrocytic transcriptional programs while activating neuronal programs (Masserdotti et al., 2015; Wapinski et al., 2013). However, since Ascl1 exhibits limited neuronal competency *in vivo*, both in the postnatal intact cortex (Galante et al., 2022a) and in the injured adult cortex (see chapter I), Ascl1-transduced astrocytes may initiate but fail to complete neuronal conversion, instead undergoing cell death. Microglial identity is tightly maintained by a network of transcription factors, and disruption of this network destabilizes microglial identity, leading to functional silencing or apoptosis (Lavin et al., 2014). Notably, a similar phenomenon has been reported after NeuroD1 overexpression, while initial studies reported NeuroD1-mediated microglia-to-neuron conversion (Matsuda et al., 2019), subsequent work demonstrated that NeuroD1 overexpression instead induces microglial apoptosis (Rao et al., 2021). Thus, expression of incompatible lineage transcription factors, such as Ascl1, may similarly compromise microglial viability.

Together, these observations suggest that OPCs are more permissive to Ascl1 activity, whereas astrocytes and microglia appear less able to sustain Ascl1-driven programs, likely due to a combination of epigenetic and environmental constraints.

5.6. Ascl1 does not induce lineage fate reprogramming of reactive astrocytes in the injured adult cortex

The reduction in transduced reactive astrocytes following Ascl1 overexpression in the injured cortex was also hypothesized to be due to conversion of astrocytes towards an oligodendroglial fate. Such lineage conversion has been demonstrated *in vivo*, with Sox10 overexpression converting astrocytes into oligodendroglial-like cells (Mokhtarzadeh Khanghahi et al., 2018). However, genetic fate-mapping using Aldh1l1-CreERTM/RCE (Marichal et al., 2024; Sousa et al., 2009; Srinivasan et al., 2016), showed that only a small subset of Ascl1- or Ascl1-Bcl2-transduced cells derived from reactive astrocytes (Figure 26D, E). These fate-mapped cells did not acquire Sox10 expression, nor incorporated EdU (Figure 26F, G), demonstrating that astrocytes contribute minimally to the Ascl1-transduced population and do not give rise to proliferating OPCs in the injured adult cortex.

Reactive astrocytes also contributed minimally to Ascl1SA6-Bcl2-derived iNs. In contrast, in the postnatal intact cortex, astrocytes were the primary cellular source for iNs generated by the same reprogramming factors (Marichal et al., 2024), suggesting that either age or injury-related changes reduce astrocyte competence for Ascl1-mediated reprogramming.

Although Ascl1 rapidly remodels chromatin and transcriptional programs and suppresses astrocytic gene expression (Masserdotti et al., 2015; Wapinski et al., 2013), in this study, reactive astrocytes did not progress toward neuronal or oligodendroglial identity after Ascl1 expression. After injury, reactive astrocytes activate Notch signalling, which has been shown to antagonize Ascl1 activity and stabilize astrocytic identity (Tan et al., 2022). Similarly, studies in the retina indicated that injury-induced NF-kB signalling in Müller glia limits Ascl1 chromatin binding and suppresses Ascl1-mediated regeneration (Jorstad et al., 2020; Palazzo et al., 2023). Finally, injury can also promote reactive astrocytes to acquire neurotoxic features (Liddelow et al., 2017), and C3-expressing neurotoxic reactive astrocytes were found present in the reprogramming milieu and are likely among retroviral-transduced cells (see chapter I). Such a reactive subtype may be intrinsically less susceptible to undergoing Ascl1-mediated lineage reprogramming.

Taken together, these findings demonstrate that Ascl1 does not induce astrocyte-to-oligodendroglial reprogramming in the injured cortex and suggest that the injury environment imposes intrinsic and extrinsic constraints for reactive astrocyte reprogramming.

5.7. OPCs constitute the primary cellular source of Ascl1-induced expansion in the injured adult cortex

The marked increase in the proportion of transduced oligodendroglial cells and in overall oligodendroglial density following Ascl1 overexpression could arise from enhanced proliferation of pre-existing OPCs or lineage conversion of other glial types into oligodendroglia. Although short-pulse EdU incorporation revealed ~ 17% of transduced OPCs undergoing proliferation (Figure 24B, C), oligodendroglia cell density (Sox10 cells/mm^2) increased almost 50% around the lesion site (Figure 24D, E), suggesting that proliferation alone might not fully account for this expansion.

Genetic fate-mapping revealed that Ascl1-mediated astrocyte-to-oligodendroglia is not achieved by Ascl1 in the injury adult cortex (Figure 26B, C, D). In contrast, Ascl1-transduced cells were partially fate-mapped to OPCs and a subset of these fate-mapped cells incorporated EdU (Figure 27B, C, D). Ascl1 also increased the proportion of Sox10-expressing fate-mapped cells, which is consistent with its role in OPC specification and differentiation in development (Nakatani et al., 2013; Parras et al., 2007). These observations suggest that Ascl1 acts primarily on pre-existing OPCs, instead of recruiting other glial types, such as reactive astrocytes into oligodendroglial programs, and reinforces oligodendroglial identity while driving proliferative expansion of OPCs.

Importantly, the contribution of pre-existing OPC is likely underestimated in this study. NG2-CreER^{TM}/RCE typically achieves partial labeling of OPCs in adults under standard tamoxifen regimens (reviewed in Guo et al., 2021), which aligns with the labeling efficiency achieved in this study (~56%). Alternative Cre lines with higher labeling efficiency, such as PDGFRα-CreER^{T2}, which reports >90% labeling of adult OPCs (O'Rourke et al., 2016), could expose a more robust contribution of OPCs to Ascl1-mediated expansion. Nevertheless, both NG2 and PDGFRα are also expressed in other cell types such as pericytes (Ozerdem et al., 2001) and result in their labeling (Nikolakopoulou et al., 2019). Despite this technical limitation, these observations suggest that Ascl1 acts primarily on pre-existing OPCs, enhancing their proliferation and reinforcing oligodendroglial identity, rather than recruiting other glial types such as reactive astrocytes into oligodendroglial programs.

5.8. Proliferative effect induced by Ascl1 is sustained long-term in the injured adult cortex

Injury-induced OPC proliferation is typically transient, peaking rapidly after cortical insult and returning toward baseline as the inflammatory response resolves (Dean et al., 2023; Simon et al., 2011). In contrast, Ascl1 overexpression induced a strikingly sustained proliferative response in a subset of transduced OPCs that extended beyond the early post-injury phase (4 dpi or 7 days post-lesion) and persisted for over 70 days post-lesion (Figure 29B, D). Notably, although the proportion of EdU-incorporating transduced OPCs slightly decreased over time, the overall proliferation rate remained mostly stable across time-points (~16-12%). These observations suggest that Ascl1 not only enhances OPC proliferation but also sustains it long-term in the injured cortex.

This prolonged effect likely reflects continuous transcriptional activation by constitutive Ascl1 overexpression, contrasting with the typical oscillatory expression patterns of endogenous Ascl1 during development (Imayoshi et al., 2013). In neural progenitors, Ascl1 promotes cell cycle progression by activating cell cycle regulators (Castro et al., 2011). Moreover, oscillatory Ascl1 expression was shown to maintain proliferative progenitor states, while stable expression promotes cell cycle exit and neuronal differentiation (Imayoshi et al., 2013). Similarly, low Ascl1 activity promotes progenitor proliferation whereas an increase in Ascl1 activity arrests cell cycle and drives differentiation (reviewed in Vasconcelos & Castro, 2014). On the other hand, this effect seems highly context-dependent, as stable elevated Ascl1 expression has also been shown to maintain neuroblastoma cells in a developmental intermediate stage (Wylie et al., 2015) and to drive oncogenesis in glioblastoma (Azzarelli et al., 2022). Loss-of-function studies further demonstrate that Ascl1 ablation in neuroblastoma cells resulted in slowed cell growth (Parkinson et al., 2022) and premature cell cycle arrest in progenitors (Castro et al., 2011). These studies suggest that Ascl1 function on proliferation can also be influenced by developmental stage and cellular context rather than expression level alone.

Within the oligodendroglial lineage, Ascl1 is transiently expressed at low levels in proliferating progenitors, and its expression contributes to OPC specification. Sustained Ascl1 expression in the hippocampus has been reported to promote neuronal differentiation while inhibiting OPC formation (Sueda & Kageyama, 2021). In contrast, in the absence of Ascl1, OPC specification is impaired and proliferation is reduced in the brain and spinal cord (Kelenis et al., 2018; Nakatani et al., 2013; Parras et al., 2007; Sugimori et al., 2008). Moreover, in demyelination models, Ascl1 expression is upregulated in OPCs, required for their proliferative expansion and

subsequent remyelination (Nakatani et al., 2013). Therefore, while oscillatory Ascl1 expression was shown to be necessary for OPC expansion, the present study suggests that sustained Ascl1 expression maintained a subset of OPCs actively proliferating for up to 70 days after injury.

The persistence proliferative effect of Ascl1 may reflect the behaviour of a specific OPC subpopulation, as not all transduced OPCs incorporated EdU and the proportion of proliferating transduced OPCs remained stable over time. This observation aligns with evidence that adult OPCs are functionally heterogenous, with subpopulations exhibiting distinct proliferative behaviours, including subsets with long-term cycling capacity and others biased toward differentiation ((Baydyuk et al., 2020; Spitzer et al., 2019; Viganò et al., 2013). In this context, Ascl1 may preferentially enhance proliferation of a subset of OPCs that is intrinsically primed for sustained proliferation.

Finally, it remains unclear whether the observed Ascl1-mediated proliferative effect requires a permissive environment. Similar effects of Ascl1 on OPC proliferation have been reported in the postnatal intact brain, when developmental OPC expansion is ongoing (Galante et al., 2022b), and in demyelinating models, which actively stimulate remyelination (Nakatani et al., 2013). Testing whether Ascl1 enhances OPC proliferation in the adult intact cortex, where pro-proliferative cues may be reduced and remyelinating or developmental cues are likely absent, would reveal whether this response is sustained or context-dependent.

Together, these observations suggest that Ascl1 enhances proliferation in a subset of OPCs and sustains it long-term in the injured adult cortex.

5.9. Ascl1 does not prevent OPC differentiation into oligodendrocytes in the injured adult cortex

Having demonstrated that Ascl1 induces a sustained increase in OPCs, it was hypothesized that the observed proliferative effect of Ascl1 would simultaneously impair or delay OPC differentiation into oligodendrocytes. Surprisingly, Ascl1-transduced pre-myelinating OPCs were detected both at 28- and 70 dpi (Figure 30B, C; Figure 31B, C). These observations suggest that transduced OPCs retain the ability to undergo differentiation despite prolonged Ascl1 expression. This finding aligns with recent evidence that OPCs undergo constitutive differentiation attempts at a relatively constant rate, independent of their proliferative state or environmental signals (Mironova et al., 2026). Rather than proliferation and differentiation being mutually exclusive states, OPCs appear to maintain an intrinsic constitutive differentiation program that continues regardless of enhanced proliferation. This suggests that Ascl1-mediated expansion of the OPC pool does not suppress the constitutive differentiation mechanism, but rather increases the number of progenitors available to undergo this process. Moreover, Ascl1's established role in oligodendrogenesis also supports this observation, as its activity has been shown to be required for oligodendrocyte development in the spinal cord and forebrain (Nakatani et al., 2013; Sueda & Kageyama, 2021; Sugimori et al., 2008).

Notably, co-expression with Bcl2 significantly increased the fraction of pre-myelinating oligodendrocytes compared to Ascl1 alone at 28 dpi, suggesting that Bcl2 may enhance the survival of newly differentiated cells, consistent with its pro-survival role during reprogramming (Gascón et al., 2016). Additionally, pre-myelinating transduced oligodendrocytes seemed to progress in their maturation over time, as a subset of transduced cells expressed mature oligodendrocyte markers (APC/CC1) at 70 dpi (Figure 30B, D), suggesting that at least a fraction of Ascl1-expressing OPCs can undergo differentiation in the injured adult cortex. This aligns with previous reports showing that OPCs undergo differentiation into myelinating oligodendrocytes and contribute to myelin regeneration following spinal cord injury (Duncan et al., 2020), demyelinating cortical lesions (Strijbis et al., 2017), ischemic stroke (Zhang et al., 2013), and cortical impact injury (Song et al., 2022). Moreover, loss-of-function studies demonstrated that Ascl1 ablation reduces OPC proliferation without impairing their ability to differentiate in the spinal cord (Sueda & Kageyama, 2021), supporting that Ascl1 may primarily regulate proliferative dynamics rather than differentiation competence.

Overall, these results indicate that Ascl1-induced OPC proliferation does not prevent subsequent oligodendroglial differentiation in the injured cortex, and instead enhanced proliferation and lineage progression co-exist following cortical stab-wound.

5.10. Future perspectives and conclusive remarks

The findings in this study suggest that Ascl1-mediated effect on glial cell lineage decisions in the injured adult cortex is constrained by a combination of extrinsic and intrinsic factors. In particular, the inflammatory response and the emergence of neurotoxic reactive astrocytes following injury constrain reprogramming efficiency, while glial cells display intrinsic differences in their susceptibility to Ascl1-mediated fate modulation. In addition, achieving successful neuronal maturation and long-term survival of iNs remains a challenge, highlighting the need to optimize this approach for its application in brain repair. However, these findings also revealed alternative therapeutic opportunities that extend beyond neuronal replacement. While wild-type Ascl1 preferentially enhances OPC proliferation, phosphomutant Ascl1SA6 and Bcl2, promotes generation of iNs in the injured adult cortex. Altogether, these observations suggest that the context-dependent activity of Ascl1, shaped by its phosphorylation state and the local environment, may enable distinct therapeutic applications to promote regeneration following cortical injury.

5.10.1 Potential of Ascl1 for oligodendroglial repair after cortical injury

Cortical traumatic brain injury frequently results in demyelination due to axonal injury and loss of myelinating oligodendrocytes (Armstrong et al., 2016; Lotocki et al., 2011). Following traumatic injury, myelin debris accumulate and are mainly cleared by microglia. In the CNS, this is a relatively slow process that can prolong or exacerbate the inflammatory response (Clarner et al., 2012; Vargas & Barres, 2007). While OPCs respond to demyelination by proliferating and migrating to lesion areas, recent work has demonstrated that myelin repair occurs primarily through constitutive differentiation of OPCs rather than injury-mediated induction, with differentiation attempts remaining relatively constant despite of oligodendrocyte loss or the extent of demyelination (Mironova et al., 2026). However, their differentiation into myelinating oligodendrocytes is often limited in chronic injuries due to persistent inflammatory signaling that actively suppresses OPC differentiation attempts (Franklin & ffrench-Constant, 2008; Kuhlmann et al., 2008; Mironova et al., 2026). This suggests that the primary constraint on remyelination may not be the differentiation capacity of existing OPCs, but rather the available OPC pool and the permissiveness of the local environment.

The observation that Ascl1 enhances OPC proliferation, while preserving their capacity to differentiate into oligodendrocytes suggests a potential application for remyelination-based therapeutic strategies. By locally expanding the OPC pool, Ascl1

overexpression could increase the number of progenitors undergoing constitutive differentiation, thereby enhancing overall oligodendrocyte generation. This approach may be particularly relevant in chronic demyelinating diseases such as multiple sclerosis, where progressive depletion of the OPC pool and persistent inflammation contribute to remyelination failure (reviewed in Franklin & ffrench-Constant, 2008). In these contexts, repeated cycles of demyelination and incomplete remyelination, together with persistent inflammatory signalling progressively exhaust the OPC population (Kuhlmann et al., 2008; Sim et al., 2002), while sustained inflammatory cytokine signalling, particularly interferon gamma (IFN-γ) has been shown to induce OPC quiescence and inhibit differentiation (Saraswat et al., 2021). Additionally, the slow clearance of myelin debris, which contain components inhibitory to OPC differentiation, further hinder remyelination and likely also reflect impaired microglial trophic support (Tiwari et al., 2024). The sustained proliferative effect observed following Ascl1 overexpression suggests that this approach may support maintenance of a long-term reservoir of cycling OPCs that retain differentiation competence, potentially helping to overcome the OPC depletion that limits repair in chronic demyelinating conditions.

Testing Ascl1 overexpression in demyelination animal models, such as cuprizone-induced demyelination or experimental autoimmune encephalomyelitis, would provide important insights into its potential to support remyelination. Combining Ascl1-mediated OPC expansion with strategies that reduce inflammation or promote differentiation may achieve more robust remyelination. Several strategies are being investigated to enhance OPC differentiation, including blocking IFN-y signalling and enhancement of myelin debris clearance by microglia (Cantoni et al., 2015; Saraswat et al., 2021; Song et al., 2022). More direct approaches to induce OPCs differentiation include the use of compounds, such as PDE7 and GSK-3 inhibitors (Medina-Rodríguez et al., 2017), vitamin C (Guo et al., 2018) and Clemastine (Yamazaki & Ohno, 2025).

Finally, the observation that Ascl1-mediated proliferation persists for months after transduction raises some important questions, including whether a transient modulation of Ascl1 expression could promote both OPC expansion and subsequent differentiation. Strategies that enable temporal control of Ascl1 expression, such as inducible systems (e.g., Tet-ON), would help determine whether blocking Ascl1 expression after OPC expansion promotes cell cycle exit, and differentiation into oligodendrocytes in this context. It also remains unknown whether Ascl1-transduced proliferating OPCs eventually exit cell cycle, or whether a subset retains prolonged enhanced proliferative activity that could potentially pose a risk of dysregulated

growth. Addressing these questions through long-term studies extending beyond 70 days post-injection will be required for evaluating the translational potential and safety of Ascl1-based strategies for OPC expansion and remyelination.

5.10.2 Current limitations and optimization strategies for Ascl1SA6-Bcl2-mediated neuronal repair after cortical injury

Cortical traumatic injuries mainly lead to neuronal loss and long-lasting functional impairment, while the regenerative ability of the adult mammalian brain remains limited. Consequently, functional recovery requires strategies aimed at replacing lost neurons, such as direct neuronal reprogramming. However, this cell replacement approach faces major biological and technical barriers in the injured brain, including a pro-inflammatory microenvironment, region-specific differences in glial competence, and a limited capacity for iNs to mature and integrate into host circuitry (reviewed in Gascón et al., 2017; Grande et al., 2013; Hu et al., 2019).

While Ascl1 showed potential for oligodendroglial regeneration and myelin repair by expanding the progenitor pool without preventing differentiation, its phospho-mutant, Ascl1SA6, combined with Bcl2, exhibited neurogenic capacity by inducing the conversion of OPCs into iNs. Nevertheless, the present findings suggest that Ascl1SA6-Bcl2-mediated neuronal reprogramming is constrained by the hostile injury environment. These results also highlight the distinct responsiveness of OPCs to Ascl1-mediated modulation, as OPCs are susceptible to Ascl1-mediated proliferation and Ascl1SA6-Bcl2-mediated neuronal reprogramming following cortical injury.

The rapid and widespread morphological changes observed following Ascl1SA6-Bcl2 overexpression, together with the delayed and limited expression of neuronal markers, suggest a slow acquisition of neuronal identity or incomplete neuronal conversion in the injured adult cortex. This contrast with findings in the postnatal intact cortex, where iNs progressively mature, acquire subtype-specification and functional properties (Marichal et al., 2024). These differences suggest that additional transcription factor co-expression or complementary treatments may be required overcome injury-associated barriers. For example, co-expression of transcription factors such as Myt1l has been shown to repress non-neuronal lineage programs, including oligodendroglial gene expression (Mall et al., 2017), thereby facilitating neuronal fate acquisition. Similarly, antioxidant treatments such as α-Tocotrienol were shown to accelerate iNs differentiation and maturation (Gascón et al., 2016).

The timing of viral delivery may also influence reprogramming outcomes. In this study, retroviral vectors were delivered at 3 days post-injury, while this timing

was chosen to target glial cells at their proliferative peak, cells undergoing conversion are also exposed to substantial inflammatory stress (Amlerova et al., 2024; Heinrich et al., 2014; Gascón et al., 2016). Consistent with the notion that timing relative to injury response affects cellular outcomes, delaying transplantation of embryonic-derived motor neurons into the injured cortex by 10 days (~14 days post-injury) resulted in improved graft survival and integration compared to transplantation at earlier time-points (Péron et al., 2017), suggesting that the early post-injury inflammatory phase may be particularly hostile to newly generated or transplanted cells. Testing whether delayed retroviral delivery (e.g., 5-7 days post-injury) or the use of inducible systems to temporally control transgene expression improves reprogramming efficiency would help identify the optimal window for neuronal conversion induction. Alternatively, transgenic approaches that enable conditional expression of reprogramming factors, such as those reported in Chen et al. (2025), could provide more precise temporal and spatial control over transgene expression while avoiding the additional inflammatory burden associated with viral vector delivery. In addition, modulation of the injury environment, for example by preventing the emergence of C3-expressing neurotoxic reactive astrocytes during reprogramming may alleviate inflammatory signaling that limits induced neuron survival and maturation.

An alternative to address these limitations could involve a sequential approach, in which Ascl1 overexpression is first used to maintain a robust proliferative OPC pool, followed by delayed induction of neuronal conversion using Ascl1SA6 and Bcl2. Such strategy could increase the pool of accessible starter cells, while temporally separating proliferation expansion from neuronal reprogramming. Similarly, inducible systems such as a Tet-ON system, could enable controlled activation of Ascl1SA6-Bcl2 expression at later time-points after injury. These approaches may allow neuronal reprogramming to occur outside the peak inflammatory window, which in cortical stab-wound models can correspond to the first 2 weeks post-injury (Bardehle et al., 2013; Buffo et al., 2008), thereby limiting the exposure of iNs to hostile environmental cues. Nevertheless, the optimal temporal window for neuronal reprogramming following injury remains unknown.

Altogether, successful neuronal reprogramming in the injured adult cortex will require systematic optimization to address multiple barriers. These include choice and combination of reprogramming factors, viral delivery strategies, identification of competent starter cell populations, additional metabolic support, and modulation of the hostile inflammatory environment. Beyond conversion efficiency, therapeutic relevance requires subtype specification and functional integration into host circuits. Evidence from disease models, including epilepsy (Lentini et al., 2021), Parkinson's

disease (Rivetti Di Val Cervo et al., 2017), and Alzheimer's disease (Guo et al., 2014), suggests that iNs can achieve partial functional integration under favourable conditions.

While the present study demonstrates that Ascl1SA6-Bcl2-mediated conversion of OPCs into iNs and early stages of iNs maturation can be achieved in the injured cortex, conversion efficiency, as well as morphological and molecular maturation, remain limited. Several pending questions remain, including the relative contribution of the inflammatory environment versus cell-intrinsic barriers to reprogramming outcomes, whether iNs survive long-term and the extent to which iNs continue to mature over time and whether they acquire subtype-specificity. Importantly, it also remains to be determined whether iNs could eventually acquire functional properties and integrate into existing circuits. Addressing these questions will be essential to determine whether Ascl1SA6-Bcl2-mediated reprogramming can ultimately support neuronal repair following cortical injury.

6. Bibliography

Addis, R. C., Hsu, F.-C., Wright, R. L., Dichter, M. A., Coulter, D. A., & Gearhart, J. D. (2011). Efficient Conversion of Astrocytes to Functional Midbrain Dopaminergic Neurons Using a Single Polycistronic Vector. *PLoS ONE*, *6*(12), e28719. https://doi.org/10.1371/journal.pone.0028719

Aguilar-Arredondo, A., & Zepeda, A. (2018). Memory retrieval-induced activation of adult-born neurons generated in response to damage to the dentate gyrus. *Brain Structure and Function*, *223*(6), 2859–2877.

Aimone, J. B., Deng, W., & Gage, F. H. (2011). Resolving New Memories: A Critical Look at the Dentate Gyrus, Adult Neurogenesis, and Pattern Separation. *Neuron*, *70*(4), 589–596. https://doi.org/10.1016/j.neuron.2011.05.010

Alam, A., Thelin, E. P., Tajsic, T., Khan, D. Z., Khellaf, A., Patani, R., & Helmy, A. (2020). Cellular infiltration in traumatic brain injury. *Journal of Neuroinflammation*, *17*(1), 328. https://doi.org/10.1186/s12974-020-02005-x

Ali, F. R., Cheng, K., Kirwan, P., Metcalfe, S., Livesey, F. J., Barker, R. A., & Philpott, A. (2014). The phosphorylation status of Ascl1 is a key determinant of neuronal differentiation and maturation *in vivo* and *in vitro*. *Development*, *141*(11), 2216–2224. https://doi.org/10.1242/dev.106377

Alshebib, Y., Hori, T., Goel, A., Fauzi, A. A., & Kashiwagi, T. (2023). Adult human neurogenesis: A view from two schools of thought. *IBRO Neuroscience Reports*, *15*, 342–347. https://doi.org/10.1016/j.ibneur.2023.07.004

Altman, J. (1962). Are new neurons formed in the brains of adult mammals? *Science*, *135*(3509), 1127–1128.

Altman, J., & Das, G. D. (1965). Autoradiographic and histological evidence of postnatal hippocampal neurogenesis in rats. *Journal of Comparative Neurology*, *124*(3), 319–335. https://doi.org/10.1002/cne.901240303

Alves, J. L. (2014). Blood–brain barrier and traumatic brain injury. *Journal of Neuroscience Research*, *92*(2), 141–147. https://doi.org/10.1002/jnr.23300

Amamoto, R., & Arlotta, P. (2014). Development-inspired reprogramming of the mammalian central nervous system. *Science*, *343*(6170), 1239882.

Amamoto, R., Huerta, V. G. L., Takahashi, E., Dai, G., Grant, A. K., Fu, Z., & Arlotta, P. (2016). Adult axolotls can regenerate original neuronal diversity in response to brain injury. *eLife*, *5*, e13998. https://doi.org/10.7554/eLife.13998

Amlerova, Z., Chmelova, M., Anderova, M., & Vargova, L. (2024). Reactive gliosis in traumatic brain injury: A comprehensive review. *Frontiers in Cellular Neuroscience*, *18*, 1335849. https://doi.org/10.3389/fncel.2024.1335849

Armstrong, R. C., Mierzwa, A. J., Sullivan, G. M., & Sanchez, M. A. (2016). Myelin and oligodendrocyte lineage cells in white matter pathology and plasticity after traumatic brain injury. *Neuropharmacology*, *110*, 654–659. https://doi.org/10.1016/j.neuropharm.2015.04.029

Arvidsson, A., Collin, T., Kirik, D., Kokaia, Z., & Lindvall, O. (2002). Neuronal replacement from endogenous precursors in the adult brain after stroke. *Nature Medicine*, *8*(9), 963–970. https://doi.org/10.1038/nm747

Assinck, P., Duncan, G. J., Plemel, J. R., Lee, M. J., Stratton, J. A., Manesh, S. B., Liu, J., Ramer, L. M., Kang, S. H., Bergles, D. E., Biernaskie, J., & Tetzlaff, W. (2017). Myelinogenic Plasticity of Oligodendrocyte Precursor Cells following Spinal Cord Contusion Injury. *The Journal of Neuroscience*, *37*(36), 8635–8654. https://doi.org/10.1523/JNEUROSCI.2409-16.2017

Aydin, B., Kakumanu, A., Rossillo, M., Moreno-Estellés, M., Garipler, G., Ringstad, N., Flames, N., Mahony, S., & Mazzoni, E. O. (2019). Proneural factors Ascl1 and Neurog2 contribute to neuronal subtype identities by establishing distinct chromatin landscapes. *Nature Neuroscience*, *22*(6), 897–908.

Azzarelli, R., Gillen, S., Connor, F., Lundie-Brown, J., Puletti, F., Drummond, R., Raffaelli, A., & Philpott, A. (2024). Phospho-regulation of ASCL1-mediated chromatin opening during cellular reprogramming. *Development*, *151*(24), dev204329. https://doi.org/10.1242/dev.204329

Azzarelli, R., McNally, A., Dell'Amico, C., Onorati, M., Simons, B., & Philpott, A. (2022). ASCL1 phosphorylation and ID2 upregulation are roadblocks to glioblastoma stem cell differentiation. *Scientific Reports*, *12*(1), 2341. https://doi.org/10.1038/s41598-022-06248-x

Bardehle, S., Krüger, M., Buggenthin, F., Schwausch, J., Ninkovic, J., Clevers, H., Snippert, H. J., Theis, F. J., Meyer-Luehmann, M., Bechmann, I., Dimou, L., & Götz, M. (2013). Live imaging of astrocyte responses to acute injury reveals selective

juxtavascular proliferation. *Nature Neuroscience*, *16*(5), 580–586. https://doi.org/10.1038/nn.3371

Barres, B. A., Hart, I. K., Coles, H. S. R., Burne, J. F., Voyvodic, J. T., Richardson, W. D., & Raff, M. C. (1992). Cell death and control of cell survival in the oligodendrocyte lineage. *Cell*, *70*(1), 31–46. https://doi.org/10.1016/0092-8674(92)90531-G

Battiste, J., Helms, A. W., Kim, E. J., Savage, T. K., Lagace, D. C., Mandyam, C. D., Eisch, A. J., Miyoshi, G., & Johnson, J. E. (2007). Ascl1 defines sequentially generated lineage-restricted neuronal and oligodendrocyte precursor cells in the spinal cord. *Development*, *134*(2), 285–293. https://doi.org/10.1242/dev.02727

Baydyuk, M., Morrison, V. E., Gross, P. S., & Huang, J. K. (2020). Extrinsic factors driving oligodendrocyte lineage cell progression in CNS development and injury. *Neurochemical Research*, *45*(3), 630–642.

Bazarek, S. F., Thaqi, M., King, P., Mehta, A. R., Patel, R., Briggs, C. A., Reisenbigler, E., Yousey, J. E., Miller, E. A., & Stutzmann, G. E. (2023). Engineered neurogenesis in naive adult rat cortex by Ngn2-mediated neuronal reprogramming of resident oligodendrocyte progenitor cells. *Frontiers in Neuroscience*, *17*, 1237176.

Bergles, D. E., & Richardson, W. D. (2016). Oligodendrocyte Development and Plasticity. *Cold Spring Harbor Perspectives in Biology*, *8*(2), a020453. https://doi.org/10.1101/cshperspect.a020453

Bergles, D. E., Roberts, J. D. B., Somogyi, P., & Jahr, C. E. (2000). Glutamatergic synapses on oligodendrocyte precursor cells in the hippocampus. *Nature*, *405*(6783), 187–191. https://doi.org/10.1038/35012083

Bernier, P. J., Bédard, A., Vinet, J., Lévesque, M., & Parent, A. (2002). Newly generated neurons in the amygdala and adjoining cortex of adult primates. *Proceedings of the National Academy of Sciences*, *99*(17), 11464–11469. https://doi.org/10.1073/pnas.172403999

Berninger, B., Costa, M. R., Koch, U., Schroeder, T., Sutor, B., Grothe, B., & Götz, M. (2007). Functional properties of neurons derived from in vitro reprogrammed postnatal astroglia. *Journal of Neuroscience*, *27*(32), 8654–8664.

Bertrand, N., Castro, D. S., & Guillemot, F. (2002). Proneural genes and the specification of neural cell types. *Nature Reviews Neuroscience*, *3*(7), 517–530. https://doi.org/10.1038/nrn874

Bhardwaj, R. D., Curtis, M. A., Spalding, K. L., Buchholz, B. A., Fink, D., Björk-Eriksson, T., Nordborg, C., Gage, F. H., Druid, H., Eriksson, P. S., & Frisén, J. (2006). Neocortical neurogenesis in humans is restricted to development. *Proceedings of the National Academy of Sciences*, *103*(33), 12564–12568. https://doi.org/10.1073/pnas.0605177103

Björklund, A., Dunnett, S. B., Brundin, P., Stoessl, A. J., Freed, C. R., Breeze, R. E., Levivier, M., Peschanski, M., Studer, L., & Barker, R. (2003). Neural transplantation for the treatment of Parkinson's disease. *The Lancet Neurology*, *2*(7), 437–445. https://doi.org/10.1016/S1474-4422(03)00442-3

Bocchi, R., Masserdotti, G., & Götz, M. (2022). Direct neuronal reprogramming: Fast forward from new concepts toward therapeutic approaches. *Neuron*, *110*(3), 366–393. https://doi.org/10.1016/j.neuron.2021.11.023

Bodnar, C. N., Watson, J. B., Higgins, E. K., Quan, N., & Bachstetter, A. D. (2021). Inflammatory Regulation of CNS Barriers After Traumatic Brain Injury: A Tale Directed by Interleukin-1. *Frontiers in Immunology*, *12*, 688254. https://doi.org/10.3389/fimmu.2021.688254

Bonaguidi, M. A., Song, J., Ming, G., & Song, H. (2012). A unifying hypothesis on mammalian neural stem cell properties in the adult hippocampus. *Current Opinion in Neurobiology*, *22*(5), 754–761. https://doi.org/10.1016/j.conb.2012.03.013

Boshans, L. L., Factor, D. C., Singh, V., Liu, J., Zhao, C., Mandoiu, I., Lu, Q. R., Casaccia, P., Tesar, P. J., & Nishiyama, A. (2019). The Chromatin Environment Around Interneuron Genes in Oligodendrocyte Precursor Cells and Their Potential for Interneuron Reprograming. *Frontiers in Neuroscience*, *13*, 829. https://doi.org/10.3389/fnins.2019.00829

Boshans, L. L., Soh, H., Wood, W. M., Nolan, T. M., Mandoiu, I. I., Yanagawa, Y., Tzingounis, A. V., & Nishiyama, A. (2021). Direct reprogramming of oligodendrocyte precursor cells into GABAergic inhibitory neurons by a single homeodomain transcription factor Dlx2. *Scientific Reports*, *11*(1), 3552.

Boulton, M., & Al-Rubaie, A. (2025). Neuroinflammation and neurodegeneration following traumatic brain injuries. *Anatomical Science International*, *100*(1), 3–14.

Breton-Provencher, V., Lemasson, M., Peralta, M. R., & Saghatelyan, A. (2009). Interneurons Produced in Adulthood Are Required for the Normal Functioning of the Olfactory Bulb Network and for the Execution of Selected Olfactory Behaviors. *The Journal of Neuroscience*, *29*(48), 15245–15257. https://doi.org/10.1523/JNEUROSCI.3606-09.2009

Buchanan, J., Elabbady, L., Collman, F., Jorstad, N. L., Bakken, T. E., Ott, C., Glatzer, J., Bleckert, A. A., Bodor, A. L., Brittain, D., Bumbarger, D. J., Mahalingam, G., Seshamani, S., Schneider-Mizell, C., Takeno, M. M., Torres, R., Yin, W., Hodge, R. D., Castro, M., ... Da Costa, N. M. (2022). Oligodendrocyte precursor cells ingest axons in the mouse neocortex. *Proceedings of the National Academy of Sciences*, *119*(48), e2202580119. https://doi.org/10.1073/pnas.2202580119

Buffo, A., Rite, I., Tripathi, P., Lepier, A., Colak, D., Horn, A.-P., Mori, T., & Götz, M. (2008). Origin and progeny of reactive gliosis: A source of multipotent cells in the injured brain. *Proceedings of the National Academy of Sciences*, *105*(9), 3581–3586. https://doi.org/10.1073/pnas.0709002105

Buffo, A., Vosko, M. R., Ertürk, D., Hamann, G. F., Jucker, M., Rowitch, D., & Götz, M. (2005). Expression pattern of the transcription factor Olig2 in response to brain injuries: Implications for neuronal repair. *Proceedings of the National Academy of Sciences*, *102*(50), 18183–18188. https://doi.org/10.1073/pnas.0506535102

Burda, J. E., & Sofroniew, M. V. (2014). Reactive Gliosis and the Multicellular Response to CNS Damage and Disease. *Neuron*, *81*(2), 229–248. https://doi.org/10.1016/j.neuron.2013.12.034

Bush, T. G., Puvanachandra, N., Horner, C. H., Polito, A., Ostenfeld, T., Svendsen, C. N., Mucke, L., Johnson, M. H., & Sofroniew, M. V. (1999). Leukocyte Infiltration, Neuronal Degeneration, and Neurite Outgrowth after Ablation of Scar-Forming, Reactive Astrocytes in Adult Transgenic Mice. *Neuron*, *23*(2), 297–308. https://doi.org/10.1016/S0896-6273(00)80781-3

Butler, C. R., Boychuk, J. A., & Smith, B. N. (2015). Effects of Rapamycin Treatment on Neurogenesis and Synaptic Reorganization in the Dentate Gyrus after Controlled Cortical Impact Injury in Mice. *Frontiers in Systems Neuroscience*, *9*. https://doi.org/10.3389/fnsys.2015.00163

Cai, J., Qi, Y., Hu, X., Tan, M., Liu, Z., Zhang, J., Li, Q., Sander, M., & Qiu, M. (2005). Generation of Oligodendrocyte Precursor Cells from Mouse Dorsal Spinal Cord

Independent of Nkx6 Regulation and Shh Signaling. *Neuron*, *45*(1), 41–53. https://doi.org/10.1016/j.neuron.2004.12.028

Caiazzo, M., Dell'Anno, M. T., Dvoretskova, E., Lazarevic, D., Taverna, S., Leo, D., Sotnikova, T. D., Menegon, A., Roncaglia, P., & Colciago, G. (2011). Direct generation of functional dopaminergic neurons from mouse and human fibroblasts. *Nature*, *476*(7359), 224–227.

Cantoni, C., Bollman, B., Licastro, D., Xie, M., Mikesell, R., Schmidt, R., Yuede, C. M., Galimberti, D., Olivecrona, G., & Klein, R. S. (2015). TREM2 regulates microglial cell activation in response to demyelination in vivo. *Acta Neuropathologica*, *129*(3), 429–447.

Carter, J. L., Halmai, J. A. N. M., & Fink, K. D. (2020). The iNs and Outs of Direct Reprogramming to Induced Neurons. *Frontiers in Genome Editing*, *2*, 7. https://doi.org/10.3389/fgeed.2020.00007

Casarosa, S., Fode, C., & Guillemot, F. (1999). Mash1 regulates neurogenesis in the ventral telencephalon. *Development*, *126*(3), 525–534.

Castro, D. S., Martynoga, B., Parras, C., Ramesh, V., Pacary, E., Johnston, C., Drechsel, D., Lebel-Potter, M., Garcia, L. G., Hunt, C., Dolle, D., Bithell, A., Ettwiller, L., Buckley, N., & Guillemot, F. (2011). A novel function of the proneural factor Ascl1 in progenitor proliferation identified by genome-wide characterization of its targets. *Genes & Development*, *25*(9), 930–945. https://doi.org/10.1101/gad.627811

Castro, D. S., Skowronska-Krawczyk, D., Armant, O., Donaldson, I. J., Parras, C., Hunt, C., Critchley, J. A., Nguyen, L., Gossler, A., Göttgens, B., Matter, J.-M., & Guillemot, F. (2006). Proneural bHLH and Brn Proteins Coregulate a Neurogenic Program through Cooperative Binding to a Conserved DNA Motif. *Developmental Cell*, *11*(6), 831–844. https://doi.org/10.1016/j.devcel.2006.10.006

Chanda, S., Ang, C. E., Davila, J., Pak, C., Mall, M., Lee, Q. Y., Ahlenius, H., Jung, S. W., Südhof, T. C., & Wernig, M. (2014). Generation of induced neuronal cells by the single reprogramming factor ASCL1. *Stem Cell Reports*, *3*(2), 282–296.

Chang, E. H., Adorjan, I., Mundim, M. V., Sun, B., Dizon, M. L., & Szele, F. G. (2016). Traumatic brain injury activation of the adult subventricular zone neurogenic niche. *Frontiers in Neuroscience*, *10*, 332.

Chen, F., Liu, X., Zhong, X., Chen, X., Nicholson, E., Liu, K., Chen, H., Lin, Y., Shu, Y., & Zhou, W. (2025). Neurons derived from NeuroD1-expressing astrocytes transition through transit-amplifying intermediates but lack functional maturity. *Science Advances*, *11*(30), eadw9296.

Chen, Y.-C., Ma, N.-X., Pei, Z.-F., Wu, Z., Do-Monte, F. H., Keefe, S., Yellin, E., Chen, M. S., Yin, J.-C., Lee, G., Minier-Toribio, A., Hu, Y., Bai, Y.-T., Lee, K., Quirk, G. J., & Chen, G. (2020). A NeuroD1 AAV-Based Gene Therapy for Functional Brain Repair after Ischemic Injury through In Vivo Astrocyte-to-Neuron Conversion. *Molecular Therapy*, *28*(1), 217–234. https://doi.org/10.1016/j.ymthe.2019.09.003

Cieri, M. B., & Ramos, A. J. (2025). Astrocytes, reactive astrogliosis, and glial scar formation in traumatic brain injury. *Neural Regeneration Research*, *20*(4), 973–989. https://doi.org/10.4103/NRR.NRR-D-23-02091

Cieri, M. B., Villarreal, A., Gomez-Cuautle, D. D., Mailing, I., & Ramos, A. J. (2023). Progression of reactive gliosis and astroglial phenotypic changes following stab wound-induced traumatic brain injury in mice. *Journal of Neurochemistry*, *167*(2), 183–203. https://doi.org/10.1111/jnc.15941

Clark, D. P. Q., Perreau, V. M., Shultz, S. R., Brady, R. D., Lei, E., Dixit, S., Taylor, J. M., Beart, P. M., & Boon, W. C. (2019). Inflammation in Traumatic Brain Injury: Roles for Toxic A1 Astrocytes and Microglial–Astrocytic Crosstalk. *Neurochemical Research*, *44*(6), 1410–1424. https://doi.org/10.1007/s11064-019-02721-8

Clarner, T., Diederichs, F., Berger, K., Denecke, B., Gan, L., Van der Valk, P., Beyer, C., Amor, S., & Kipp, M. (2012). Myelin debris regulates inflammatory responses in an experimental demyelination animal model and multiple sclerosis lesions. *Glia*, *60*(10), 1468–1480.

Clayton, B. L., & Liddelow, S. A. (2025). Heterogeneity of astrocyte reactivity. *Annual Review of Neuroscience*, *48*(1), 231–249.

Cook, R., Zima, L., Khazaal, J., & Williams, J. (2024). Low-velocity penetrating brain injury: A review of the literature and illustrative case. *Brain Injury*, *38*(8), 668–674. https://doi.org/10.1080/02699052.2024.2336067

Cooper, A., Garcia Mora, A., Herrera-Oropeza, G., Beltran Arranz, A., Marichal, N., Shi, Y., Leaman, S., Lozano Gonzalez, K., Strom, M., & Fursham, H. (2026). Dlx2 reprograms the transcriptome and laminar position of glia-derived Ascl1-induced interneurons. *bioRxiv*, 2026.01. 02.697435.

Damisah, E. C., Hill, R. A., Tong, L., Murray, K. N., & Grutzendler, J. (2017). A fluoro-Nissl dye identifies pericytes as distinct vascular mural cells during in vivo brain imaging. *Nature Neuroscience*, *20*(7), 1023–1032.

Dash, P. K., Mach, S. A., & Moore, A. N. (2001). Enhanced neurogenesis in the rodent hippocampus following traumatic brain injury. *Journal of Neuroscience Research*, *63*(4), 313–319. https://doi.org/10.1002/1097-4547(20010215)63:4%253C313::AID-JNR1025%253E3.0.CO;2-4

Davis, W. C., Marusic, S., Lewin, H. A., Splitter, G. A., Perryman, L. E., McGuire, T. C., & Gorham, J. R. (1987). The development and analysis of species specific and cross reactive monoclonal antibodies to leukocyte differentiation antigens and antigens of the major histocompatibility complex for use in the study of the immune system in cattle and other species. *Veterinary Immunology and Immunopathology*, *15*(4), 337–376.

Dawson, M. (2003). NG2-expressing glial progenitor cells: An abundant and widespread population of cycling cells in the adult rat CNS. *Molecular and Cellular Neuroscience*, *24*(2), 476–488. https://doi.org/10.1016/S1044-7431(03)00210-0

Dean, T., Ghaemmaghami, J., Corso, J., & Gallo, V. (2023). The cortical NG2 -glia response to traumatic brain injury. *Glia*, *71*(5), 1164–1175. https://doi.org/10.1002/glia.24342

Dent, K. A., Christie, K. J., Bye, N., Basrai, H. S., Turbic, A., Habgood, M., Cate, H. S., & Turnley, A. M. (2015). Oligodendrocyte Birth and Death following Traumatic Brain Injury in Adult Mice. *PLOS ONE*, *10*(3), e0121541. https://doi.org/10.1371/journal.pone.0121541

Dias, D. O., & Göritz, C. (2018). Fibrotic scarring following lesions to the central nervous system. *Matrix Biology*, *68–69*, 561–570. https://doi.org/10.1016/j.matbio.2018.02.009

Dimou, L., & Gallo, V. (2015). NG 2-glia and their functions in the central nervous system. *Glia*, *63*(8), 1429–1451. https://doi.org/10.1002/glia.22859

Dimou, L., & Götz, M. (2014). Glial Cells as Progenitors and Stem Cells: New Roles in the Healthy and Diseased Brain. *Physiological Reviews*, *94*(3), 709–737. https://doi.org/10.1152/physrev.00036.2013

Dimou, L., Simon, C., Kirchhoff, F., Takebayashi, H., & Götz, M. (2008). Progeny of Olig2-Expressing Progenitors in the Gray and White Matter of the Adult Mouse Cerebral Cortex. *The Journal of Neuroscience*, *28*(41), 10434–10442. https://doi.org/10.1523/JNEUROSCI.2831-08.2008

Dixon, S. J., Lemberg, K. M., Lamprecht, M. R., Skouta, R., Zaitsev, E. M., Gleason, C. E., Patel, D. N., Bauer, A. J., Cantley, A. M., & Yang, W. S. (2012). Ferroptosis: An iron-dependent form of nonapoptotic cell death. *Cell*, *149*(5), 1060–1072.

Donat, C. K., Scott, G., Gentleman, S. M., & Sastre, M. (2017). Microglial Activation in Traumatic Brain Injury. *Frontiers in Aging Neuroscience*, *9*, 208. https://doi.org/10.3389/fnagi.2017.00208

Duncan, G. J., Manesh, S. B., Hilton, B. J., Assinck, P., Plemel, J. R., & Tetzlaff, W. (2020). The fate and function of oligodendrocyte progenitor cells after traumatic spinal cord injury. *Glia*, *68*(2), 227–245.

Edward Dixon, C., Clifton, G. L., Lighthall, J. W., Yaghmai, A. A., & Hayes, R. L. (1991). A controlled cortical impact model of traumatic brain injury in the rat. *Journal of Neuroscience Methods*, *39*(3), 253–262. https://doi.org/10.1016/0165-0270(91)90104-8

Elbaz, B., & Popko, B. (2019). Molecular Control of Oligodendrocyte Development. *Trends in Neurosciences*, *42*(4), 263–277. https://doi.org/10.1016/j.tins.2019.01.002

Emery, B., & Lu, Q. R. (2015). Transcriptional and Epigenetic Regulation of Oligodendrocyte Development and Myelination in the Central Nervous System. *Cold Spring Harbor Perspectives in Biology*, *7*(9), a020461. https://doi.org/10.1101/cshperspect.a020461

Eriksson, P. S., Perfilieva, E., Björk-Eriksson, T., Alborn, A.-M., Nordborg, C., Peterson, D. A., & Gage, F. H. (1998). Neurogenesis in the adult human hippocampus. *Nature Medicine*, *4*(11), 1313–1317. https://doi.org/10.1038/3305

Escartin, C., Galea, E., Lakatos, A., O'Callaghan, J. P., Petzold, G. C., Serrano-Pozo, A., Steinhäuser, C., Volterra, A., Carmignoto, G., Agarwal, A., Allen, N. J., Araque, A., Barbeito, L., Barzilai, A., Bergles, D. E., Bonvento, G., Butt, A. M., Chen, W.-T., Cohen-Salmon, M., ... Verkhratsky, A. (2021). Reactive astrocyte nomenclature, definitions, and future directions. *Nature Neuroscience*, *24*(3), 312–325. https://doi.org/10.1038/s41593-020-00783-4

Evans, J., Sumners, C., Moore, J., Huentelman, M. J., Deng, J., Gelband, C. H., & Shaw, G. (2002). Characterization of Mitotic Neurons Derived From Adult Rat Hypothalamus and Brain Stem. *Journal of Neurophysiology*, *87*(2), 1076–1085. https://doi.org/10.1152/jn.00088.2001

Faulkner, J. R., Herrmann, J. E., Woo, M. J., Tansey, K. E., Doan, N. B., & Sofroniew, M. V. (2004). Reactive Astrocytes Protect Tissue and Preserve Function after Spinal Cord Injury. *The Journal of Neuroscience*, *24*(9), 2143–2155. https://doi.org/10.1523/JNEUROSCI.3547-03.2004

Feeney, D. M., Boyeson, M. G., Linn, R. T., Murray, H. M., & Dail, W. G. (1981). Responses to cortical injury: I. Methodology and local effects of contusions in the rat. *Brain Research*, *211*(1), 67–77.

Fesharaki-Zadeh, A., & Datta, D. (2024). An overview of preclinical models of traumatic brain injury (TBI): Relevance to pathophysiological mechanisms. *Frontiers in Cellular Neuroscience*, *18*, 1371213.

Festa, L. K., Jordan-Sciutto, K. L., & Grinspan, J. B. (2025). Neuroinflammation: An oligodendrocentric view. *Glia*, *73*(6), 1113–1129.

Fogarty, M., Richardson, W. D., & Kessaris, N. (2005). A subset of oligodendrocytes generated from radial glia in the dorsal spinal cord. *Development*, *132*(8), 1951–1959. https://doi.org/10.1242/dev.01777

Franklin, R. J., & Ffrench-Constant, C. (2017). Regenerating CNS myelin—From mechanisms to experimental medicines. *Nature Reviews Neuroscience*, *18*(12), 753–769.

Franklin, R. J. M., & ffrench-Constant, C. (2008). Remyelination in the CNS: From biology to therapy. *Nature Reviews Neuroscience*, *9*(11), 839–855. https://doi.org/10.1038/nrn2480

Freed, C. R., Greene, P. E., Breeze, R. E., Tsai, W.-Y., DuMouchel, W., Kao, R., Dillon, S., Winfield, H., Culver, S., & Trojanowski, J. Q. (2001). Transplantation of embryonic dopamine neurons for severe Parkinson's disease. *New England Journal of Medicine*, *344*(10), 710–719.

Frik, J., Merl-Pham, J., Plesnila, N., Mattugini, N., Kjell, J., Kraska, J., Gómez, R. M., Hauck, S. M., Sirko, S., & Götz, M. (2018). Cross-talk between monocyte invasion

and astrocyte proliferation regulates scarring in brain injury. *EMBO Reports*, *19*(5), e45294. https://doi.org/10.15252/embr.201745294

Gage, F. H., Coates, P. W., Palmer, T. D., Kuhn, H. G., Fisher, L. J., Suhonen, J. O., Peterson, D. A., Suhr, S. T., & Ray, J. (1995). Survival and differentiation of adult neuronal progenitor cells transplanted to the adult brain. *Proceedings of the National Academy of Sciences*, *92*(25), 11879–11883. https://doi.org/10.1073/pnas.92.25.11879

Galante, C., Marichal, N., Scarante, F. F., Ghayad, L. M., Shi, Y., Schuurmans, C., Berninger, B., & Péron, S. (2022b). Enhanced proliferation of oligodendrocyte progenitor cells following retrovirus mediated Achaete-scute complex-like 1 overexpression in the postnatal cerebral cortex in vivo. *Frontiers in Neuroscience*, *16*, 919462. https://doi.org/10.3389/fnins.2022.919462

Galante, C., Marichal, N., Schuurmans, C., Berninger, B., & Péron, S. (2022a). Low-efficiency conversion of proliferative glia into induced neurons by Ascl1 in the postnatal mouse cerebral cortex in vivo. *bioRxiv*, 2022.04. 13.488173.

Gao, X., & Chen, J. (2013). Moderate traumatic brain injury promotes neural precursor proliferation without increasing neurogenesis in the adult hippocampus. *Experimental Neurology*, *239*, 38–48. https://doi.org/10.1016/j.expneurol.2012.09.012

Gascón, S., Masserdotti, G., Russo, G. L., & Götz, M. (2017). Direct Neuronal Reprogramming: Achievements, Hurdles, and New Roads to Success. *Cell Stem Cell*, *21*(1), 18–34. https://doi.org/10.1016/j.stem.2017.06.011

Gascón, S., Murenu, E., Masserdotti, G., Ortega, F., Russo, G. L., Petrik, D., Deshpande, A., Heinrich, C., Karow, M., & Robertson, S. P. (2016). Identification and successful negotiation of a metabolic checkpoint in direct neuronal reprogramming. *Cell Stem Cell*, *18*(3), 396–409.

Ghajar, J. (2000). Traumatic brain injury. *The Lancet*, *356*(9233), 923–929.

Goedhart, J., Van Weeren, L., Adjobo-Hermans, M. J., Elzenaar, I., Hink, M. A., & Gadella Jr, T. W. (2011). Quantitative co-expression of proteins at the single cell level–application to a multimeric FRET sensor. *PloS One*, *6*(11), e27321.

Goldman, S. A., & Nottebohm, F. (1983). Neuronal production, migration, and differentiation in a vocal control nucleus of the adult female canary brain. *Proceedings of the National Academy of Sciences*, *80*(8), 2390–2394. https://doi.org/10.1073/pnas.80.8.2390

Götz, M., & Bocchi, R. (2021). Neuronal replacement: Concepts, achievements, and call for caution. *Current Opinion in Neurobiology*, *69*, 185–192. https://doi.org/10.1016/j.conb.2021.03.014

Götz, M., Sirko, S., Beckers, J., & Irmler, M. (2015). Reactive astrocytes as neural stem or progenitor cells: In vivo lineage, in vitro potential, and genome-wide expression analysis. *Glia*, *63*(8), 1452–1468.

Grande, A., Sumiyoshi, K., López-Juárez, A., Howard, J., Sakthivel, B., Aronow, B., Campbell, K., & Nakafuku, M. (2013). Environmental impact on direct neuronal reprogramming in vivo in the adult brain. *Nature Communications*, *4*(1), 2373.

Greenhalgh, A. D., David, S., & Bennett, F. C. (2020). Immune cell regulation of glia during CNS injury and disease. *Nature Reviews Neuroscience*, *21*(3), 139–152. https://doi.org/10.1038/s41583-020-0263-9

Guilfoyle, M. R., Carpenter, K. L. H., Helmy, A., Pickard, J. D., Menon, D. K., & Hutchinson, P. J. A. (2015). Matrix Metalloproteinase Expression in Contusional Traumatic Brain Injury: A Paired Microdialysis Study. *Journal of Neurotrauma*, *32*(20), 1553–1559. https://doi.org/10.1089/neu.2014.3764

Guillemot, F. (2007). Cell fate specification in the mammalian telencephalon. *Progress in Neurobiology*, *83*(1), 37–52.

Guo, Q., Scheller, A., & Huang, W. (2021). Progenies of NG2 glia: What do we learn from transgenic mouse models? *Neural Regeneration Research*, *16*(1), 43–48.

Guo, Y., Suo, N., Cui, X., Yuan, Q., & Xie, X. (2018). Vitamin C promotes oligodendrocytes generation and remyelination. *Glia*, *66*(7), 1302–1316.

Guo, Z., Zhang, L., Wu, Z., Chen, Y., Wang, F., & Chen, G. (2014). In vivo direct reprogramming of reactive glial cells into functional neurons after brain injury and in an Alzheimer's disease model. *Cell Stem Cell*, *14*(2), 188–202.

Gurdon, J. B. (1962). The developmental capacity of nuclei taken from intestinal epithelium cells of feeding tadpoles. *Development*, *10*(4), 622–640.

Gusel'Nikova, V. V., & Korzhevskiy, D. (2015). NeuN as a neuronal nuclear antigen and neuron differentiation marker. *Acta Naturae (Англоязычная Версия)*, *7*(2 (25)), 42–47.

Guttenplan, K. A., Stafford, B. K., El-Danaf, R. N., Adler, D. I., Münch, A. E., Weigel, M. K., Huberman, A. D., & Liddelow, S. A. (2020). Neurotoxic Reactive Astrocytes Drive Neuronal Death after Retinal Injury. *Cell Reports*, *31*(12), 107776. https://doi.org/10.1016/j.celrep.2020.107776

Gyoneva, S., & Ransohoff, R. M. (2015). Inflammatory reaction after traumatic brain injury: Therapeutic potential of targeting cell–cell communication by chemokines. *Trends in Pharmacological Sciences*, *36*(7), 471–480. https://doi.org/10.1016/j.tips.2015.04.003

Hackett, A. R., Yahn, S. L., Lyapichev, K., Dajnoki, A., Lee, D.-H., Rodriguez, M., Cammer, N., Pak, J., Mehta, S. T., Bodamer, O., Lemmon, V. P., & Lee, J. K. (2018). Injury type-dependent differentiation of NG2 glia into heterogeneous astrocytes. *Experimental Neurology*, *308*, 72–79. https://doi.org/10.1016/j.expneurol.2018.07.001

Haslund-Vinding, J., McBean, G., Jaquet, V., & Vilhardt, F. (2017). NADPH oxidases in oxidant production by microglia: Activating receptors, pharmacology and association with disease. *British Journal of Pharmacology*, *174*(12), 1733–1749.

Heinrich, C., Bergami, M., Gascón, S., Lepier, A., Viganò, F., Dimou, L., Sutor, B., Berninger, B., & Götz, M. (2014). Sox2-mediated conversion of NG2 glia into induced neurons in the injured adult cerebral cortex. *Stem Cell Reports*, *3*(6), 1000–1014.

Heinrich, C., Blum, R., Gascón, S., Masserdotti, G., Tripathi, P., Sánchez, R., Tiedt, S., Schroeder, T., Götz, M., & Berninger, B. (2010). Directing astroglia from the cerebral cortex into subtype specific functional neurons. *PLoS Biology*, *8*(5), e1000373.

Heins, N., Malatesta, P., Cecconi, F., Nakafuku, M., Tucker, K. L., Hack, M. A., Chapouton, P., Barde, Y.-A., & Götz, M. (2002). Glial cells generate neurons: The role of the transcription factor Pax6. *Nature Neuroscience*, *5*(4), 308–315.

Heo, D., Kim, A. A., Neumann, B., Doze, V. N., Xu, Y. K. T., Mironova, Y. A., Slosberg, J., Goff, L. A., Franklin, R. J. M., & Bergles, D. E. (2025). Transcriptional profiles of mouse oligodendrocyte precursor cells across the lifespan. *Nature Aging*, *5*(4), 675–690. https://doi.org/10.1038/s43587-025-00840-2

Hernandez, M. L., Chatlos, T., Gorse, K. M., & Lafrenaye, A. D. (2019). Neuronal Membrane Disruption Occurs Late Following Diffuse Brain Trauma in Rats and Involves a Subpopulation of NeuN Negative Cortical Neurons. *Frontiers in Neurology*, *10*, 1238. https://doi.org/10.3389/fneur.2019.01238

Herrero-Navarro, Á., Puche-Aroca, L., Moreno-Juan, V., Sempere-Ferràndez, A., Espinosa, A., Susín, R., Torres-Masjoan, L., Leyva-Díaz, E., Karow, M., Figueres-Oñate, M., López-Mascaraque, L., López-Atalaya, J. P., Berninger, B., & López-Bendito, G. (2021). Astrocytes and neurons share region-specific transcriptional signatures that confer regional identity to neuronal reprogramming. *Science Advances*, *7*(15), eabe8978. https://doi.org/10.1126/sciadv.abe8978

Hitoshi, N., Ken-ichi, Y., & Jun-ichi, M. (1991). Efficient selection for high-expression transfectants with a novel eukaryotic vector. *Gene*, *108*(2), 193–199. https://doi.org/10.1016/0378-1119(91)90434-D

Horky, L. L., Galimi, F., Gage, F. H., & Horner, P. J. (2006). Fate of endogenous stem/progenitor cells following spinal cord injury. *Journal of Comparative Neurology*, *498*(4), 525–538. https://doi.org/10.1002/cne.21065

Hu, X., Qin, S., Huang, X., Yuan, Y., Tan, Z., Gu, Y., Cheng, X., Wang, D., Lian, X.-F., & He, C. (2019). Region-restrict astrocytes exhibit heterogeneous susceptibility to neuronal reprogramming. *Stem Cell Reports*, *12*(2), 290–304.

Huang, H., Rubenstein, J. L., & Qiu, M. (2021). Cracking the Codes of Cortical Glial Progenitors: Evidence for the Common Lineage of Astrocytes and Oligodendrocytes. *Neuroscience Bulletin*, *37*(4), 437–439. https://doi.org/10.1007/s12264-021-00675-y

Hughes, E. G., Kang, S. H., Fukaya, M., & Bergles, D. E. (2013). Oligodendrocyte progenitors balance growth with self-repulsion to achieve homeostasis in the adult brain. *Nature Neuroscience*, *16*(6), 668–676. https://doi.org/10.1038/nn.3390

Huntemer-Silveira, A., Patil, N., Brickner, M. A., & Parr, A. M. (2021). Strategies for Oligodendrocyte and Myelin Repair in Traumatic CNS Injury. *Frontiers in Cellular Neuroscience*, *14*, 619707. https://doi.org/10.3389/fncel.2020.619707

Imayoshi, I., Isomura, A., Harima, Y., Kawaguchi, K., Kori, H., Miyachi, H., Fujiwara, T., Ishidate, F., & Kageyama, R. (2013). Oscillatory control of factors determining multipotency and fate in mouse neural progenitors. *Science*, *342*(6163), 1203–1208.

Jorstad, N. L., Wilken, M. S., Todd, L., Finkbeiner, C., Nakamura, P., Radulovich, N., Hooper, M. J., Chitsazan, A., Wilkerson, B. A., & Rieke, F. (2020). STAT signaling modifies Ascl1 chromatin binding and limits neural regeneration from Muller glia in adult mouse retina. *Cell Reports*, *30*(7), 2195-2208. e5.

Jurkowski, M. P., Bettio, L., K. Woo, E., Patten, A., Yau, S.-Y., & Gil-Mohapel, J. (2020). Beyond the Hippocampus and the SVZ: Adult Neurogenesis Throughout the Brain. *Frontiers in Cellular Neuroscience*, *14*, 576444. https://doi.org/10.3389/fncel.2020.576444

Kamen, Y., Chapman, T. W., Piedra, E. T., Ciolkowski, M. E., & Hill, R. A. (2025). Transient Upregulation of Procaspase-3 during Oligodendrocyte Fate Decisions. *The Journal of Neuroscience*, *45*(12), e2066242025. https://doi.org/10.1523/JNEUROSCI.2066-24.2025

Kang, S. H., Fukaya, M., Yang, J. K., Rothstein, J. D., & Bergles, D. E. (2010). NG2+ CNS Glial Progenitors Remain Committed to the Oligodendrocyte Lineage in Postnatal Life and following Neurodegeneration. *Neuron*, *68*(4), 668–681. https://doi.org/10.1016/j.neuron.2010.09.009

Karow, M., Camp, J. G., Falk, S., Gerber, T., Pataskar, A., Gac-Santel, M., Kageyama, J., Brazovskaja, A., Garding, A., & Fan, W. (2018). Direct pericyte-to-neuron reprogramming via unfolding of a neural stem cell-like program. *Nature Neuroscience*, *21*(7), 932–940.

Karow, M., Sánchez, R., Schichor, C., Masserdotti, G., Ortega, F., Heinrich, C., Gascón, S., Khan, M. A., Lie, D. C., & Dellavalle, A. (2012). Reprogramming of pericyte-derived cells of the adult human brain into induced neuronal cells. *Cell Stem Cell*, *11*(4), 471–476.

Katayama, Y., Becker, D. P., Tamura, T., & Hovda, D. A. (1990). Massive increases in extracellular potassium and the indiscriminate release of glutamate following concussive brain injury. *Journal of Neurosurgery*, *73*(6), 889–900.

Kawabata, S., Takano, M., Numasawa-Kuroiwa, Y., Itakura, G., Kobayashi, Y., Nishiyama, Y., Sugai, K., Nishimura, S., Iwai, H., Isoda, M., Shibata, S., Kohyama, J., Iwanami, A., Toyama, Y., Matsumoto, M., Nakamura, M., & Okano, H. (2016). Grafted Human iPS Cell-Derived Oligodendrocyte Precursor Cells Contribute to Robust Remyelination of Demyelinated Axons after Spinal Cord Injury. *Stem Cell Reports*, *6*(1), 1–8. https://doi.org/10.1016/j.stemcr.2015.11.013

Keirstead, H. S., Levine, J. M., & Blakemore, W. F. (1998). Response of the oligodendrocyte progenitor cell population (defined by NG2 labelling) to demyelination of the adult spinal cord. *Glia*, *22*(2), 161–170. https://doi.org/10.1002/(SICI)1098-1136(199802)22:2%253C161::AID-GLIA7%253E3.0.CO;2-A

Kelenis, D. P., Hart, E., Edwards-Fligner, M., Johnson, J. E., & Vue, T. Y. (2018). ASCL 1 regulates proliferation of NG 2-glia in the embryonic and adult spinal cord. *Glia*, *66*(9), 1862–1880.

Kempermann, G., & Kronenberg, G. (2003). Depressed new Neurons?—Adult hippocampal neurogenesis and a cellular plasticity hypothesis of major depression. *Biological Psychiatry*, *54*(5), 499–503. https://doi.org/10.1016/S0006-3223(03)00319-6

Kessaris, N., Fogarty, M., Iannarelli, P., Grist, M., Wegner, M., & Richardson, W. D. (2006). Competing waves of oligodendrocytes in the forebrain and postnatal elimination of an embryonic lineage. *Nature Neuroscience*, *9*(2), 173–179. https://doi.org/10.1038/nn1620

Kim, E. J., Leung, C. T., Reed, R. R., & Johnson, J. E. (2007). *In Vivo* Analysis of Ascl1 Defined Progenitors Reveals Distinct Developmental Dynamics during Adult Neurogenesis and Gliogenesis. *The Journal of Neuroscience*, *27*(47), 12764–12774. https://doi.org/10.1523/JNEUROSCI.3178-07.2007

Kim, J., Efe, J. A., Zhu, S., Talantova, M., Yuan, X., Wang, S., Lipton, S. A., Zhang, K., & Ding, S. (2011). Direct reprogramming of mouse fibroblasts to neural progenitors. *Proceedings of the National Academy of Sciences*, *108*(19), 7838–7843.

Kim, K. K., Adelstein, R. S., & Kawamoto, S. (2009). Identification of neuronal nuclei (NeuN) as Fox-3, a new member of the Fox-1 gene family of splicing factors. *Journal of Biological Chemistry*, *284*(45), 31052–31061.

Kim, M., Oh, S., Kim, S., Kim, I.-S., Kim, J., Han, J., Ahn, J. W., Chung, S., Jang, J.-H., Shin, J. E., & Park, K. I. (2024). In vivo neural regeneration via AAV-NeuroD1 gene delivery to astrocytes in neonatal hypoxic-ischemic brain injury. *Inflammation and Regeneration*, *44*(1), 33. https://doi.org/10.1186/s41232-024-00349-y

Kirby, L., Jin, J., Cardona, J. G., Smith, M. D., Martin, K. A., Wang, J., Strasburger, H., Herbst, L., Alexis, M., Karnell, J., Davidson, T., Dutta, R., Goverman, J., Bergles, D., & Calabresi, P. A. (2019). Oligodendrocyte precursor cells present antigen and are cytotoxic targets in inflammatory demyelination. *Nature Communications*, *10*(1), 3887. https://doi.org/10.1038/s41467-019-11638-3

Kirdajova, D., Valihrach, L., Valny, M., Kriska, J., Krocianova, D., Benesova, S., Abaffy, P., Zucha, D., Klassen, R., Kolenicova, D., Honsa, P., Kubista, M., & Anderova, M. (2021). Transient astrocyte-like NG2 glia subpopulation emerges solely

following permanent brain ischemia. *Glia*, *69*(11), 2658–2681. https://doi.org/10.1002/glia.24064

Koehl, M., & Abrous, D. N. (2011). A new chapter in the field of memory: Adult hippocampal neurogenesis. *European Journal of Neuroscience*, *33*(6), 1101–1114. https://doi.org/10.1111/j.1460-9568.2011.07609.x

Koupourtidou, C., Schwarz, V., Aliee, H., Frerich, S., Fischer-Sternjak, J., Bocchi, R., Simon-Ebert, T., Bai, X., Sirko, S., Kirchhoff, F., Dichgans, M., Götz, M., Theis, F. J., & Ninkovic, J. (2024). Shared inflammatory glial cell signature after stab wound injury, revealed by spatial, temporal, and cell-type-specific profiling of the murine cerebral cortex. *Nature Communications*, *15*(1), 2866. https://doi.org/10.1038/s41467-024-46625-w

Kremer, L. P. M., Cerrizuela, S., El-Sammak, H., Al Shukairi, M. E., Ellinger, T., Straub, J., Korkmaz, A., Volk, K., Brunken, J., Kleber, S., Anders, S., & Martin-Villalba, A. (2024). DNA methylation controls stemness of astrocytes in health and ischaemia. *Nature*, *634*(8033), 415–423. https://doi.org/10.1038/s41586-024-07898-9

Kriks, S., Shim, J.-W., Piao, J., Ganat, Y. M., Wakeman, D. R., Xie, Z., Carrillo-Reid, L., Auyeung, G., Antonacci, C., Buch, A., Yang, L., Beal, M. F., Surmeier, D. J., Kordower, J. H., Tabar, V., & Studer, L. (2011). Dopamine neurons derived from human ES cells efficiently engraft in animal models of Parkinson's disease. *Nature*, *480*(7378), 547–551. https://doi.org/10.1038/nature10648

Kuhlmann, T., Miron, V., Cuo, Q., Wegner, C., Antel, J., & Brück, W. (2008). Differentiation block of oligodendroglial progenitor cells as a cause for remyelination failure in chronic multiple sclerosis. *Brain*, *131*(7), 1749–1758.

Kuhn, H., Dickinson-Anson, H., & Gage, F. (1996). Neurogenesis in the dentate gyrus of the adult rat: Age-related decrease of neuronal progenitor proliferation. *The Journal of Neuroscience*, *16*(6), 2027–2033. https://doi.org/10.1523/JNEUROSCI.16-06-02027.1996

Kuhn, S., Gritti, L., Crooks, D., & Dombrowski, Y. (2019). Oligodendrocytes in Development, Myelin Generation and Beyond. *Cells*, *8*(11), 1424. https://doi.org/10.3390/cells8111424

La Rosa, C., Parolisi, R., & Bonfanti, L. (2020). Brain Structural Plasticity: From Adult Neurogenesis to Immature Neurons. *Frontiers in Neuroscience*, *14*, 75. https://doi.org/10.3389/fnins.2020.00075

Labusch, M., Mancini, L., Morizet, D., & Bally-Cuif, L. (2020). Conserved and Divergent Features of Adult Neurogenesis in Zebrafish. *Frontiers in Cell and Developmental Biology*, *8*, 525. https://doi.org/10.3389/fcell.2020.00525

Lange Canhos, L., Chen, M., Falk, S., Popper, B., Straub, T., Götz, M., & Sirko, S. (2021). Repetitive injury and absence of monocytes promote astrocyte self-renewal and neurological recovery. *Glia*, *69*(1), 165–181.

Lavin, Y., Winter, D., Blecher-Gonen, R., David, E., Keren-Shaul, H., Merad, M., Jung, S., & Amit, I. (2014). Tissue-Resident Macrophage Enhancer Landscapes Are Shaped by the Local Microenvironment. *Cell*, *159*(6), 1312–1326. https://doi.org/10.1016/j.cell.2014.11.018

Le, N., Vu, T.-D., Palazzo, I., Pulya, R., Kim, Y., Blackshaw, S., & Hoang, T. (2024). Robust reprogramming of glia into neurons by inhibition of Notch signaling and nuclear factor I (NFI) factors in adult mammalian retina. *Science Advances*, *10*(28), eadn2091.

Leaman, S., Marichal, N., & Berninger, B. (2022). Reprogramming cellular identity *in vivo*. *Development*, *149*(4), dev200433. https://doi.org/10.1242/dev.200433

Lentini, C., d'Orange, M., Marichal, N., Trottmann, M.-M., Vignoles, R., Foucault, L., Verrier, C., Massera, C., Raineteau, O., & Conzelmann, K.-K. (2021). Reprogramming reactive glia into interneurons reduces chronic seizure activity in a mouse model of mesial temporal lobe epilepsy. *Cell Stem Cell*, *28*(12), 2104-2121. e10.

Levine, J. M., Reynolds, R., & Fawcett, J. W. (2001). The oligodendrocyte precursor cell in health and disease. *Trends in Neurosciences*, *24*(1), 39–47. https://doi.org/10.1016/S0166-2236(00)01691-X

Li, S., Mattar, P., Dixit, R., Lawn, S. O., Wilkinson, G., Kinch, C., Eisenstat, D., Kurrasch, D. M., Chan, J. A., & Schuurmans, C. (2014). RAS/ERK Signaling Controls Proneural Genetic Programs in Cortical Development and Gliomagenesis. *The Journal of Neuroscience*, *34*(6), 2169–2190. https://doi.org/10.1523/JNEUROSCI.4077-13.2014

Lian, H., Litvinchuk, A., Chiang, A. C.-A., Aithmitti, N., Jankowsky, J. L., & Zheng, H. (2016). Astrocyte-microglia cross talk through complement activation modulates amyloid pathology in mouse models of Alzheimer's disease. *Journal of Neuroscience*, *36*(2), 577–589.

Liddelow, S. A., Guttenplan, K. A., Clarke, L. E., Bennett, F. C., Bohlen, C. J., Schirmer, L., Bennett, M. L., Münch, A. E., Chung, W.-S., Peterson, T. C., Wilton, D. K., Frouin, A., Napier, B. A., Panicker, N., Kumar, M., Buckwalter, M. S., Rowitch, D. H., Dawson, V. L., Dawson, T. M., ... Barres, B. A. (2017). Neurotoxic reactive astrocytes are induced by activated microglia. *Nature*, *541*(7638), 481–487. https://doi.org/10.1038/nature21029

Liddelow, S. A., Marsh, S. E., & Stevens, B. (2020). Microglia and Astrocytes in Disease: Dynamic Duo or Partners in Crime? *Trends in Immunology*, *41*(9), 820–835. https://doi.org/10.1016/j.it.2020.07.006

Lighthall, J. W. (1988). Controlled Cortical Impact: A New Experimental Brain Injury Model. *Journal of Neurotrauma*, *5*(1), 1–15. https://doi.org/10.1089/neu.1988.5.1

Lindvall, O., & Kokaia, Z. (2010). Stem cells in human neurodegenerative disorders—Time for clinical translation? *Journal of Clinical Investigation*, *120*(1), 29–40. https://doi.org/10.1172/JCI40543

Lindvall, O., Widner, H., Rehncrona, S., Brundin, P., Odin, P., Gustavii, B., Frackowiak, R., Leenders, K. L., Sawle, G., Rothwell, J. C., Ourklund, A. B., & Marsden, C. D. (1992). Transplantation of fetal dopamine neurons in Parkinson's disease: One-year clinical and neurophysiological observations in two patients with putaminal implants. *Annals of Neurology*, *31*(2), 155–165. https://doi.org/10.1002/ana.410310206

Liu, F., Zhang, Y., Chen, F., Yuan, J., Li, S., Han, S., Lu, D., Geng, J., Rao, Z., Sun, L., Xu, J., Shi, Y., Wang, X., & Liu, Y. (2021). Neurog2 directly converts astrocytes into functional neurons in midbrain and spinal cord. *Cell Death & Disease*, *12*(3), 225. https://doi.org/10.1038/s41419-021-03498-x

Liu, T., Cao, F., Xu, Y., & Feng, S. (2015). Upregulated Ras/Raf/ERK1/2 signaling pathway: A new hope in the repair of spinal cord injury. *Neural Regeneration Research*, *10*(5), 792. https://doi.org/10.4103/1673-5374.156984

Liu, Y., Miao, Q., Yuan, J., Han, S., Zhang, P., Li, S., Rao, Z., Zhao, W., Ye, Q., Geng, J., Zhang, X., & Cheng, L. (2015). Ascl1 Converts Dorsal Midbrain Astrocytes into Functional Neurons In Vivo. *Journal of Neuroscience*, *35*(25), 9336–9355. https://doi.org/10.1523/JNEUROSCI.3975-14.2015

Liu, Y., Wu, Q., Jiang, B., Hou, T., Wu, C., Wu, M., & Song, H. (2024). Distinct regulation of ASCL1 by the cell cycle and chemotherapy in small cell lung cancer. *Molecular Cancer Research*, *22*(7), 613–624.

Loane, D. J., & Kumar, A. (2016). Microglia in the TBI brain: The good, the bad, and the dysregulated. *Experimental Neurology*, *275*, 316–327. https://doi.org/10.1016/j.expneurol.2015.08.018

Lois, C., & Alvarez-Buylla, A. (1994). Long-Distance Neuronal Migration in the Adult Mammalian Brain. *Science*, *264*(5162), 1145–1148. https://doi.org/10.1126/science.8178174

Lotocki, G., de Rivero Vaccari, J., Alonso, O., Molano, J. S., Nixon, R., Safavi, P., Dietrich, W. D., & Bramlett, H. M. (2011). Oligodendrocyte vulnerability following traumatic brain injury in rats. *Neuroscience Letters*, *499*(3), 143–148.

Lucin, K. M., & Wyss-Coray, T. (2009). Immune activation in brain aging and neurodegeneration: Too much or too little? *Neuron*, *64*(1), 110–122.

Lundie-Brown, J., Puletti, F., Philpott, A., & Azzarelli, R. (2025). Cell fate acquisition and reprogramming by the proneural transcription factor ASCL1. *Open Biology*, *15*(6), 250018.

Ma, Y., Xie, H., Du, X., Wang, L., Jin, X., Zhang, Q., Han, Y., Sun, S., Wang, L., & Li, X. (2021). In vivo chemical reprogramming of astrocytes into neurons. *Cell Discovery*, *7*(1), 12.

Magavi, S. S., Leavitt, B. R., & Macklis, J. D. (2000). Induction of neurogenesis in the neocortex of adult mice. *Nature*, *405*(6789), 951–955. https://doi.org/10.1038/35016083

Magnusson, J. P., Göritz, C., Tatarishvili, J., Dias, D. O., Smith, E. M., Lindvall, O., Kokaia, Z., & Frisén, J. (2014). A latent neurogenic program in astrocytes regulated by Notch signaling in the mouse. *Science*, *346*(6206), 237–241.

Magnusson, J. P., Zamboni, M., Santopolo, G., Mold, J. E., Barrientos-Somarribas, M., Talavera-Lopez, C., Andersson, B., & Frisén, J. (2020). Activation of a neural stem cell transcriptional program in parenchymal astrocytes. *eLife*, *9*, e59733. https://doi.org/10.7554/eLife.59733

Maimon, R., Chillon-Marinas, C., Snethlage, C. E., Singhal, S. M., McAlonis-Downes, M., Ling, K., Rigo, F., Bennett, C. F., Da Cruz, S., Hnasko, T. S., Muotri, A. R., &

Cleveland, D. W. (2021). Therapeutically viable generation of neurons with antisense oligonucleotide suppression of PTB. *Nature Neuroscience*, *24*(8), 1089–1099. https://doi.org/10.1038/s41593-021-00864-y

Mall, M., Kareta, M. S., Chanda, S., Ahlenius, H., Perotti, N., Zhou, B., Grieder, S. D., Ge, X., Drake, S., & Euong Ang, C. (2017). Myt1l safeguards neuronal identity by actively repressing many non-neuronal fates. *Nature*, *544*(7649), 245–249.

Marichal, N., Péron, S., Beltrán Arranz, A., Galante, C., Franco Scarante, F., Wiffen, R., Schuurmans, C., Karow, M., Gascón, S., & Berninger, B. (2024). Reprogramming astroglia into neurons with hallmarks of fast-spiking parvalbumin-positive interneurons by phospho-site–deficient Ascl1. *Science Advances*, *10*(43), eadl5935. https://doi.org/10.1126/sciadv.adl5935

Masserdotti, G., Gillotin, S., Sutor, B., Drechsel, D., Irmler, M., Jørgensen, H. F., Sass, S., Theis, F. J., Beckers, J., & Berninger, B. (2015). Transcriptional mechanisms of proneural factors and REST in regulating neuronal reprogramming of astrocytes. *Cell Stem Cell*, *17*(1), 74–88.

Matsuda, T., Irie, T., Katsurabayashi, S., Hayashi, Y., Nagai, T., Hamazaki, N., Adefuin, A. M. D., Miura, F., Ito, T., & Kimura, H. (2019). Pioneer factor NeuroD1 rearranges transcriptional and epigenetic profiles to execute microglia-neuron conversion. *Neuron*, *101*(3), 472-485. e7.

Mattugini, N., Bocchi, R., Scheuss, V., Russo, G. L., Torper, O., Lao, C. L., & Götz, M. (2019). Inducing different neuronal subtypes from astrocytes in the injured mouse cerebral cortex. *Neuron*, *103*(6), 1086-1095. e5.

Mattugini, N., Merl-Pham, J., Petrozziello, E., Schindler, L., Bernhagen, J., Hauck, S. M., & Götz, M. (2018). Influence of white matter injury on gray matter reactive gliosis upon stab wound in the adult murine cerebral cortex. *Glia*, *66*(8), 1644–1662. https://doi.org/10.1002/glia.23329

Mayoral, S. R., & Chan, J. R. (2016). The environment rules: Spatiotemporal regulation of oligodendrocyte differentiation. *Current Opinion in Neurobiology*, *39*, 47–52. https://doi.org/10.1016/j.conb.2016.04.002

McIntosh, T. K., Vink, R., Yamakami, I., & Faden, A. I. (1989). Magnesium protects against neurological deficit after brain injury. *Brain Research*, *482*(2), 252–260. https://doi.org/10.1016/0006-8993(89)91188-8

Medina-Rodríguez, E. M., Bribián, A., Boyd, A., Palomo, V., Pastor, J., Lagares, A., Gil, C., Martínez, A., Williams, A., & de Castro, F. (2017). Promoting in vivo remyelination with small molecules: A neuroreparative pharmacological treatment for Multiple Sclerosis. *Scientific Reports*, *7*(1), 43545.

Menon, D. K., Schwab, K., Wright, D. W., & Maas, A. I. (2010). Position Statement: Definition of Traumatic Brain Injury. *Archives of Physical Medicine and Rehabilitation*, *91*(11), 1637–1640. https://doi.org/10.1016/j.apmr.2010.05.017

Mira, R. G., Lira, M., & Cerpa, W. (2021). Traumatic Brain Injury: Mechanisms of Glial Response. *Frontiers in Physiology*, *12*, 740939. https://doi.org/10.3389/fphys.2021.740939

Mircea, M., & Semrau, S. (2021). How a cell decides its own fate: A single-cell view of molecular mechanisms and dynamics of cell-type specification. *Biochemical Society Transactions*, *49*(6), 2509–2525.

Miron, V. E., Boyd, A., Zhao, J.-W., Yuen, T. J., Ruckh, J. M., Shadrach, J. L., Van Wijngaarden, P., Wagers, A. J., Williams, A., Franklin, R. J. M., & ffrench-Constant, C. (2013). M2 microglia and macrophages drive oligodendrocyte differentiation during CNS remyelination. *Nature Neuroscience*, *16*(9), 1211–1218. https://doi.org/10.1038/nn.3469

Mironova, Y. A., Dang, B., Heo, D., Xu, Y. K. T., Hsu, A. Y.-H., Eugenin von Bernhardi, J., Molina-Castro, G. C., Kim, A. A., Lin, J.-P., & Reich, D. S. (2026). Myelin is repaired by constitutive differentiation of oligodendrocyte progenitors. Science, 391(6783), eadu2896.

Mokhtarzadeh Khanghahi, A., Satarian, L., Deng, W., Baharvand, H., & Javan, M. (2018). In vivo conversion of astrocytes into oligodendrocyte lineage cells with transcription factor Sox10; Promise for myelin repair in multiple sclerosis. *PloS One*, *13*(9), e0203785.

Munoz-Ballester, C., Mahmutovic, D., Rafiqzad, Y., Korot, A., & Robel, S. (2022). Mild traumatic brain injury-induced disruption of the blood-brain barrier triggers an atypical neuronal response. *Frontiers in Cellular Neuroscience*, *16*, 821885.

Nakatani, H., Martin, E., Hassani, H., Clavairoly, A., Maire, C. L., Viadieu, A., Kerninon, C., Delmasure, A., Frah, M., Weber, M., Nakafuku, M., Zalc, B., Thomas, J.-L., Guillemot, F., Nait-Oumesmar, B., & Parras, C. (2013). Ascl1/Mash1 Promotes

Brain Oligodendrogenesis during Myelination and Remyelination. *Journal of Neuroscience*, *33*(23), 9752–9768. https://doi.org/10.1523/JNEUROSCI.0805-13.2013

Naso, M. F., Tomkowicz, B., Perry III, W. L., & Strohl, W. R. (2017). Adeno-associated virus (AAV) as a vector for gene therapy. *BioDrugs*, *31*(4), 317–334.

Nato, G., Caramello, A., Trova, S., Avataneo, V., Rolando, C., Taylor, V., Buffo, A., Peretto, P., & Luzzati, F. (2015). Striatal astrocytes produce neuroblasts in an excitotoxic model of Huntington's disease. *Development*, *142*(5), 840–845.

Neuberger, E. J., Swietek, B., Corrubia, L., Prasanna, A., & Santhakumar, V. (2017). Enhanced Dentate Neurogenesis after Brain Injury Undermines Long-Term Neurogenic Potential and Promotes Seizure Susceptibility. *Stem Cell Reports*, *9*(3), 972–984. https://doi.org/10.1016/j.stemcr.2017.07.015

Newville, J., Jantzie, L., & Cunningham, L. (2017). Embracing oligodendrocyte diversity in the context of perinatal injury. *Neural Regeneration Research*, *12*(10), 1575. https://doi.org/10.4103/1673-5374.217320

Nikolakopoulou, A. M., Montagne, A., Kisler, K., Dai, Z., Wang, Y., Huuskonen, M. T., Sagare, A. P., Lazic, D., Sweeney, M. D., & Kong, P. (2019). Pericyte loss leads to circulatory failure and pleiotrophin depletion causing neuron loss. *Nature Neuroscience*, *22*(7), 1089–1098.

Nishiyama, A., Suzuki, R., & Zhu, X. (2014). NG2 cells (polydendrocytes) in brain physiology and repair. *Frontiers in Neuroscience*, *8*. https://doi.org/10.3389/fnins.2014.00133

Niu, J., Tsai, H.-H., Hoi, K. K., Huang, N., Yu, G., Kim, K., Baranzini, S. E., Xiao, L., Chan, J. R., & Fancy, S. P. J. (2019). Aberrant oligodendroglial–vascular interactions disrupt the blood–brain barrier, triggering CNS inflammation. *Nature Neuroscience*, *22*(5), 709–718. https://doi.org/10.1038/s41593-019-0369-4

Niu, W., Zang, T., Smith, D. K., Vue, T. Y., Zou, Y., Bachoo, R., Johnson, J. E., & Zhang, C.-L. (2015). SOX2 reprograms resident astrocytes into neural progenitors in the adult brain. *Stem Cell Reports*, *4*(5), 780–794.

Niu, W., Zang, T., Zou, Y., Fang, S., Smith, D. K., Bachoo, R., & Zhang, C.-L. (2013). In vivo reprogramming of astrocytes to neuroblasts in the adult brain. *Nature Cell Biology*, *15*(10), 1164–1175.

Obernier, K., & Alvarez-Buylla, A. (2019). Neural stem cells: Origin, heterogeneity and regulation in the adult mammalian brain. *Development*, *146*(4), dev156059. https://doi.org/10.1242/dev.156059

Ogino, Y., Bernas, T., Greer, J. E., & Povlishock, J. T. (2022). Axonal injury following mild traumatic brain injury is exacerbated by repetitive insult and is linked to the delayed attenuation of NeuN expression without concomitant neuronal death in the mouse. Brain Pathology, 32(2), e13034.

Ohab, J. J., & Carmichael, S. T. (2008). Poststroke Neurogenesis: Emerging Principles of Migration and Localization of Immature Neurons. *The Neuroscientist*, *14*(4), 369–380. https://doi.org/10.1177/1073858407309545

Olanow, C. W., Goetz, C. G., Kordower, J. H., Stoessl, A. J., Sossi, V., Brin, M. F., Shannon, K. M., Nauert, G. M., Perl, D. P., & Godbold, J. (2003). A double-blind controlled trial of bilateral fetal nigral transplantation in Parkinson's disease. *Annals of Neurology*, *54*(3), 403–414.

O'Rourke, M., Cullen, C. L., Auderset, L., Pitman, K. A., Achatz, D., Gasperini, R., & Young, K. M. (2016). Evaluating tissue-specific recombination in a Pdgfrα-CreERT2 transgenic mouse line. *PloS One*, *11*(9), e0162858.

Ory, D. S., Neugeboren, B. A., & Mulligan, R. C. (1996). A stable human-derived packaging cell line for production of high titer retrovirus/vesicular stomatitis virus G pseudotypes. *Proceedings of the National Academy of Sciences*, *93*(21), 11400–11406. https://doi.org/10.1073/pnas.93.21.11400

Osier, N. D., & Dixon, C. E. (2016). The Controlled Cortical Impact Model: Applications, Considerations for Researchers, and Future Directions. *Frontiers in Neurology*, *7*. https://doi.org/10.3389/fneur.2016.00134

Otsu, N. (1979). A Threshold Selection Method from Gray-Level Histograms. *IEEE Transactions on Systems, Man, and Cybernetics*, *9*(1), 62–66. https://doi.org/10.1109/TSMC.1979.4310076

Ozerdem, U., Grako, K. A., Dahlin-Huppe, K., Monosov, E., & Stallcup, W. B. (2001). NG2 proteoglycan is expressed exclusively by mural cells during vascular morphogenesis. *Developmental Dynamics: An Official Publication of the American Association of Anatomists*, *222*(2), 218–227.

Palazzo, I., Kelly, L., Koenig, L., & Fischer, A. J. (2023). Patterns of NFkB activation resulting from damage, reactive microglia, cytokines, and growth factors in the mouse retina. *Experimental Neurology*, *359*, 114233.

Palmer, T. D., Takahashi, J., & Gage, F. H. (1997). The Adult Rat Hippocampus Contains Primordial Neural Stem Cells. *Molecular and Cellular Neuroscience*, *8*(6), 389–404. https://doi.org/10.1006/mcne.1996.0595

Pannell, D., & Ellis, J. (2001). Silencing of gene expression: Implications for design of retrovirus vectors. *Reviews in Medical Virology*, *11*(4), 205–217.

Parent, A., Cicchetti, F., & Beach, T. G. (1995). Calretinin-immunoreactive neurons in the human striatum. *Brain Research*, *674*(2), 347–351. https://doi.org/10.1016/0006-8993(95)00124-9

Parkinson, L. M., Gillen, S. L., Woods, L. M., Chaytor, L., Marcos, D., Ali, F. R., Carroll, J. S., & Philpott, A. (2022). The proneural transcription factor ASCL1 regulates cell proliferation and primes for differentiation in neuroblastoma. *Frontiers in Cell and Developmental Biology*, *10*, 942579.

Parras, C. M., Hunt, C., Sugimori, M., Nakafuku, M., Rowitch, D., & Guillemot, F. (2007). The Proneural Gene *Mash1* Specifies an Early Population of Telencephalic Oligodendrocytes. *The Journal of Neuroscience*, *27*(16), 4233–4242. https://doi.org/10.1523/JNEUROSCI.0126-07.2007

Parras, C. M., Schuurmans, C., Scardigli, R., Kim, J., Anderson, D. J., & Guillemot, F. (2002). Divergent functions of the proneural genes Mash1 and Ngn2 in the specification of neuronal subtype identity. *Genes & Development*, *16*(3), 324–338.

Pavlou, M. A. S., Grandbarbe, L., Buckley, N. J., Niclou, S. P., & Michelucci, A. (2019). Transcriptional and epigenetic mechanisms underlying astrocyte identity. *Progress in Neurobiology*, *174*, 36–52. https://doi.org/10.1016/j.pneurobio.2018.12.007

Peferoen, L., Kipp, M., Van Der Valk, P., Van Noort, J. M., & Amor, S. (2014). Oligodendrocyte-microglia cross-talk in the central nervous system. *Immunology*, *141*(3), 302–313. https://doi.org/10.1111/imm.12163

Pereira, M., Birtele, M., Shrigley, S., Benitez, J. A., Hedlund, E., Parmar, M., & Ottosson, D. R. (2017). Direct reprogramming of resident NG2 glia into neurons with properties of fast-spiking parvalbumin-containing interneurons. *Stem Cell Reports*, *9*(3), 742–751.

Péron, S., Droguerre, M., Debarbieux, F., Ballout, N., Benoit-Marand, M., Francheteau, M., Brot, S., Rougon, G., Jaber, M., & Gaillard, A. (2017). A Delay between Motor Cortex Lesions and Neuronal Transplantation Enhances Graft Integration and Improves Repair and Recovery. *The Journal of Neuroscience*, *37*(7), 1820–1834. https://doi.org/10.1523/JNEUROSCI.2936-16.2017

Peters, A. (2004). A fourth type of neuroglial cell in the adult central nervous system. *Journal of Neurocytology*, *33*(3), 345–357. https://doi.org/10.1023/B:NEUR.0000044195.64009.27

Petrosyan, H. A., Hunanyan, A. S., Alessi, V., Schnell, L., Levine, J., & Arvanian, V. L. (2013). Neutralization of Inhibitory Molecule NG2 Improves Synaptic Transmission, Retrograde Transport, and Locomotor Function after Spinal Cord Injury in Adult Rats. *The Journal of Neuroscience*, *33*(9), 4032–4043. https://doi.org/10.1523/JNEUROSCI.4702-12.2013

Ponti, G., Obernier, K., Guinto, C., Jose, L., Bonfanti, L., & Alvarez-Buylla, A. (2013). Cell cycle and lineage progression of neural progenitors in the ventricular-subventricular zones of adult mice. *Proceedings of the National Academy of Sciences*, *110*(11). https://doi.org/10.1073/pnas.1219563110

Povlishock, J. T., & Jenkins, L. W. (1995). Are the Pathobiological Changes Evoked by Traumatic Brain Injury Immediate and Irreversible? *Brain Pathology*, *5*(4), 415–426. https://doi.org/10.1111/j.1750-3639.1995.tb00620.x

Povlishock, J. T., & Katz, D. I. (2005). Update of neuropathology and neurological recovery after traumatic brain injury. *The Journal of Head Trauma Rehabilitation*, *20*(1), 76–94.

Puglisi, M., Lao, C. L., Wani, G., Masserdotti, G., Bocchi, R., & Götz, M. (2024). Comparing Viral Vectors and Fate Mapping Approaches for Astrocyte-to-Neuron Reprogramming in the Injured Mouse Cerebral Cortex. *Cells*, *13*(17), 1408. https://doi.org/10.3390/cells13171408

Qian, H., Kang, X., Hu, J., Zhang, D., Liang, Z., Meng, F., Zhang, X., Xue, Y., Maimon, R., Dowdy, S. F., Devaraj, N. K., Zhou, Z., Mobley, W. C., Cleveland, D. W., & Fu, X.-D. (2020). Reversing a model of Parkinson's disease with in situ converted nigral neurons. *Nature*, *582*(7813), 550–556. https://doi.org/10.1038/s41586-020-2388-4

Ramón y Cajal, S. (1909). *Histologie du système nerveux de l'homme & des vertébrés*. Maloine. https://doi.org/10.5962/bhl.title.48637

Rao, Y., Du, S., Yang, B., Wang, Y., Li, Y., Li, R., Zhou, T., Du, X., He, Y., Wang, Y., Zhou, X., Yuan, T.-F., Mao, Y., & Peng, B. (2021). NeuroD1 induces microglial apoptosis and cannot induce microglia-to-neuron cross-lineage reprogramming. *Neuron*, *109*(24), 4094-4108.e5. https://doi.org/10.1016/j.neuron.2021.11.008

Raposo, A. A. S. F., Vasconcelos, F. F., Drechsel, D., Marie, C., Johnston, C., Dolle, D., Bithell, A., Gillotin, S., van den Berg, D. L. C., Ettwiller, L., Flicek, P., Crawford, G. E., Parras, C. M., Berninger, B., Buckley, N. J., Guillemot, F., & Castro, D. S. (2015). Ascl1 Coordinately Regulates Gene Expression and the Chromatin Landscape during Neurogenesis. *Cell Reports*, *10*(9), 1544–1556. https://doi.org/10.1016/j.celrep.2015.02.025

Reynolds, B. A., & Weiss, S. (1992). Generation of Neurons and Astrocytes from Isolated Cells of the Adult Mammalian Central Nervous System. *Science*, *255*(5052), 1707–1710. https://doi.org/10.1126/science.1553558

Richardson, W. D., Young, K. M., Tripathi, R. B., & McKenzie, I. (2011). NG2-glia as Multipotent Neural Stem Cells: Fact or Fantasy? *Neuron*, *70*(4), 661–673. https://doi.org/10.1016/j.neuron.2011.05.013

Rivetti Di Val Cervo, P., Romanov, R. A., Spigolon, G., Masini, D., Martín-Montañez, E., Toledo, E. M., La Manno, G., Feyder, M., Pifl, C., & Ng, Y.-H. (2017). Induction of functional dopamine neurons from human astrocytes in vitro and mouse astrocytes in a Parkinson's disease model. *Nature Biotechnology*, *35*(5), 444–452.

Roe, T., Reynolds, T. C., Yu, G., & Brown, P. O. (1993). Integration of murine leukemia virus DNA depends on mitosis. *The EMBO Journal*, *12*(5), 2099–2108. https://doi.org/10.1002/j.1460-2075.1993.tb05858.x

Russo, G. L., Sonsalla, G., Natarajan, P., Breunig, C. T., Bulli, G., Merl-Pham, J., Schmitt, S., Giehrl-Schwab, J., Giesert, F., & Jastroch, M. (2021). CRISPR-mediated induction of neuron-enriched mitochondrial proteins boosts direct glia-to-neuron conversion. *Cell Stem Cell*, *28*(3), 524-534. e7.

Russo, M. V., & McGavern, D. B. (2016). Inflammatory neuroprotection following traumatic brain injury. *Science*, *353*(6301), 783–785. https://doi.org/10.1126/science.aaf6260

Salas-Briceno, K., Zhao, W., & Ross, S. R. (2024). Murine leukemia virus infection of non-dividing dendritic cells is dependent on nucleoporins. *PLoS Pathogens*, *20*(1), e1011640.

Salewski, R. P., Mitchell, R. A., Li, L., Shen, C., Milekovskaia, M., Nagy, A., & Fehlings, M. G. (2015). Transplantation of Induced Pluripotent Stem Cell-Derived Neural Stem Cells Mediate Functional Recovery Following Thoracic Spinal Cord Injury Through Remyelination of Axons. *Stem Cells Translational Medicine*, *4*(7), 743–754. https://doi.org/10.5966/sctm.2014-0236

Santiago, F. S., Lowe, H. C., Day, F. L., Chesterman, C. N., & Khachigian, L. M. (1999). Early Growth Response Factor-1 Induction by Injury Is Triggered by Release and Paracrine Activation by Fibroblast Growth Factor-2. *The American Journal of Pathology*, *154*(3), 937–944. https://doi.org/10.1016/S0002-9440(10)65341-2

Saraswat, D., Shayya, H. J., Polanco, J. J., Tripathi, A., Welliver, R. R., Pol, S. U., Seidman, R. A., Broome, J. E., O'Bara, M. A., & van Kuppervelt, T. H. (2021). Overcoming the inhibitory microenvironment surrounding oligodendrocyte progenitor cells following experimental demyelination. *Nature Communications*, *12*(1), 1923.

Sawamoto, N., Doi, D., Nakanishi, E., Sawamura, M., Kikuchi, T., Yamakado, H., Taruno, Y., Shima, A., Fushimi, Y., Okada, T., Kikuchi, T., Morizane, A., Hiramatsu, S., Anazawa, T., Shindo, T., Ueno, K., Morita, S., Arakawa, Y., Nakamoto, Y., ... Takahashi, J. (2025). Phase I/II trial of iPS-cell-derived dopaminergic cells for Parkinson's disease. *Nature*, *641*(8064), 971–977. https://doi.org/10.1038/s41586-025-08700-0

Schweitzer, J. S., Song, B., Herrington, T. M., Park, T.-Y., Lee, N., Ko, S., Jeon, J., Cha, Y., Kim, K., Li, Q., Henchcliffe, C., Kaplitt, M., Neff, C., Rapalino, O., Seo, H., Lee, I.-H., Kim, J., Kim, T., Petsko, G. A., ... Kim, K.-S. (2020). Personalized iPSC-Derived Dopamine Progenitor Cells for Parkinson's Disease. *New England Journal of Medicine*, *382*(20), 1926–1932. https://doi.org/10.1056/NEJMoa1915872

Shigemoto-Mogami, Y., Hoshikawa, K., & Sato, K. (2018). Activated Microglia Disrupt the Blood-Brain Barrier and Induce Chemokines and Cytokines in a Rat in vitro Model. *Frontiers in Cellular Neuroscience*, *12*, 494. https://doi.org/10.3389/fncel.2018.00494

Shohami, E., Novikov, M., Bass, R., Yamin, A., & Gallily, R. (1994). Closed Head Injury Triggers Early Production of TNFα and IL-6 by Brain Tissue. *Journal of Cerebral Blood Flow & Metabolism*, *14*(4), 615–619. https://doi.org/10.1038/jcbfm.1994.76

Sim, F. J., Zhao, C., Penderis, J., & Franklin, R. J. (2002). The age-related decrease in CNS remyelination efficiency is attributable to an impairment of both oligodendrocyte progenitor recruitment and differentiation. *Journal of Neuroscience*, *22*(7), 2451–2459.

Simon, C., Götz, M., & Dimou, L. (2011). Progenitors in the adult cerebral cortex: Cell cycle properties and regulation by physiological stimuli and injury. *Glia*, *59*(6), 869–881. https://doi.org/10.1002/glia.21156

Simon, D. W., McGeachy, M. J., Bayır, H., Clark, R. S. B., Loane, D. J., & Kochanek, P. M. (2017). The far-reaching scope of neuroinflammation after traumatic brain injury. *Nature Reviews Neurology*, *13*(3), 171–191. https://doi.org/10.1038/nrneurol.2017.13

Sirko, S., Behrendt, G., Johansson, P. A., Tripathi, P., Costa, M. R., Bek, S., Heinrich, C., Tiedt, S., Colak, D., & Dichgans, M. (2013). Reactive glia in the injured brain acquire stem cell properties in response to sonic hedgehog. *Cell Stem Cell*, *12*(4), 426–439.

Sirko, S., Schichor, C., Della Vecchia, P., Metzger, F., Sonsalla, G., Simon, T., Bürkle, M., Kalpazidou, S., Ninkovic, J., & Masserdotti, G. (2023). Injury-specific factors in the cerebrospinal fluid regulate astrocyte plasticity in the human brain. Nature Medicine, 29(12), 3149–3161.

Sofroniew, M. V. (2009). Molecular dissection of reactive astrogliosis and glial scar formation. *Trends in Neurosciences*, *32*(12), 638–647. https://doi.org/10.1016/j.tins.2009.08.002

Son, E. Y., Ichida, J. K., Wainger, B. J., Toma, J. S., Rafuse, V. F., Woolf, C. J., & Eggan, K. (2011). Conversion of mouse and human fibroblasts into functional spinal motor neurons. *Cell Stem Cell*, *9*(3), 205–218.

Song, S., Hasan, M. N., Yu, L., Paruchuri, S. S., Bielanin, J. P., Metwally, S., Oft, H. C. M., Fischer, S. G., Fiesler, V. M., Sen, T., Gupta, R. K., Foley, L. M., Hitchens, T. K., Dixon, C. E., Cambi, F., Sen, N., & Sun, D. (2022). Microglial–oligodendrocyte interactions in myelination and neurological function recovery after traumatic brain injury. *Journal of Neuroinflammation*, *19*(1), 246. https://doi.org/10.1186/s12974-022-02608-6

Soomro, S. H., Jie, J., & Fu, H. (2018). Oligodendrocytes Development and Wnt Signaling Pathway. *International Journal of Human Anatomy*, *1*(3), 17–35. https://doi.org/10.14302/issn.2577-2279.ijha-18-2407

Sousa, V. H., Miyoshi, G., Hjerling-Leffler, J., Karayannis, T., & Fishell, G. (2009). Characterization of Nkx6-2-derived neocortical interneuron lineages. *Cerebral Cortex*, *19*(suppl_1), i1–i10.

Spencer, D. D., Robbins, R. J., Naftolin, F., Marek, K. L., Vollmer, T., Leranth, C., Roth, R. H., Price, L. H., Gjedde, A., & Bunney, B. S. (1992). Unilateral transplantation of human fetal mesencephalic tissue into the caudate nucleus of patients with Parkinson's disease. *New England Journal of Medicine*, *327*(22), 1541–1548.

Spitzer, S. O., Sitnikov, S., Kamen, Y., Evans, K. A., Kronenberg-Versteeg, D., Dietmann, S., de Faria, O., Agathou, S., & Káradóttir, R. T. (2019). Oligodendrocyte progenitor cells become regionally diverse and heterogeneous with age. *Neuron*, *101*(3), 459-471. e5.

Srinivasan, R., Lu, T.-Y., Chai, H., Xu, J., Huang, B. S., Golshani, P., Coppola, G., & Khakh, B. S. (2016). New transgenic mouse lines for selectively targeting astrocytes and studying calcium signals in astrocyte processes in situ and in vivo. *Neuron*, *92*(6), 1181–1195.

Stevens, B., Allen, N. J., Vazquez, L. E., Howell, G. R., Christopherson, K. S., Nouri, N., Micheva, K. D., Mehalow, A. K., Huberman, A. D., & Stafford, B. (2007). The classical complement cascade mediates CNS synapse elimination. *Cell*, *131*(6), 1164–1178.

Stricker, S. H., & Götz, M. (2021). Epigenetic regulation of neural lineage elaboration: Implications for therapeutic reprogramming. *Neurobiology of Disease*, *148*, 105174.

Strijbis, E. M., Kooi, E.-J., van der Valk, P., & Geurts, J. J. (2017). Cortical remyelination is heterogeneous in multiple sclerosis. *Journal of Neuropatholgy & Experimental Neurology*, *76*(5), 390–401.

Sueda, R., & Kageyama, R. (2021). Oscillatory expression of Ascl1 in oligodendrogenesis. *Gene Expression Patterns*, *41*, 119198.

Sugawara, T., Fujimura, M., Noshita, N., Kim, G. W., Saito, A., Hayashi, T., Narasimhan, P., Maier, C. M., & Chan, P. H. (2004). Neuronal death/survival signaling pathways in cerebral ischemia. *NeuroRx*, *1*(1), 17–25.

Sugimori, M., Nagao, M., Parras, C. M., Nakatani, H., Lebel, M., Guillemot, F., & Nakafuku, M. (2008). Ascl1 is required for oligodendrocyte development in the spinal cord. *Development*, *135*(7), 1271–1281. https://doi.org/10.1242/dev.015370

Tai, W., Wu, W., Wang, L.-L., Ni, H., Chen, C., Yang, J., Zang, T., Zou, Y., Xu, X.-M., & Zhang, C.-L. (2021). In vivo reprogramming of NG2 glia enables adult neurogenesis and functional recovery following spinal cord injury. *Cell Stem Cell*, *28*(5), 923-937. e4.

Takahashi, K., & Yamanaka, S. (2006). Induction of pluripotent stem cells from mouse embryonic and adult fibroblast cultures by defined factors. *Cell*, *126*(4), 663–676.

Tan, Z., Qin, S., Liu, H., Huang, X., Pu, Y., He, C., Yuan, Y., & Su, Z. (2024). Small molecules reprogram reactive astrocytes into neuronal cells in the injured adult spinal cord. *Journal of Advanced Research*, *59*, 111–127.

Tan, Z., Qin, S., Yuan, Y., Hu, X., Huang, X., Liu, H., Pu, Y., He, C., & Su, Z. (2022). NOTCH1 signaling regulates the latent neurogenic program in adult reactive astrocytes after spinal cord injury. *Theranostics*, *12*(10), 4548–4563. https://doi.org/10.7150/thno.71378

Tepavčević, V., & Lubetzki, C. (2022). Oligodendrocyte progenitor cell recruitment and remyelination in multiple sclerosis: The more, the merrier? *Brain*, *145*(12), 4178–4192.

Tiane, A., Schepers, M., Rombaut, B., Hupperts, R., Prickaerts, J., Hellings, N., Van Den Hove, D., & Vanmierlo, T. (2019). From OPC to Oligodendrocyte: An Epigenetic Journey. *Cells*, *8*(10), 1236. https://doi.org/10.3390/cells8101236

Tiwari, V., Prajapati, B., Asare, Y., Damkou, A., Ji, H., Liu, L., Naser, N., Gouna, G., Leszczyńska, K. B., & Mieczkowski, J. (2024). Innate immune training restores pro-reparative myeloid functions to promote remyelination in the aged central nervous system. *Immunity*, *57*(9), 2173-2190. e8.

Todd, L., Palazzo, I., Suarez, L., Liu, X., Volkov, L., Hoang, T. V., Campbell, W. A., Blackshaw, S., Quan, N., & Fischer, A. J. (2019). Reactive microglia and IL1β/IL-1R1-

signaling mediate neuroprotection in excitotoxin-damaged mouse retina. *Journal of Neuroinflammation*, *16*(1), 118.

Todd, L., Jenkins, W., Finkbeiner, C., Hooper, M. J., Donaldson, P. C., Pavlou, M., Wohlschlegel, J., Ingram, N., Mu, X., & Rieke, F. (2022). Reprogramming Müller glia to regenerate ganglion-like cells in adult mouse retina with developmental transcription factors. Science Advances, 8(47), eabq7219.

Torper, O., Ottosson, D. R., Pereira, M., Lau, S., Cardoso, T., Grealish, S., & Parmar, M. (2015). In vivo reprogramming of striatal NG2 glia into functional neurons that integrate into local host circuitry. *Cell Reports*, *12*(3), 474–481.

Torper, O., Pfisterer, U., Wolf, D. A., Pereira, M., Lau, S., Jakobsson, J., Björklund, A., Grealish, S., & Parmar, M. (2013). Generation of induced neurons via direct conversion in vivo. *Proceedings of the National Academy of Sciences*, *110*(17), 7038–7043.

Trounson, A., & McDonald, C. (2015). Stem Cell Therapies in Clinical Trials: Progress and Challenges. *Cell Stem Cell*, *17*(1), 11–22. https://doi.org/10.1016/j.stem.2015.06.007

Varadarajan, S. G., Hunyara, J. L., Hamilton, N. R., Kolodkin, A. L., & Huberman, A. D. (2022). Central nervous system regeneration. *Cell*, *185*(1), 77–94.

Vargas, M. E., & Barres, B. A. (2007). Why is Wallerian degeneration in the CNS so slow? *Annu. Rev. Neurosci.*, *30*(1), 153–179.

Vasan, L., Park, E., David, L. A., Fleming, T., & Schuurmans, C. (2021). Direct Neuronal Reprogramming: Bridging the Gap Between Basic Science and Clinical Application. *Frontiers in Cell and Developmental Biology*, *9*, 681087. https://doi.org/10.3389/fcell.2021.681087

Vasconcelos, F. F., & Castro, D. S. (2014). Transcriptional control of vertebrate neurogenesis by the proneural factor Ascl1. *Frontiers in Cellular Neuroscience*, *8*. https://doi.org/10.3389/fncel.2014.00412

Vierbuchen, T., Ostermeier, A., Pang, Z. P., Kokubu, Y., Südhof, T. C., & Wernig, M. (2010). Direct conversion of fibroblasts to functional neurons by defined factors. *Nature*, *463*(7284), 1035–1041.

Vierbuchen, T., & Wernig, M. (2012). Molecular roadblocks for cellular reprogramming. *Molecular Cell*, *47*(6), 827–838.

Viganò, F., Möbius, W., Götz, M., & Dimou, L. (2013). Transplantation reveals regional differences in oligodendrocyte differentiation in the adult brain. *Nature Neuroscience*, *16*(10), 1370–1372.

Vignoles, R., Lentini, C., d'Orange, M., & Heinrich, C. (2019). Direct Lineage Reprogramming for Brain Repair: Breakthroughs and Challenges. *Trends in Molecular Medicine*, *25*(10), 897–914. https://doi.org/10.1016/j.molmed.2019.06.006

Waddington, C. H. (1957). *The Strategy of the Genes. Allen*. Unwin, London.

Wang, J.-H., Gessler, D. J., Zhan, W., Gallagher, T. L., & Gao, G. (2024). Adeno-associated virus as a delivery vector for gene therapy of human diseases. *Signal Transduction and Targeted Therapy*, *9*(1), 78. https://doi.org/10.1038/s41392-024-01780-w

Wang, L.-L., Serrano, C., Zhong, X., Ma, S., Zou, Y., & Zhang, C.-L. (2021). Revisiting astrocyte to neuron conversion with lineage tracing in vivo. *Cell*, *184*(21), 5465-5481. e16.

Wang, L.-L., Su, Z., Tai, W., Zou, Y., Xu, X.-M., & Zhang, C.-L. (2016). The p53 pathway controls SOX2-mediated reprogramming in the adult mouse spinal cord. *Cell Reports*, *17*(3), 891–903.

Wang, N. B., Lende-Dorn, B. A., Beitz, A. M., Han, P., Adewumi, H. O., O'Shea, T. M., & Galloway, K. E. (2025). Proliferation history and transcription factor levels drive direct conversion to motor neurons. *Cell Systems*, *16*(4).

Wang, S., Cheng, H., Dai, G., Wang, X., Hua, R., Liu, X., Wang, P., Chen, G., Yue, W., & An, Y. (2013). Umbilical cord mesenchymal stem cell transplantation significantly improves neurological function in patients with sequelae of traumatic brain injury. *Brain Research*, *1532*, 76–84. https://doi.org/10.1016/j.brainres.2013.08.001

Wang, X., Wang, Q., Hou, L., Wei, G., He, C., Li, H., & Liu, L. (2025). Advances in ERK Signaling Pathway in Traumatic Brain Injury: Mechanisms and Therapeutic Potential. *Neurochemical Research*, *50*(3), 191. https://doi.org/10.1007/s11064-025-04449-0

Wapinski, O. L., Vierbuchen, T., Qu, K., Lee, Q. Y., Chanda, S., Fuentes, D. R., Giresi, P. G., Ng, Y. H., Marro, S., & Neff, N. F. (2013). Hierarchical mechanisms for direct reprogramming of fibroblasts to neurons. *Cell*, *155*(3), 621–635.

Waisman, A., Ginhoux, F., Greter, M., & Bruttger, J. (2015). Homeostasis of microglia in the adult brain: Review of novel microglia depletion systems. Trends in Immunology, 36(10), 625–636.

Williams, A. J., Hartings, J. A., Lu, X.-C. M., Rolli, M. L., Dave, J. R., & Tortella, F. C. (2005). Characterization of a new rat model of penetrating ballistic brain injury. *Journal of Neurotrauma*, *22*(2), 313–331.

Witcher, K. G., Bray, C. E., Chunchai, T., Zhao, F., O'Neil, S. M., Gordillo, A. J., Campbell, W. A., McKim, D. B., Liu, X., Dziabis, J. E., Quan, N., Eiferman, D. S., Fischer, A. J., Kokiko-Cochran, O. N., Askwith, C., & Godbout, J. P. (2021). Traumatic Brain Injury Causes Chronic Cortical Inflammation and Neuronal Dysfunction Mediated by Microglia. *The Journal of Neuroscience*, *41*(7), 1597–1616. https://doi.org/10.1523/JNEUROSCI.2469-20.2020

Woods, L. M., Ali, F. R., Gomez, R., Chernukhin, I., Marcos, D., Parkinson, L. M., Tayoun, A. N. A., Carroll, J. S., & Philpott, A. (2022). Elevated ASCL1 activity creates de novo regulatory elements associated with neuronal differentiation. *BMC Genomics*, *23*(1), 255. https://doi.org/10.1186/s12864-022-08495-8

Wylie, L. A., Hardwick, L. J. A., Papkovskaia, T. D., Thiele, C. J., & Philpott, A. (2015). Ascl1 phospho-status regulates neuronal differentiation in a *Xenopus* developmental model of neuroblastoma. *Disease Models & Mechanisms*, *8*(5), 429–441. https://doi.org/10.1242/dmm.018630

Xiang, Z., He, S., Chen, R., Liu, S., Liu, M., Xu, L., Zheng, J., Jiang, Z., Ma, L., & Sun, Y. (2024). Two-photon live imaging of direct glia-to-neuron conversion in the mouse cortex. *Neural Regeneration Research*, *19*(8), 1781–1788.

Xiang, Z., Xu, L., Liu, M., Wang, Q., Li, W., Lei, W., & Chen, G. (2021). Lineage tracing of direct astrocyte-to-neuron conversion in the mouse cortex. *Neural Regeneration Research*, *16*(4), 750. https://doi.org/10.4103/1673-5374.295925

Xiao, Y., & Czopka, T. (2023). Myelination-independent functions of oligodendrocyte precursor cells in health and disease. *Nature Neuroscience*, *26*(10), 1663–1669. https://doi.org/10.1038/s41593-023-01423-3

Xie, Y., Zhou, J., Wang, L.-L., Zhang, C.-L., & Chen, B. (2023). New AAV tools fail to detect Neurod1-mediated neuronal conversion of Müller glia and astrocytes in vivo. *eBioMedicine*, *90*, 104531. https://doi.org/10.1016/j.ebiom.2023.104531

Xiong, Y., Mahmood, A., & Chopp, M. (2013). Animal models of traumatic brain injury. *Nature Reviews Neuroscience*, *14*(2), 128–142. https://doi.org/10.1038/nrn3407

Yamashita, M., Nakahira, N., Hashimoto, K., Kobayashi, H., Nakashima, M., Ikeshima-Kataoka, H., & Miyamoto, Y. (2025). Reactive astrocyte-derived neurotoxicity is mitigated by vitronectin in traumatic brain injury mouse model. *IBRO Neuroscience Reports*, *19*, 300–306. https://doi.org/10.1016/j.ibneur.2025.07.009

Yamashita, T., Ninomiya, M., Acosta, P. H., García-Verdugo, J. M., Sunabori, T., Sakaguchi, M., Adachi, K., Kojima, T., Hirota, Y., & Kawase, T. (2006). Subventricular zone-derived neuroblasts migrate and differentiate into mature neurons in the post-stroke adult striatum. *Journal of Neuroscience*, *26*(24), 6627–6636.

Yamashita, T., Shang, J., Nakano, Y., Morihara, R., Sato, K., Takemoto, M., Hishikawa, N., Ohta, Y., & Abe, K. (2019). In vivo direct reprogramming of glial linage to mature neurons after cerebral ischemia. *Scientific Reports*, *9*(1), 10956.

Yamazaki, R., & Ohno, N. (2025). The potential of repurposing clemastine to promote remyelination. *Frontiers in Cellular Neuroscience*, *19*, 1582902.

Yang, Y., Vanin, E. F., Whitt, M. A., Fornerod, M., Zwart, R., Schneiderman, R. D., Grosveld, G., & Nienhuis, A. W. (1995). Inducible, high-level production of infectious murine leukemia retroviral vector particles pseudotyped with vesicular stomatitis virus G envelope protein. *Human Gene Therapy*, *6*(9), 1203–1213.

Yasuhara, T., Kawauchi, S., Kin, K., Morimoto, J., Kameda, M., Sasaki, T., Bonsack, B., Kingsbury, C., Tajiri, N., Borlongan, C. V., & Date, I. (2020). Cell therapy for central nervous system disorders: Current obstacles to progress. *CNS Neuroscience & Therapeutics*, *26*(6), 595–602. https://doi.org/10.1111/cns.13247

Yin, H., Brian, D., Weber, R. Z., Lyden, P. D., & Rust, R. (2025). "Time Is Brain" – for Cell Therapies. *Advanced Science*, e19579. https://doi.org/10.1002/advs.202519579

Young, K. M., Psachoulia, K., Tripathi, R. B., Dunn, S.-J., Cossell, L., Attwell, D., Tohyama, K., & Richardson, W. D. (2013). Oligodendrocyte Dynamics in the Healthy Adult CNS: Evidence for Myelin Remodeling. *Neuron*, *77*(5), 873–885. https://doi.org/10.1016/j.neuron.2013.01.006

Young, K., & Morrison, H. (2018). Quantifying microglia morphology from photomicrographs of immunohistochemistry prepared tissue using ImageJ. *Journal of Visualized Experiments: JoVE*, *136*, 57648.

Yu, F., Wang, Y., Stetler, A. R., Leak, R. K., Hu, X., & Chen, J. (2022). Phagocytic microglia and macrophages in brain injury and repair. *CNS Neuroscience & Therapeutics*, *28*(9), 1279–1293.

Yun, S. P., Kam, T.-I., Panicker, N., Kim, S., Oh, Y., Park, J.-S., Kwon, S.-H., Park, Y. J., Karuppagounder, S. S., & Park, H. (2018). Block of A1 astrocyte conversion by microglia is neuroprotective in models of Parkinson's disease. *Nature Medicine*, *24*(7), 931–938.

Zamanian, J. L., Xu, L., Foo, L. C., Nouri, N., Zhou, L., Giffard, R. G., & Barres, B. A. (2012). Genomic Analysis of Reactive Astrogliosis. *The Journal of Neuroscience*, *32*(18), 6391–6410. https://doi.org/10.1523/JNEUROSCI.6221-11.2012

Zamboni, M., Llorens-Bobadilla, E., Magnusson, J. P., & Frisén, J. (2020). A widespread neurogenic potential of neocortical astrocytes is induced by injury. *Cell Stem Cell*, *27*(4), 605-617. e5.

Zawadzka, M., Rivers, L. E., Fancy, S. P. J., Zhao, C., Tripathi, R., Jamen, F., Young, K., Goncharevich, A., Pohl, H., Rizzi, M., Rowitch, D. H., Kessaris, N., Suter, U., Richardson, W. D., & Franklin, R. J. M. (2010). CNS-Resident Glial Progenitor/Stem Cells Produce Schwann Cells as well as Oligodendrocytes during Repair of CNS Demyelination. *Cell Stem Cell*, *6*(6), 578–590. https://doi.org/10.1016/j.stem.2010.04.002

Zhang, L., Lei, Z., Guo, Z., Pei, Z., Chen, Y., Zhang, F., Cai, A., Mok, G., Lee, G., Swaminathan, V., Wang, F., Bai, Y., & Chen, G. (2020). Development of Neuroregenerative Gene Therapy to Reverse Glial Scar Tissue Back to Neuron-Enriched Tissue. *Frontiers in Cellular Neuroscience*, *14*, 594170. https://doi.org/10.3389/fncel.2020.594170

Zhang, R., Chopp, M., & Zhang, Z. G. (2013). Oligodendrogenesis after cerebral ischemia. *Frontiers in Cellular Neuroscience*, *7*, 201.

Zhang, R. L., Chopp, M., Roberts, C., Jia, L., Wei, M., Lu, M., Wang, X., Pourabdollah, S., & Zhang, Z. G. (2011). Ascl1 Lineage Cells Contribute to Ischemia-Induced Neurogenesis and Oligodendrogenesis. *Journal of Cerebral Blood Flow & Metabolism*, *31*(2), 614–625. https://doi.org/10.1038/jcbfm.2010.134

Zhao, M., Momma, S., Delfani, K., Carlén, M., Cassidy, R. M., Johansson, C. B., Brismar, H., Shupliakov, O., Frisén, J., & Janson, A. M. (2003). Evidence for neurogenesis in the adult mammalian substantia nigra. *Proceedings of the National Academy of Sciences*, *100*(13), 7925–7930. https://doi.org/10.1073/pnas.1131955100

Zhao, Q., Zhang, J., Li, H., Li, H., & Xie, F. (2023). Models of traumatic brain injury-highlights and drawbacks. *Frontiers in Neurology*, *14*, 1151660.

Zhu, B., Eom, J., & Hunt, R. F. (2019). Transplanted interneurons improve memory precision after traumatic brain injury. *Nature Communications*, *10*(1), 5156. https://doi.org/10.1038/s41467-019-13170-w

Zhu, X., Hill, R. A., Dietrich, D., Komitova, M., Suzuki, R., & Nishiyama, A. (2011). Age-dependent fate and lineage restriction of single NG2 cells. *Development*, *138*(4), 745–753.

Zincarelli, C., Soltys, S., Rengo, G., & Rabinowitz, J. E. (2008). Analysis of AAV serotypes 1–9 mediated gene expression and tropism in mice after systemic injection. *Molecular Therapy*, *16*(6), 1073–1080.

Zufferey, R., Donello, J. E., Trono, D., & Hope, T. J. (1999). Woodchuck hepatitis virus posttranscriptional regulatory element enhances expression of transgenes delivered by retroviral vectors. *Journal of Virology*, *73*(4), 2886–2892.

7. Appendix

Appendix 1: Experimental animals used and analyses performed. Total number of animals (n) used per experiment and corresponding chapters and figures.

Experiment	Strain	Initial Age (w)	Retrovirus (RV)	n	Chapter, figure and analyses
SWI 0 dpi	C57BL/6J	8	-	3	Chapter I: Fig.16 – EdU; C3; GFAP
SWI + RV 4 dpi	C57BL/6J	8	DsRed	3	Chapter I: Fig.5 – Sox10; GFAP; Iba1; DCX Fig.6 – Sox10; GFAP Fig.7 – DCX; NeuN Chapter II: Fig.18 – EdU; Sox10 Fig.19 – Sox10 Fig.20 – Sox10; EdU Fig.21 – GFAP; EdU Fig.22 – Iba1; EdU
	C57BL/6J	8	Ascl1	3	Chapter I: Fig.6 – Sox10; GFAP Fig.7 – DCX; NeuN Chapter II: Fig.19 – Sox10 Fig.20 – Sox10; EdU Fig.21 – GFAP; EdU Fig.22 – Iba1; EdU
	C57BL/6J	8	Ascl1SA6	3	Chapter I: Fig.6 – Sox10; GFAP Fig.7 – DCX; NeuN Chapter II: Fig.19 – Sox10 Fig.20 – Sox10; EdU Fig.21 – GFAP; EdU Fig.22 – Iba1; EdU
	C57BL/6J	8	Bcl2	3	Chapter II: Fig.19 – Sox10 Fig.20 – Sox10; EdU Fig.21 – GFAP; EdU Fig.22 – Iba1; EdU
	C57BL/6J	8	Ascl1-Bcl2	3	Chapter II: Fig.19 – Sox10 Fig.20 – Sox10; EdU Fig.21 – GFAP; EdU Fig.22 – Iba1; EdU

SWI + RV 12 dpi	C57BL/6J	8	DsRed	3	Chapter I: Fig.8 – DCX; NeuN Fig.9 –NeuN; Neurotrace Chapter II: Fig.23 – Sox10 Fig.24 – Sox10; EdU Fig.25 – GFAP; EdU
	C57BL/6J	8	Ascl1SA6-Bcl2	3	Chapter I: Fig.8 – DCX; NeuN Fig.9 – NeuN; Neurotrace Fig.10 – Sox10; GFAP
	C57BL/6J	9	Ascl1SA6	3	Chapter I: Fig.13 – Iba1; GFAP; CD45 Fig.14 – C3; GFAP; Iba1 Fig.15 – C3 mRNA
	C57BL/6J	9	Ascl1-Bcl2	3	Chapter I: Fig.8 – DCX; NeuN Fig.9 – NeuN; Neurotrace Fig.10 – Sox10; GFAP
	C57BL/6J	9	Ascl1	3	Chapter II: Fig.23 – Sox10 Fig.24 – Sox10; EdU Fig.25 – GFAP; EdU
	C57BL/6J	9	Ascl1-Bcl2	3	Chapter II: Fig.23 – Sox10 Fig.24 – Sox10; EdU Fig.25 – GFAP; EdU
	C57BL/6J	9	Bcl2	3	Chapter II: Fig.23 – Sox10 Fig.24 – Sox10; EdU Fig.25 – GFAP; EdU
	C57BL/6J	8	Ascl1-Bcl2	3	Chapter II: Fig.17 –NeuN; Neurotrace Fig.28 – EdU; Sox10 Fig.30 – BCAS1; Sox10
	C57BL/6J	8	Ascl1SA6-Bcl2	3	Chapter I: Fig.17 –NeuN; Neurotrace
SWI + RV 28 dpi	C57BL/6J	9	Ascl1	3	Chapter II: Fig.28 – EdU; Sox10 Fig.30 – BCAS1; Sox10
	C57BL/6J	9	Bcl2	3	Chapter II: Fig.28 – EdU; Sox10 Fig.30 – BCAS1; Sox10
	C57BL/6J	9	DsRed	3	Chapter II: Fig.18 – EdU; Sox10 Fig.28 – EdU; Sox10 Fig.30 – BCAS1; Sox10
SWI + RV	C57BL/6J	8	DsRed	3	Chapter II: Fig.18 – EdU; Sox10

70 dpi					Fig.29 – EdU; Sox10 Fig.30 – BCAS1; Sox10 Fig.31 – CC1; Sox10
	C57BL/6J	8	Asc1-Bcl2	3	Chapter II: Fig.29 – EdU; Sox10 Fig.30 – BCAS1; Sox10 Fig.31 – CC1; Sox10
	C57BL/6J	8	Ascl1	3	Chapter II: Fig.29 – EdU; Sox10 Fig.30 – BCAS1; Sox10 Fig.31 – CC1; Sox10
SWI + RV 12 dpi	Aldh1l1-CreER^{T2}/RCE	8-12	DsRed	3	Chapter II: Fig.26 – GFP; Sox9; Sox10; EdU
	Aldh1l1-CreER^{T2}/RCE	8-12	Ascl1	3	Chapter II: Fig.26 – GFP; Sox9; Sox10; EdU
	Aldh1l1-CreER^{T2}/RCE	8-12	Ascl1-Bcl2	3	Chapter II: Fig.26 – GFP; Sox9; Sox10; EdU
	Aldh1l1-CreER^{T2}/RCE	8-12	Ascl1SA6-Bcl2	3	Chapter I: Fig.11 – GFP; Sox9; NeuN; Neurotrace
	NG2-CreER^{TM}/RCE	8-12	DsRed	3	Chapter II: Fig.27 – GFP; PDGFRα; Sox10 EdU
	NG2-CreER^{TM}/RCE	8-12	Ascl1	3	Chapter II: Fig.27 – GFP; PDGFRα; Sox10 EdU
	NG2-CreER^{TM}/RCE	8-12	Ascl1-Bcl2	3	Chapter II: Fig.27 – GFP; PDGFRα; Sox10 EdU
	NG2-CreER^{TM}/RCE	8-12	Asc1SA6-Bcl2	3	Chapter II: Fig.12 – GFP; Sox9; NeuN; Neurotrace